SILICA BASED IMMUNOASSAYS

FOR A COVALENTLY ATTACHED ANTIGEN

By

KATHRYN MELZAK

B.Sc., University of British Columbia, 1986

A THESIS SUBMITTED IN PARTIAL FULFILLMENT OF

THE REQUIREMENTS FOR THE DEGREE OF

DOCTOR OF PHILOSOPHY

in

THE FACULTY OF GRADUATE STUDIES

DEPARTMENT OF CHEMISTRY

We accept this thesis as conforming

to the required standard

THE UNIVERSITY OF BRITISH COLUMBIA

August 1993

In presenting this thesis in partial fulfilment of the requirements for an advanced degree at the University of British Columbia, I agree that the Library shall make it freely available for reference and study. I further agree that permission for extensive copying of this thesis for scholarly purposes may be granted by the head of my department or by his or her representatives. It is understood that copying or publication of this thesis for financial gain shall not be allowed without my written permission.

(Signature) _____

Department of Chemistry

The University of British Columbia
Vancouver, Canada

Date Oct 15 1993

Abstract

An immunoassay was developed using a monoclonal antibody and an antigen covalently immobilized on silica, showing that silica is a potentially useful assay substrate.

Silica beads prepared from tetraethyl orthosilicate (0.78 μm diameter) and fused quartz slides were thoroughly cleaned and modified with 3-aminopropyltriethoxysilane. Amine groups on the modified slides and beads were used for carbodiimide mediated coupling to carboxyl groups on a peptide antigen. High surface concentrations of antigen were achieved.

Antibody binding to the antigen-modified beads and slides was measured using an iodinated monoclonal antibody. The equilibrium constant for the antibody binding on the beads was ten times higher than on the flat silica, but the maximum amount bound was lower.

Immunoassays performed using a second enzyme-labelled antibody to detect the monoclonal antibody bound to the silica permitted detection of the antigen at 10^{-8} M using the modified beads and at 10^{-7} M using the slides.

Table of Contents

List of Tables

List of Figures

Abbreviations

Ab.....antibody

AC3.....the name of the hybridoma cell line used to produce the antibody used in most of the experiments, and the name of the antibody produced by that cell line.

Ag.....antigen

BALB/c.....an inbred strain of mice

BCA.....bicinchoninic acid

BSA.....bovine serum albumin

C_{sat}^{*}.....a proposed minimum silicic acid concentration required to initiate nucleation.

CD-1.....a strain of mice

d.....sampling depth. In XPS measurements, this denotes the depth of the region from which the measured photoelectrons originate.

DME.....Dulbecco's modified Eagle medium

DMSO.....dimethyl sulfoxide

DNA.....deoxyribonucleic acid

Eb.....binding energy

EDC.....1-ethyl-3-(3-dimethylaminopropyl carbodiimide)

EDTA ehylene diamine tetraacetic acid

$E_{h\nu}$.....photon energy

E_{KE}.....electron kinetic energy

ELISA.....enzyme-linked immunosorbent assay

Fab.....the *a*ntigen *b*inding *f*ragment of immunoglobulins (see Fig. 3)

FBS.....fetal bovine serum

Fc.....the *c*rystallizable *f*ragment of immunoglobulins

FOX-NY.....a myeloma cell line derived from BALB/c mice

ΔG°.....the change in the standard state free energy

HAT.....hypoxanthine, adenine and thymidine

HRP.....horseradish peroxidase

HT.....hypoxanthine and thymidine

Ig.....immunoglobulin. Different classes are designated as IgA, IgD, IgE, IgG and IgM.

K.....equilibrium constant

ka.....association constant

kd.....dissociation constant

KLH.....keyhole limpet haemocyanin

PBS.....phosphate buffered saline

PBS-Tweem..phosphate buffered saline with 0.5% Tween 80

PEG.....polyethylene glycol

R.....the gas constant

SDS.....sodium dodecyl sulfate

SDS-PAGE...sodium dodecyl sulfate polacrylamide gel electrophoresis

SEM.....scanning electron microscopy

TEM.....transmission electron microscopy

TEOS.....tetraethyl orthosilicate

tlc.....thin layer chromatography

TMB.....tetramethyl benzidine

Tris.....tris(hydroxymethyl)aminomethane

Tween 80...polyoxyethylene sorbitan monooleate

XPS.....X-ray photoelectron spectroscopy

α.....used to denote specificity of antibody, eg goat α-rabbit is goat antibody against rabbit.

θ.....angle away from normal at which measurements are made for XPS

σ.....surface charge density

Acknowledgements

I would like to thank all the people who have offered me advice and good cheer while I have been working on this project, including:

-Don Brooks, who always listened if things were going badly, and who could usually point out that things weren't that bad after all,

-my parents, who always had faith in me

-Adam, who may consider that AC3 stands for Adam's company (cubed)

-the meanest mouse of all, who made it all possible,

-and all the people in the Brooks lab, who have made the days brighter and easier and altogether more cheerful.

Chapter 1

Introduction

1.1 General background

Immunoassays use the sensitive and specific antibody-antigen interaction to detect either antibodies or antigens. Detection of antibodies is used clinically to diagnose disease, and detection of antigens is used for a variety of clinical, agricultural and research purposes (1-3).

Antibodies are produced *in vivo* as part of the immune response to most foreign substances and will bind specifically to the antigen stimulating the response. The antibody and antigen associate reversibly to form a complex, with an equilibrium constant K defined as shown below (4).

[1] $$K = \frac{[Ab\text{-}Ag]}{[Ab][Ag]}$$

where [Ab-Ag] = concentration of the antibody-antigen complex
[Ab]= concentration of unoccupied binding sites on the antibody
[Ag]= concentration of unbound antigen

Measured equilibrium constants range from less than 10^5 litre mol^{-1} for low affinity systems with weak binding to greater than 10^{12} litre mol^{-1} for high affinity systems (5,6). High affinity systems can be used to detect antigens at concentrations as low as pmol/l (7).

There are many different sorts of immunoassay designs, with some common features that can be used for classification. Assays measure analyte bound in an antibody-antigen complex, and must therefore be able

to differentiate between the bound and unbound analyte. One of the ways to classify assays is by the method of differentiation used: in homogeneous assays, there is a detectable change in a reagent when the antibody antigen complex is formed (8, 9), and in the more common heterogeneous assays (10), the bound and unbound reagent are separated before quantitation. A simple way to effect the separation is to attach either the antigen or antibody to a solid phase, so that unbound reagent can be washed away.

Assays can also be classified by the different methods used to detect the reagents. Radioactive (11, 12), enzyme (13, 14, 15), particulate (16), and fluorescent (17) labels can be detected at the low concentrations and small volumes required in a sensitive and convenient assay. The labels can be attached directly to the antibody or antigen being measured, or can be attached to secondary reagents.

Enzyme-linked immunosorbent assays (ELISAs, 13) are a common form of immunoassay that use an enzyme label to determine antibody concentration. The antibody-antigen interaction takes place at a solid-liquid interface with one of the reagents attached to the solid substrate; unbound reagent left in solution can be washed away. One of the simplest formats of ELISAs is shown in Fig. 1. The assay shown has an enzyme linked to a secondary antibody; this antibody binds to the primary antibody being measured (the primary antibody is a target of the secondary antibody).

Commonly used enzyme substrates have coloured products that can be detected spectrophotometrically. Under appropriate conditions, the intensity of the colour in the developed assay is proportional to the amount of enzyme present, which is, in turn, related to the amount of antibody being measured. Results from an assay such as the one described

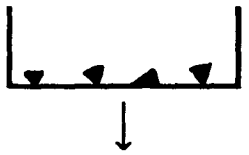

The antigen is immobilized on a solid support. Commercially available assay plates contain different wells that are used as separate incubation chambers.

An antibody solution is added to the antigen-coated substrate. Antibodies towards the antigen on the substrate will reach an equilibrium with a portion of the antibody on the plate and a portion in solution. Different concentrations of antibodies can be added to the different wells.

The unbound antibody can be washed away. The amount of antibody left on the substrate will depend on the amount of immobilized antigen, the antigen-antibody affinity and the amount of antibody in solution.

A second, enzyme-labelled antibody is incubated with the assay plates. The secondary antibody will bind generally to antibodies from a particular species.

Unbound enzyme-labelled antibody is washed away. If there is an excess of the secondary antibody, then the amount bound will not depend on the solution concentration of enzyme-labelled antibody, but will, instead, reflect the amount of the primary antibody bound.

The enzyme substrate is added in the final assay step to determine the amount of antibody bound. Enzyme that is associated with the surface will catalyze conversion of the substrate to a coloured or otherwise readily detectable reaction product.

Figure 1: An indirect ELISA for detecting antibodies.

in Fig. 1 are usually presented as absorbance against the initial solution antibody concentration applied to the assay plate. Antibody concentration in an unknown sample can be determined using a suitable standard curve.

Antigen concentration can be determined using a displacement assay similar to the assay described above (Fig. 2). A known concentration of antibody is incubated with a sample containing an unknown concentration of antigen prior to being added to the assay plate. If there is free antigen present in the sample, it will compete with the antigen adsorbed to the plate for binding sites on the antibody. More antigen in solution will result in less antibody being bound to the plate, and in less intense colour after the substrate is added.

1.2 Development and applications of immunoassays: some historical notes

Applications of early immunoassays were limited due to their lack of sensitivity. The antigen-antibody binding could be followed by appearance of visible aggregates formed when divalent antibodies interacted with multivalent antigens (18), but this required large amounts of antibody and antigen (19). Red blood cells were attached to the antibody to make the aggregates more visible (and to decrease the amount of antibody required to form a visible aggregate (20)), but this gave unreliable results (21). Assays measuring formation of visible precipitates (turbidimetric assays) are still used to measure serum proteins, where larger volumes of relatively concentrated samples are available (22).

Immunoassays developed during the 1950s greatly increased the range of antigen concentration that could be measured. Latex agglutination assays were first described in 1954 by Singer and Plotz (23) as a method

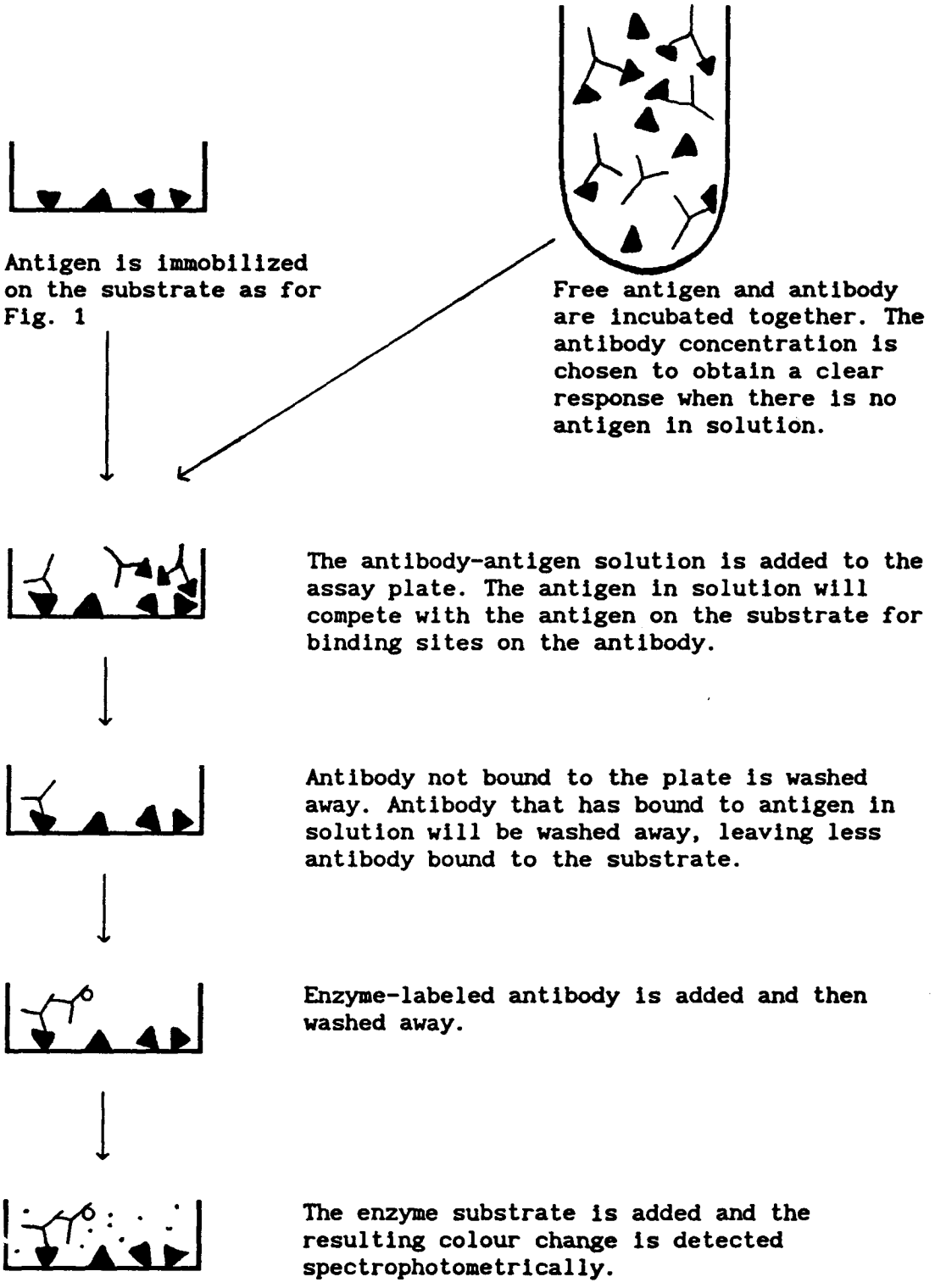

Figure 2: A competitive ELISA for detecting antigen

for diagnosing rheumatoid arthritis. Latex particles (0.77 μm diameter) were coated with antibody and mixed with serum from patients. If the patients had rheumatoid arthritis, antigens present in their serum caused the particles to aggregate. Latex agglutination assays were more consistent and reliable than the assays involving red blood cells, and are still widely used. One of the common applications is to test for human chorionic gonadotrophin as a means for diagnosing pregnancy (24).

Radioimmunoassays were developed in 1959 by Berson and Yalow as a quantitative measurement for insulin in human plasma (12). Insulin labelled with ^{131}I was incubated with antibody, after which bound and free insulin were separated electrophoretically and quantitated using the iodine label. Insulin in human plasma was determined by addition of a plasma sample to the labelled insulin; insulin in the plasma competed for antigen binding sites on a limited amount of antibody, and caused a decrease in the amount of bound radiolabelled insulin measured.

Radioimmunoassays are sensitive (insulin can be detected at the normal plasma concentration of about 0.1 nmol/l), specific (due to the specific nature of the antigen-antibody interaction) and conceptually simple. The method is also widely applicable, since it can be used to measure any molecule against which an antibody can be raised. Radioimmunoassays have been used to measure hormones (25, 26), drugs and drug metabolites (27,28), serum proteins (29) and viruses (30, 31), and were at one time a commonly used clinical assay (32). The popularity of radioimmunoassays has declined due to problems associated with radioisotopes.

Enzymes linked to antibodies gave a sensitive detection method that did not require the use of radioisotopes and expensive counting equipment (13, 32). Enzyme linked antibodies have been used for several

different assays (15, 33); one of the most common of these is the ELISA that was developed and named by Engvall and Perlmann in 1971 (13). Several factors have contributed to the popularity of ELISAs: reagents are stable, non-hazardous and readily available, commercial assay plates used as the substrate typically have 96 wells and can be used for processing multiple samples, and the assay results after the final step in the procedure (see Fig. 1) can be determined using a spectrophotometer that will read all the wells in an assay plate simultaneously.

Clinical uses of ELISAs include detection of viruses (33-35), bacteria (36), antibodies (37, 38) and plasma protein levels. The assays are also popular in research laboratories: the Medline computer data base of biological journals lists more than 13 000 papers that have described developments or applications of ELISAs.

Immunoassays today are used as a sensitive and specific means to detect antibodies and any molecule that can be used to raise an antibody. Since there is a wide range of molecules that can be used for raising antibodies (39), there is an equally wide range of immunoassay applications: assays have been used to detect drugs and drug metabolites (40), antibiotics (41), food additives (42) and toxins (43), as well as metabolites, infectious agents and antibodies measured for clinical diagnoses.

1.3 Immunogens, epitopes, haptens and antigens

1.3a Immunogens

Immunogens are agents that will induce an immunological response *in vivo* (44). Whether or not a chemical structure will be immunogenic is determined by the mechanism of the response (section **1.5c**): immunogens

must have a binding site for which an antibody is available and must have a second region to promote the cellular interactions that comprise part of the immune response. Immunogens have several features in common: they are perceived as foreign to the individual producing the response, are chemically complex, and have a high molecular weight (45).

Healthy individuals do not respond immunologically to their own tissues. This is because the cells that would produce such a response are removed or inactivated early in the individual's life (46).

The size requirements of immunogens derive from the need for an antibody binding site and for a second region to promote cellular interaction (47). Compounds with a molecular weight of less than 3 000 g/mol are generally not immunogenic (48).

Immunogenic compounds must also be chemically complex. High molecular weight homopolymers of amino acids will not be immunogenic unless they are chemically modified so that they are no longer a regularly repeating unit.

1.3b Epitopes

Although molecules inducing an immunological response are relatively large, an antibody only binds to a small region of the immunogen called the epitope. Epitopes have been shown to have a size of approximately 7x12x35 Å (49). One immunogen can have several different epitopes.

1.3c Haptens (and carriers)

Molecules that do not have a region that promotes the cellular interaction necessary for the immune response are not immunogenic by themselves but can be conjugated to carrier molecules to produce a complex that will be immunogenic. An immunological response induced

against the conjugated complex can result in antibodies that will bind to the first molecule in the absence of the carrier. Non-immunogenic molecules treated this way to raise antibodies are called haptens.

Regions identified as possible promoters of the cellular interaction in mice are peptides with a molecular weight of 1000 to 2000 g/mol (50). A synthetic peptide with the appropriate sequence could be used by itself as a carrier, but might not be effective in the strain and species of animal used (51). Larger proteins are generally used as carriers to ensure a good response.

1.3d Antigens

An antigen is the material to which an antibody binds. Antigens can be whole cells, large molecules or haptens, and can contain one or more epitopes; antigens with several epitopes can interact with several different antibodies. Since the term "antigen" refers specifically to the reagent that interacts with an antibody, it is usually used in discussions of antibody binding.

1.3e Conjugating haptens to carrier molecules

The two most commonly used protein carriers are keyhole limpet haemocyanin (KLH) and bovine serum albumin (BSA) (52). Some of the residues of the twenty different amino acids commonly found in proteins have functional groups that can be conjugated to haptens. Useful groups include amino groups (on lysine residues and the amino terminus), carboxyl groups (on glutamic and aspartic acid residues and the carboxyl terminus), sulfhydryl groups (on cysteine residues) and phenolic hydroxyls (on tyrosine residues).

The conjugation method used depends on the groups available on the

hapten. The hapten functional group used should be chosen so that epitopes of interest remain unmodified.

Water soluble carbodiimides can be used to couple carboxyl or amino groups on the hapten directly to the carrier, forming a peptide bond ((53), section **2.10a**). Various small bifunctional cross linkers can also be used to conjugate different pairs of the groups listed above (54).

1.4 Antibodies

1.4a Different classes of antibodies and their functions

Antibodies are proteins found in the blood and in various secretions. They are produced in response to immunogens and will bind specifically to different epitopes on the immunogen surface. By binding to the foreign particles or molecules, antibodies can perform a variety of functions: they can, among other things, neutralize toxins, agglutinate microorganisms, precipitate soluble antigens, neutralize viruses and make foreign cells targets for killer cells produced by the immune system. In humans, there are five different classes of antibodies, which are also known as immunoglobulins (Fig. 3). The different classes have a similarly shaped subunit, a Y-shaped tetrameric protein with two identical heavy polypeptide chains and two identical lighter chains (Fig. 3). The subunits are symmetric, with identical binding sites on each arm of the Y.

Immunoglobulin G (IgG) is found in the blood, where it constitutes about 15% of the total serum protein (55), and in milk. It can also cross the placental barrier to confer immunity on the fetus. Since IgG is divalent, it can interact with multivalent antigens to form a precipitate, which is engulfed and removed by phagocytic cells in the blood. The IgG molecule can also bind to foreign cells with the Fab

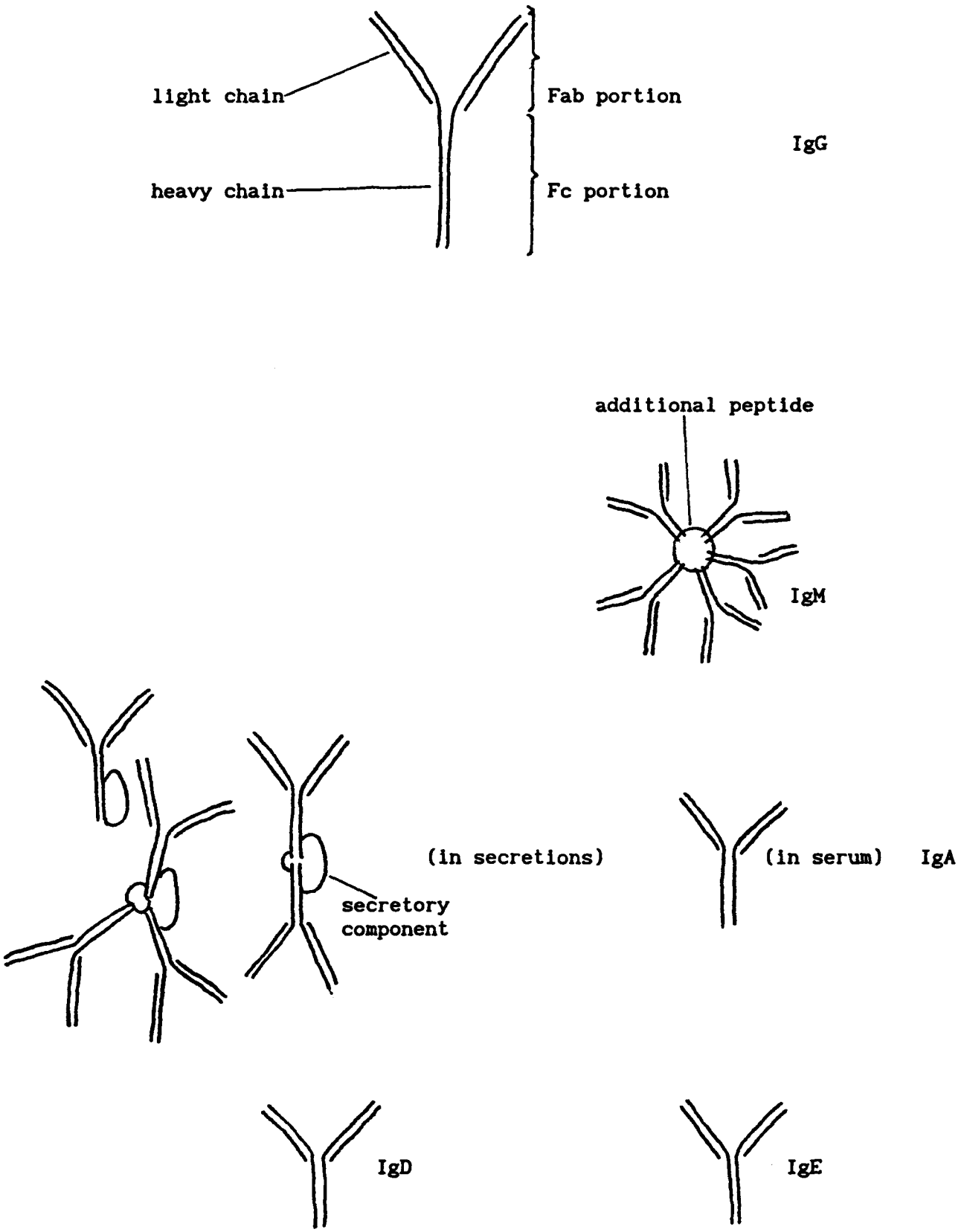

Figure 3: The different classes of immunoglobulins

portion (Fig. 3), and then with the Fc portion (Fig. 3) to natural killer cells found in the blood; the killer cells then release substances that destroy the foreign cell. Immunoglobulin G bound to foreign cells can also activate the complement system resulting in cell lysis, and can cause immobilization of motile microorganisms by clumping flagella or cilia. Viruses can be inactivated by IgG bound to the region required for attachment to the target cell. Toxins can also be neutralized by bound IgG.

Immunoglobulin G is produced after the second and subsequent exposures to an immunogen. Elevated levels of IgG indicate presence of an antigen, and many clinical assays test for an increase in serum concentrations of a particular specificity of IgG in order to make a diagnosis (56, 57). Assays testing for the presence of antigen commonly use IgG because it can be isolated readily from the serum of immunized animals.

There are subclasses of IgG with different conserved amino acid sequences on the heavy polypeptide chain. Each subclass can also have different classes of light chains (58).

Immunoglobulin M (IgM) is produced after the first exposure to an antigen. Elevated IgM levels can indicate recent infection or ongoing exposure to an antigen that does not cause production of IgG (59, 60). Immunoglobulin M can agglutinate antigens and can activate the complement pathway resulting in lysis of foreign cells.

Immunoglobulin A is present in serum, where it may have several poorly understood functions, and in secretions such as tears and mucus, where it keeps organisms from attaching to and infecting the epithelial surface (61).

Immunoglobulin D is present on the surface of cells called B

lymphocytes, and may be involved in cellular development (62).

Immunoglobulin E is present on the surface of some cells circulating in the blood, and in low concentrations in the serum. Allergic reactions are mediated by IgE.

1.4b Structure of Immunoglobulin G

Immunoglobulin G is a Y shaped glycoprotein (Fig. 4) with (when produced *in vivo*) two identical light polypeptide chains that are combined with two identical heavy chains to form a tetramer having a total molecular weight of about 160 000 g/mol. The light and heavy chains are held together by a combination of disulfide and non-covalent bonds, in an arrangement shown in Fig. 5. Regions of the polypeptide chains with conserved amino acid sequences form globular domains (Figs. 4 and 5) and give IgG its characteristic structure. Proline residues in the hinge region disrupt the folding of the polypeptide chain, giving the IgG molecule flexibility and permitting the Fab region (the arms of the Y) to open and close. The amino terminal of the light and heavy chains (at the ends of the arms) contains a variable region with an amino acid sequence that is not as strongly conserved as the constant domains. Hypervariable regions within this amino terminal domain combine to form the antigen binding site, conferring the antibody specificity.

The folding of the polypeptide chains and the overall molecular shape of IgG (Fig. 4) have been determined by X-ray crystallography (63, 64).

1.4c Clonal selection and the mechanism of antibody production

Antibodies are produced by the combined actions of several different sorts of cells, following a complex procedure which is briefly

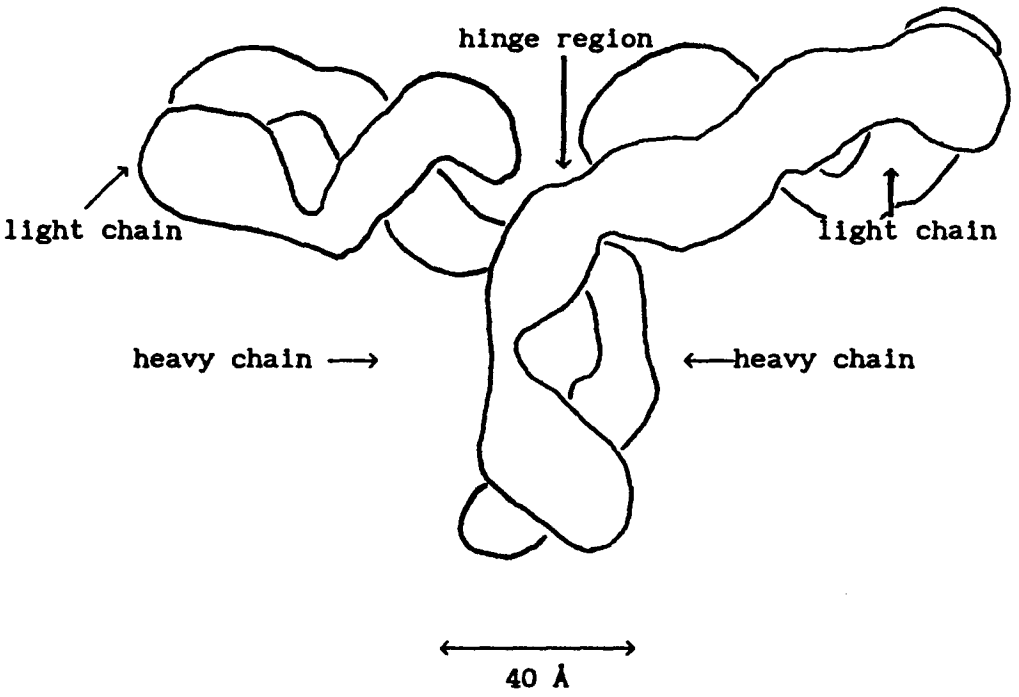

Figure 4: Shape of the IgG molecule (63)

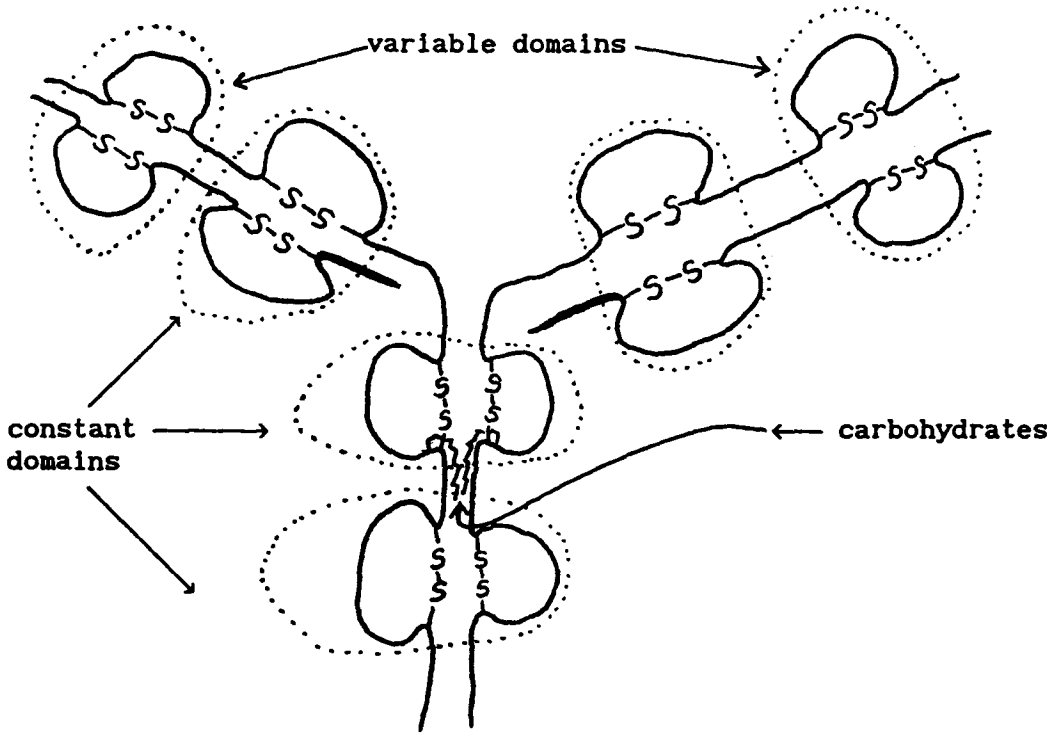

Figure 5: Structure of the IgG molecule

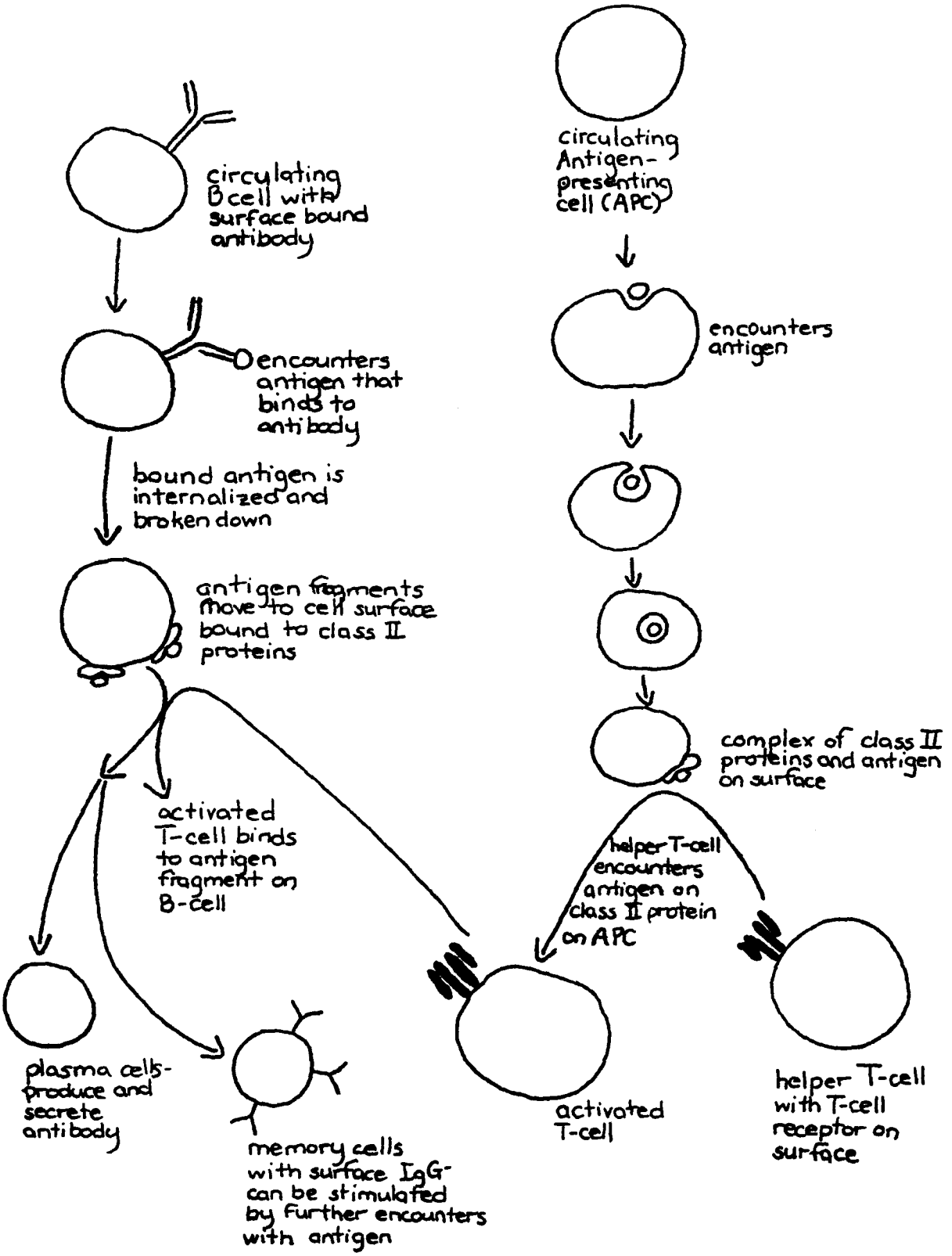

Figure 6: Antibody production *in vivo*

summarized here and in Fig. 6. Two different sorts of cells, helper T lymphocytes and B lymphocytes, proliferate after stimulation by an appropriate antigen and then bind to each other, with subsequent differentiation of the B cells into antibody producing cells. The B cells have modified antibodies on the cell surface, with the same antigen binding specificity as the antibody that will be produced by the differentiated cells. Receptors on the T cells will also recognize and bind to a specific antigen. B cells with different surface receptors and the potential to make different antibodies are present in the spleen and other secondary lymphoid organs before contact with an immunogen, but only cells having a receptor to which an antigen binds are stimulated to proliferate and produce antibody. A large repertoire of different antigen binding sites is created by rearrangements of the DNA that codes for the antibodies. Variable regions of the DNA are combined randomly to produce the mature DNA coding for the light or heavy chains of the antibody. Light and heavy chains can also combine randomly; in mice, there are about 10^7 different potential antigen binding sites that can be generated this way (65). After binding to the receptors on the B cells, the antigen is degraded by the cell and antigen fragments are presented on the cell surface bound to receptors called class II proteins (these are glycoprotein dimers encoded by the genes of the major histocompatibility complex and involved in interactions of some T cells).

Helper T cells are stimulated to proliferate by antigen fragments bound to class II proteins on the surface of a third group of cells called antigen presenting cells, which process antigen non-specifically. Receptors on the T cells recognize specific antigen-class II protein complexes, with the additional requirement that the antigen fragment

must contain one of a group of conserved amino acid sequences. The stimulated T cells will also bind to the antigen-class II protein complex on the surface of the B cells. Contact between the B cells and T cells causes the B cells to proliferate and differentiate into plasma cells and memory cells.

Plasma cells produce IgM, and cause a short lived primary response to an antigen starting about seven to ten days after immunization. If the antigen is cleared out of the body by the IgM, the plasma cells die, leaving the memory B cells and helper T cells. Second and subsequent exposures to an antigen result in memory B cells interacting with the T cells to produce more plasma cells. Plasma cells involved in the secondary response produce predominantly IgG with a high affinity for the antigen. The change from IgM to IgG is effected by a rearrangement of the DNA that switches the constant region of the heavy chain that determines the subclass, but leaves intact the variable region that determines the specificity.

Assays for IgM are used to detect the primary response against infection or response to antigens that do not cause class switching from IgM to IgG (59, 60), and assays for IgG are used to detect the secondary response (56, 57).

1.4d Monoclonal antibody production

Antibodies isolated from the serum of immunized animals have a mixture of different antigen-binding specificities. This can present problems in some immunoassays, since the antibody preparation used will contain an unknown proportion of antibody binding to the antigen being studied, and antibodies that do bind to the antigen in question will bind to different epitopes with a range of different affinities.

A homogeneous antibody preparation can be obtained by isolating

antibodies from one B cell, since each cell is only capable of producing antibody with one antigen-binding specificity. Although B cells will not grow in culture by themselves, the terminally differentiated plasma cells that produce antibodies can be fused with myeloma cells that grow and divide in culture to produce a hybridoma cell that will proliferate in culture and will continue to produce antibodies.

Immunoglobulin G producing plasma cells from the secondary response can be obtained from the spleen of an immunized animal. After an initial injection of immunogen, different epitopes on the antigen bind to B cells with appropriate receptors, stimulating the B cells to differentiate into plasma cells and memory cells. After the immunogen is cleared from the system and the IgM producing plasma cells involved in the primary response die off, the animal can be given another injection of immunogen. The second injection causes differentiation of the memory cells into IgG producing plasma cells which can then be fused with the immortal myeloma cells.

Bone marrow tumours called myelomas can be induced in the inbred strain of BALB/c mice by mineral oil injected into the peritoneum. Cell lines derived from BALB/c myelomas and adapted for continuous culture are available commercially, and have become the most widely used myeloma cells for monoclonal antibody production. Most of the BALB/c myeloma cell lines, including the FOX-NY cell line that was used in these experiments, produce light chains that are not secreted by themselves but that are incorporated into the antibody produced by the spleen cell-myeloma hybrid (66). If the light chains originating from the spleen cell and the myeloma cell are incorporated randomly into the antibody, 25 % of the molecules will have two light chains from the myeloma and no antigen binding site, 50 % will have one binding site, and 25 % will

have two binding sites. A myeloma cell line that does not produce light chains has been isolated (67), but is not available from the American Type Culture Collection (68), which is the non-profit agency used as the most common source of cell lines in North America.

Commonly used cell lines have a mutation in the gene coding for one of the enzymes involved in a salvage pathway for production of purine bases for nucleic acids. Addition of toxic compounds such as aminopterin that block the *de novo* synthesis pathway will kill the cells, since they will not be able to use the salvage pathway for conversion of other nucleotide bases to the required product. Unfused myeloma cells remaining after the fusion of the myeloma cells with the spleen cells can be rapidly killed by addition of aminopterin to cell culture medium.

Polyethylene glycol (PEG) is the most common cell fusing agent used in monoclonal antibody production (69). Addition of sufficiently high concentrations of PEG will result in fusion of the plasma cell membranes of adjacent cells and formation of hybrid cells with two or more nuclei. The first division of the hybrids gives cells with one nucleus each. The cells initially have a large number of extra chromosomes, some of which are lost during the early cell divisions before a stable cell line is obtained.

Unfused spleen cells will not grow in culture and unfused myeloma cells can be killed off by addition of aminopterin, leaving only the spleen cell-myeloma hybrids. The cell culture medium is screened for secreted antibodies, and cells producing antibody are kept and allowed to proliferate. Positive cell lines are subcloned to ensure that the cell line originates from only one cell and thus produces only one antibody. To subclone, the cells are diluted and added to a 96 well plate at a calculated concentration of about one cell per well. Wells

with growing cells are inspected visually to check that the cells grow from one colony. Cells are sometimes subcloned two or three times to ensure stability and purity of the cell line.

A homogeneous preparation of antibody with a unique specificity can be isolated from the hybridoma supernatant. The hybridomas can also be frozen and stored and then thawed later to provide a constant source of antibody.

1.5 Antigen-antibody interactions: chemistry and thermodynamics

1.5a Binding of antigen to antibody

The antigen binding sites are located at the ends of the arms of the IgG molecules, in shallow pockets formed by the variable regions of the light and heavy chains. Three polypeptide loops from each of the light and heavy chains protrude into the pockets. The loops correspond to the hypervariable regions of DNA and can determine the antigen binding specificity by providing an appropriately shaped binding site and allowing for a variety of non-covalent interactions (71).

Amino acid side chains can be polar, non-polar, aromatic, and at physiological pH, can also be positively or negatively charged. The amino acid side chains and peptide bonds of the antibody can bind to the antigen through electrostatic interactions, hydrogen bonds, Lifshitz-van der Waals interactions and hydrophobic interactions. Since the interactions are relatively short range and are separately weak, there must be an area of close contact between the antibody and antigen for strong antibody-antigen interactions to occur. Crystallographic studies with cocrystals of antibody bound to antigen have shown that the area of contact can be as large as 750 $Å^2$ and that binding can occur without deformation of the antibody (70).

1.5b Equilibrium constants and affinities for monovalent antibodies and antigens interacting in solution

The binding of one epitope to one antigen-binding site on an antibody is reversible (71) under physiological conditions, due to the nature of the interactions involved. Antigen (Ag) and antibody (Ab) in solution can reach an equilibrium with the antigen-antibody complex, where the rate of formation of the complex is equal to the spontaneous rate of dissociation. At this point, the equilibrium constant can be defined from the concentrations of reactants. For the simplest case, where the antigen and antibody are monovalent, the binding reaction will be:

$$Ag + Ab \rightleftharpoons Ag\text{-}Ab$$

The equilibrium constant K will then be (72):

$$K = \frac{[Ag\text{-}Ab]}{[Ag][Ab]} = \frac{ka}{kd} \qquad [2]$$

where Ag-Ab is the antigen-antibody complex, square brackets denote equilibrium concentration of the reagents and ka and kd are the association and dissociation rate constants for the reaction.

The antibody affinity is defined as the negative of the standard free energy change of the binding reaction, and can be calculated from the equilibrium constant K:

$$A = -\Delta G^{\circ} = RT\ln K \qquad [3]$$

where R is the gas constant and T the absolute temperature. The equilibrium constant is usually used by itself to describe the strength of the antibody-antigen reaction, with antigen-antibody systems being referred to generally as high or low affinity, depending on the value of K.

1.5c Equilibrium constant for a divalent antibody and monovalent antigen in solution

Intact IgG produced *in vitro* is divalent, meaning that a sequence of two antigen binding reactions can occur:

$$Ag + Ab \rightleftharpoons Ag\text{-}Ab$$

$$Ag\text{-}Ab + Ag \rightleftharpoons Ag_2\text{-}Ab$$

If the antigen and antibody are both in solution, the equilibrium constants are similar, although there may be some cooperativity (73). If the constants are assumed to be the same, then the binding can be described as a special case of the general multiple equilibria problem. For a macromolecule with n equivalent sites (i.e., all sites have the same intrinsic association constant, K, for Ag) which are independent (no cooperativity) the average number of sites filled, ν, at an equilibrium concentration [Ag] of antigen, is given by (74):

$$\nu = \frac{n\ K\ [Ag]}{1 + K\ [Ag]} \qquad [4]$$

where n is the total number of sites per macromolecule (74). For a divalent Ab, n = 2. The treatment which provides [4] allows the distribution of ligand occupation to be calculated from:

$$c_i = \frac{c_o\ n!\ ([Ag]\ K)^i}{(n-i)!\ i!} \qquad [5]$$

where c_i is the concentration of the macromolecule with i of the n sites filled and the other symbols are as defined above.

1.5d Some comments on the antibody preparation used

The myeloma cells that were used for antibody production produced their own light chains, which would not have provided an antigen binding site for the antigen used. If the light chains were produced in equal amounts and incorporated randomly into the antibody molecules, then there would be a distribution of antibody molecules with zero, one and two binding sites, in a 1:2:1 ratio.

1.5e Antibody binding to antigen on a solid surface: kinetics and equilibrium constants

If the antigen is adsorbed to a solid phase, the antibody-antigen interaction will be more complex than the reactions in solution. The antibody must be transported to the interface from the bulk phase. There it may also diffuse in two dimensions before associating with the antigen, and it must be transported away from the interface after dissociation. In experiments in which the antibody solution is unstirred, the solution will become depleted of antibody near the interface, after which the rate of reaction will be limited by the rate of diffusion of antibody from the bulk of the sample (75). If the solution is well stirred, the rate of the antibody binding to the surface will be limited by the intrinsic rate of the reaction (75). Reactions occurring on small spheres also tend to remain reaction-rate limited, due to the geometry of the system (75).

If the surface concentration of antigen is sufficiently high, one divalent antibody molecule can bind to two antigen epitopes. The reaction of the second antigen binding site on the antibody molecule will be fast. Dissociation of the divalent antibody from the surface will be slow, since both binding sites would have to dissociate from the

antigen at once.

Other effects are also active in decreasing the rate of dissociation of the antibody from the surface-bound antigen, since monovalent portions of antibody molecules will also show a decreased rate of dissociation relative to free solution reactions (76). The same non-specific forces responsible for adsorption of any protein to a surface will affect the antibody binding. Slow dissociation may also be due to attractive forces between the antibodies or antibody fragments, which have been implied by some experiments: antibodies immobilized on a phospholipid layer have been shown to form a two-dimensional crystal lattice (77) and high affinity antibodies bound to surface-immobilized antigen have been shown to increase the apparent affinity of low affinity antibodies in an experiment measuring binding of a mixture of low and high affinity antibodies (78). Lateral attractive forces are not observed for all systems with IgG binding to a surface. For instance, IgG binding to bovine serum albumin coated latex has a large excluded area relative to the molecular cross-sectional area (79).

The maximum amount of antibody bound on the surface can also be limited by steric constraints if the antigen is smaller than the antibody and is packed sufficiently closely on the surface. The geometric constraints lead to what has been called the large ligand effect (80). Obviously, if the average area of surface associated with each molecule of antigen is much smaller than the area of the antibody when bound to surface-bound antigen, the molecular surface concentration (molecules per unit area) of Ab will not coincide with one half the Ag surface concentration, which would be the theoretical limit in the absence of geometric effects.

The dissociation rate for antibodies bound to surface immobilized

antigen is decreased to such an the extent that the binding has been described as irreversible (81, 82). However, the off rate is not zero and the apparent irreversibility just depends on the time scale considered.

A decrease in the dissociation rate constant for antibodies bound to individual epitopes will cause an increase in the measured apparent equilibrium constant. The above discussion does not, however, imply an increase in the magnitude of the free energy change associated with epitope interacting with the antigen binding site on the antibody.

Since the system reaches equilibrium, a single apparent equilibrium constant can usually be measured. The apparent or macroscopic constant represents the overall reaction of the antibody binding to the surface and is a function of the microscopic constants for interactions such as those described above (including the antibody-antigen binding). The apparent equilibrium constant cannot be interpreted in terms of the individual reaction steps without kinetic analyses of the reactions involved. Some analyses have been formulated to account for different aspects of the problem (83-85) and to interpret the apparent constant in terms of the free energy change associated with the antibody-antigen interaction, but these will not be used here. The apparent equilibrium constants will be calculated for the antibody interacting with the surface bound antigen and will be discussed with respect to the various effects described above.

The apparent equilibrium constant for monovalent antibody fragments binding to antigen immobilized on the surface at a low enough density to avoid geometric effects and assuming no non-specific binding of antibody occurs will be given by an equation of the same form as [4] (86):

$$[\text{Ag-Ab}] = \frac{n\,K\,[\text{Ab}]}{1 + K\,[\text{Ab}]} \qquad [6]$$

where [Ag-Ab] = surface concentration of bound Ab (mass or number of moles per unit area)

n = maximum surface concentration of bound Ab possible

K = apparent association constant

[Ab] = Ab concentration in equilibrium with surface

For sufficiently well separated molecules of surface-bound antigen, it would be expected that n, determined from the saturation value of the Ab binding isotherm, should equal the surface concentration of Ag. This is generally not observed, however, because as the antigen density decreases, more of the underlying substrate becomes available to the antibody and non-specific adsorption of the protein results. This non-specific adsorption can overwhelm the specific adsorption if the substrate is a good protein adsorbent (e.g., hydrophobic solid polymer). The non-specific adsorption can be minimized by adsorbing an uninvolved "blocking" protein to the substrate before exposure to the antibody solution. Protein adsorption is sufficiently slow to reverse (87) that non-specific binding of antibody to the blocked areas can be greatly reduced.

For the antibody preparation used in this work, with a distribution of divalent, monovalent, and non-binding antibodies, for a surface antigen concentration low enough that an antibody cannot form a bridge between adjacent binding sites (a condition that will be referred to as dilute surface antigen concentration) the equilibrium will obey:

$$[\text{Ag-Ab}] = \frac{3\,n\,K\,[\text{Ab}]}{4 + 3\,K\,[\text{Ab}]} \qquad [7]$$

since only 3/4 of the antibodies can bind and monovalent and divalent can be assumed to behave similarly towards isolated Ags on the surface.

At higher surface concentrations of antigen, the equilibrium surface concentration of antibody will also tend to increase at a given equilibrium concentration, since n increases in [7]. Formation of bridges between adjacent epitopes and attractive lateral forces between the bound antibody molecules will cause an increase in the calculated affinity since they will both act to decrease the desorption of the antibody. Increased surface concentrations of antigen have been shown to cause variations of several orders of magnitude in the measured apparent equilibrium constant (83).

1.5f Free antigen in solution inhibiting binding of antibody to the surface-bound antigen: another interaction involved in the equilibrium

The binding of antibody to surface-immobilized antigen can be inhibited by free antigen in solution as shown in Fig. 2. Free antibody and antigen in solution will reach an equilibrium with concentrations of free and bound reagents that are a function of the initial concentrations and of the equilibrium constant for the reaction. If the solution of antibody and antigen is then applied to a surface bearing bound antigen, a new equilibrium will be reached: some of the free antibody will bind to the surface and, since the antibody-antigen reaction in solution is reversible, some antibody will dissociate from the antibody-antigen complex in solution. For a fixed surface concentration of immobilized antigen and a fixed initial antibody concentration, the amount of antibody bound on the surface will decrease with increasing initial concentrations of free antigen.

For a system with a known apparent equilibrium constant for the antibody binding to antigen on the surface, solution inhibition measurements can be used to calculate an equilibrium constant for the antibody-antigen interaction in solution, following the procedure outlined in Appendix 1 (D. E. Brooks, unpublished).

1.5g Experimental determination of equilibrium constants: information required and methods of calculation

The apparent equilibrium constant for antibody binding to antigen immobilized on a surface can be calculated from equation [6], knowing the surface concentration of antibody as a function of antibody concentration in solution. The concentrations of bound and free antibody can be measured accurately using a radiolabelled IgG. For a fixed Ag surface density, the surface concentration of bound antibody can be plotted as a function of the equilibrium solution concentration to give a binding isotherm as shown in Fig. 7.

The surface concentration of antibody binding sites, n, can be calculated from the maximum amount bound at high solution concentrations of antibody. The equilibrium constant will affect the shape of the curve as shown in Fig. 7 and can be calculated from a direct non-linear least squares fit of equation [6] to the measured data. However, it is often more revealing to re-cast equation [6] into a linear form known as the Scatchard equation since the shape of the resulting plot can provide information on the binding mechanisms if the equation is not followed. It is also straightforward to obtain estimates of n and K from such a plot from linear least square fits of the data. The equation (74) is:

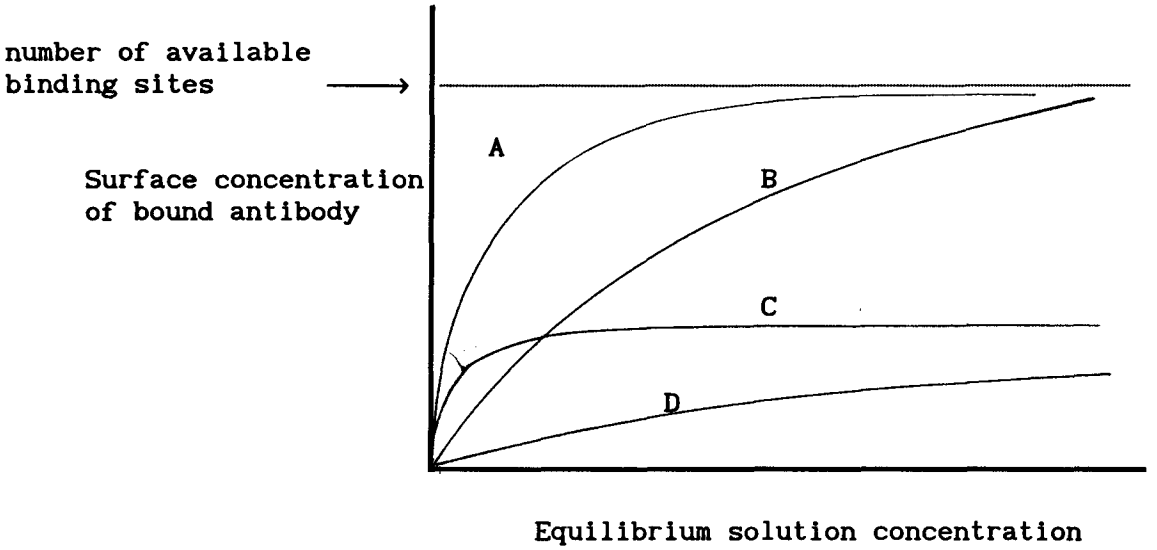

Figure 7: Adsorption isotherms. A = high affinity and large number of binding sites, B = low affinity and large number of binding sites, C = high affinity and low number of binding sites, D = low affinity and low number of binding sites.

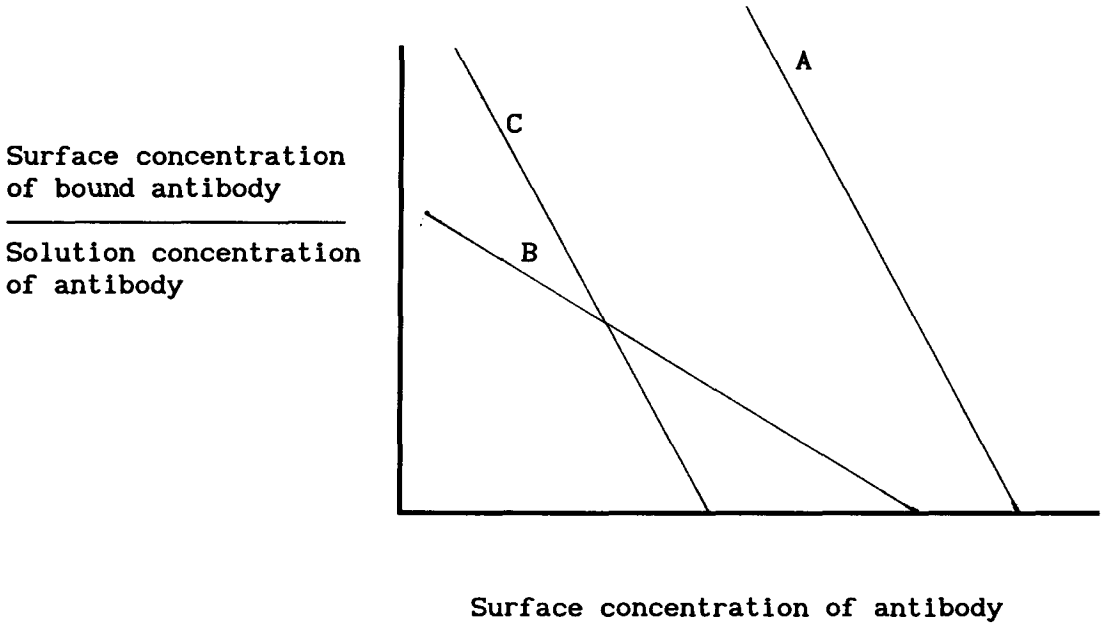

Figure 8: Scatchard plots. A = high affinity and large number of binding sites, B = low affinity and large number of binding sites, C = high affinity and low number of binding sites.

$$\frac{[Ag\text{-}Ab]}{[Ab]} = -K\,[Ag\text{-}Ab] + K\,n \qquad [8]$$

A plot of [Ag-Ab]/[Ab] vs [Ag-Ab] will be linear with slope -K and x-intercept n if [8] is obeyed; a plot is illustrated in Fig. 8. In the particular case of the antibody preparation with 1/4 of the molecules unable to bind, [Ab] would be taken to be 3/4 of the IgG protein in the experiment.

These calculations do not take into account the possibility of bridging between epitopes at higher surface antigen concentrations. The simplest treatment of this possibility would be to assume that binding of both valences on IgG would simply double the free energy difference associated with one site binding so the affinity would double and the association constant would be squared. However, the factors discussed in the earlier sections suggest this would be an unwarranted simplification.

There does not appear to be a suitable way to treat all the complications associated with the interpretation of divalent Ab binding to surfaces of the type of interest here. Instead, since it is known that equation [5] was capable of describing binding in related systems (80) in which Ab binding to mobile surface-bound antigens was studied, the approach will be to estimate values of K from experimental measurements employing a Scatchard plot and try to interpret the apparent values derived.

1.6 Measuring the antibody-antigen interaction with ELISAs

1.6a Limitations of ELISAs

Although ELISAs can in principle be used for determining the equilibrium constants as described in section **1.5g**, they are generally

used only to determine the concentration of a specific antibody or antigen in an unknown sample by comparison to standards under carefully controlled conditions (88). There is generally insufficient information for further calculations.

The solid substrate used for ELISAs is usually a polymer with unknown surface characteristics. Commercially available 96 well plates and strips of detachable wells are made from polystyrene (89), polyvinyl chloride (89) or other plastics not specified by the manufacturer (90). For a given brand of ELISA plate, there can be variation in the binding capacity in different batches or even between different wells in one plate (92).

The antigen is usually adsorbed non-specifically to the wells of the ELISA plate. The surface concentration of antigen can be increased or decreased by changing the initial concentration used for coating the plates, but is not usually measured. Protein antigens will usually saturate polystyrene plates at solution concentrations of less than 4 $\mu g\ ml^{-1}$ (93).

The absorbance measured after addition of the substrate solution in the final step of the assay is related to the amount of antibody on the surface. The absorbance can be calibrated to give a measure of the surface concentration of the antibody (94), but since there are several steps separating the binding of antibody from the production of colour in the final assay step, the relationship between the antibody concentration and the absorbance may not be simple.

The initial concentrations of antibody added to the different wells in the ELISA plate is measured, rather than the equilibrium solution

concentration after some antibody has adsorbed to the wells. This makes determination of the concentration in an unknown sample simpler, but makes interpretation of the binding more complex.

1.6b Calibration curves for ELISAs

The calibration curves for ELISAs are obtained by plotting absorbance after addition of the substrate against the initial concentration of antibody or initial solution concentration of antigen. Since the interactions involved in ELISAs are not usually modeled by equations, a choice must be made about how to obtain a line from the data points. Separate points are often connected with straight lines. Although this may cause less bias in drawing the calibration curve (95), it can cause greater error for regions in the middle of the straight line segments. Curves are also fit by eye or by splines (96), which are continuous curves formed by connecting segments of different polynomials.

The useful region of the calibration curve is one in which there is a change in the measured absorbance with a change in the analyte being measured. At high surface concentrations of antibody, the surface will be saturated and will not show a change in the absorbance; at low surface concentrations of antibody there may be insufficient change to be distinguishable from the background.

Clinically used assays are often sold as kits complete with standards.

1.6c Experimental requirements

There must be a stable bond between the substrate and the antigen, so that the antigen does not desorb during the course of the assay.

Hydrophobic surfaces are usually used to minimize desorption of protein antigens (93). Larger antigens will often adsorb effectively irreversibly to surfaces because of multiple attachment points (87, 91) but smaller molecules may not bind or may desorb slowly in the presence of molecules competing for adsorption sites (91). Small molecules can be conjugated to larger molecules that will adsorb to the surface being used, but this creates the possibility of cross reaction of the antibody preparation with the protein carrier if a monoclonal antibody is not used. Small molecules can be attached covalently to plastic plates using gluteraldehyde or other cross linking reagents (97), but this can result in irreproducibly modified surfaces (98). In most such cases the chemistry of the coupling is obscure since the polymers involved are not reactive with the cross linking agent (e.g., polystyrene); any increase in association is more likely due to stronger adsorption of cross linked protein. It is well known that protein desorption decreases with increasing molecular weight (87, 91).

Conditions used to attach the antigen must leave the wells optically clear, since the absorbance after addition of substrate is read through the bottom of the well. Since antigens can have different functional groups available for covalent attachment, it would also be useful to be able to modify the surface with different functional groups. The process used for attaching the antigen should be simple, in order to make it viable for routine use.

Coupling a functional group on the antigen to the surface will give the antigen a defined orientation, with the functional moiety towards the surface and the other portion of the antigen presented towards the solution. If the same functional group is used for coupling the antigen to the surface and to the carrier molecule used during the

immunization, then the same portion of the antigen will be available for antibody binding.

Reproducibility is another necessary feature of ELISAs. If there is a consistent source of antibody from a hybridoma cell line, reproducibility will be only limited by substrate characteristics. The substrate should be easy to prepare and modify with antigen in very large batches or else with small batch to batch variation.

The substrate should also have a high capacity for antigen, since this will increase the sensitivity of the assay. A low capacity for non-specific binding is also necessary: if the antibody binds to the surface in the absence of surface-immobilized antigen there will be a higher background reading and the assay will be less sensitive. As noted above, blocking agents are routinely used to minimize this problem.

1.6d Covalent enzyme-linked immunoassays on polystyrene substrates

Polystyrene and polystyrene derivative plates are available with surface carboxyl groups (99), aldehyde groups (100), and with irradiated surfaces that will bind to carboxyl groups in the presence of a carbodiimide (101). Coupling procedures can be used to give surfaces that are more extensively modified than those resulting from non-specific adsorption, with subsequent higher assay signals (99, 101).

1.6e Advantages of silica

Silica is a useful substrate for attachment of covalent antigens, because it can be functionalized with a large variety of groups (102, 103). The silica surface can be modified by reaction with compounds of the form $R_nSiX_{(4-n)}$, where X is a hydrolyzable group and R contains the functional group to be used for covalent attachment of the antigen. The

reaction occurs as shown in Fig. 9, and leaves the silica surface covalently modified with the organosilane used. There is a large variety of commercially available organosilanes to provide surfaces modified with different functional groups.

Monodisperse silica beads can be made in large quantities from tetraethylorthosilicate (104, 105) and can likewise be modified with a silane. Beads can be used to provide a large surface area for assays or for characterization studies. The geometrical surface area of the beads can be determined and used for calculations because the surface of the bead appears smooth at the level of electron microscopic images.

Silica is also optically clear, resistant to solvents that could be used in any modification step and autoclavable so that the substrate can be readily sterilized. Silica beads are mechanically stable and can be centrifuged without damage.

1.7 Characterizing a modified surface

1.7a Information that will describe a substrate

If a surface is modified with functional groups to be used for covalent coupling of the antigen, it is useful to know the extent of the modification. The silica can also be characterized prior to modification, to ensure that the surface is clean so the silane will be able to modify the surface evenly. Since pure silica contains no carbon, measuring carbon present on the surface will give an indication of the cleanliness of the surface.

Silica used in these experiments was modified with 3-aminopropyltriethoxy silane, to give a surface covered with amino groups that could be used for coupling to the carboxyl groups of the antigen. The atomic percentage of nitrogen and number of amino groups on

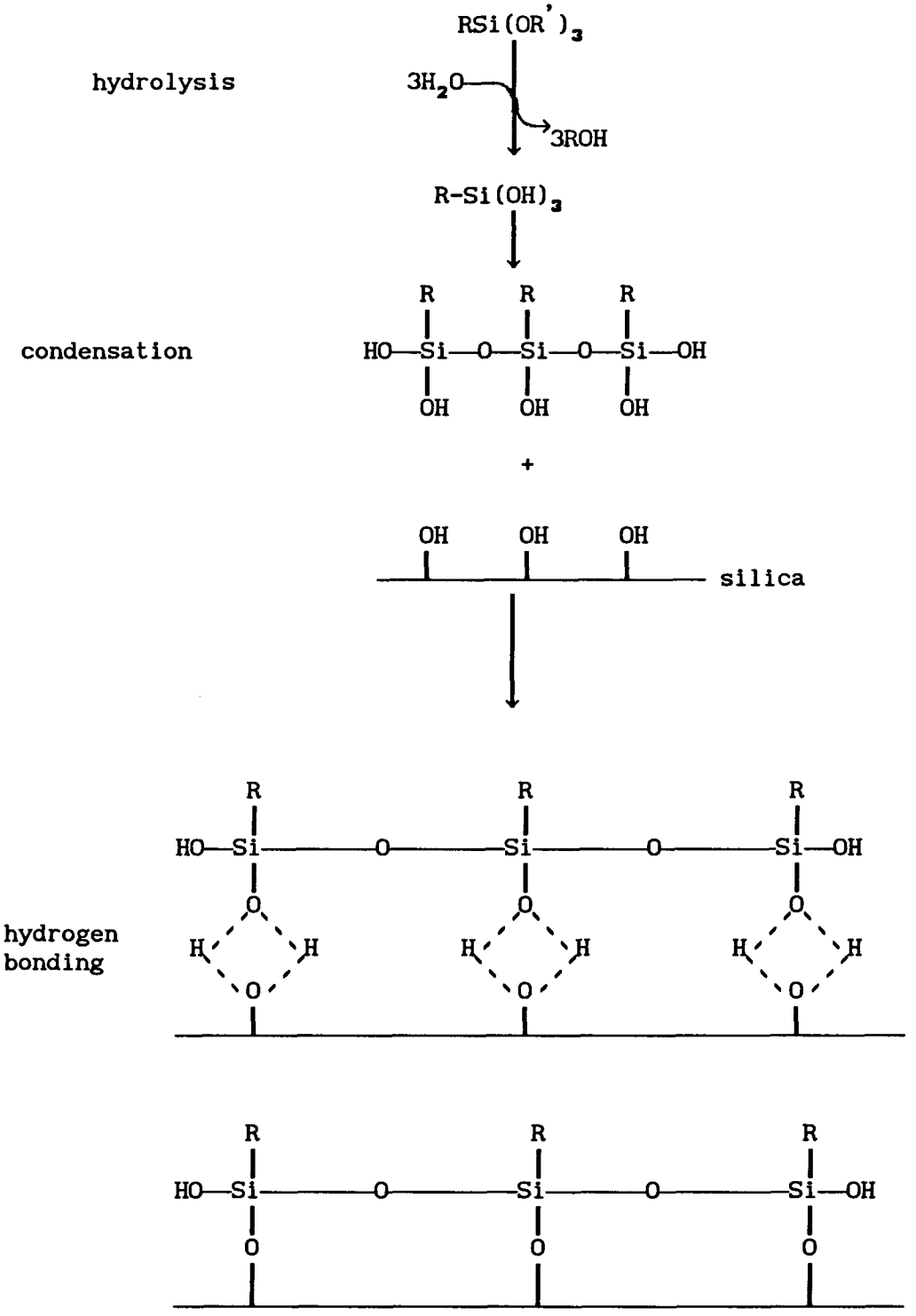

Figure 9: Deposition of silanes on silica

the surface was measured to determine the extent of the modification. The electrophoretic mobility of the beads was also measured to allow calculation of the electrokinetic charge density; unmodified beads have surface silanols which will give the beads a negative charge in water and modified beads will have a positive charge.

1.7b Ninhydrin assays

Ninhydrin reacts with primary amines on the beads to give a coloured complex that will diffuse away from the bead surface and remain in solution. The absorbance of the solution can then be measured and combined with geometric information to calculate the surface density of the amines (106).

1.7c X-ray photoelectron spectroscopy

X-ray photoelectron spectroscopy can be used for identification and semi-quantitative measurement of elements near the surface of a sample. The principle of the method is as follows (107, 108). Initially, an X-ray is directed onto the sample being studied and is absorbed by atoms in the surface region. When the X-ray photon is absorbed, its energy is transferred to a core electron in one of these atoms. Because the energy from the photon is greater than the binding energy of the electron, the electron is ejected from the atom. The kinetic energy of the photoelectron can be measured and used to calculate the binding energy from:

$$E_B = E_{hv} - E_{KE} - \Phi \qquad [9]$$

where E_B is the binding energy, E_{hv} is the X-ray energy, E_{KE} is the kinetic energy of the photoelectron and Φ is a constant for the particular instrument being used.

The XPS spectrum is presented as intensity vs. binding energy, where intensity is a measure of the number of scattered photoelectrons. The binding energy is characteristic of the orbital and element; the relative intensities of the different peaks can be used to determine the relative amounts of elements present.

The binding energy of the core electrons varies with the molecular bonding environment and oxidation state of the element. In general, the binding energy for electrons in a given element and orbital will increase with increasing oxidation state and decreased interatomic distance to the nearest neighbours (108).

The intensity of the peaks is a function of the intensity of the X-ray source, the atomic density of the element in question, the cross-section of the orbital and various instrumental factors.

Silica samples are non-conducting and will build up a charge after loss of photoelectrons due to ionisation by X-rays. To maintain a constant charge, the sample is bombarded with electrons from a low energy flood gun. Compensation is made for the change in binding energy due to the surface charge by assigning a reference peak in the XPS spectrum to a known binding energy and shifting the other peaks accordingly. Since aliphatic carbon is present on the surface of virtually all samples as a contaminant, it is often used for a reference peak (108).

Photoelectrons can be scattered inelastically by atoms. This accounts for the surface sensitivity of XPS: only photoelectrons produced in the surface region pass out of the sample. Although a fixed sample depth is often given for XPS measurements (about 100 Å for organic samples, (108)), the sensitivity decreases exponentially with increasing depth in the sample. Non-destructive depth profiling can be

done by changing the angle at which the photoelectrons are detected (Fig. 10). The maximum sampling depth will be obtained when the photoelectrons are detected normal to the surface. If the photoelectrons are detected at high angle θ away from the normal, the electrons will travel the same distance d through the sample, but will originate from atoms that are $d\cos\theta$ away from the surface.

X-ray photoelectron spectroscopy was used to determine the efficiency of cleaning procedures for the silica surfaces prior to modification with the silane by measuring the percentage of carbon in the surface region. The extent of modification with the silane was determined by measuring the percentage of nitrogen. The Fe 2p XPS signal was used to confirm the presence of antigen on the surface, since the substrate does not contain iron.

The extent of coverage of the surface can be determined by following the disappearance of the Si 2p signal originating from the substrate. If the surface is covered by a sufficiently thick overlying layer, then none of the Si 2p signal will be detected. The thickness of an even overlying layer can be obtained from the relative strengths of a characteristic signal from the substrate with and without the layer present, if the mean free path length of the photoelectrons in the layer is known (109). Information about the distribution of an overlying layer can be obtained from angularly resolved measurements (110, 111). If the layer is continuous, at sufficiently large angles away from the normal the sampling depth will be small enough (Fig. 11) that the signal from the substrate disappears. If the overlying layer forms discontinuous patches on the surface, then there will be signal from the substrate at all measurement angles.

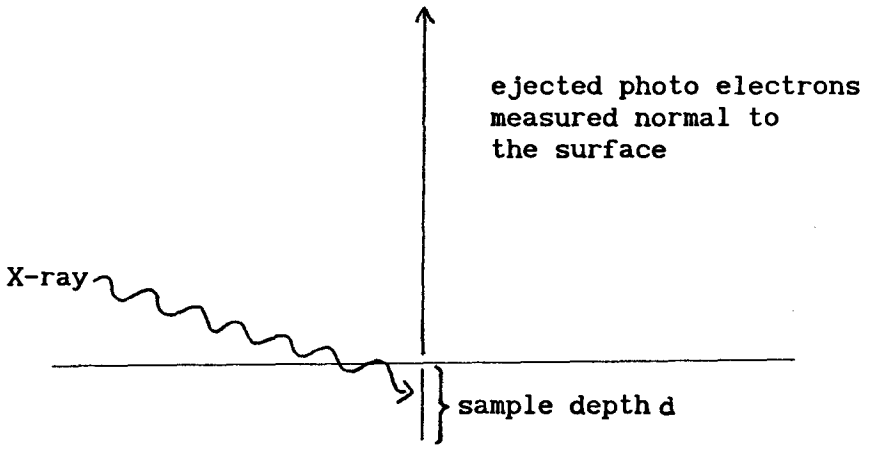

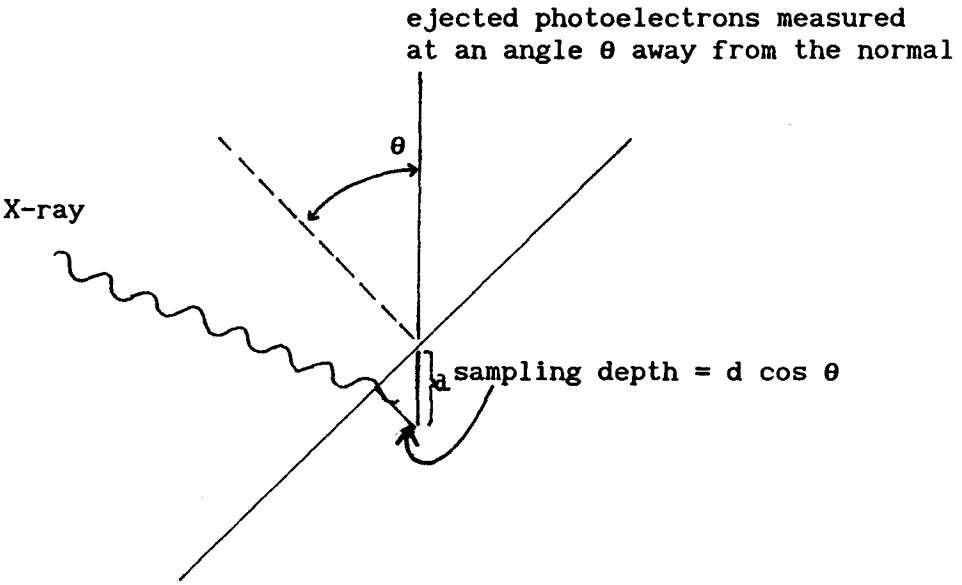

Figure 10: Depth profiles by XPS measurements

1.7d Electrophoretic mobility of beads

The mobility of particles in an electric field can be used to calculate the electrokinetic surface charge density. The electrophoretic mobility u, defined as the particle velocity per unit electric field strength, is related to σ, the surface charge density at the shear plane (the hydrodynamic boundary of the particle) by (112):

$$\sigma = \kappa \eta u \qquad [10]$$

where σ = surface charge density (esu/cm^2)

$\kappa = [8 \pi N_a e^2 I/1{,}000 \varepsilon k T]^{1/2}$ (cm^{-1}) is the Debye-Hückel parameter

N_a = Avogadro's number

e = electron charge

I = ionic strength = $1/2 \sum_i c_i z_i^2$

c_i = molar concentration of i^{th} ionic species in suspending medium

z_i = valence of i^{th} ionic species in suspending medium

k = Boltzmann constant

T = absolute temperature

ε = dielectric constant of suspending medium

η = viscosity of the suspending medium (Pa-s)

Equation [10] holds providing the particle radius, a, obeys ($\kappa a > 300$) and providing the surface potential is "small", i.e., providing:

$$(4 \pi \sigma e/\kappa \varepsilon k T) << 1 \qquad [11]$$

where $(4\pi\sigma/\kappa\varepsilon) = \zeta$, the zeta potential or potential at the plane of shear. For larger surface zeta potentials the charge density can be calculated from [12] (112), where $z = |z_i|$:

$$\sigma = \frac{(2 \varepsilon k t n_o)^{1/2}}{\pi} \sinh \frac{z e \zeta}{2 k T} \qquad [12]$$

The electrophoretic mobility can be determined experimentally for a given electric field strength and solution viscosity. The surface charge density can be calculated by comparison of the mobility to that of a well characterized particle such as a red blood cell measured in the same system.

The hydroxyl groups on the surface of the silica beads will give the beads a net negative charge in water. As the silica surface is modified and the silanol groups react, the charge will decrease. Since the beads were modified with a silane having an amine group, the surface would be expected to be positive for the silylated beads.

1.8 The silica surface

Glass and silica surfaces that have been standing in air have a surface covered with a contaminating layer of aliphatic hydrocarbons (108). If the surface is to be modified, then the reactive groups on the surface must be accessible to the reagents in solution, and the surface should be clean. Glass and silica have been cleaned with solvents, hydrofluoric acid etching, sodium hydroxide, hot nitric acid, hot ammoniacal hydrogen peroxide (113-116), and hot chromic acid (117, 118).

The extent of contamination left on the surface after the cleaning procedure can be monitored by measuring the percentage of carbon in the surface region, using a surface sensitive technique such as Auger (116) or X-ray photoelectron spectroscopy (113)(section **1.8c**). The surface will become more hydrophobic as hydrocarbon contaminants are deposited. Water droplets will spread on a clean silica surface to give water-silica contact angle of 0°, and increasing contact angles will be indicative of the hydrophobicity due to surface contamination.

1.9 Characterizing the antigen-modified substrate

1.9a Measuring the surface concentration of antigen

The surface concentration of antigen on the beads can be measured indirectly from solution depletion measurements during the modification procedure or directly from assays that are sufficiently sensitive to detect the antigen on the beads.

The antigen used for these experiments was a ferric trihydroxamate that absorbs strongly around 436 nm; the concentration of the antigen in solution was followed by absorbance measurements. The Fe^{3+} ion could be detected by XPS and used to confirm the presence of the antigen on the flat silica.

1.9b Determining whether or not the antigen is attached covalently

The presence of a covalent bond can usually only be inferred indirectly from stability of the attachment between the antigen and the substrate. If the antigen can be removed from the surface when adsorbed non-specifically but remains on after being attached to the surface under conditions expected to produce a covalent bond, this is used as evidence for formation of the covalent bond.

The clearest evidence for formation of a covalent bond between the antigen and the substrate would be detection of the bond itself by some suitable spectroscopic technique.

1.10 Measuring antibody on the surface and in solution

The amount of antibody on the surface and in solution must be determined accurately for the calculations outlined in section **1.5g**. The antibody can be labelled with ^{125}I; the protein can then be detected at low concentrations using a γ-counter.

1.11 This project

This project was the development and detailed characterization of assays analogous to the ELISAs shown in Figs. 1 and 2. The substrate used as a solid phase for the assays was silica, which was modified with amine groups for covalent attachment to a carboxyl containing antigen. Covalent attachment of the antigen has an advantage over conventional ELISAs using non-specifically adsorbed reagent, since a stable bond can be formed between the small antigen used and the substrate (see section 1.6c).

Silica slides and beads (0.78 μm diameter) were both used for assays because they could be characterized in different ways, in order to obtain additional information. The silica beads provided a high surface area for more accurate measurement of surface amine groups and surface antigen concentration and could also be used for particle electrophoresis measurements to determine the surface charge on the beads after different modifications. The silica slides had a smooth flat surface and were used for XPS measurements determining the cleaning procedure prior to silylation and the amount of nitrogen on the surface after silylation. The XPS measurements were also used to detect antigen on the slides.

The silica slides and beads were cleaned thoroughly to increase the accessibility of the surface silanols to reagents in solution. The beads and slides were both modified with 3-aminopropyltriethoxy silane, to give a surface covered with amine groups. The surface concentration of amine groups on the silylated beads was measured using a ninhydrin assay and the surface concentration of nitrogen was measured using XPS.

The antigen used in the assays was ferrichrome A, a cyclic hexapeptide that chelates iron through three hydroxamate groups.

Ferrichrome A was chosen as an antigen because of several useful features: the ferric hydroxamate group absorbs at 436 nm and can be used to determine the peptide concentration, there are three carboxyl groups per molecule for covalent attachment to the amine-modified silica, the iron can be distinguished by XPS and the isolation results in a high yield of antigen which can be readily purified.

A water soluble carbodiimide, (1-ethyl-3-(3-dimethylaminopropyl) carbodiimide, EDC) was used to promote the formation of an amide bond between the antigen and the silylated silica. The surface concentration of ferrichrome A on the beads was measured as a function of solution concentration. Some evidence is presented for formation of a covalent bond.

Ferrichrome A was coupled to a carrier protein using EDC in order to produce an antibody. A monoclonal antibody was obtained against ferrichrome A and used in later studies so that the antibody preparation would have only one binding specificity and the antibody binding measurements would be simpler to interpret.

The surface concentration of antibody bound to the antigen-modified beads and flat silica was measured as a function of solution concentration of antibody and surface concentration of antigen, using an ^{125}I labelled antibody. The equilibrium binding constant for the antibody-antigen reaction at the substrate surface was calculated for the different surface concentrations of ferrichrome A used. An estimate of the solution binding constant was obtained as described in Appendix 1 using a series of different solution concentrations of antigen to inhibit antibody binding to flat slides modified with ferrichrome A.

The slides and beads were both used for ELISAs measuring the concentration of antibody and antigen in solution.

Chapter 2

Methods and materials: preparation of the antigen, antibody and modified substrate

2.1 Isolation of the antigen

Where not otherwise specified, the chemicals used in all experiments were reagent grade products from BDH (Vancouver) or Fisher (Vancouver).

Ferrichrome A is one of a large group of related compounds that are secreted by microorganisms in order to chelate extracellular ferric ions and transport them into the cell. Because ferrichrome A is secreted externally to the cell, it can be isolated readily from the culture supernatant (see Fig. 11 for structure of ferrichrome A).

Ferrichrome A was isolated (119) from *Ustilago sphaerogena* Burril which was obtained from the American Type Culture Collection (cat. no. 12421), with an import permit from Agriculture Canada. The initial freeze dried fungus was grown in 10 ml of a low iron medium (composition, Table I) in a 125 ml Erlenmeyer flask. The cell line was maintained in 125 ml Erlenmeyer flasks with re-inoculation of fresh medium every ten days. The fungus was grown at 30 °C in a reciprocal shaker. Larger amounts of culture used for isolation of ferrichrome A were grown in 500 ml of medium in a 2.8 litre Fernbach flask.

Three or four days after inoculation of the large flask, the cells were removed by centrifugation. Ferric chloride was added to the culture supernatant to produce the coloured iron hydroxamate. The supernatant was then saturated with ammonium sulphate and extracted with benzyl alcohol. After addition of diethyl ether to the organic phase, the

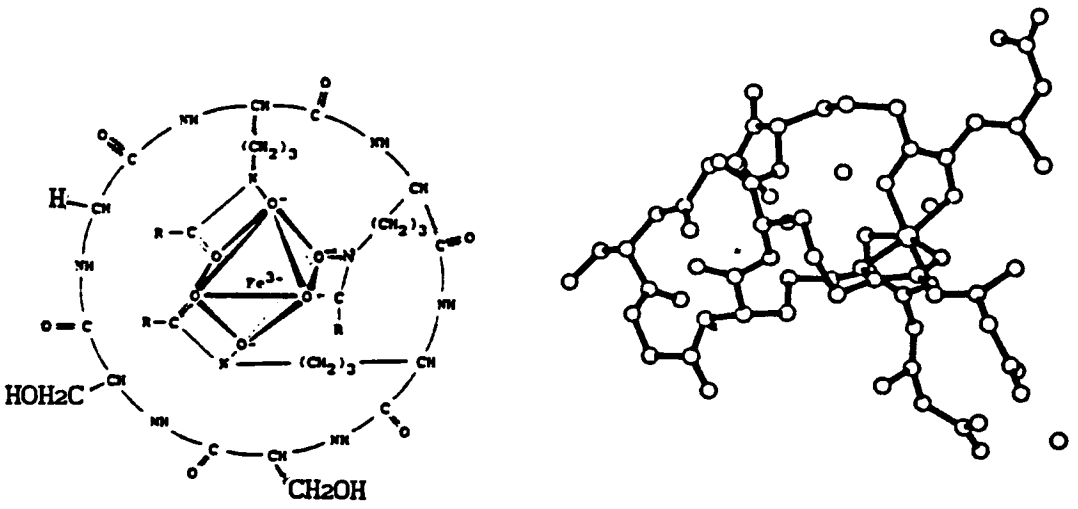

Figure 11: (a) Structure of ferrichrome A, where R = trans -CH=C(CH3)CH2COOH (b) Crystallographic structure of ferrichrome A (120).

Table I: Preparation of growth medium for *Ustilago sphaerogena*

1. Solution A was made in an EDTA washed test tube to minimize iron adsorbed to the glass: 5 mg thiamine hydrochloride in 5 ml H_2O. Freshly made solution A was used.

2. Solution B was made and stored in an EDTA washed bottle: 4.5 mg $CuSO_4.5H_2O$, 32.0 mg $MnSO_4.4H_2O$ and 2.0 g $ZnSO_4.7H_2O$ were added to 100 ml of water.

3. The growth medium was then made up in a Fernbach flask with 520 ml of H_2O, to which the following ingredients were added:

		Final concentration
K_2SO_4	0.52 g	1.0 g/l
K_2HPO_4	1.56 g	3.0 g/l
NH_4COOCH_3	1.56 g	3.0 g/l
sucrose	10.4 g	20.0 g/l
citric acid	0.569 g	1.0 g/l
solution A (thiamine)	0.52 ml	2.0 mg/l
$MgSO_4.7H_2O$	0.422 g	Mg 80.0 mg/l
solution B (trace salts)	0.174 ml	Cu 0.005 mg/ml
		Mn 0.035 mg/ml
		Zn 2.0 mg/ml

4. The pH of the solution was adjusted to 6.8 with concentrated ammonium hydroxide.

5. The solution was sterilized by autoclaving.

ferrichrome A was extracted using water and was obtained as a dark red crystalline material. The ferrichrome A was purified by recrystallization from water.

Ferrichrome A absorbs strongly in the visible region of the spectrum (λmax at 436 nm) because of the iron hydroxamate centre. Absorbance (A) was measured with a Hewlett-Packard 8450A UV/VIS spectrophotometer. The extinction coefficient at λ=436 nm was determined to be $\varepsilon = 2.778$ ml mg^{-1} cm^{-1}.

The derivative curve ($dA/d\lambda$) was also used to determine the concentration of ferrichrome A (121). This method has the advantage of eliminating most of the effects due to low concentrations of suspended particles and was used in later experiments measuring adsorption of ferrichrome A to silica beads, because of problems with beads in the samples. Light scattering due to the particles will increase the absorbance reading, but because the increase in light scattering is nearly linear with decreasing wavelength (for the particle size and wavelength range used), the difference between the derivative at any two wavelengths will remain unaffected by increased light scattering (Fig. 12, sample spectra are included in Appendix 3). The difference between the maximum and minimum points on the derivative curve was determined; this corresponds to the sum of the absolute values of the slopes at the inflection points on the absorbance curve at 389nm and 492nm. The sum of the slopes was shown to vary linearly with concentration (Fig. 13), and the concentration of ferrichrome A in mg/ml was found to be equal to the sum divided by 0.05986±0.00017, where the error is the standard deviation in the slope of the calibration curve (Fig. 13).

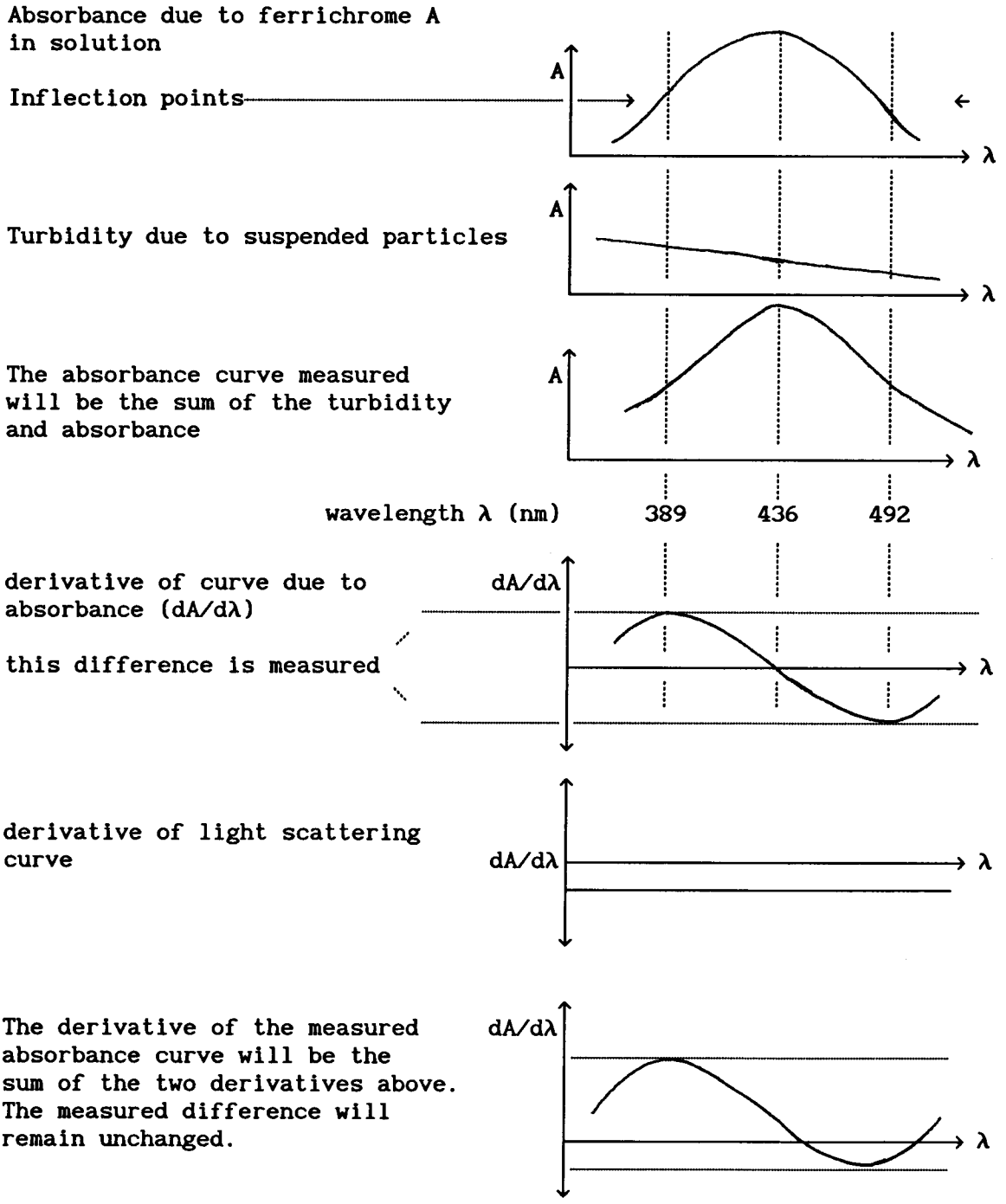

Figure 12: The effect of light scattering on the derivative of the absorbance curve.

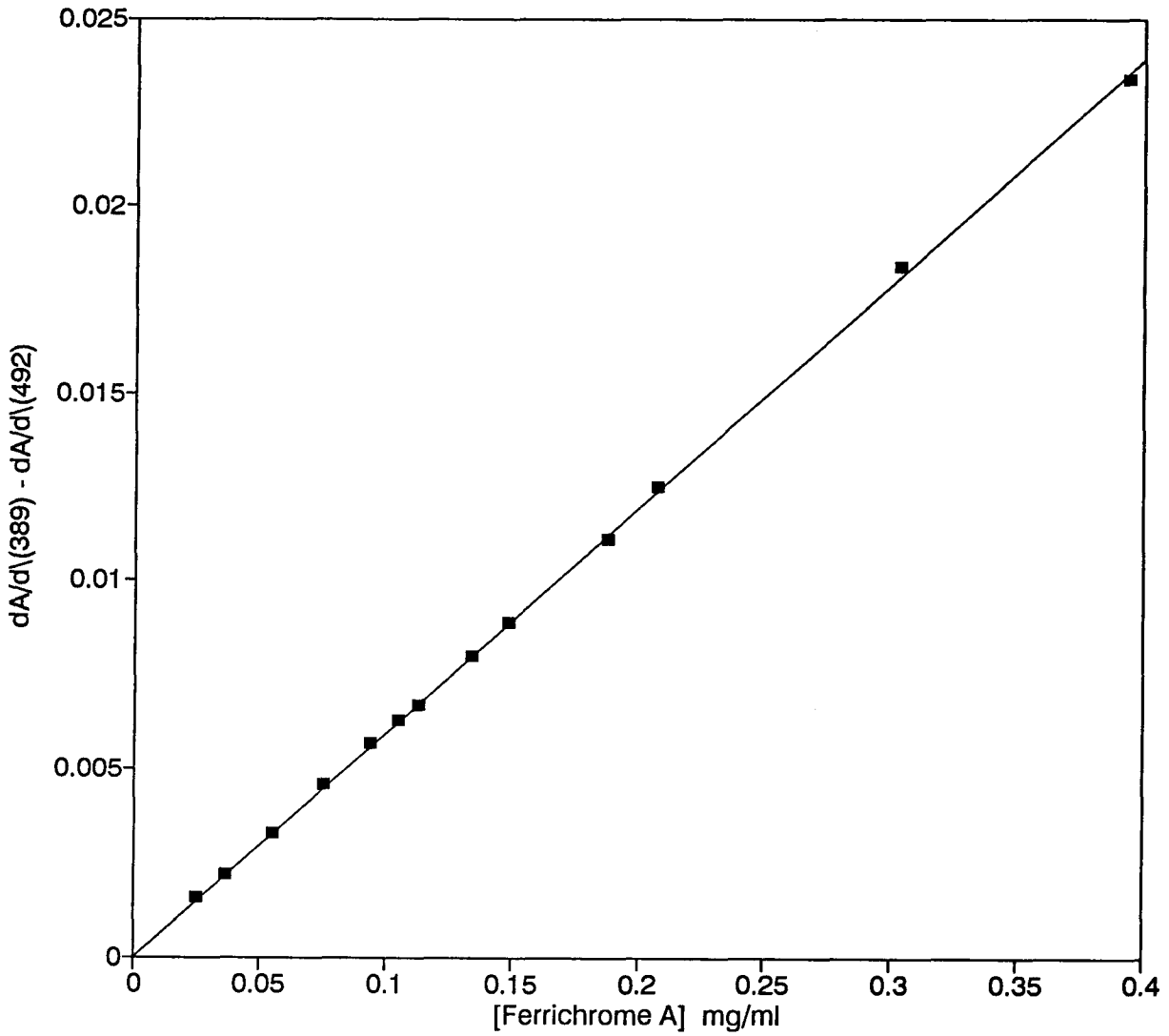

Figure 13: Determining the concentration of ferrichrome A from the derivative of the absorbance spectrum ($dA/d\lambda$). The sum of the absolute values of the slopes at the inflection points at either side of the absorbance peak is plotted against concentration of ferrichrome A.

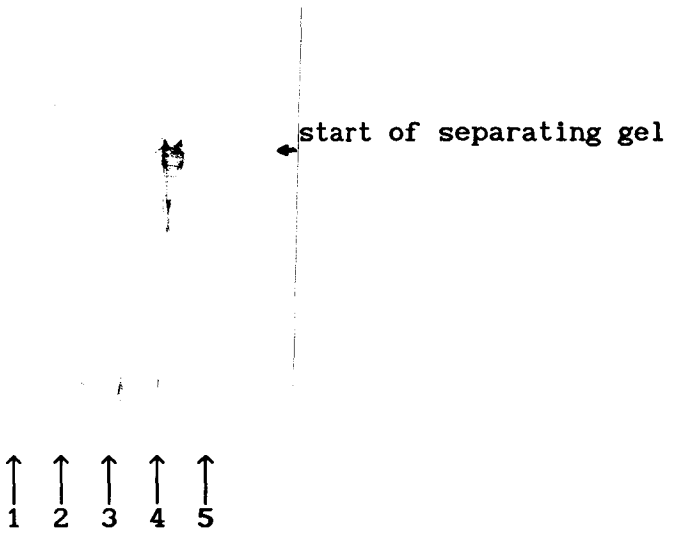

Figure 14: Western blot showing that the antigen is coupled to KLH. The outline on the blot marks the position of the gel. Higher molecular weight samples are near the top of the gel. The different lanes are for 1) molecular weight standards 2) KLH 3) KLH mixed with ferrichrome A 4) KLH coupled to ferrichrome A using EDC 5) ferrichrome A.

2.2 Coupling antigen to KLH and BSA

2.2a Coupling Procedure

Keyhole limpet haemocyanin (KLH, Calbiochem, San Diego) was used as a carrier molecule for raising both the rabbit polyclonal and mouse monoclonal antibodies and was coupled to ferrichrome A using 1-ethyl-3-(3-dimethylaminopropyl) carbodiimide (EDC). Ferrichrome A was dispersed in water (5 mg/ml); most of the ferrichrome A dissolved after addition of a 34x molar excess of EDC. Keyhole limpet haemocyanin (5 mg/ml) was added and the mixture was stirred at room temperature for one hour, after which it was dialyzed against water at 4 $^{\circ}$C for 48 hr using dialysis tubing with a molecular weight cut off of 50 000 g/mol (Spectrapor, Spectrum Industries, Los Angeles). This left an aggregated mass of undissolved KLH and a clear supernatant; both were orange, indicating that there was still free ferrichrome A remaining after dialysis. Both the supernatant and the precipitate (termed collectively ferrichrome A/KLH) were used for eliciting the antibodies.

Ferrichrome A/BSA was prepared the same way as ferrichrome A/KLH, but had no precipitate because the BSA dissolved completely.

2.2b Western Blot with ferrichrome A/KLH: an indication of the success of the coupling procedure

A Western blot (122) on the clear supernatant from the KLH/ferrichrome A preparation using one of the monoclonal antibodies raised as described later showed that the antibody interacted with a high molecular weight antigen, indicating that the ferrichrome A in solution was attached to KLH.

Samples in solution were mixed at a 1:1 volume ratio with PBS containing 2% SDS and 5% v/v β-mercaptoethanol, and boiled for two

minutes to denature and reduce the sample. The initial electrophoretic separation of the proteins was carried out using the automated Pharmacia Phastsystem with precast 8-25% polyacrylamide gels and sodium dodecyl sulfate (SDS) buffer strips. The samples were electroblotted onto nitrocellulose membrane with a 0.45 μm pore size in pH 8.3 transfer buffer with 25 mM Tris (tris[hydroxymethyl]aminomethane) 192 mM glycine and 20% methanol. The nitrocellulose membrane was incubated overnight with supernatant from the AC3 cell line grown in serum free medium (described in section **2.4**) diluted 1:15 in PBS with 0.5% Tween 20 and 3% BSA to block non-specific binding. Antibody produced by the AC3 cell line was shown to interact with ferrichrome A (section **2.4c**, Fig. 25). The membrane was washed using PBS with 0.5% Tween 20 and developed with horseradish peroxidase conjugated antibody and substrate from the Bio-Rad Immun-blot kit with 4-chloro-1-naphthol as a substrate.

The Western blot indicates the species to which the antibody binds. The antibody bound to the ferrichrome A/KLH but not to the KLH by itself with EDC, indicating that the monoclonal antibody bound to ferrichrome A. No band was seen for ferrichrome A on the initial gel or on the blot. This may be because ferrichrome A was too small to be distinguishable from the solvent front on the gel used or because ferrichrome A alone does not stain with Coomassie blue and does not adsorb to the blotting membrane. No band was seen for ferrichrome A mixed with KLH without EDC, indicating that the EDC was required for the coupling.

The band for the ferrichrome A/KLH is a smear, indicating that there was a range of molecular weights for the species in solution. The KLH by itself can form aggregates that could be cross-linked by EDC to give a product with a molecular weight too high to run onto the gel (samples that do not run onto the gel can be seen as a band between the sample

application layer and the separating gel). Aggregation does not pose a problem and can help stimulate antibody production (123).

2.3 Developing an ELISA prior to raising a monoclonal antibody

An enzyme linked immunosorbent assay (ELISA) was developed using rabbit and mouse polyclonal antibodies, so that an assay would be available to detect the monoclonal antibody when it was produced.

2.3a ELISA with serum from an immunized rabbit

A rabbit polyclonal antibody was elicited against the ferrichrome A/KLH preparation described in section 2.2a (124). One New Zealand White rabbit was injected subcutaneously at the back of the neck with one ml of a 1:1 emulsion of ferrichrome A/KLH (containing 0.5 mg of KLH) and Freund's complete adjuvant (Difco Laboratories, Detroit). The rabbit was given a subcutaneous booster injection one month later with one ml of a 1:1 emulsion of ferrichrome A/KLH and Freund's incomplete adjuvant (Difco). Blood was obtained from an ear vein five days after the second injection.

An ELISA was developed with commercial plates, following the ELISA protocol for the Vancouver Research Station of Agriculture Canada (125). Figure 15 provides a general description of the ELISA procedure.

Ferrichrome A adsorbed directly to ELISA plates gave a poor assay response, so the ferrichrome A was cross-linked with EDC, ethylene diamine and triethylamine to give a higher molecular weight product that would remain adsorbed to the plates. Since the ferrichrome A has three carboxyl groups per molecule, EDC coupling of the carboxyl groups with the amino groups on a polyamine will result in a cross linked product. Ferrichrome A, ethylene diamine, EDC and triethylamine were mixed together in water at a mole ratio of 2:3:6:6. The unpurified product was

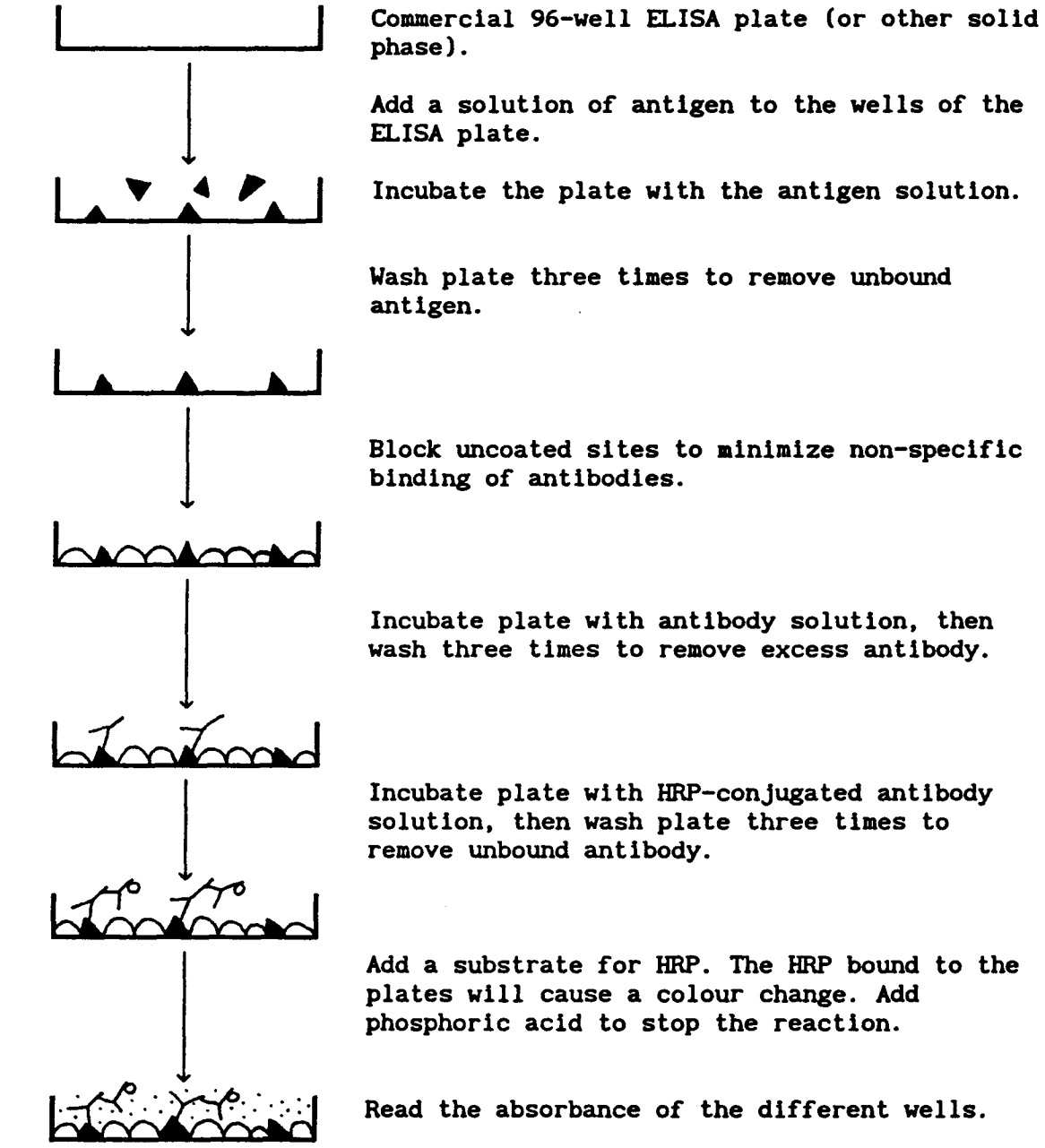

Figure 15: The ELISA procedure

adsorbed to Immulon 2 plates (Dynatech, from Fisher, Vancouver) overnight at room temperature in 100 mM acetate buffer pH 4.5 at a concentration equivalent to 5 μg/ml free ferrichrome A and a volume of 100 μl/well. The uncoated sites were blocked with 0.2% Carnation skim milk in phosphate buffered saline with 0.05% Tween 80 (blocking buffer) for half an hour at 37 °C, to minimize non-specific adsorption of antibodies in subsequent steps (Tween 80 is a non-ionic detergent, poly-oxyethylene sorbitan mono-oleate). The ELISA plate was washed three times with PBS containing 0.05% Tween 80 (PBS-Tween) after all adsorption steps.

A dilution series of the rabbit serum in blocking buffer was adsorbed to the plates for one hour at 37 °C, and then washed off. A secondary horseradish peroxidase conjugated goat anti-rabbit antibody (HRP-gαr Ab, Cappel, Cooper Biomedical, West Chester, P.A.) was diluted in blocking buffer and incubated with the plates for one hour at 37 °C. The plate was developed using tetramethyl benzidine (TMB) as a substrate for the horseradish peroxidase (Table II gives the composition of the substrate solution). Substrate solution was added to the plates (100 μl/well) and left at room temperature for two to three minutes before the reaction was stopped in all wells by addition of 50 μl of 2.0 M phosphoric acid/well. The absorbance of each well was read at 450 nm with a reference at 620 nm (where the substrate has minimal absorbance) using an SLT Instruments plate reader.

The ELISA procedure outlined above gave a clear positive response for the rabbit serum (Fig. 16).

2.3b An ELISA with blood from an immunized mouse

Two BALB/c mice were also used to raise antibodies against

Table II: Preparation of substrate solution for ELISAs (126)

1. Stock solutions. The following stock solutions were made up.

acetate/citrate buffer	200 mM sodium citrate was added to 200 mM sodium acetate to give a solution with a final pH of 6.0.
tetramethylbenzidine (TMB)	TMB (Sigma, St. Louis) was dissolved in dimethylsulfoxide (DMSO) at a concentration of 10 mg/ml.

2. Substrate solution. The substrate solution was made up immediately before use, with reagents added in the order listed.

acetate/citrate buffer	4 ml
water	16 ml
TMB solution	200 µl
3% w/w H_2O_2	20 µl

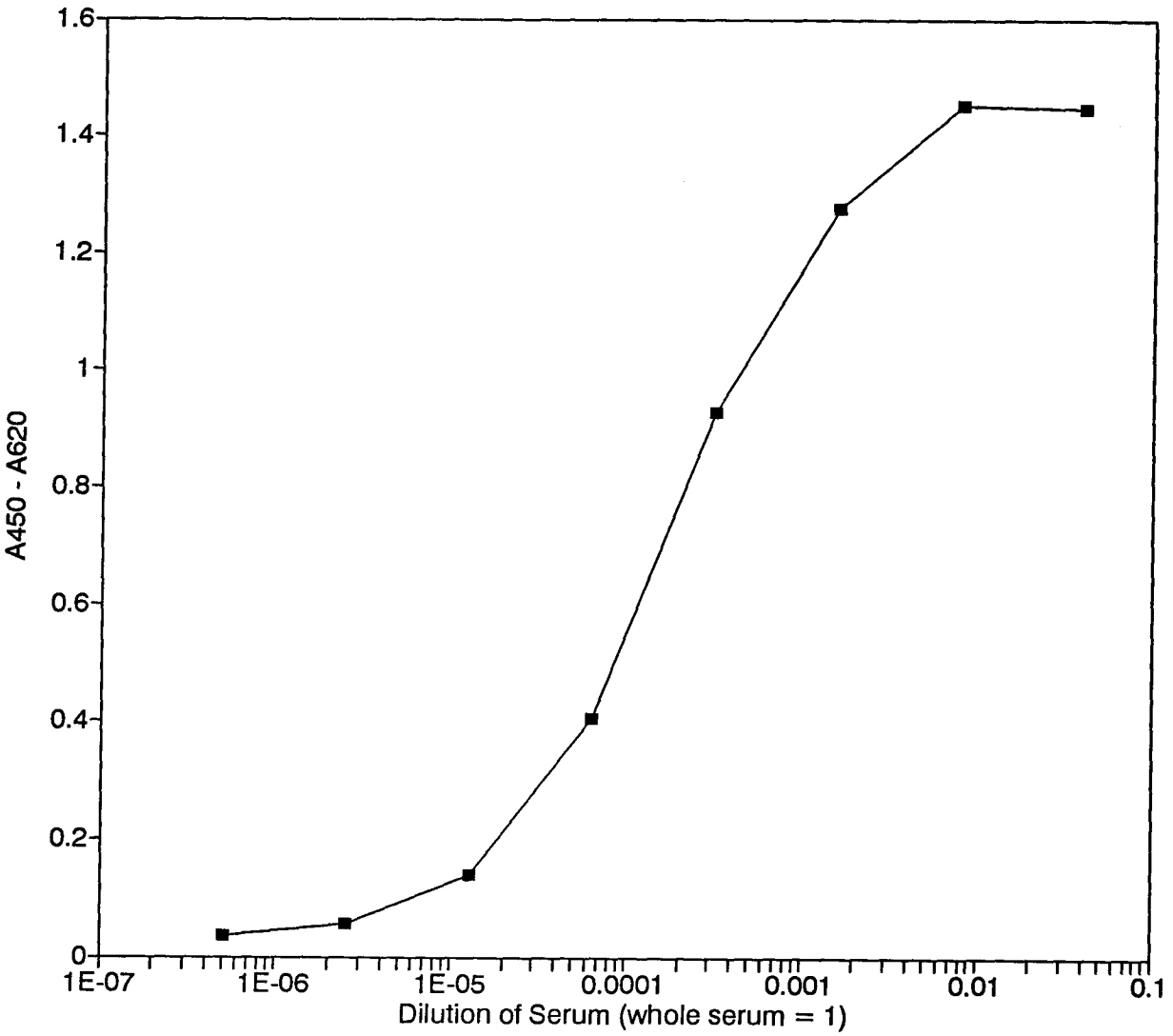

Figure 16: An ELISA with ferrichrome A adsorbed to Immulon 2 plates and rabbit serum as antibody. The rabbit serum was diluted in blocking buffer with an initial dilution of 1:25 and subsequent five-fold stepwise dilutions.

ferrichrome A/KLH. A 1:1 emulsion of ferrichrome A/KLH prepared as described in section 2.2a was injected subcutaneously in the sides of the mice (100 µl total volume). An intraperitoneal boost of ferrichrome A/KLH in PBS (0.5 ml total volume) was administered 28 days after the initial immunization. Blood was obtained by tail bleeding three days after the boost.

Blood from immunized mice did not give a positive reaction on the ELISA (Fig. 17). Mice were later shown to produce antibodies against ferrichrome A (section 2.4), but the rabbit serum may have contained more antibodies against ferrichrome A because of species differences in the immune response (127).

2.3c A second ELISA with blood from immunized mice

An ELISA with mouse serum as the antibody and ferrichrome A/BSA adsorbed to the ELISA plates as the antigen (adsorbed at a concentration of 1 µg/ml BSA in PBS) gave a strong positive response (Fig. 18), but a further ELISA showed that this response was not due to antibodies that were active against free ferrichrome A.

Inhibition of the antibody binding by free ferrichrome A was measured using antibody at a constant concentration (1:3000 dilution of mouse blood in blocking buffer) and varying concentrations of ferrichrome A. The diluted mouse blood was incubated with the ferrichrome A for 30 min at 37 °C before being added to the ELISA plates.

Free ferrichrome A did not inhibit the ELISA response, as would be expected if the ferrichrome A in solution were competing with the ferrichrome A on the ELISA plates for binding sites on the antibody molecules (Fig. 19).

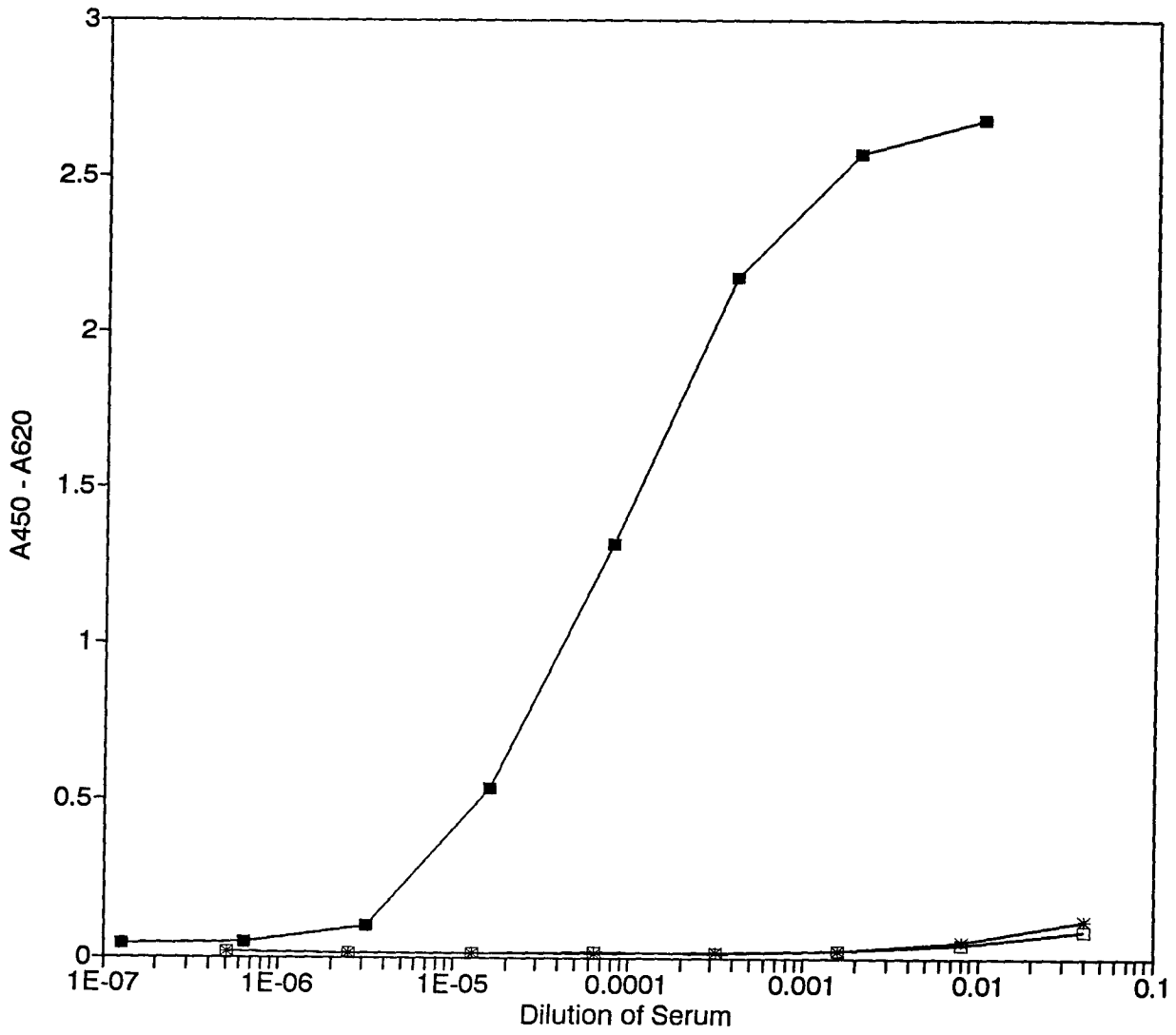

Figure 17: An ELISA with ferrichrome A adsorbed to Immulon 2 plates: comparison of the ELISA results for blood from two mice (x and □) and a rabbit (■).

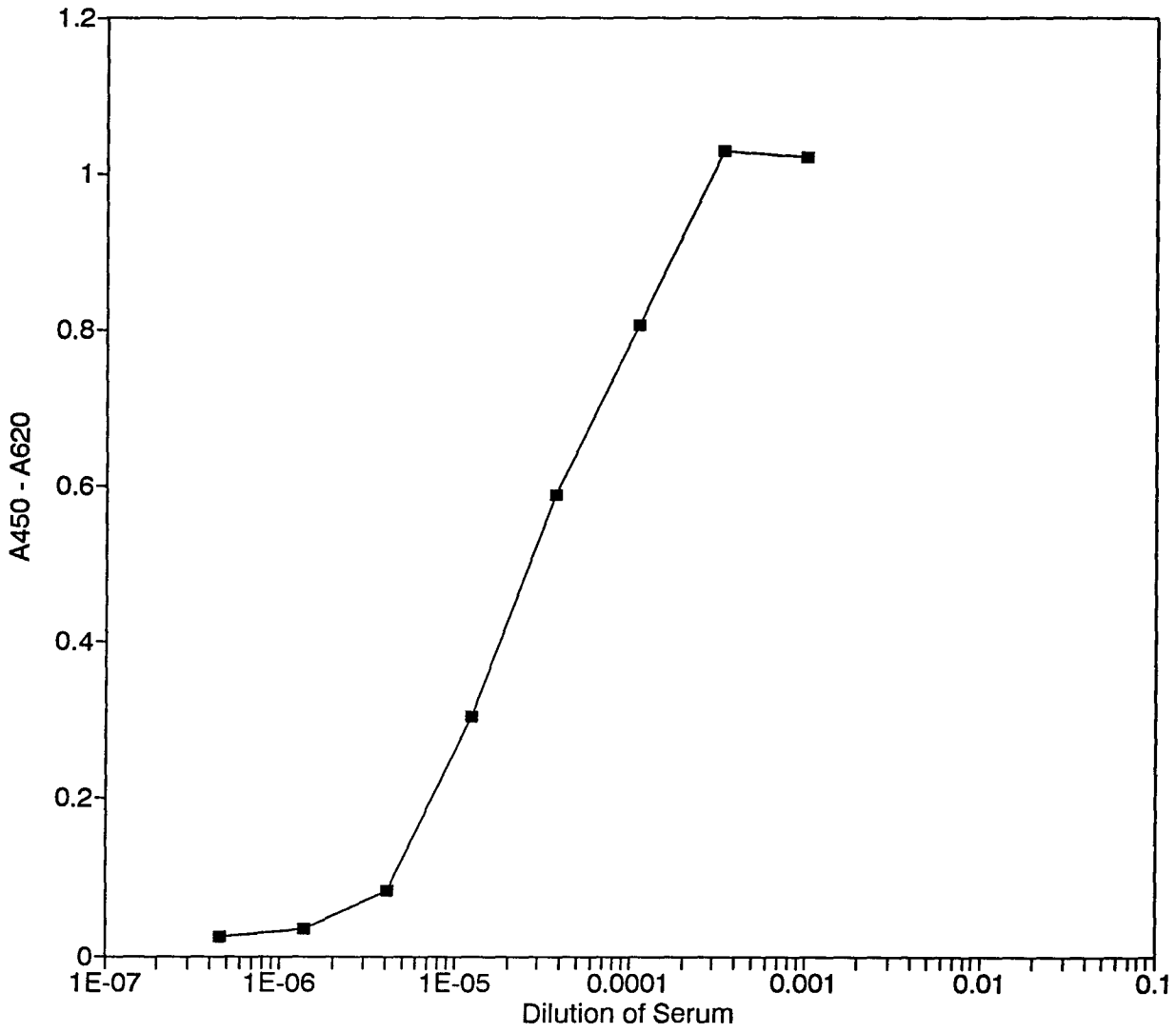

Figure 18: An ELISA with ferrichrome A/BSA adsorbed to Immulon 2 plates and serum from an immunized mouse as antibody.

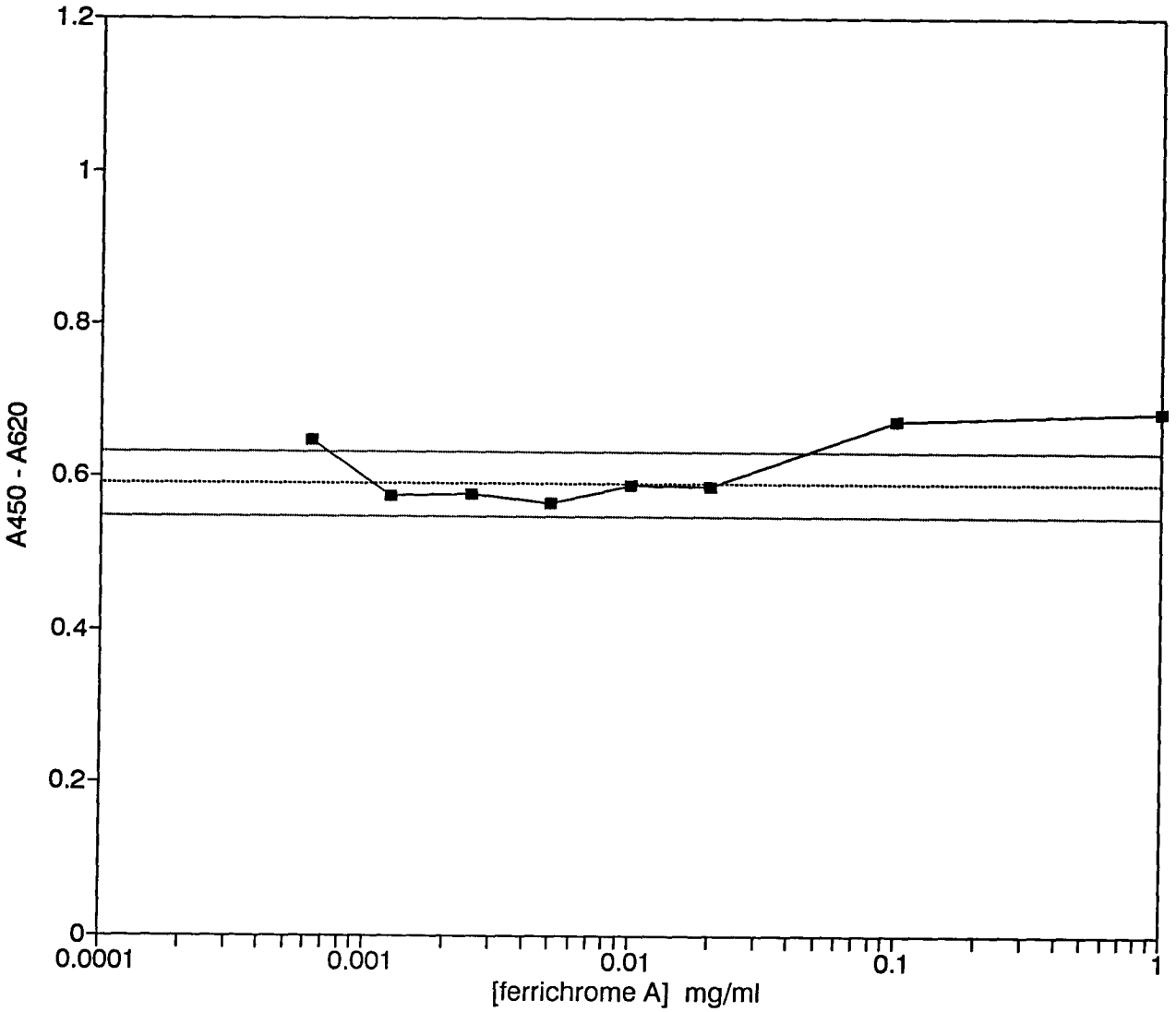

Figure 19: An ELISA with ferrichrome A/BSA adsorbed to Immulon 2 plates. The antibody used was blood from an immunized mouse diluted 1:3000. Ferrichrome A at different concentrations was pre-incubated with antibody and added to the ELISA plate (■). The absorbance resulting from antibody with no inhibiting ferrichrome A is also shown (----), with error limits (———).

Typical epitopes on proteins comprise six to eight amino acid residues (49). Most of the antibodies produced by the mouse may be active against the ferrichrome A together with one or more amino acid residues on the protein. This problem could be minimized by using a spacer molecule when attaching the ferrichrome A (54).

2.3d Comparing the efficiencies of skim milk and BSA as blocking reagents

The efficiencies of skim milk powder and BSA as blocking reagents were compared for polystyrene plates. The assays were carried out as described for the previous ELISAs with BSA/ferrichrome A adsorbed to the plates, but without Tween in the PBS at any point and adding the blocking reagents only in the first 30 minute blocking step (0.2% skim milk powder in PBS or 0.2% BSA in PBS). The antibody and HRP conjugated antibody were made up in PBS with no Tween or blocking agent. A mouse antibody against an unrelated antigen was also used, to determine non-specific binding. The results obtained are shown in Figure 20. The non-specific binding, as determined by the unrelated antibody, was higher with the BSA block. This curve also seemed to form the baseline for the results obtained with the AC3 antibody with a BSA block in PBS. Skim milk powder was used initially in adherence to the procedure described by the Agriculture Canada monoclonal antibody laboratory, and these results were taken to justify continued use of skim milk powder as a blocking reagent.

2.3e The effect of Tween 80 on the ELISA

The effect of Tween 80 in the buffer was also studied for assays on polystyrene plates. The plates were coated as before with ferrichrome A/ BSA in PBS. One plate was then washed with PBS Tween, and blocked with

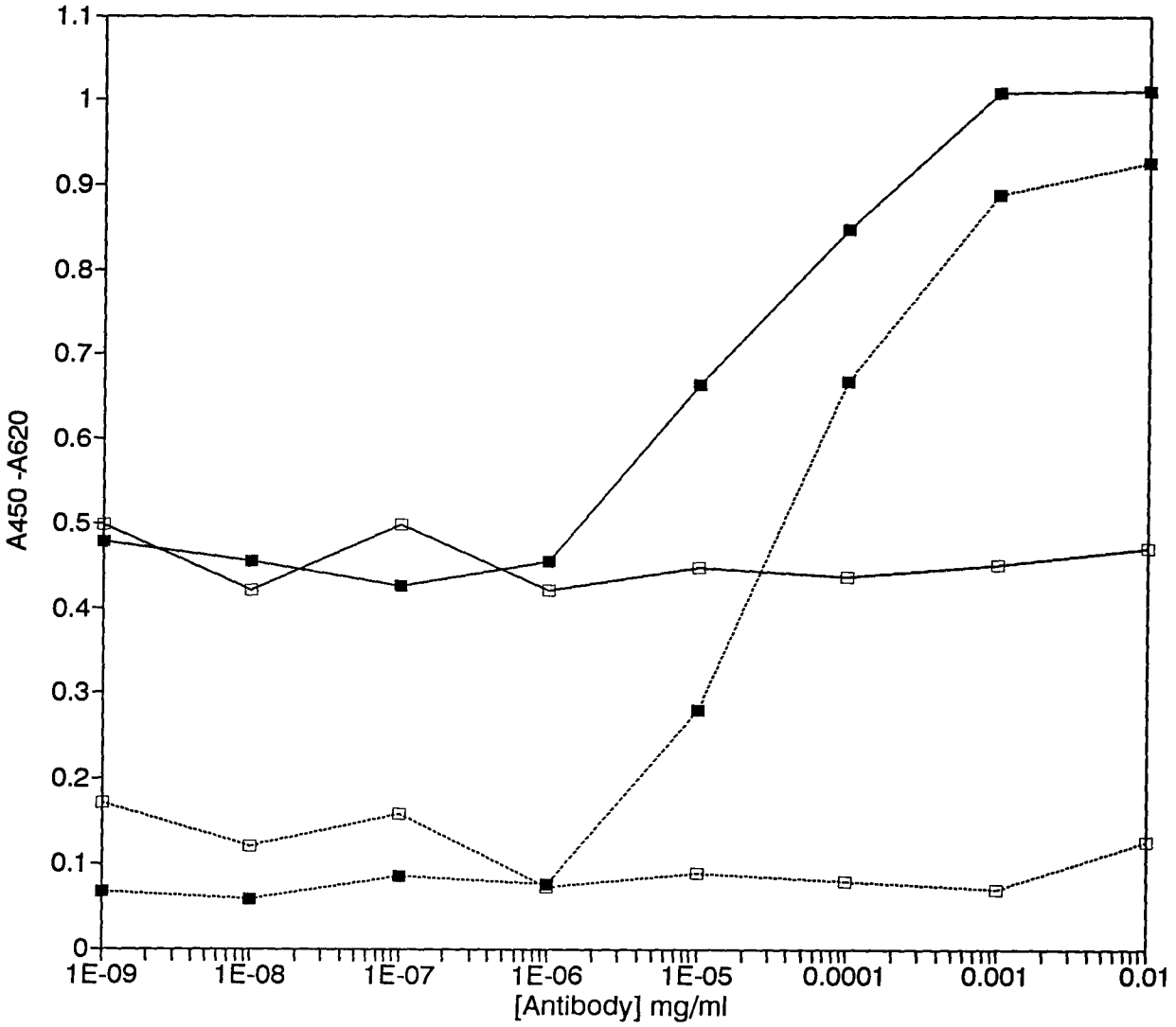

Figure 20: An ELISA comparing the efficiency of 0.2% BSA and 0.2% skim milk as blocking agents. Results are shown for an antibody to ferrichrome A with BSA (■—■) and with skim milk (■---■), and for an unrelated antibody with BSA (□——□) and skim milk (□---□) as blocking agents. ■ = anti-ferr. A, □ = other antibody, —— = BSA,--- = skim milk.

0.2% BSA or skim milk in PBS Tween. Antibody and HRP conjugated antibody were also added in PBS Tween. A second plate was treated the same way, but all washes and solutions were in PBS without Tween. The results from these experiments (Fig. 21) show that BSA is an effective blocking agent when there is detergent in the solution. The results also show that Tween seems to enhance the affinity of the antibody for the antigen.

2.3f Absorbance of the substrate solution as a function of HRP-conjugated antibody concentration and evidence that there is a large excess of HRP-conjugated antibody used in the ELISAs

Dilute solutions of HRP-conjugated antibody solution were added directly to the substrate to determine if the absorbance increased linearly with increasing enzyme concentration. A series of HRP-conjugated antibody solutions was made up in dilutions ranging from 1:100 000 to 1:1 000 of a commercial stock solution. A 20 µl volume of each solution was added to the substrate solution described above and left at room temperature for three minutes. The absorbance of each solution was read after the enzyme reaction was stopped by addition of phosphoric acid. The absorbance is plotted as a function of dilution of the stock solution in Figs. 22 and 23. In solutions having an absorbance of up to 1.5 after three minutes, the absorbance was a linear function of the amount of HRP-conjugated antibody present. At absorbances greater than 2.5, there was almost no increase in absorbance with increasing amounts of the HRP-conjugated enzyme. This is not merely a function of response of the spectrophotometer. The absorbance was measured with a shorter optical path length and used to calculate the total absorbance; this gave a similarly shaped curve, with a non-linear response seen for HRP-conjugated antibody concentrations giving absorbances higher than

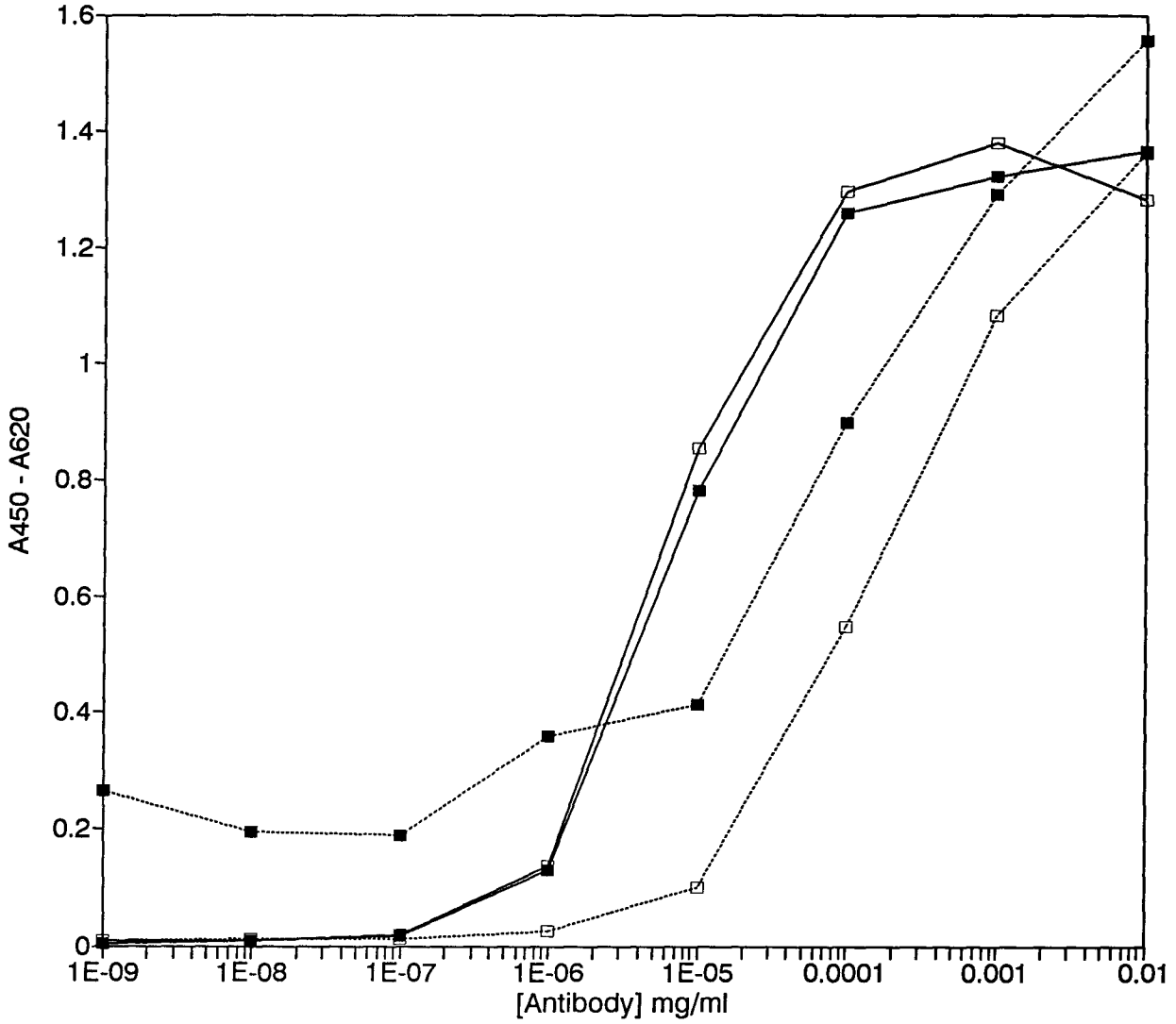

Figure 21: The effect of Tween 80 on the ELISA. Results are shown for an antibody to ferrichrome A using BSA as a blocking agent with plates washed with PBS-Tween (■——■) and PBS (■---■) and using skim milk as a blocking agent, with plates washed with PBS-Tween (□——□) or PBS (□---□).

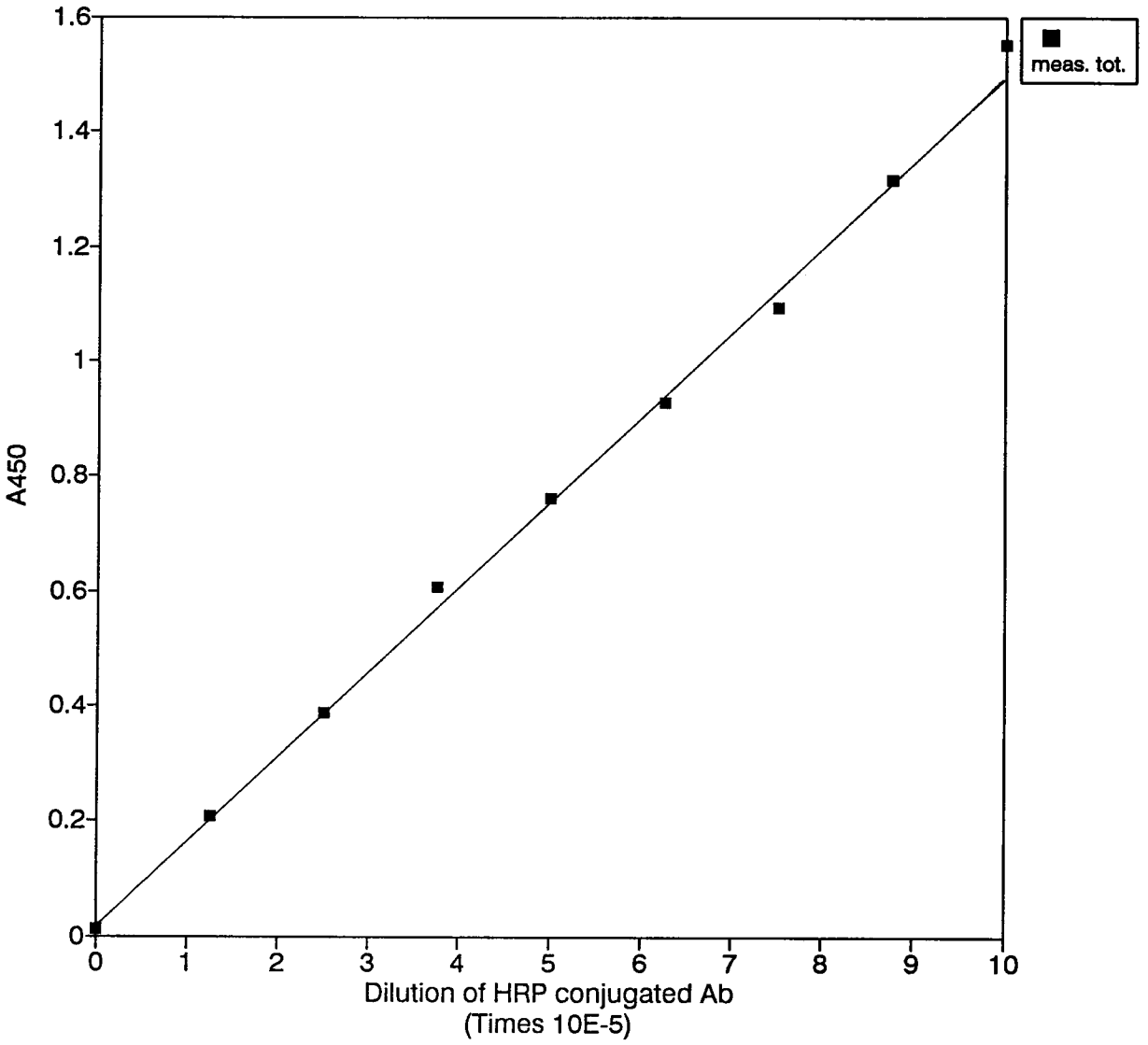

Figure 22: Absorbance of the ELISAs as a function of low HRP concentrations

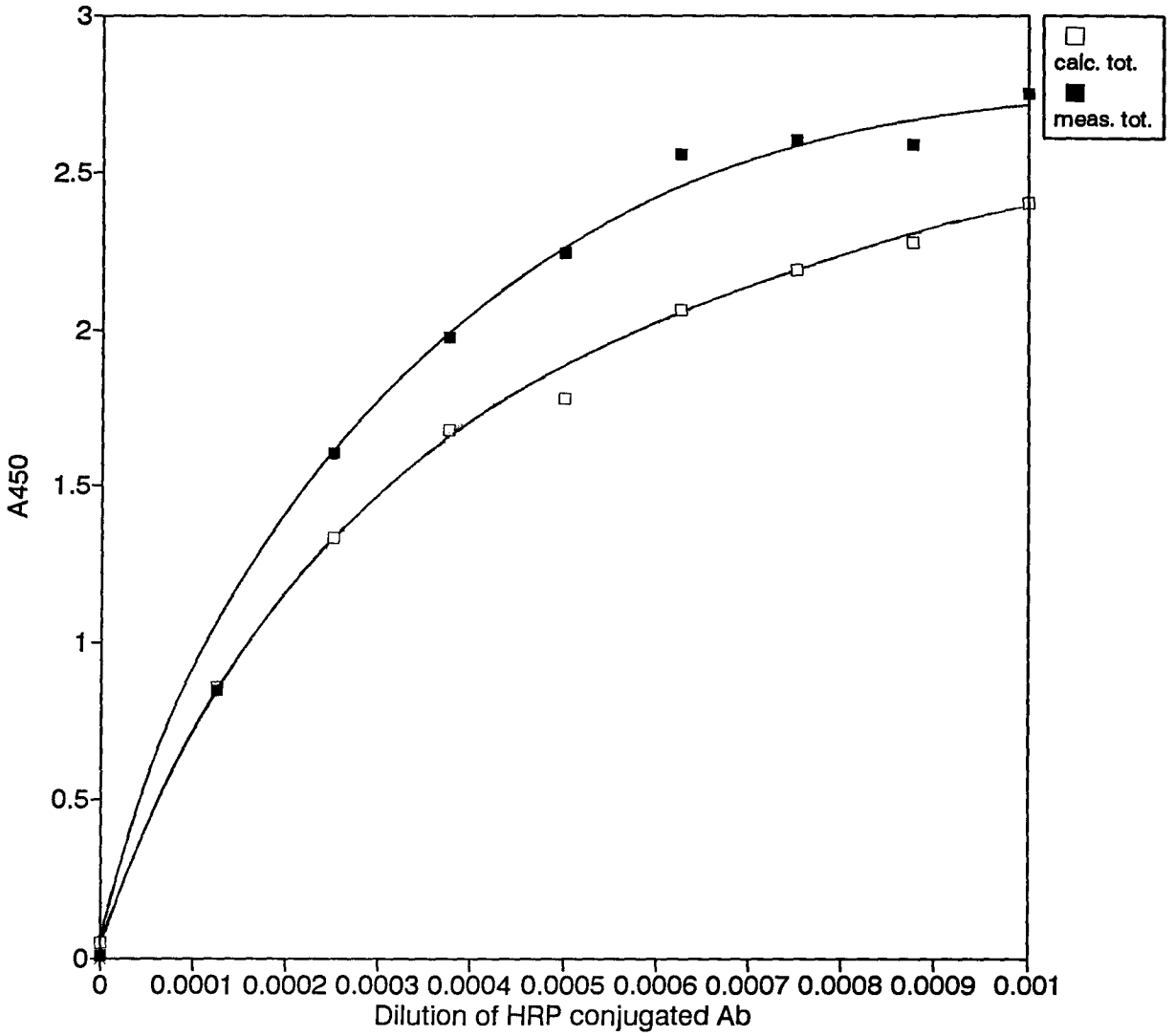

Figure 23: Absorbance of the ELISA as a function of higher HRP concentrations ■ = direct measurement, □ = absorbance for total sample calculated from measurement with a short optical path length.

1.5. The calculated value for the absorbance was slightly lower than the measured value; this may be due to the fact that the optical path length was calculated assuming a level surface of liquid, and the path length through the centre of the smaller volume would have been affected more by the shape of the meniscus.

For the ELISAs, 100 µl of a 1:1000 dilution of the HRP-conjugated antibody was added to the wells. The amount of HRP-conjugated enzyme remaining on the plates after rinsing was sufficient to cause an absorbance of about 1. If the activity of the surface bound enzyme is the same of that of the enzyme in solution, then about a 300-fold excess of the conjugated enzyme is added.

2.4 Production and purification of the monoclonal antibody, with SDS-PAGE to determine the antibody purity

2.4a Antibody production

The monoclonal antibody was made following the procedure of the Vancouver Research Station of Agriculture Canada (125).

Three BALB/c mice were injected subcutaneously with ferrichrome A/KLH and complete Freund's adjuvant at zero days. The mice were injected intraperitoneally with ferrichrome A/KLH in buffer at 30 days. Serum obtained by tail bleeding at 33 days was tested for antibodies using an ELISA with ferrichrome A/BSA adsorbed to the ELISA plate. At 34 days, the spleen from the mouse with the highest serum antibody titre was removed and placed in a Petri dish with 10 ml of Dulbecco's modified Eagle medium (DME from GIBCO, Grand Island; for composition see Table III). The spleen cells were separated by covering the spleen with a piece of gauze and squeezing the spleen with the end of a syringe plunger. The DME, containing the spleen cells, was pipetted off, and the cells were

Table III: Preparation of Dulbecco's Modified Eagle medium

1. DME was made up from powdered packets from Gibco (cat. no. 430-1600, low glucose medium with L-glutamine and sodium pyruvate). One litre of medium was made up at a time and contained components in the following concentrations (128):

	mg/l
Inorganic salts	
$CaCl_2.2H_2O$	264.9
$Fe(NO_3)_3.9H_2O$	0.100
KCl	400.0
$MgSO_4$	97.7
NaCl	6400.0
NaH_2PO_4	125.0
Other components	
glucose	1000.0
phenol red, sodium salt	15.0
sodium pyruvate	110.0
Amino acids	
L-arginine.HCl	84.00
L-cystine, disodium salt	56.78
L-glutamine	584.0
glycine	30.00
L-histidine.HCl.H_2O	42.00
L-isoleucine	104.8
L-leucine	104.8
L-lysine.HCl	146.2
L-methionine	30.00
L-phenylanine	66.00
L-serine	42.00
L-threonine	95.20
L-tryptophan	16.00
L-tyrosine	72.00
L-valine	93.60
Vitamins	
D-Ca pantothenate	4.00
choline chloride	4.00
folic acid	4.00
i-inositol	7.00
nicotinamide	4.00
pyridoxal.HCl	4.00
riboflavin	0.4000
thiamin.HCl	4.00

2. The DME solution was sterilized by filtration with Falcon Easy Flow™ filtration units (0.22 μm pore size), and stored in autoclaved bottles at 4 °C.

3. If the DME solution had been stored for more than ten days, additional glutamine was added immediately before use. Glutamine was added at a 1:100 dilution from a 29.2 mg/ml L-glutamine solution from Flow laboratories.

collected by centrifugation and washed twice with fresh DME.

FOX-NY myeloma cells (129)(ATCC CRL1732) frozen in DME with 20% fetal bovine serum (FBS, Hyclone, Logan) were thawed at 30 days, washed with DME, added to DME with 5% FBS, and plated out in five 15x100 mm Petri dishes (Fisherbrand, Fisher Scientific, Ottawa). The cells were grown under 10% CO_2 and were collected at 34 days and washed twice with DME.

PEG 4000 (Serva, Heidelberg) was used to fuse the myeloma and spleen cells. Five grams of PEG 4000 were dissolved with heating in four ml of DME. The cooled PEG solution was sterilized by filtration through a 0.22 μm filter after addition of one ml DMSO (BDH Assured, BDH, Toronto) and stored at 37 °C.

The spleen cells and the FOX-NY myeloma cells were suspended in DME in a 12 ml round bottom tube, the cells were centrifuged, and all the liquid was removed. The myeloma cells and spleen cells were then fused, with careful attention to the mixing times. The bottom of the tube with cell pellet was immersed in a 37 °C water bath. One ml of the 50% PEG 10% DMSO mixture was added to the cells with a 5 ml serological pipette and the cells were mixed with the pipette tip for one minute. One ml of DME was added over the second minute while continuing to mix the cells with the pipette tip, two ml of DME was added over the third minute, and six ml of DME was added over the following five minutes.

The cells were washed in DME and resuspended in DME with 20% FBS and added HAT (hypoxanthine, aminopterin and thymidine, obtained as a 100x concentrate from GIBCO). Thymocytes were collected from the thymuses of two four week old CD-1 mice following the same procedure used to collect the spleen cells. The thymocyte and the fused myeloma and spleen cell mixture was diluted to 50 ml in DME with 20% FBS and added HAT, and plated out in 96 well tissue culture plates (with 100 μl cell

suspension/well).

Four days after the fusion, the cells were fed by adding 100 µl of DME with 20% FBS and added HT (hypoxanthine and thymidine) to each well.

Seven days after the fusion, 160 µl of medium was removed from each well and 160 µl of fresh HT medium was added.

Ten days after the fusion, the wells were screened for supernatants that gave a positive reaction in an ELISA with adsorbed ferrichrome A/ BSA and a negative reaction in an ELISA with adsorbed KLH.

Positive cell lines were transferred to 24 well plates and subcloned at 18 days after the fusion. The number of viable cells/ml was counted using a haemocytometer and erythrosin B (80 mg/ml final concentration) to stain the dead cells. The cell suspension was diluted out to 5, 20 or 50 viable cells/ml. Thymocytes from one four week old CD-1 mouse were added and the cells were plated out at 100 µl/well in 96 well plates, with one plate for each dilution of cells. The colonies in each well were counted and the wells were checked for antibody production using the same ELISA procedure that was used after the fusion.

Cells from wells that had one colony and were positive in the ELISA were grown and then stored in liquid nitrogen. Cells from large Petri dishes were diluted one or two days before freezing to ensure that they would be in logarithmic growth phase. The cells from three or four 15x100 mm petri dishes were collected by centrifugation and resuspended in 10ml DME (with 20% FBS and 10% DMSO) that had been equilibrated in 10% CO_2 at 37 °C. One ml aliquots of cell suspension were added to ten freezer vials, and the vials were stored in a styrofoam box in a -70 °C freezer overnight before being transferred to liquid nitrogen.

After subcloning, three positive cell lines were obtained: AC3, AA3 and CC3. The isotypes were determined to be IgG2bκ (AA3 and CC3) and

IgG1κ and λ (AC3). The AC3 cell line was subcloned two more times; after each cycle the supernatants from all subcloned wells with cells were positive for both the κ and λ light chains.

The cells were grown on a large scale in serum free medium with supplements (see Table IV). The cells were grown in 15x100 mm Petri dishes and were diluted slowly, with no more than a two-fold dilution in one day. The supernatants from the cultures were filtered with a 0.22 μm filter to remove residual cell and cell fragments left in suspension after centrifugation, and were filtered with a YM-100 Amicon filter to concentrate the antibody. The antibodies were purified as follows using a column modified with protein A, a protein isolated from the cell wall of *S. aureus* that binds specifically to the Fc portion of antibodies (protein A modified column from Pharmacia, Dorval).

2.4b Antibody purification

The IgG1 from the AC3 cell line was purified (130) in high salt to increase binding to the protein A column. The concentrated tissue culture supernatant was transferred to 3.0 M NaCl with 0.1 M sodium borate, pH 8.9, using the Amicon filter to retain the protein while the buffer was exchanged. The protein solution was applied to the protein A column, which was then rinsed with 10 column volumes of 3.0 M NaCl with 50 mM borate pH 8.9, and with another ten column volumes of 3.0 M NaCl with 10 mM borate. The bound protein was eluted with 0.5 ml aliquots of 0.1 M glycine (pH 3.0). Fractions of 0.5 ml volume were collected and were mixed immediately with 50 μl of 1M Tris pH 8.0. The protein-containing fractions were determined by measurement of the absorbance at 280 nm, and were pooled and stored at -70 °C. The protein A column was cleaned after each use by washing sequentially with 10

Table IV: Supplements for serum - free medium (131)

1. Stock solutions of supplements were made up or purchased at concentrations listed below. The protein solutions and oleic acid were stored at -20 °C, and all other solutions were stored at 4 °C.

insulin	bovine insulin (Sigma) 2 mg/ml in water that had been adjusted to pH 2.5 with HCl
transferrin	Human transferrin (Sigma) 2 mg/ml in DME
ethanolamine	ethanolamine (Sigma) 2mM in DME
sodium selenite	Na_2SeO_3 (Sigma) 200 μM in DME
oleic acid	sodium oleate (Sigma) 431 μg/ml in DME (to give a free acid concentration of 400 μg/ml)
pyruvate	100 mM solution from Gibco
amino acids	10 mM non-essential amino acids solution from Gibco.

2. Final concentrations of supplements in serum-free medium:

insulin	5	μg/ml
transferrin	35	μg/ml
ethanolamine	20	μM
sodium selenite	2	μM
oleic acid	4	μM
pyruvate	1	mM
non-essential amino acids	0.1	mM

column volumes of 2M urea, 1M LiCl and 100 mM glycine.

The IgG2b from the AA3 and CC3 cell lines was purified (132) in low salt. The pH of the culture supernatant was adjusted to 8.0 by addition of 1/10 volume of 1.0 M Tris pH 8.0. The antibody solution was applied to the column which was then rinsed with 10 column volumes of 100 mM Tris pH 8.0 and with another ten column volumes of 10 mM Tris pH 8.0. The bound protein was eluted the same way as the IgG1.

2.4c ELISA results with the monoclonal antibodies

The three monoclonal antibodies obtained from the cell fusion were purified in order to increase the chances of obtaining an antibody that would perform well in a solid phase immunoassay. Since monoclonal antibodies have only one binding specificity, it is possible for antigens in an inappropriate orientation on a surface to present no antibody binding site towards the surrounding solution. Since the three antibodies raised seemed to have similar affinities for ferrichrome A on the assay plates (Fig. 24), only one was chosen for use in this project. The antibody AC3 was chosen because the the other two antibodies were of the subclass IgG2b, which tends to precipitate in low salt concentrations (133) (it also had a slightly higher affinity for ferrichrome A).

The binding of the antibody AC3 was inhibited by free ferrichrome A in solution (Fig. 25).

2.4d SDS-PAGE procedure for the antibody AC3

Polyacrylamide gel electrophoresis in sodium dodecylsulfate (SDS-PAGE, 134) was used to estimate the purity of the AC3 antibody preparation. Reagents were combined as described in Table V and cast as rod gels on 125 mm long glass tubes with an inner diameter of 5 mm. An

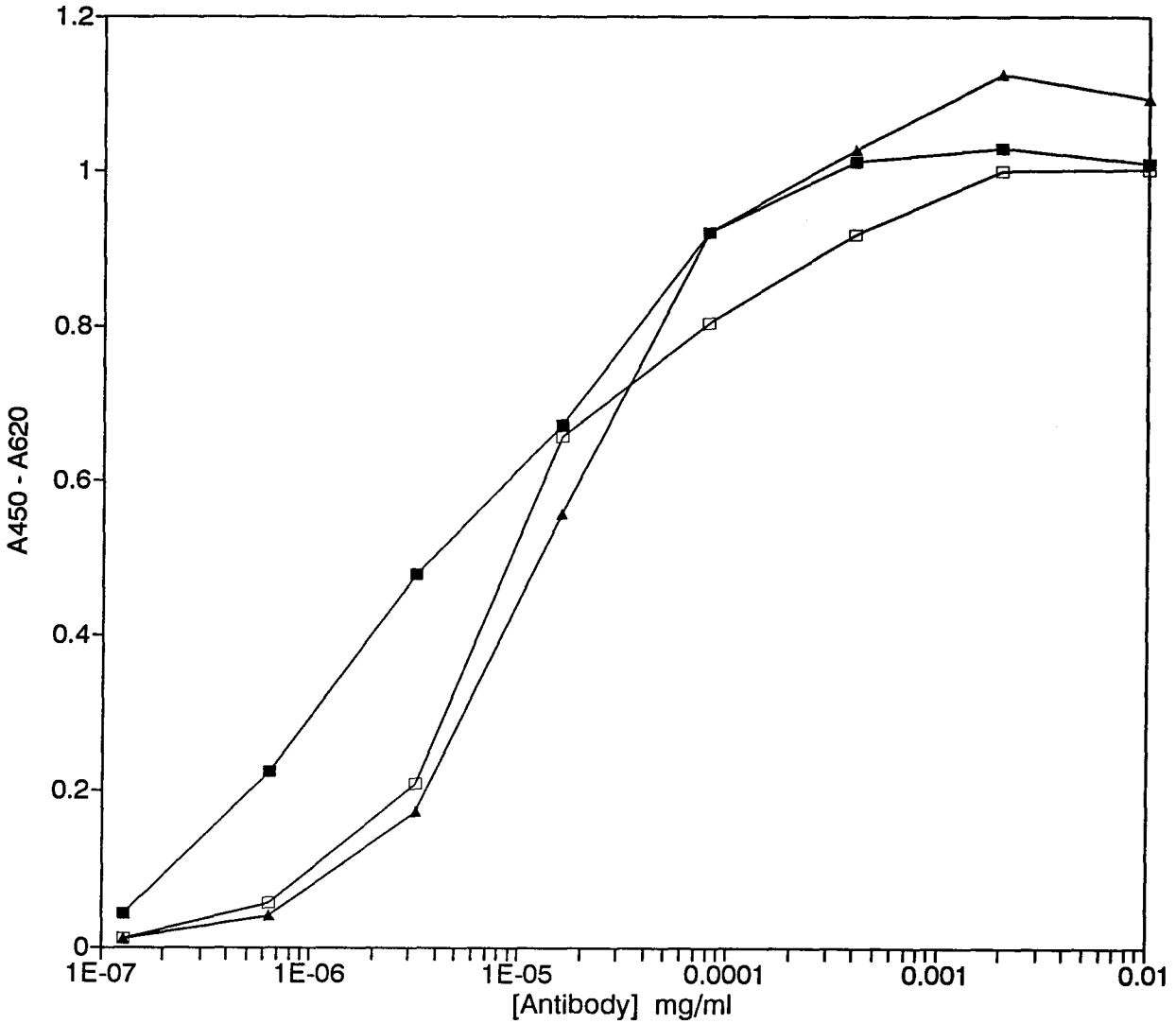

Figure 24: ELISA with the purified monoclonal antibodies and ferrichrome A/BSA adsorbed to the plate. Results are shown for AC3 (■), CC3 (□) and AA3 (Δ).

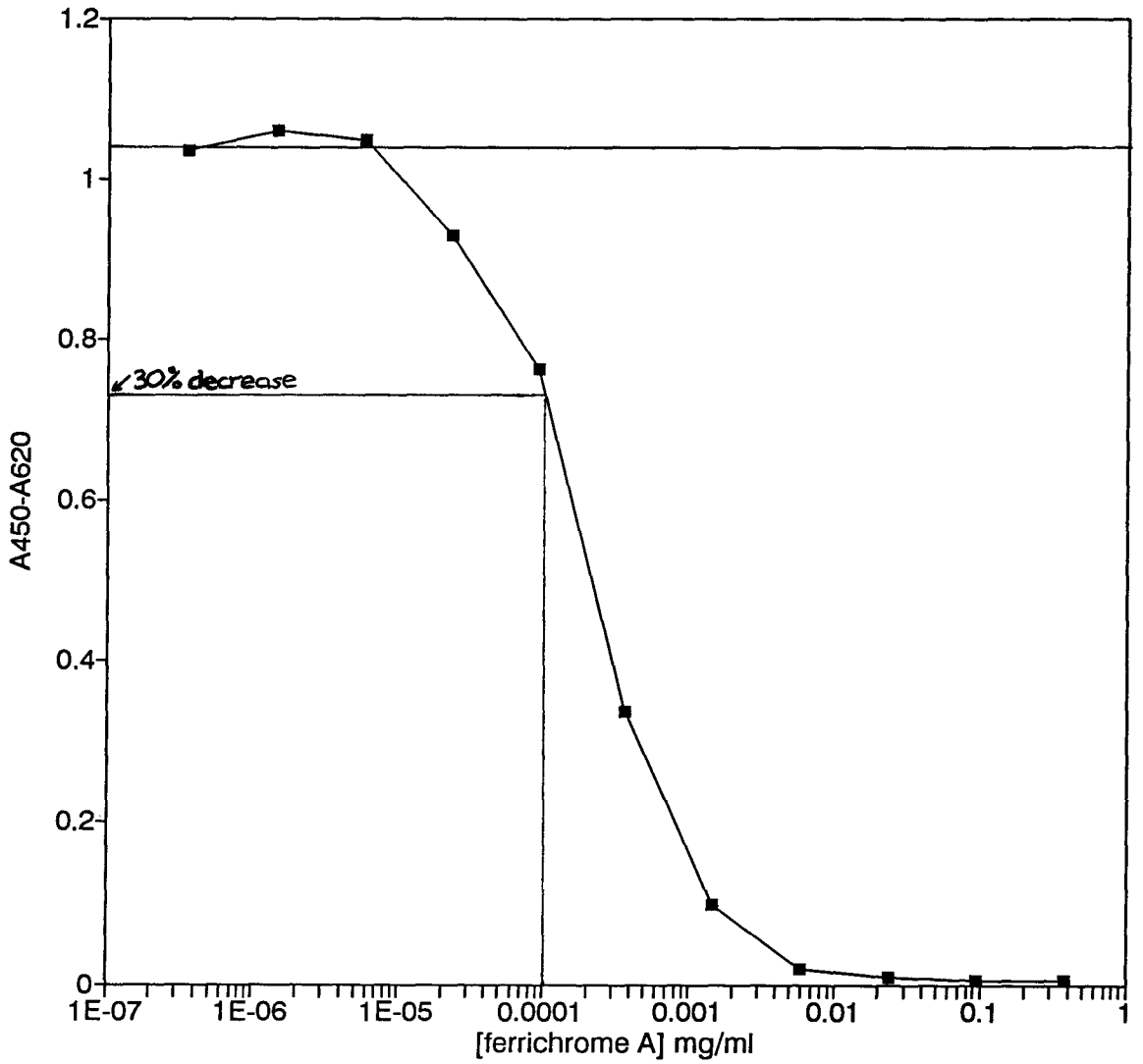

Figure 25: ELISA with monoclonal antibody and ferrichrome A/BSA adsorbed to the plates: inhibiting the antibody with free ferrichrome A.
—— indicates absorbance for antibody with no ferrichrome A in solution (antibody concentration = 1.4×10^{-5} mg/ml).

overlay of the gel solution without acrylamide was added to ensure a flat upper surface on the gel. After the acrylamide had gelled at room temperature, the overlay solution was flushed away with running buffer, the samples were mounted in a Bio-Rad model 150A electrophoresis chamber, and the apparatus was equilibrated at 4 °C. The antibody in buffer was mixed with reducing or non-reducing sample preparation buffer (Table V) at a 1:1 ratio by volume and boiled for one minute. Samples were layered on to the gel surface and the current was set at 0.5 mA per tube until the samples entered the gel. The electrophoresis was then carried out at 4 °C at a current of 6 mA per tube.

Gels were removed from the tubes with a 2% w/v solution of glycerol in water added with a flexible hypodermic needle inserted between the gel and the tube wall. The position of the pyronin Y tracking dye was marked with ink and the gels were stained and fixed for one hour with Coomassie Blue solution (Table V), followed by destaining in a solution of 30% v/v methanol and 5% v/v acetic acid (135).

The gels were scanned for dye binding at a wavelength of 595 nm in a Beckman Model 25 spectrophotometer fitted with a gel scanning attachment.

2.4e SDS-PAGE results for AC3: an indication of the antibody purity

The characteristic proteins in human serum were used as molecular weight standards for the gel scans (Fig. 26). Molecular weight was plotted as a function of mobility on the gel and the calibration curve thus obtained was used to estimate the molecular weights of the protein in the antibody samples (Appendix 2). The non-reduced IgG showed a molecular weight of about 101 000 g/mol. This is much lower than the actual molecular weight for mouse IgG of about 160 000, but mouse IgG1

Table V: Preparation of gels and reagents for SDS-PAGE

1. Stock solutions. The following solutions were made up for use in preparation, running and staining of the SDS-PAGE gels:

10x buffer	0.4 M Tris, 0.2 M sodium acetate, 0.02 M EDTA, pH 7.4
30% acrylamide/BIS	30% w/v acrylamide (Bio-Rad, Richmond CA), 1.2% w/v N,N'-methylene-bis-acrylamide (Bio-Rad) The acrylamide/BIS solution was degassed before use.
Running buffer	100 ml 10x buffer and 50 ml 4% SDS (Bio-Rad), made up to one litre with water.
Sample reagent	20 mM Tris-HCl, 2 mM EDTA, 2% w/v SDS, 14% w/v sucrose, 20 μg/ml pyronin Y, with pH adjusted to 8 using acetic acid.
Reducing sample reagent	as above with 50 mM 2-mercaptoethanol
Coomassie blue stain/fix	0.2 g Coomassie Blue G250, 27.5 ml methanol, 30.5 ml acetic acid, made up to 500 ml with water.

2. Reagents for casting gels. Reagents were combined in the order listed, to give a final acrylamide concentration of 3%.

30% acrylamide/BIS	3 ml
10x buffer	3 ml
4% w/v SDS	1.5 ml
0.5% w/v N,N,N',N'-Tetramethylethylenediamine (TEMED, Bio-Rad)	1.5 ml
water	18 ml
1.5% w/v ammonium persulfate (Bio-Rad)	3 ml

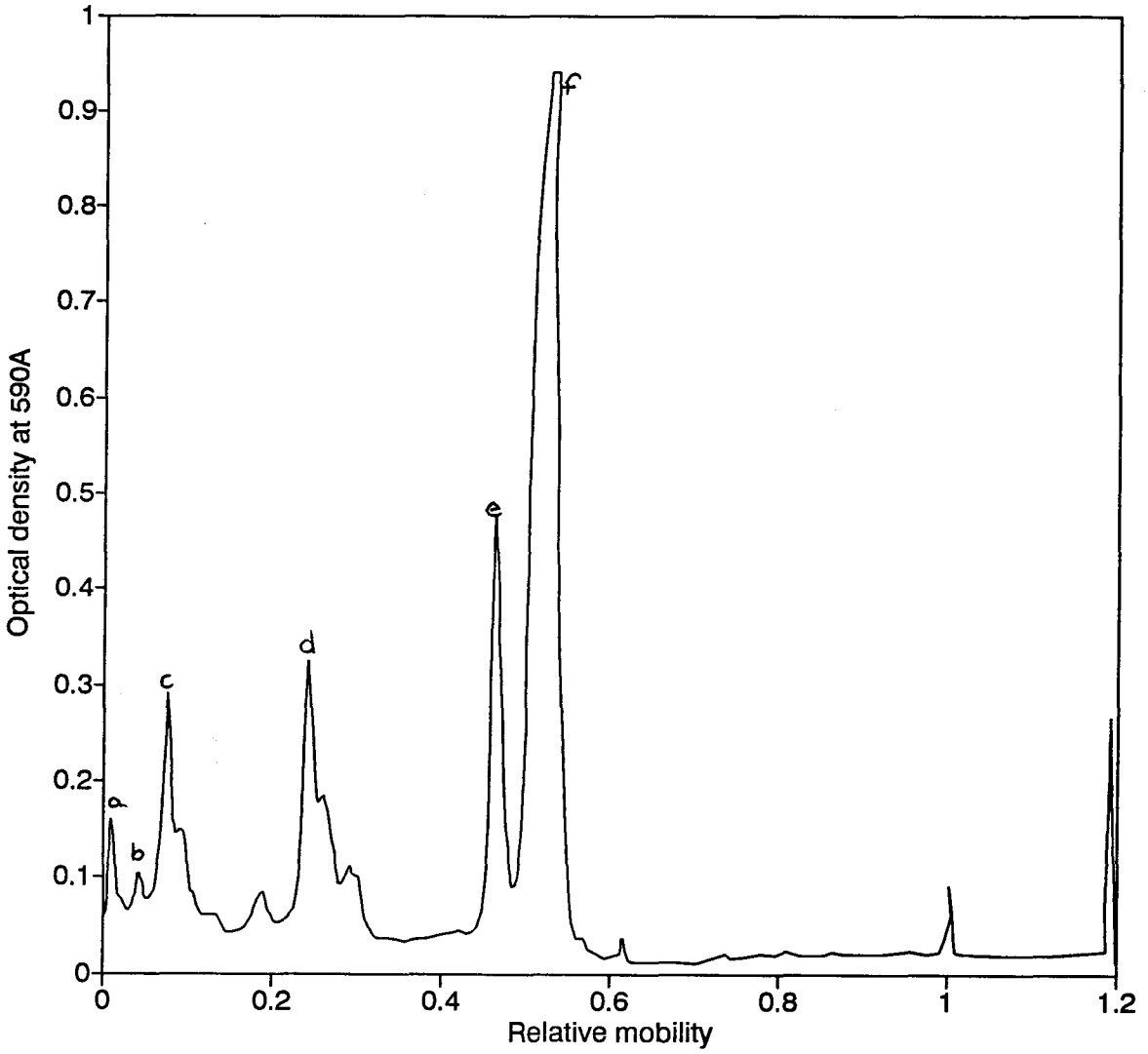

Figure 26: SDS-PAGE of human plasma proteins as molecular weight standards (a= IgM, 950 kD, b= α_2M, 750 kD, c= fibrinogen, 340 kD, d= IgG, 160 kD, e= transferrin, 76 kD, e= transferrin, 76 kD, f= albumin, 66 kD (136)

has been reported to have a fast electrophoretic mobility (133) that would give it a low apparent molecular weight.

The gel scans show one band for the non-reduced sample and two bands for the reduced sample, as expected for IgG (Figs. 27 and 28), indicating that there was no Coomassie Blue staining protein impurity present in greater than trace amounts. Addition of mercaptoethanol reduces the disulfide bonds that help hold the IgG tetramer (Fig. 5) together. Addition of the SDS disrupts the remainder of the bonds maintaining the integrity of the IgG so that the heavy and light chains separate and run as distinct bands.

2.5 Synthesis of silica beads

Silica beads were made by hydrolysis of tetraethyl orthosilicate (TEOS, Aldrich, Milwaukee) and subsequent condensation of silicic acid (104). Monodisperse beads are probably formed as a result of a limited number of nucleation sites being produced at the start of the reaction, when the concentration of silicic acid exceeds a critical value C_{sat}^* (132). If C_{sat}^* is greater than the saturation concentration of silicic acid in solution, the silicic acid will condense on the sites that have been formed and eventually lower the concentration below C_{sat}^*, after which particle growth will continue, but no new nucleation will occur. If nucleation sites are only formed over a short period of time, then the final bead preparation will have a narrow size distribution.

The reaction mixture contained ethanol, water and TEOS in proportions of 150:30:6 by volume (100). An ethanol/water solution (464.6 g ethanol, 117.5g water) was saturated with ammonia at 4 °C by bubbling ammonia through the solution until the solution volume stopped increasing. This resulted in 179.7 g of ammonia being dissolved in the

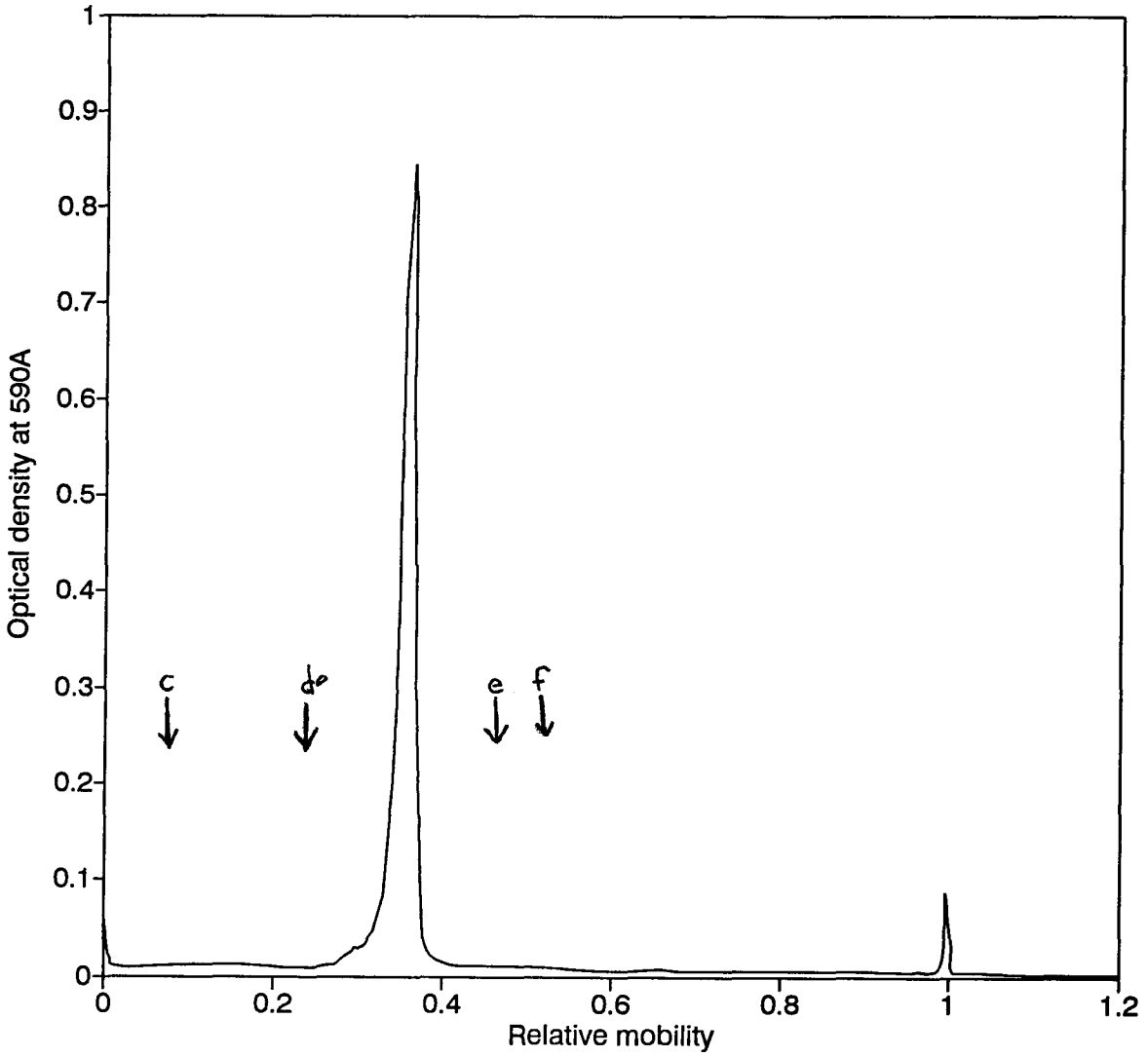

Figure 27: SDS-PAGE of the non-reduced monoclonal antibody AC3. Arrows indicate position of the human plasma protein standards (Fig. 26) (c= fibrinogen, 340 kD, d= IgG, 160 kD, e= transferrin, 76 kD, f= albumin, 66 kD).

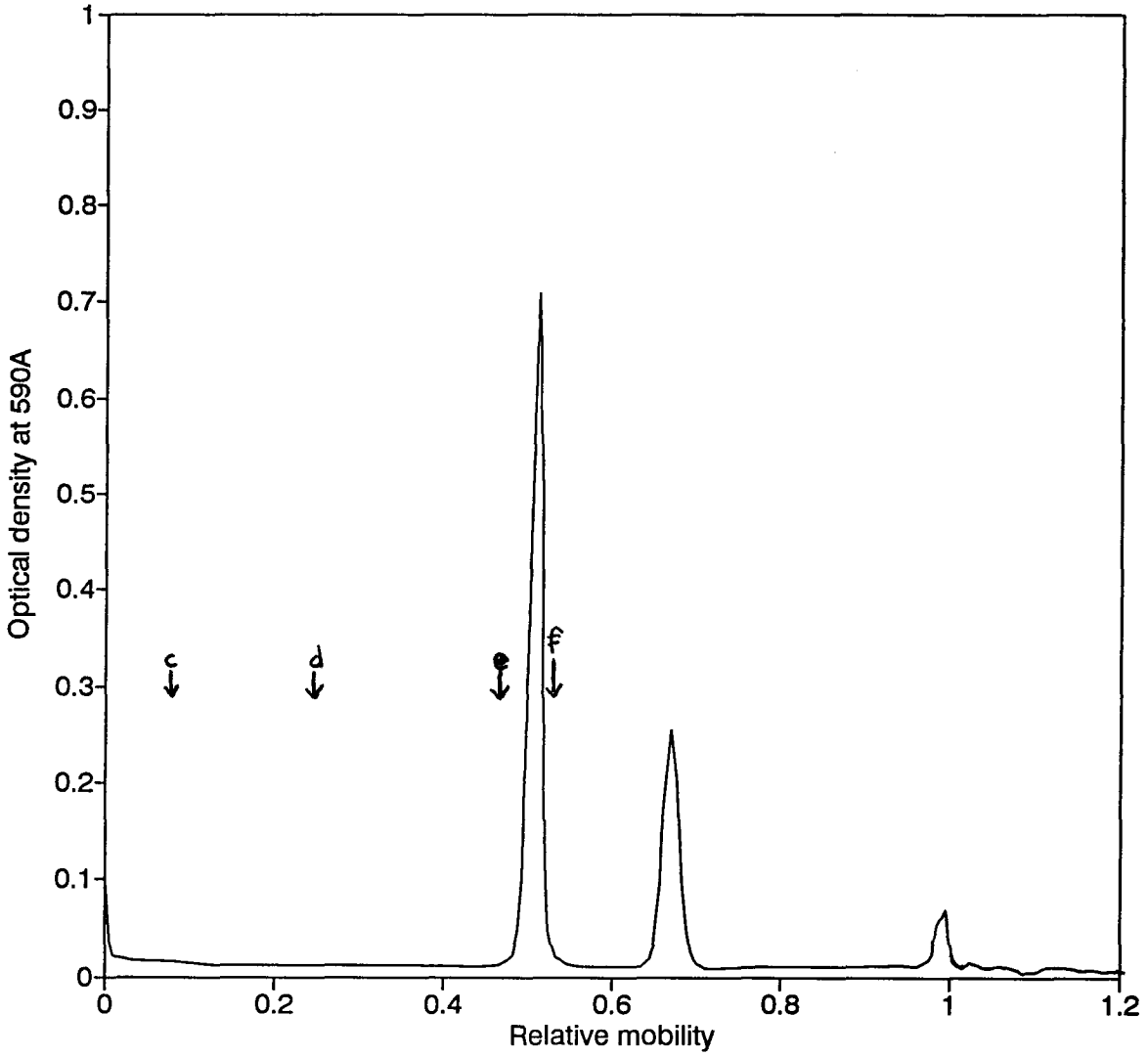

Figure 28: SDS-PAGE of the reduced antibody AC3. Arrows indicate position of the human plasma protein standards (Fig. 26) (c= fibrinogen, 340 kD, d= IgG, 160 kD, e= transferrin, 76 kD, f= albumin, 66 kD).

solution. The reaction flask was transferred to a -20 °C cold room and equilibrated in an ethylene glycol bath. Distilled TEOS (21.75 g) was added to a glass syringe and also equilibrated at -20 °C. The TEOS was added as rapidly as possible through the syringe while the ethanol/water/ammonia solution was being stirred rapidly.

The reaction mixture turned opalescent four minutes and 30 seconds after addition of the TEOS, indicating formation of the nucleation sites. The reaction was allowed to proceed overnight, after which the silica beads were collected by centrifugation.

All glassware used in producing the silica beads was cleaned with chromic acid before use to minimize contamination on the surface of the beads.

Spherical beads with a fairly uniform size distribution were obtained (Fig. 29). The bead size distribution was determined using photographs with a total of 314 beads. The area of each bead was determined by tracing the photograph on a digitizing board and using commercial analytical software (Bioquant). The diameter of the beads was calculated by assuming that images of the beads were circular. An average diameter of 0.779 ±0.042 μm (± 1 s.d.) was calculated, with a bead size distribution shown in Fig. 30. As can be seen from the photograph and from the size distribution, the scatter in the bead diameter results from bead aggregation (or from nucleated sites aggregating before the polymerization has finished). Larger non-spherical beads can be seen in the photographs and appear to be the result of aggregates that have formed during the polymerization.

The density of the silica beads was measured by centrifugation in a sulfuric acid solution. The beads were suspended in the acid solution by

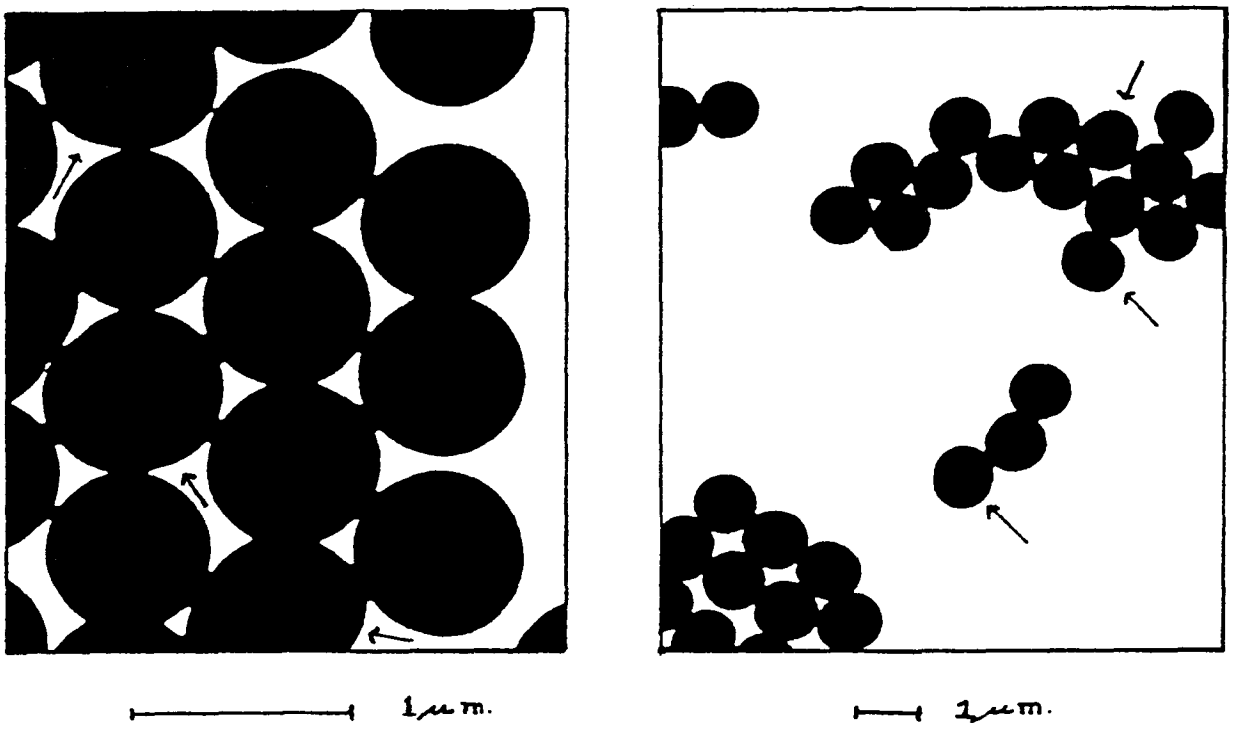

Figure 29: TEM photograph of silica beads. Arrows indicate examples of non-spherical beads.

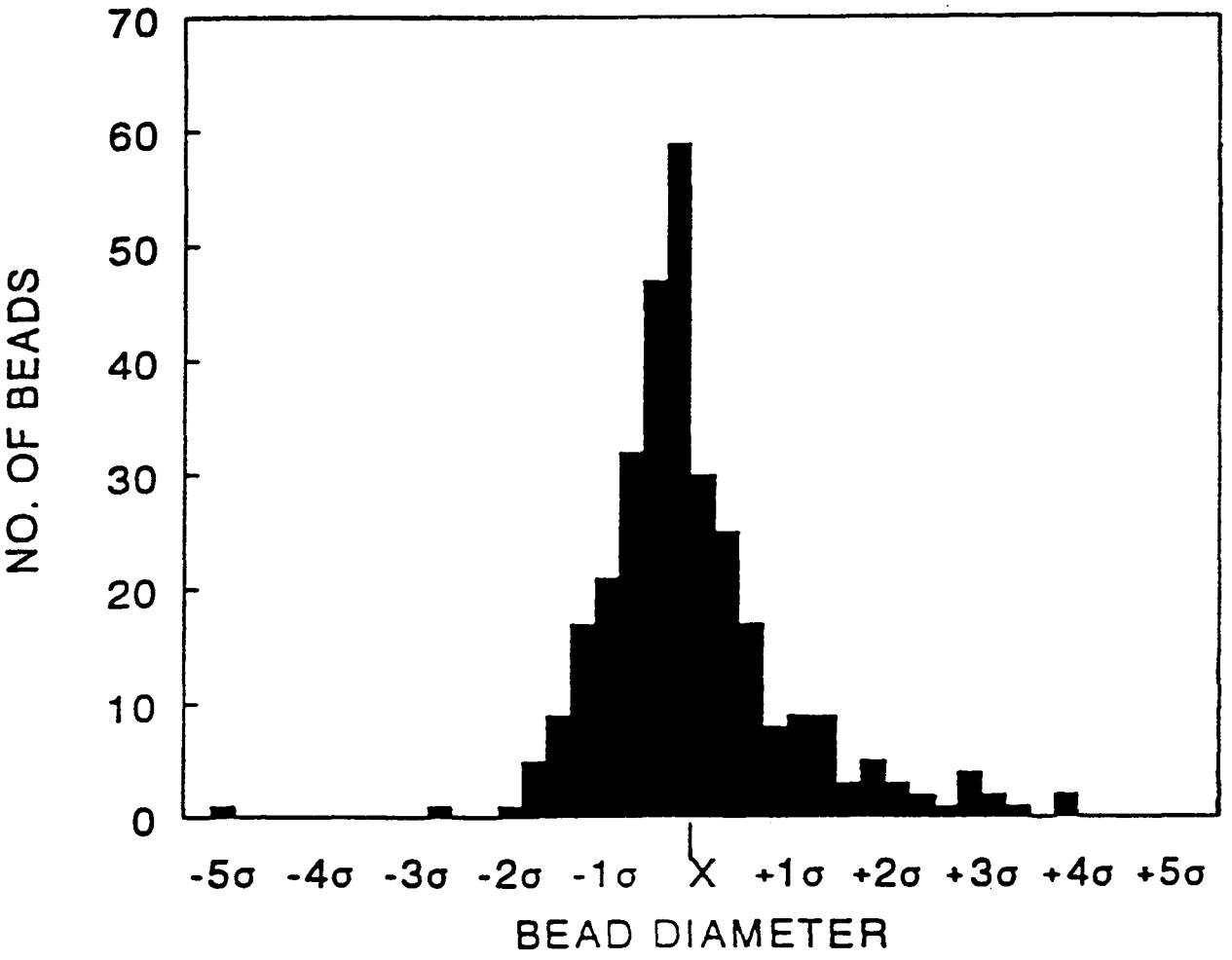

Figure 30: Silica bead size distribution showing the number of beads as a function of bead diameter, where bead diameter is shown as $X \pm n\sigma$ (X = 0.779 μm and σ = 0.042 μm)

sonication and vortexing and then centrifuged at 5 500 x g. In concentrated sulfuric acid solutions, the beads floated to the top after the centrifugation. The density of the sulfuric acid for the isopycnic system was measured and found to be 1.83 g cm^{-3}.

The specific area of the beads was 4.2 x 10^4 cm^2 g^{-1}.

2.6 XPS measurements

X-ray photoelectron spectroscopy (XPS) measurements were done by Dr. Philip Wong using a Leybold Heraeus MAX 200 spectrometer. Silica or glass slides cleaned as described in section 2.7 were put under vacuum and were stored for up two months before analysis. The samples were mounted on the sample holder using copper strips and transferred through air to the loading chamber of the XPS machine, which was evacuated overnight to a final pressure of approximately 1x10^{-8} mbar. The samples were then transferred to the analysis chamber and analyzed at a pressure of 8x10^{-9} mbar using a 2x4 mm sample area near the centre of the slide, chosen visually to avoid the copper binding strips. Samples were analyzed using an Alkα 1486.6 eV X-ray source (excitation voltage 15.0 kV, emission current 25.0 mA) or with a Mgkα 1253.6 eV source (excitation voltage 15.0 kV, emission current 20.0 mA).

Ejected photoelectrons were measured normal to the surface of the silica unless otherwise specified. The kinetic energy of the photoelectrons was measured using a hemispherical analyzer at a constant pass energy of 192 eV. The carbon 1s peak at 285.0 eV (108) was used for charge correction of the measured binding energies.

The relative amounts present were calculated for all elements detected with photoelectrons in the binding energy range of 100-1100 eV (Mgkα X-ray source) or 100-1300 eV (Alkα X-ray source). Areas under

characteristic peaks for each element were measured from narrow scans of the peak region, with baselines determined visually. Atomic percentages for the elements were calculated using the elemental sensitivity factors provided by the instrument manufacturer.

2.7 Cleaning the silica

Silica was cleaned before modification with the silane in order to remove the contaminating surface layer of hydrocarbon. Since there should be no carbon present in the substrate, samples can easily be checked for contamination by taking XPS measurements to determine the atomic % of carbon in the surface region, as described in section 2.6.

Initial studies were made using glass slides (Canlab). Various cleaning and drying procedures were tried to minimize the amount of carbon at the surface. Subsequent studies were carried out with clear fused quartz microscope slides (Quartz Scientific International, Fairport Harbour). The slides had trace impurities, but none in sufficient quantities to be detectable by XPS (Na 1.0 ppm by weight, Ca 0.6 ppm, Mg 0.1 ppm, and other elements in the ppm range, 133).

Silica or glass slides were cut into 8x8 mm sections, wiped clean with lens paper, and placed in separate 13x100 mm glass test tubes. All cleaning and drying procedures were carried out in these test tubes in order to minimize sample handling.

Slides were heated at 80 ^{o}C for one hour in chromic acid made with Fisher Chromerge solution and concentrated sulfuric acid or with a slurry of 5 g potassium dichromate and 5 g water added to 100 ml of concentrated sulfuric acid. Some slides were rinsed with water (distilled then deionized using a Millipore milli-Q ion exchange apparatus), and dried in a laminar flow cabinet equipped with a High

Efficiency Particle Air filter to reduce dust. Some slides were given an additional brief rinse with concentrated hydrochloric acid (BDH AnalaR) and then rinsed again with water and dried in the flow hood.

Some samples were then cleaned with the same procedure (chromic acid followed by an HCl rinse) and dried in vacuum; this resulted in a significantly lower amount of carbon at the surface (section 3.1). Samples for subsequent experiments were cleaned for one hour in chromic acid at 80 °C, rinsed with water, rinsed briefly with concentrated HCl, rinsed again with water, and then dried and stored under vacuum.

The silica beads were cleaned by the same procedure, but were cleaned in a glass centrifuge tube so that they could be rinsed by centrifugation and resuspension in the tube.

Cleaned slides were stirred for one hour in refluxing heptane (BDH OmniSolv, BDH, Toronto), the solvent used for the silylation reaction (section 2.8). The slides were dried, rinsed with water and dried again, following the same procedure used for the silylation to determine the effect of the solvent.

Some attempts were made to clean the slides with hot concentrated nitric acid, but this gave irreproducible results with some very high oxygen to silicon ratios. This may be due to the silica being oxidized.

2.8 Surface modification of the silica with silane

Silica slides and beads were modified with alkyl trialkoxysilanes, which react as shown in Figure 9. The alkoxy groups hydrolyze to form silanols, which then react by condensation with silanols on other silane molecules or on the silica surface. The water required for hydrolysis can be supplied as water adsorbed to the silica or in the solvent. The reaction is often carried out in water (137), but this can result in

polymerization of the silane in solution to form large clumps, which then react with the silica surface to form an uneven coating (134).

All glassware was cleaned with chromic acid before use. Freshly distilled silane was added to heptane (BDH OmniSolv) at a 1% w/v ratio and stirred briefly before addition of the silica beads or slides. The reaction was carried out in a 250 ml round bottom flask stirred from the bottom with a magnetic stirrer. The silica beads dispersed readily in the silane solution. The solution was heated to reflux for one hour, after which the silica was rinsed in fresh heptane, dried under vacuum, and stored overnight at room temperature (22 ^{o}C) under vacuum. The modified silica was then sonicated in water for one minute to remove any polymerized clumps of silane adsorbed to the surface, and dried under vacuum after removal of most of the water with a pipette.

2.9 Ferrichrome A on beads: non-specific adsorption

2.9a Measurement of ferrichrome A adsorption

Silica beads were modified with 3-aminopropyltriethoxy silane as described above. The amount of ferrichrome A adsorbed or attached to the beads under various conditions was determined by solution depletion measurements of ferrichrome A as measured from the absorbance.

Modified silica beads were weighed into 1.5 ml polyethylene centrifuge tubes. For a series of measurements with a given weight of beads, all samples were within 2% of the stated amount. The ferrichrome A solution was centrifuged to clarity before use to ensure that there was no undissolved ferrichrome A in suspension, and the concentration of the resulting solution was determined from the absorbance. The solution (0.75 ml) was pipetted onto the bead samples, which were immediately suspended by sonicating and vortexing. The samples were then mixed at

room temperature, after which they were centrifuged at 11 600 xg and the supernatants were collected. The supernatants were centrifuged again before the concentration of ferrichrome A in solution was measured. The concentration of ferrichrome A was determined from the derivative of the absorbance curve as described in section 2.1.

The amount of ferrichrome A which washed off the beads in PBS was also measured. All the solution on top of the pellet was removed by blotting with a piece of tissue paper. The beads were resuspended in 0.75 ml PBS using a glass stir rod followed by sonication and vortexing. The amount of ferrichrome A which washed off into PBS was measured from the derivative of the absorbance curve, and the amount of ferrichrome A left on the beads after the PBS rinse was calculated.

The weight of the beads was varied, as well as the adsorption time, ferrichrome A concentration, and salt concentration. The amount of ferrichrome A adsorbed per unit area (specific adsorption) was calculated from the amount lost from solution and the surface area of the beads. The surface area of the beads was calculated from the weight of the bead sample and the specific area of 4.2×10^4 cm^2 g^{-1} (section 2.5).

2.9b Effect of bead storage time on ferrichrome A adsorption

If the beads were stored after modification with the silane, they would not suspend readily when sonicated. Some beads were left as large (easily visible) lumps that settled out rapidly, although a portion of the beads did suspend as usual. The total amount adsorbed decreased as the beads were stored for longer periods of time (Table VI). This decrease is presumably due to a smaller area of beads being available, and does not indicate a smaller amount per unit area. A large effect was

Table VI: The amount of ferrichrome A adsorbed as a function of the storage time for the beads between the silylation and the ferrichrome A adsorption

Storage time (days)	amount adsorbed (mg/m^2)
0	2.12
2	2.0
10	1.03

Table VII: The amount of ferrichrome A adsorbed as a function of the time for adsorption (equilibrium solution concentration of ferrichrome A = 0.27 mg/ml)

adsorption time (min)	amount adsorbed (mg/m^2)
1	2.20
2	2.20
10	2.15
20	2.20
60	1.91
1200	1.18

seen if the beads were stored for a week before use. Unless otherwise specified, experiments were carried out within two days of the beads being sonicated in water and dried in the final step of the modification. Samples were checked after sonication to ensure that there were no visible aggregates remaining.

2.9c Adsorption as a function of time

The ferrichrome A adsorbed rapidly to the beads (Table VII), with no change in the amount adsorbed being observed between a one and twenty minute adsorption time. A decrease in the specific adsorption was seen as the beads settled out of suspension overnight (Table VII). A ten minute adsorption time was chosen for subsequent experiments

2.10 Reaction of ferrichrome A and EDC

2.10a Some possible reactions of ferrichrome A and EDC

Carbodiimides can be used to promote the formation of peptide bonds, by a mechanism shown in Figure 31. Figure 31 also shows an interfering side reaction: the activated ester formed by reaction of the carboxyl group with EDC can hydrolyze to give the carboxyl group as before and a urea. The rate of hydrolysis may be very rapid, with a rate constant as high as 2-3 s^{-1} at pH 4.7 (138). This would give a half life for the activated ester of 0.28 s.

Ferrichrome A could also react through the serine group to form a stable o-acylurea, or possibly through the hydroxamate groups (Fig. 11). The iron is very tightly bound (the stability constant of desferriferrichrome A and Fe^{3+} is $\cong 10^{32}$ (137)) , but will exchange freely with iron in solution, so the hydroxamate groups could be available transiently to react with EDC.

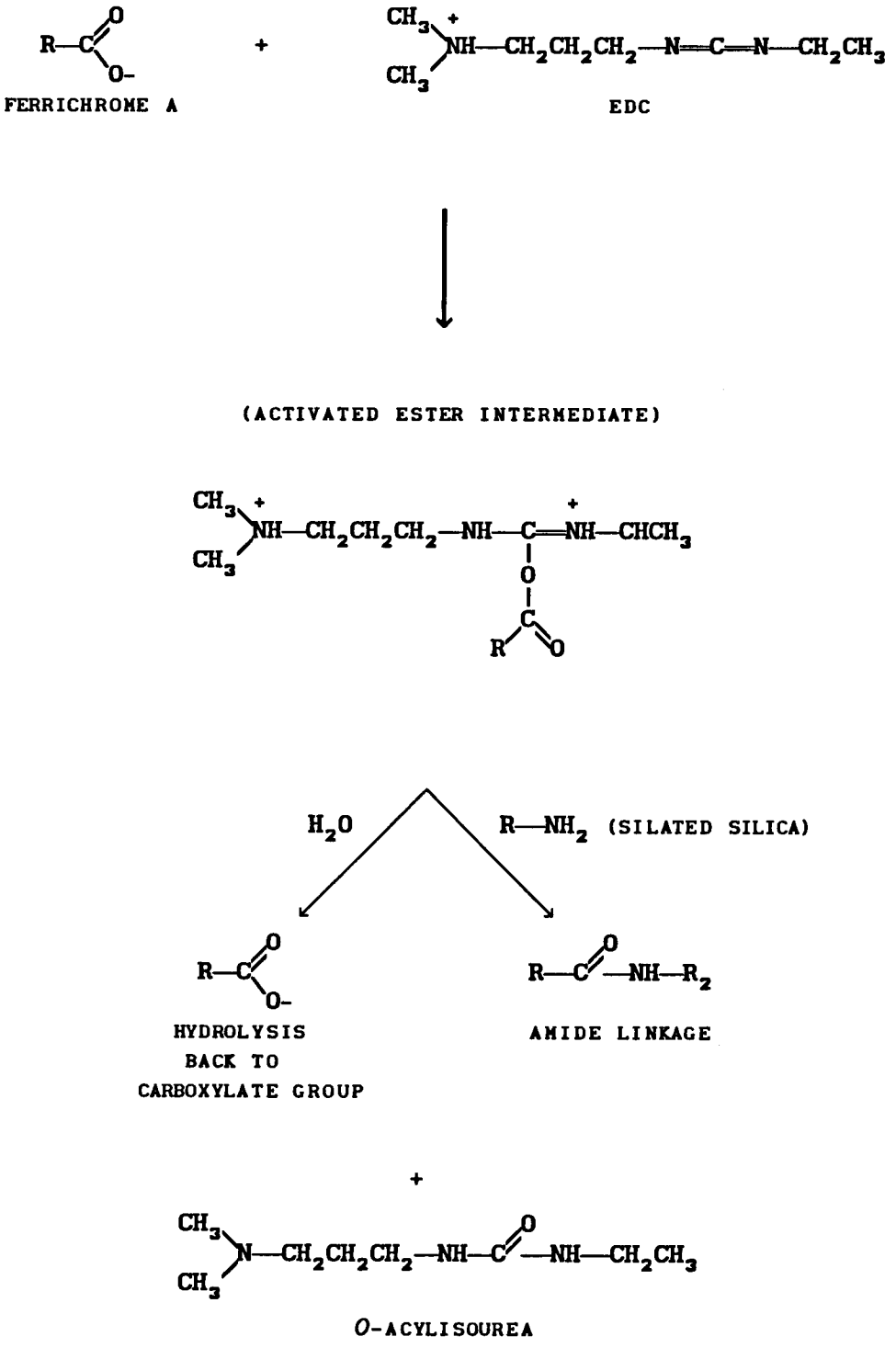

Figure 31: Carbodiimide coupling mechanism

2.10b Reactions of ferrichrome and EDC

Ferrichrome is another metabolite of *Ustilago sphaerogena* that does not have a serine residue or any carboxyl groups (Fig. 32). Ferrichrome was kindly provided by Allen Budde, Department of Plant Pathology, University of Wisconsin. Ferrichrome and EDC were mixed together to show that the peak that appears at 367 nm in absorbance spectrum of the ferrichrome A/EDC mixture is not due to the reaction of EDC with the hydroxamate groups.

2.10c The EDC:ferrichrome A mole ratio

The ratio of ferrichrome A to EDC used was chosen by determining the amount of EDC required to solubilize the ferrichrome A rapidly. Ferrichrome A is not very soluble in water, but will dissolve readily after reaction with EDC. Ferrichrome A was added to water at a concentration of 4.06 mg/ml and suspended by sonication. The suspension was pipetted into separate centrifuge tubes, and dry EDC was added to give mole ratios of EDC:ferrichrome A ranging from 0 to 68.6. The mixtures were sonicated for ten minutes, after which the undissolved ferrichrome A was separated by centrifugation and the supernatant was removed. The supernatant was diluted by a factor of 10 in water and the absorbance was measured.

Figure 33 shows that increasing amounts of ferrichrome A dissolve within ten minutes as the EDC concentration increases. All the ferrichrome A is dissolved when EDC is added at a mole ratio slightly higher than 40:1. Although this does not necessarily mean that all the carboxyl groups on ferrichrome A have reacted with EDC at this mole ratio, it does imply that up to a ratio of 40:1 of EDC:ferrichrome A,

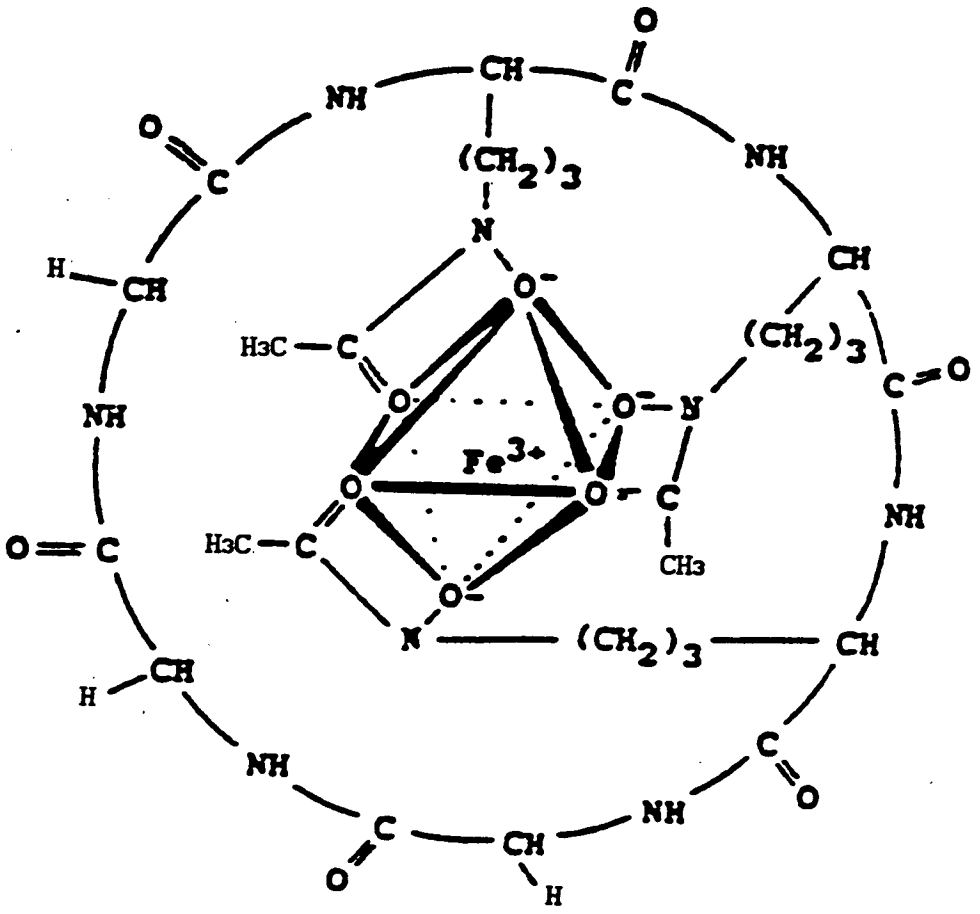

Figure 32: Structure of ferrichrome

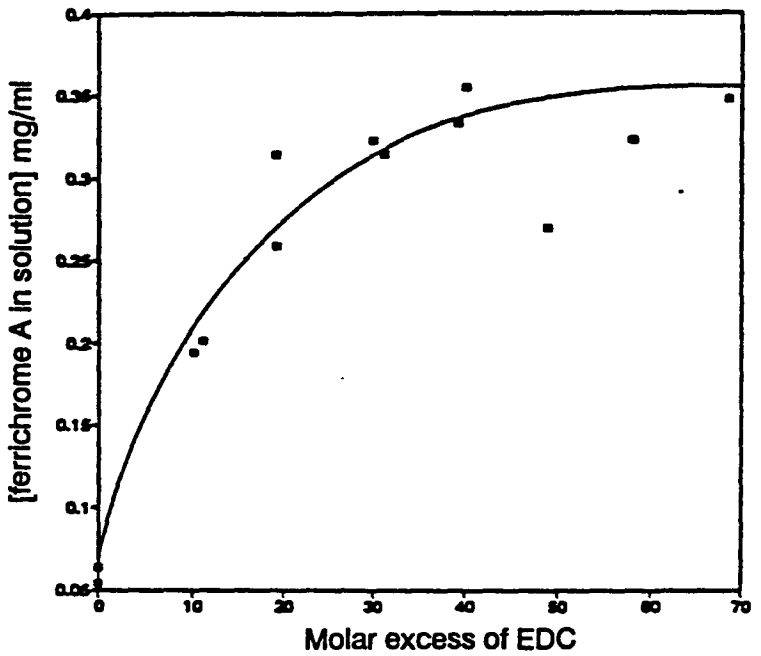

Figure 33: Choosing the EDC: ferrichrome A mole ratio. Increasing amounts of ferrichrome A were added to a 4.06 mg/ml suspension of ferrichrome A. The amount of ferrichrome A in solution after ten minutes was measured and plotted as a function of EDC:ferrichrome A mole ratio.

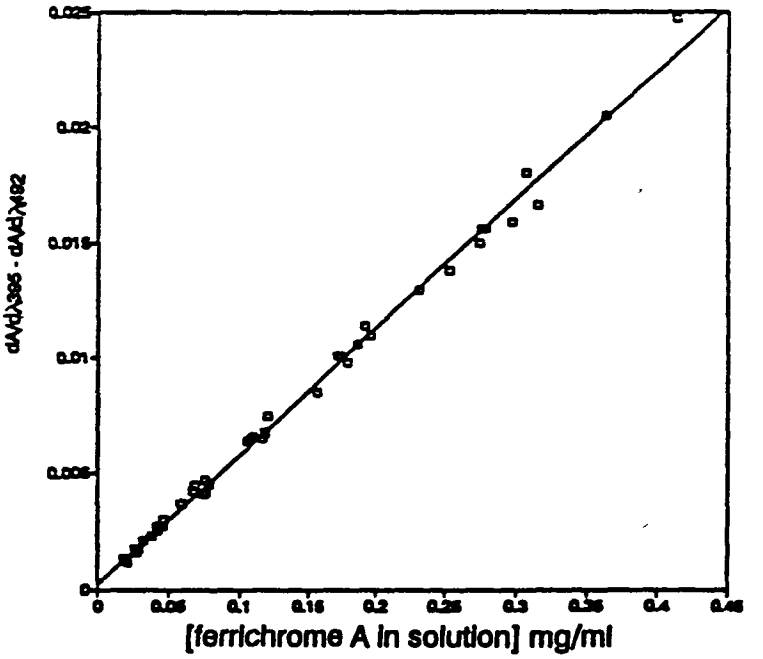

Figure 34: Determining the concentration of ferrichrome A from the derivative of the absorbance spectrum $dA/d\lambda$ for a solution with a 50:1 mole ratio of EDC: ferrichrome A.

increasing the amount of EDC will increase the extent of the reaction with ferrichrome A. A ratio of 50:1 was chosen for future experiments.

2.10d Extinction coefficient for ferrichrome A with EDC

Concentration of ferrichrome A in the presence of a 50:1 ratio of EDC was determined from the derivative of the absorbance curve at 395 nm and at 492 nm. A series of different concentration solutions of ferrichrome A was made up in water. Concentration of ferrichrome A was determined from the absorbance of the solutions. The EDC was added to the solutions at a 50:1 ratio, and the derivative of the absorbance was measured. The difference between the derivative at 395 nm and at 492 nm was plotted against concentration (Fig. 34); information from a linear least squares fit of this data was used to calculate the concentration of ferrichrome A in EDC solutions (the slope was 0.0567±0.0004, where 0.0004 = 1 σ).

2.11 Modification of silica beads with ferrichrome A and EDC

2.11a The reaction procedure

Silylated silica beads were weighed into polyethylene centrifuge tubes. Ferrichrome A solutions were made in water (unless otherwise specified), and were centrifuged to clarity before use. The ferrichrome A concentration was determined from the absorbance, and the amount of EDC required to give a 50:1 ratio was also weighed into polyethylene centrifuge tubes. The ferrichrome A solution was added to the EDC and mixed for 40 s before being pipetted onto the beads (0.75 ml). Immediately thereafter, the beads were sonicated and vortexed until a homogeneous suspension was obtained. The suspension was then mixed at room temperature (21-22 $^{\circ}$C) for 10 min before the beads were separated

by centrifugation. The supernatant was removed and stored in another polyethylene centrifuge tube and was centrifuged again to remove remaining beads before the absorbance was measured. The excess supernatant was removed from the initial bead pellet by blotting with tissue paper, and the beads were resuspended in 0.75 ml PBS by stirring with a glass rod followed by sonication. The PBS supernatant was collected after centrifugation and stored in a polyethylene centrifuge tube before the absorbance was measured. These samples were also centrifuged again before the absorbance was measured.

2.11b Some comments on the procedure

Forty seconds was chosen as the minimum convenient mixing time. This is a very long time if the rate constant for hydrolysis is on the order of 2-3 s^{-1} (138), but resulted in successful attachment of the ferrichrome A to the silica (see 3.3c).

Since ferrichrome A is a cyclic peptide, there are no amine groups and no concern about the ferrichrome A cross linking to itself before addition to the beads.

The beads could be suspended in a small volume of EDC solution, followed by addition of ferrichrome A. This would avoid the 40 s mixing time during which the activated ester could hydrolyze before addition to the beads. Although this might result in more ferrichrome A attached to the beads, the method used was chosen to simplify measuring the amount of ferrichrome A adsorbed: one ferrichrome A and EDC solution could be made in sufficient volume to add to replicate samples of beads, with solution left over to measure the concentration of ferrichrome A in the initial solution directly by absorbance rather than by calculation of dilution factors.

2.11c Varying the pH of the reaction mixture

The pH of the ferrichrome A solutions with EDC in water was about 5.7. Since the activated ester may be more stable at lower pH (138), some experiments were carried out after addition of hydrochloric acid to the ferrichrome A solution to lower the pH to 4.7 after mixing with the EDC. This resulted in a 47% decrease in the amount of ferrichrome A left on the beads after rinsing with PBS, and all subsequent experiments were carried out in water.

2.12 The ELISA procedure

2.12a The ELISA procedure for beads

Silica beads (5 or 10 mg/tube) were modified with ferrichrome A in polyethylene centrifuge tubes at a range of ferrichrome A concentrations in water, following the procedure outlined in **2.11a**. A 50:1 mole ratio of EDC: ferrichrome A was used, and the EDC and ferrichrome A were mixed for 40 s before addition to the beads. After ten minutes, the beads were separated from the solution by centrifugation and washed three times with PBS. The beads were resuspended in one ml of PBS, followed by a 1:10 dilution of the suspension in more PBS. The diluted suspension was pipetted into plastic centrifuge tubes in order to give 74 mm^2 total bead area per sample.

The beads were coated in blocking buffer, rinsed, incubated with antibody, and incubated with HRP conjugated antibody in the same way as the silica slides. The ELISAs were developed by suspending the beads in 250 µl of citrate/acetate buffer (Table II), followed by addition of a further 250 µl of substrate solution that was made up with twice the TMB and hydrogen peroxide concentrations that were used for the slides, in order to give final concentrations that were the same. The beads had to

be suspended before adding the substrate because of the time required to suspend the beads and the necessity of incubating the beads with the substrate for a precise amount of time. The reaction with the substrate was stopped by addition of 250 μl of 2.0 M phosphoric acid. The substrate solution was again transferred to an ELISA plate so that all the absorbances could be read at once, but 50 μl of solution was added to each well instead of 150 μl because of the higher absorbances found.

2.12b The ELISA procedure with flat modified silica

Pieces of flat silica were modified with 3-aminopropyl silane in several batches until enough had been accumulated for an assay. The silylated silica was stored in air between modification and use. Pieces of silica (approximately 4x8 mm^2) were placed in separate glass test tubes. Ferrichrome A solutions at a range of concentrations in water were added to EDC with a 50:1 mole ratio of EDC to ferrichrome A. The EDC and ferrichrome A were mixed for 40 s before being added to the slides (0.5 ml/test tube). The tubes were then mixed on a orbital shaker for ten minutes before the slides were removed and rinsed with PBS.

The remainder of the ELISA steps were carried out with the modified slides remaining in the same test tubes, following the procedure described in Fig. 2. Uncoated sites were blocked by incubation for 30 min at 37 °C in blocking buffer (0.2% Carnation skim milk and 0.05% Tween 80 in PBS). Slides at different surface concentrations of ferrichrome A were incubated with a dilution series of antibody in blocking buffer, then with an HRP conjugated antibody also diluted in blocking buffer. Both of the antibody incubation steps were done at 37 °C for one hour with 0.5 ml solution. The slides were rinsed three times after each incubation step by vortexing in PBS-Tween.

The slides were next transferred to clean test tubes to avoid problems with antibody adsorbed non-specifically to the walls of the tube. The ELISAs were developed with 500 µl of the TMB solution used in section 3.3a (Table II). The reaction was stopped after three minutes by addition of 250 µl of 2.0 M phosphoric acid and the substrate solution was transferred to an ELISA plate (150 µl/well) so absorbances of all the samples could be read at once with an SLT plate reader. The absorbance was read at 450 nm, with a reference at 620 nm.

Because the slides were not precisely 64 mm^2, the area of each slide was measured. The area was assumed to be directly proportional to the final absorbance reading (section 2.3f) and was used to correct the readings to that for a sample with an area of 64 mm^2. The areas were measured by photographing the slides on a background of $1mm^2$ graph paper and then digitizing and measuring the area of the photographs with the Bioquant program, using the graph paper for calibration.

2.12c The ELISA procedure for polystyrene plates

Assays with polystyrene plates were carried out as described in section 2.3.

2.12d ELISAs with plates: measuring the equilibrium concentration of antibody in solution

The antibody concentration given for the ELISA results is, unless otherwise specified, the initial concentration of the antibody solution added to the ELISA plate or test tube. As the antibody binds to the antigen on the substrate surface, the solution concentration of antibody will decrease. The surface concentration of bound antibody is a function of the equilibrium concentration of antibody (85) so the equilibrium

concentration would be a more relevant parameter for binding studies.

The equilibrium concentration of antibody after incubation was measured using AC3 labelled with ^{125}I (section 2.15a).

2.12e Inhibition of the ELISA with free ferrichrome A

The inhibition of antibody binding by free ferrichrome A in solution was also measured. The ELISAs were carried out as before, but using only one concentration of antibody, and incubating it with ferrichrome A before addition to the silica. The antibody was made up to twice the desired final concentration in blocking buffer and pipetted into a series of test tubes. An equal volume of ferrichrome A solution in blocking buffer was added and the antibody and ferrichrome A were incubated for 30 minutes before being added to the silica. The final concentrations of ferrichrome A ranged from $5x10^{-2}$ mg/ml to $5x10^{-8}$ mg/ml.

2.13 Characterization of the substrate: detection of the amines on modified silica

2.13a XPS measurements on flat silica

The silica slides were analyzed by XPS as described in section 2.6, and the percentage of nitrogen on the surface was determined.

2.13b Ninhydrin assay of amine groups on the silylated beads

The extent of modification on the beads was estimated by an assay of the amine groups using ninhydrin (139). A ninhydrin solution (0.5 ml 10 mM ninhydrin in 100 mM sodium acetate pH 5.0) was added to 10 mg of modified beads. The beads were sonicated but remained in small clumps due to the high buffer concentration. The beads and ninhydrin were then

placed in a boiling water bath for 5 minutes, during which time the beads turned blue. When the beads were shaken, the blue colour came off into solution, leaving the beads white. The remainder of the amine-ninhydrin reaction product was washed off the beads with a 50 v/v% solution of ethanol in water. The supernatants from the beads and the ethanol rinse were collected and diluted to one ml. The absorbance of this solution at 570 nm was then used to determine the amount of amines on the surface, with glycine (Fisher, Vancouver) used as a standard.

2.14 Characterization of the antigen on the substrate

2.14a Measuring the amount of ferrichrome A on the beads by solution depletion

The silylated beads used in the assays were coupled to ferrichrome A using EDC at a 50:1 EDC:ferrichrome A mole ratio in water (section 2.11). The surface concentration of ferrichrome A on the beads was determined for different equilibrium solution concentrations of ferrichrome A.

2.14b BCA assay of the amount of ferrichrome A on the beads

The amount of ferrichrome A on the beads was also measured by a bicinchoninic acid (BCA) assay (Pierce, Rockford, IL). The assay measures protein indirectly by measuring the amount of Cu^{2+} reduced to Cu^{+} by protein in alkaline medium. The BCA complexes with Cu^{+} to form a purple product that can be detected by measurement of the absorbance at 562 nm and with an appropriate standard curve the absorbance at 562 nm can be used to determine protein concentration. Since Fe^{3+} can also complex with the BCA to form a product with an absorbance at 562 nm, BCA was added to a ferrichrome A concentration

higher than that used for any of the standard curves, without addition of any Cu^{+}. No colour change was observed.

A standard curve was made up using the Pierce microassay procedure with ferrichrome A as a standard. Ten microlitres of ferrichrome A solution was added to a well in a 96 well ELISA plate. Pierce BCA reagent mixed according to instructions (containing BCA, Cu^{2+}, and buffer) was added (200 µl/well) and the plate was mixed for 30 s before being incubated at 37 °C for varying lengths of time. The absorbance was then read at 560 nm. The concentration of ferrichrome A on the beads was measured by suspending the beads at a concentration of 50 mg/ml and taking a 10 µl aliquot.

2.14c XPS measurements of ferrichrome A on the slides

Silica slides modified with ferrichrome A at different concentrations were analyzed by XPS following the procedure described in section 2.6. A slide with ferrichrome A deposited from an aqueous solution was also measured by XPS. Successive drops of ferrichrome A solution were placed on the slide and dried, until a clear red mark from the ferrichrome A could be seen on the slide.

2.14d Ninhydrin assays of slides modified with acetic acid and EDC

Silylated beads and slides were modified with acetic acid using EDC to promote formation of a peptide bond. The EDC was added to a 1.2 mM solution of acetic acid in water at a 15:1 mole ratio of EDC:acetic acid. The amine groups on the beads were assayed before and after modification to check the efficiency of the acetylation. Acetamide (Fisher, Ottawa) was used as a control for the ninhydrin assay of the amide groups.

2.15 Antibody adsorption isotherms on the modified silica

2.15a Labelling the antibody with ^{125}I

The purified AC3 was labelled with ^{125}I using Bio-Rad enzymobeads (Bio-Rad, Hercules, CA) which have covalently attached glucose oxidase and lactoperoxidase. The enzymobeads are added to a protein solution with glucose and iodide. The glucose oxidase oxidizes β-D-glucose to form hydrogen peroxide. The lactoperoxidase then reacts with the peroxide and iodide to form iodine, which reacts predominantly with the phenolic hydroxyls on tyrosine residues, displacing them and replacing them with an iodide group (140).

One vial of enzymobeads from Bio-Rad was rehydrated by addition of 0.5 ml of water. A fresh 1% glucose solution was prepared in 0.2 M sodium phosphate pH 7.2. The rehydrated enzymobead suspension (50 μl) was added to a polystyrene test tube and mixed gently. The antibody in phosphate buffer (0.2 M, pH 7.2) was added to the enzymobead suspension (200 μl of antibody solution at 0.616 mg/ml, 123 μg total). Sodium iodide with ^{125}I from Amersham (Oakville, Ont.) was added (5 μl at 2.63×10^8 dpm/ml, 1.315×10^6 total), and the reaction was started by addition of 50 μl of the glucose solution.

The free iodide was separated from the labelled protein using a Sephadex G-25 gel exclusion column. A solution of unlabelled IgG (AC3) was run through the column to minimize sticking of the labelled IgG. The labelled protein mixture was run through the column in the same phosphate buffer used in the reaction and twenty drop fractions were collected. One μl aliquots were removed from each fraction using calibrated capillary tubes which were counted with an LKB 1282 Compugamma gamma counter. The counts indicated two peaks in the eluate from the column. Since the antibody elutes in the void volume, the two highest activity

fractions from the first peak were pooled. The protein concentration was determined by absorbance at 280 nm (1 OD = 0.8 mg/ml (130)), and the activity was determined by counting ten 1 μl aliquots in capillary tubes. A specific activity of $(3.83\pm0.10)\times10^{9}$ cpm/mg was determined for the protein. The antibody solution was stored at -20 °C in 100 μl aliquots in plastic centrifuge tubes.

The amount of free label in the protein was determined using thin layer chromatography with Baker-flex silica gel IB2-F TLC sheets. The protein sample in buffer was spotted onto the TLC sheet, and the TLC was run in water. The protein stays at the origin and the iodide moves with the solvent front, so the proportion of free label can be determined by cutting up the TLC sheet and counting the region around the origin and the region around the solvent front. This gave a result of 3.7% free label.

2.15b SDS-PAGE of the labelled antibody

Gel electrophoresis with tube gels was done by Dr. Johan Janzen on native and reduced samples of the labelled and unlabelled protein, following the procedure described in section **2.4d**. The gels for the labelled protein were sliced into 100 slices using a Bio-Rad model 195 electric gel slicer and each slice was counted separately in the gamma counter. The counts at different positions on the gel were then compared to the scans for the Coomassie blue dyed unlabelled protein.

2.15c Comparing the antigen binding activity of the labelled and unlabelled antibody

The labelled and unlabelled antibodies were compared using an ELISA with BSA/ferrichrome A adsorbed to Falcon Pro-bind polystyrene ELISA

plates (Becton Dickinson, Lincoln Park, NJ) or to Immulon ELISA strip wells (Dynatech, purchased through Fisher, Ottawa). The unlabelled antibody was treated the same way as the labelled sample: a sample was transferred to 0.2 M phosphate buffer pH 7.2, diluted to the same concentration as the labelled antibody, and frozen in a 100 µl aliquot in a plastic centrifuge tube.

The ELISAs were carried out as described in section 2.3, with matching series of antibody dilutions made for the labelled and unlabelled antibody. The equilibrium solution concentration was measured by counting samples of the labelled antibody solutions after the plates were incubated with antibody for one hour. The activity of the labelled and unlabelled antibodies was compared by plotting the absorbance measured after the substrate and phosphoric acid were added against the equilibrium concentration of antibody measured for the labelled sample. Since the equilibrium concentration was assumed to be the same for both the antibody preparations, the graphs would be displaced along the y axis (A450 - A620) if the antibodies had different activities.

The amount of labelled antibody on the plates and strip wells was calculated from solution depletion measurements. The amount of labelled antibody left on the wells after the completion of the assay was measured for the strip wells by breaking the strips apart and counting the wells individually.

2.15d Measuring the antibody adsorption isotherms

The adsorption isotherms were measured for samples of beads and slides with an area of approximately 70 mm^2. The beads or slides were placed in polypropylene centrifuge tubes and incubated with a blocking buffer following the same procedure used for the ELISAs (sections 2.12a

and 2.12b). Skim milk (0.2%) was used as a blocking agent for the first isotherm measured, and 0.2% BSA (Miles Laboratories, Etobicoke, ON) was used as blocking agent in the PBS-Tween in all subsequent experiments.

The 100 μl aliquots of the labelled antibody were mixed with unlabelled antibody, and the specific activity of the new preparation was measured. A dilution series was made up in blocking buffer containing either 0.2% skim milk or 0.2% BSA; 100 μl aliquots of the different concentrations were added to the beads and 200 μl aliquots were added to the slides. Duplicate samples were used for each concentration of antibody. The larger volume for the flat silica was necessary to cover the entire slide. The precise amount added to each silica sample was determined by weighing the centrifuge tubes before and after addition of the antibody solution. The silica samples were incubated with the antibody solutions for approximately two hours at 37 °C.

The concentrations of the different solutions were determined by counting samples with an LKB Compugamma gamma counter with a five minute counting time. Samples were added to gamma tubes containing one ml of water to distribute the sample evenly in the tube and prevent geometric effects in the counting. The concentration of the initial solutions was determined from 100 or 200 μl samples, and the equilibrium antibody concentration was determined from 90 or 190 μl samples. The precise volumes of the solutions counted were determined by weighing the gamma tubes before and after addition of the samples.

The amount of antibody left on the silica after washing the samples twice was measured by placing the centrifuge tubes containing the beads directly into a gamma tube and counting the beads and centrifuge tube together and by counting the flat silica and centrifuge tubes

separately.

The amount of antibody adsorbed per unit area was calculated from solution depletion measurements and for the direct counts of samples after being washed. The protein bound to the walls of the tube was accounted for in the solution depletion calculations either by subtracting the amount left on the tube walls after the wash or by taking as the initial concentration the equilibrium concentration left in an empty tube. The area of the flat silica samples was calculated as described in section **2.12b**.

Adsorption of $Na^{125}I$ was also measured using the same procedure given above for the antibody. The free iodide washed off the silica, leaving an amount that could not be distinguished from the background radiation. Since the antibody preparation contained some free label, the specific activity used to calculate the amount of antibody on the surface was calculated for the protein only, using the amount of free label found for each experiment.

The radioactivity of the samples varied with protein concentration. The solutions measured had radiation levels of $1x10^3$ dpm to $2x10^6$ dpm per sample.

2.15e Inhibition of antibody binding with free antigen

The inhibition of antibody binding by free ferrichrome A was measured for flat silica. A low initial antibody concentration was chosen so that the concentration would not be in the range where the surface was saturated. A low solution concentration of ferrichrome A was used to modify the slides to give a low surface concentration of ferrichrome A and minimize the the difference between the initial and final concentrations of antibody as well as to minimize the proportion

of antibody molecules bound to two antigen molecules on the surface.

The initial antibody concentration was approximately $1x10^{-4}$ mg/ml, and the concentration of ferrichrome A used to modify the slides was 0.007 mg/ml. The adsorption measurements were carried out as described in section **2.12e** with BSA as a blocking agent. A dilution series of ferrichrome A was made up in a solution containing blocking buffer and antibody at a concentration of $1x10^{-4}$ mg/ml. The same slides used for the adsorption measurements were used for ELISA measurements.

2.15f Calculation of the antibody-antigen affinity

The antibody-antigen affinity was calculated from the measurements of the inhibition of antibody binding on flat silica by free ferrichrome A following the procedure outlined in Appendix 1.

2.15g SEM studies with a gold labelled secondary antibody on flat silica

Silica slides were cleaned, silylated and modified with ferrichrome A as described previously. The ferrichrome A coated slides were incubated in blocking buffer for 30 min at 37 °C, and with antibody in blocking buffer at 37 °C for another hour. Gold conjugated anti-mouse IgG (30 nm gold particles, Polysciences Inc., Warrington, PA) was transferred from a glycerol solution to blocking buffer using an Amicon micro concentrator filtration unit with a 30 000 g/mol cutoff filter (Amicon, Beverly, MA). The antibody was diluted to 1/10 the concentration of the initial commercial preparation, and one drop of the antibody solution was added to each of the silica slides. The slides were incubated with the gold conjugated antibody for one hour at 37 °C before being rinsed with buffer and freeze-dried.

Samples were attached to the conductive sample holders for the SEM

using a colloidal carbon suspension. The suspension was painted up the sides of the silica to ensure conduction between the top surface and the sample holder. The samples were coated by sputtering with a mixture of gold and platinum and photographed with a Hitachi S-570 scanning electron microscope.

2.16 Aggregation of the silica beads

Silica beads modified with a range of surface concentrations of ferrichrome A were incubated with blocking buffer and mixed with different concentrations of antibody. After the beads had been incubated with the antibody for one hour at 37 °C they were allowed to settle out of the suspension at room temperature. The beads were then gently resuspended and examined under a microscope to determine the extent of the aggregation.

2.17 Particle electrophoresis

The electrophoretic mobility u of silica particles was measured in order to calculate the surface charge density (section **1.6b**, equation [6]). Particles were suspended in 0.15 M NaCl and the suspension was added to the chamber of a Rank Mark 1 particle electrophoresis apparatus (Rank, Cambridge, U.K.). A voltage (40V, electric field 4V/cm) was applied across the sample and the movement of particles through a narrow cylindrical chamber was viewed and measured with a microscope focussed at the stationary layer where the movement of the cells is not affected by electroosmotic flow through the chamber (141).

The electrophoretic mobility was calculated from the transit time of the particles across a grid:

$$u = \frac{1}{t}\,\frac{D\,Le}{V} \qquad [12]$$

where t = transit time

D = size of grid division in μm

Le = electrical pathlength in cm, determined as described (141)

V = applied voltage

The electrophoretic mobility was determined for silica particles before and after silylation and modified with a range of surface concentrations of ferrichrome A.

Chapter 3

Results and Discussion

3.1 Silica surface

3.1a Cleaning the silica

The silica slides and beads were cleaned prior to modification with the silane. The optimum cleaning procedure was determined by comparison of the amount of carbon left on the surface as measured by XPS. Since there should be no carbon in the silica substrate, the amount of carbon left on the surface should be a good indication of the efficiency of the cleaning procedure. Uncleaned glass slides had 15.5% carbon on the surface (Table VIII). Slides were cleaned with chromic acid at 80° C, followed by rinses with hydrochloric acid and water or with water only. When the slides were dried in air (in a laminar flow hood that filtered out dust particles), very little decrease in the amount of carbon on the surface was seen. This was due to carbon from the air rapidly recontaminating the surface, since slides that were cleaned by the same procedure, with hot chromic acid followed by HCl and water rinses, and then stored under vacuum, had a large decrease in the amount of carbon on the surface (Table VIII). Only 4% carbon was observed on the surface for slides by this procedure. The slides were stored under a poor vacuum that was initially approximately 10^{-3} torr but that dissipated with increased storage time. A stronger vacuum or better sample handling with decreased time for the samples in air might result in a cleaner measured surface, but the procedure used compared well with a survey of other cleaning processes.

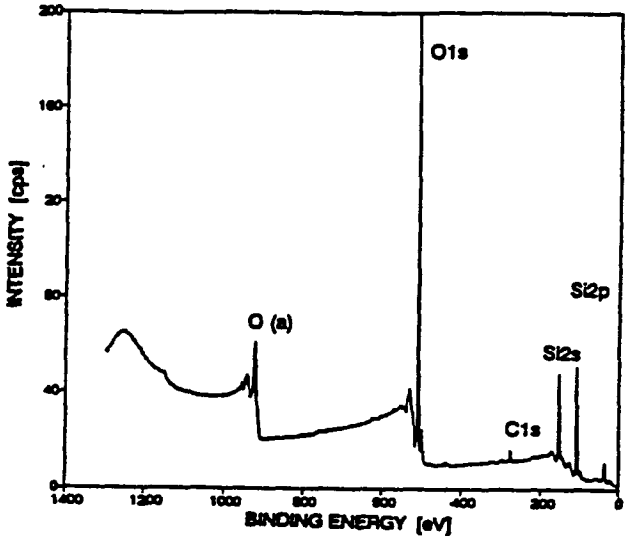

Figure 35: Wide scan XPS spectrum of silica cleaned with chromic acid at 80 °C, followed by rinses with HCl and water. The sample was dried under vacuum (Alkα X-ray source).

Table VIII. XPS measurements on clean silica and glass slides: comparing the efficiencies of the different cleaning procedures.

	Atomic % of the different elements present						
	Si2p	O1s	C1s	S2s	Na	Mg	Ca
bulk SiO_2.	33.33	66.67					
glass slides not clean.	20.73	52.31	15.53		7.58	2.02	1.83
glass slides, chromic acid cleaned, dried in flow hood.	22.15	54.82	15.35	3.99	1.56	1.47	0.68
glass cleaned with chromic acid then HCl, dried in flow hood.	26.54	57.34	13.00	0.00	0.39	1.65	1.09
glass cleaned with chromic acid and HCl, dried in vacuum.	24.83	64.03	6.85		3.04	0.64	0.61
	25.54	65.35	4.17		3.62	0.73	0.60
	25.50	64.64	5.92		2.45	0.88	0.61
SiO_2 cleaned with chromic acid and HCl dried in vacuum.	32.53	63.31	4.16				
	33.04	63.79	3.16				
	32.07	63.09	4.84				
SiO_2 cleaned as above, refluxed with heptane.	33.66	61.64	4.69				
SiO_2 cleaned with HNO_3, dried in vacuum.	13.99	83.79	2.22				
	13.62	84.37	2.01				
	34.25	61.36	4.39				

After the initial studies with glass slides, subsequent measurements used silica to obtain a cleaner spectrum and a surface closer to the silica beads.

Contact angle measurements of water droplets in air can be used to determine if the sample is clean with respect to hydrophobic contaminants, but do not give much analytical information. Water will spread on clean surfaces to give a contact angle of 0°. Clean slides can be detected visually, since a droplet placed on a clean slide will spread off the edge of the slide, but it can be difficult to measure low contact angles formed by droplets on slightly contaminated glass.

The XPS measurements have a further advantage over the contact angle measurements, since they can also detect other contamination. Sulfur from the sulfuric acid in the chromic acid mix was detected on the glass slides after the chromic acid wash. Hydrochloric acid removed the contaminating sulfur and left a surface with only carbon, silicon and oxygen detected.

Hot nitric acid was tried as a cleaning procedure, since it has been reported to be more efficient than chromic acid (116). Although the nitric acid resulted in a low concentration of carbon on the surface, it also gave an oxygen:silicon ratio of about 4:1, much higher than the bulk ratio of 2:1. Although silica is generally resistant to acids (142), the results imply that the surface is being modified in some way, so nitric acid cleaning was not used.

Flat silica was refluxed in heptane, the solvent used for the reaction. This did not cause any increase in the amount of carbon detected at the silica surface (Table VIII) implying that heptane does not adsorb to the surface or else is sufficiently volatile to desorb in vacuum.

3.1b Differences between flat silica and beads

Experiments were carried out with silica slides and beads to increase the amount of information that could be obtained about the silica surface, since different experiments could be carried out with the different systems. It is very difficult, however, to make a direct comparison of the surface properties of the beads and the slides, so the experiments with the two geometries should be thought of as being complementary rather than as being measurements on one system.

The flat silica slides are fused quartz and have a density of 2.2 g cm^{-3} (143) while the beads had a density of 1.83 g cm^{-3} as measured by centrifugation in sulfuric acid. Although the bead surface was smooth on a macroscopic scale (Fig. 29), the density difference implies a more open structure for the silica in the beads. If the surface of the beads was rough on a molecular level, there might be a greater surface area exposed to modifying reagent in solution and a greater number of hydroxyl groups available for reaction with the silane. Since silylations can result in all the surface hydroxyl groups being modified (144), a lower number of available hydroxyl groups would result in less silane on the flat silica surface than on the beads.

The flat fused quartz is produced by heating of quartz with subsequent cooling to produce an amorphous glassy state. Heating of silica is a well known way to remove hydroxyl groups from the surface and so fusion of the quartz slides may also have contributed to reducing the number of hydroxyl groups per unit area on the surface of the slides relative to the beads.

3.1c Electrophoretic measurements on the beads

The cleaned beads had a negative electrophoretic mobility (in a 25 mM sodium chloride solution) of $-3.28 \pm 0.21 \times 10^{-4}$ cm^2 V^{-1} s^{-1}, with a calculated surface charge density, from equation [10] of 5.87×10^3 esu cm^{-2} and an area per charge (equal to e/σ) of 818 $Å^2$, indicating that there are negative groups at the surface of the beads, probably dissociated silanol groups.

3.2 Silylated silica

3.2a Density of amine groups on the surface

A ninhydrin assay was used to estimate the amine content on the surface of the silylated beads. The surface concentration of amines was determined to be $(0.9\pm0.3)\times10^{-5}$ mol $-NH_2/m^2$, corresponding to an area per group of 18 $Å^2$. This implies a surface that has very closely packed amine groups. Since the surface area was calculated from the bead radius assuming a smooth sphere, the true surface area may be higher and the surface concentration of amine groups might be lower. However, modification of silica surfaces with other silanes has been shown to result in modification of all the surface hydroxyl groups, implying that a high degree of modification of the surface can be achieved (144).

The error given for the ninhydrin assay measurement is the standard deviation for four samples. A similar error was observed for the solution measurements of the standards.

3.2b Charge density on the surface and surface pH: effect on EDC coupling

Electrophoretic measurements showed that silylated beads had a positive surface potential in 25 mM NaCl. The electrophoretic mobility

was 3.86 ±0.2 x 10^{-4} cm^2 V^{-1} s^{-1}. This gives a calculated charge density of 7.27 x 10^3 esu/cm^2, with a corresponding area per charge of 660 $Å^2$. The surface charge density was lower than the value that would be expected from the ninhydrin assay of the surface amines. This is partly due to the effect of surface pH on ionization of the surface amine groups discussed below. However, it likely also reflects the fact that the beads were stored prior to the electrophoresis measurement, permitting adsorption of negatively charged contaminants.

Charged surfaces will affect the distribution of ions in solution adjacent to the surface, giving rise to what is known as the electric double layer (112). Hydrogen and hydroxide ions in aqueous solution close to the surface will also be affected, causing a change in the pH of solutions close to a charged surface (112). The surface pH may be calculated from the bulk pH and the zeta potential, making the usual assumption that the surface and zeta potentials are equal. The relevant ion distribution is just given by the Boltzmann equation, which for the present case may be written, for the proton concentration adjacent to a surface whose surface potential is assumed to be ζ:

$$H_s^+ = H_b^+ \exp(-e\zeta/kT) \qquad [13]$$

where H_s^+ = hydrogen ion concentration adjacent to surface

H_b^+ = hydrogen ion concentration in bulk phase.

In terms of surface pH this equation becomes:

$$pH_s = pH_b + e\zeta/2.303kT \qquad [14]$$

If in the calculation of surface pH the surface concentration implied by the ninhydrin assay is used and it is assumed each propyl amine group is charged, the surface potential is calculated by inverting equation [10]. When used in [14], the value of pH_s is calculated to be

about 10, close to the pKa of the group. This means the assumption that each amine bears a positive charge is likely incorrect. If instead the zeta potential is calculated from the measured electrophoretic mobility and used as the basis for the calculation, the surface pH associated with the silylated bead surface is increased above the bulk value by only 0.94 units.

The EDC coupling is affected by pH. The EDC mediated coupling between acetylglycine and glycine methyl ester in solution has a broad optimum between pH 5 and 7 (145). The pH of the solution of ferrichrome A and EDC was 5.6 before addition of the beads and 6.01 after addition of the beads. An increase of 0.94 over 6.01 would still leave the pH at surface within the optimum range for the reaction. The problems with the EDC mediated coupling on the bead surface are that the EDC-carboxylate adduct can hydrolyze before reaction with the surface and that the positively charged surface would repel the positively charged group on the EDC. The rate of hydrolysis should not be greatly affected by the surface pH, since most of the EDC-ferrichrome A product remains in the bulk of the solution.

Electrophoretic measurements with the ferrichrome A-modified beads (section **3.3f**, Fig. 44) showed that the beads had a negative charge, implying that not all the carboxyl groups on the ferrichrome A had reacted and that the ferrichrome A-EDC product would not be repelled from the surface. If the antigen used had not had more than one carboxyl group per molecule, use of a positively charged carbodiimide might have resulted in lower amounts of antigen bound on the surface. Problems with this could be solved by use of a negatively charged water soluble carbodiimide.

3.2c Thickness of the amine layer

Silylation of silica surfaces in aqueous solutions can result in deposition of seven to ten molecular layers of the silane (137). Trihydroxysilanes can condense in solution after hydrolysis of the alkoxy groups and since the condensation is not limited to two dimensions, it can produce a thick layer of silanes which can then react with the surface (see Fig. 9 for general reaction of silanes with silica). Condensation of the silane into such "lumps" might result in an unevenly modified surface, so the reaction was not carried out in aqueous solution.

Heptane was chosen as a solvent for the reaction because it takes up only a small amount of water, and could provide sufficient water for hydrolysis of the silane while minimizing the condensation of silane in solution. The 3-aminopropyltrihydroxy silane used in these experiments appeared to coat the beads rapidly; the silica beads could be suspended readily in a solution of the silane in heptane but not in the heptane alone. This could be due to the hydroxyl groups on the silica interacting with amine groups on the silane.

Angularly resolved XPS measurements on a silylated silica slide (that had also been modified with ferrichrome A) showed a shift in the Si2p peak at higher angles away from the normal (Fig. 36). The Si2p peak for clean unmodified silica is also shown. When measurements on the modified silica were taken normal to the surface to achieve a greater sampling depth (Fig. 10), the observed peak was closer to that for the unmodified silica. As the measurement angle moved away from the normal, the sampling depth became shallower and the signal from silicon in the silane layer became enhanced relative to the signal from the underlying silica. When the photoelectrons were detected at 70° away from the

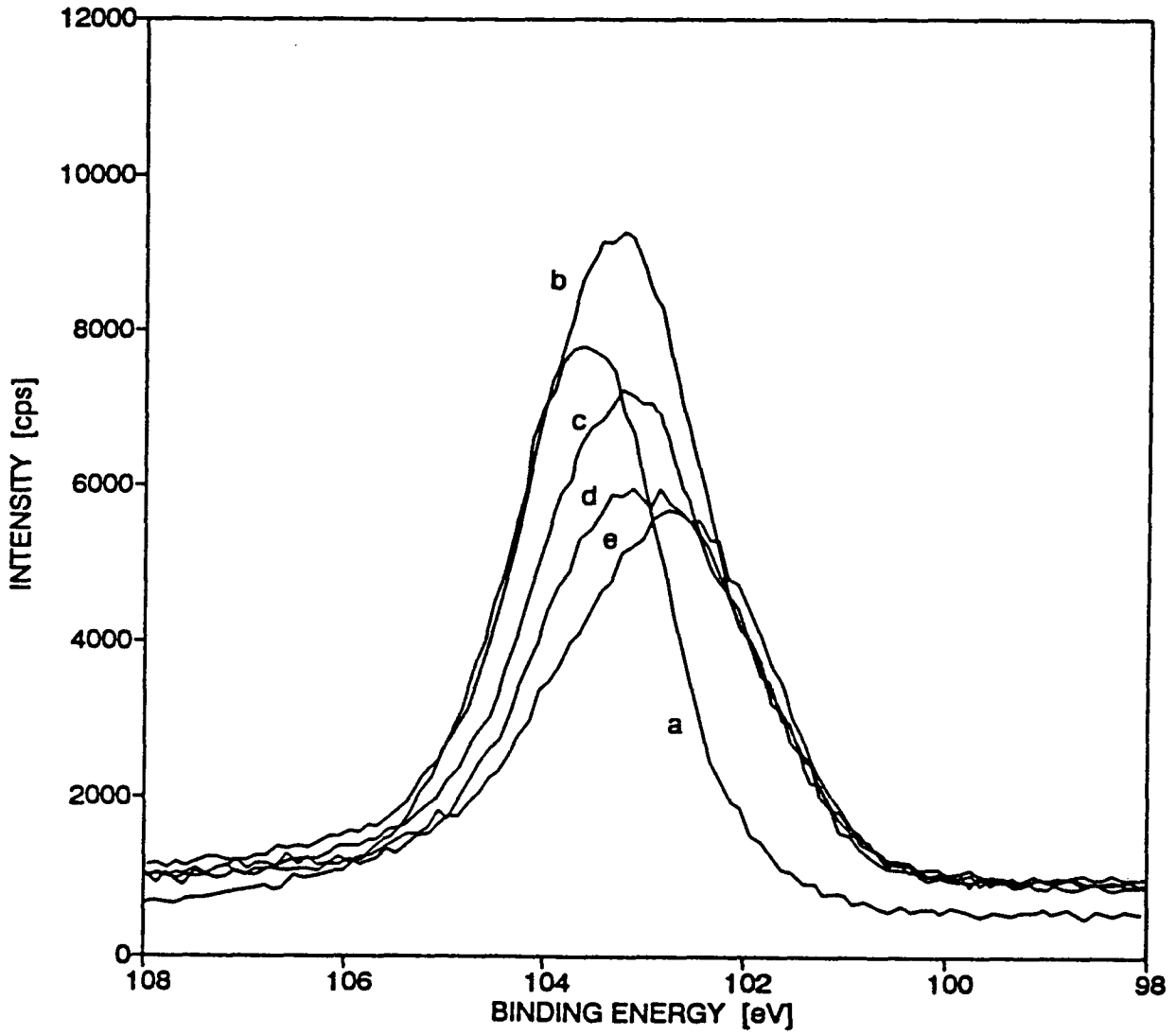

Figure 36: Angularly resolved measurements on silylated silica, showing the shift in the Si2p peak away from the value for unmodified silica, as the angle of measurement away from the normal becomes larger and the sampling depth becomes shallower (a= clean silica at 90°, normal to the surface, b-e = the silylated surface, b= 90°, c= 45°, d= 30°, e= 20°)

normal, there seemed to be very little signal contributed from the underlying silica layer.

These measurements imply that there is a continuous layer of silane, since if the silane were present as islands on the silica surface, there would be some of the underlying silica at the surface and distinguishable at all takeoff angles (111). The silane layer is thin enough that signal from the underlying silica can be seen. The intensity of the signal decreases at high takeoff angles because of the ferrichrome A covering the silica.

X-ray photoelectron spectroscopy measurements showed only 2.4% nitrogen on the flat silica (Table IX), less than the amount of carbon detected on the cleaned surface. This low measurement is in contrast to the high surface concentration of amines measured by the ninhydrin assay, and may reflect the fact that the amines are at the top of the silane layer.

3.3 Silica with ferrichrome A

3.3a Some comments on ferrichrome A

Figure 37 is a crystallographic structure of ferrichrome A showing the face with the three carboxyl groups. If the carboxyl groups all interacted with the positively charged amine groups on the silylated silica, the ferrichrome A would be adsorbed with the carboxyl face down and a molecular cross-sectional area of about 70 $Å^2$ (all numbers are obtained using Silicon Graphics and the ferrichrome A coordinates (120) from the Cambridge Data Base).

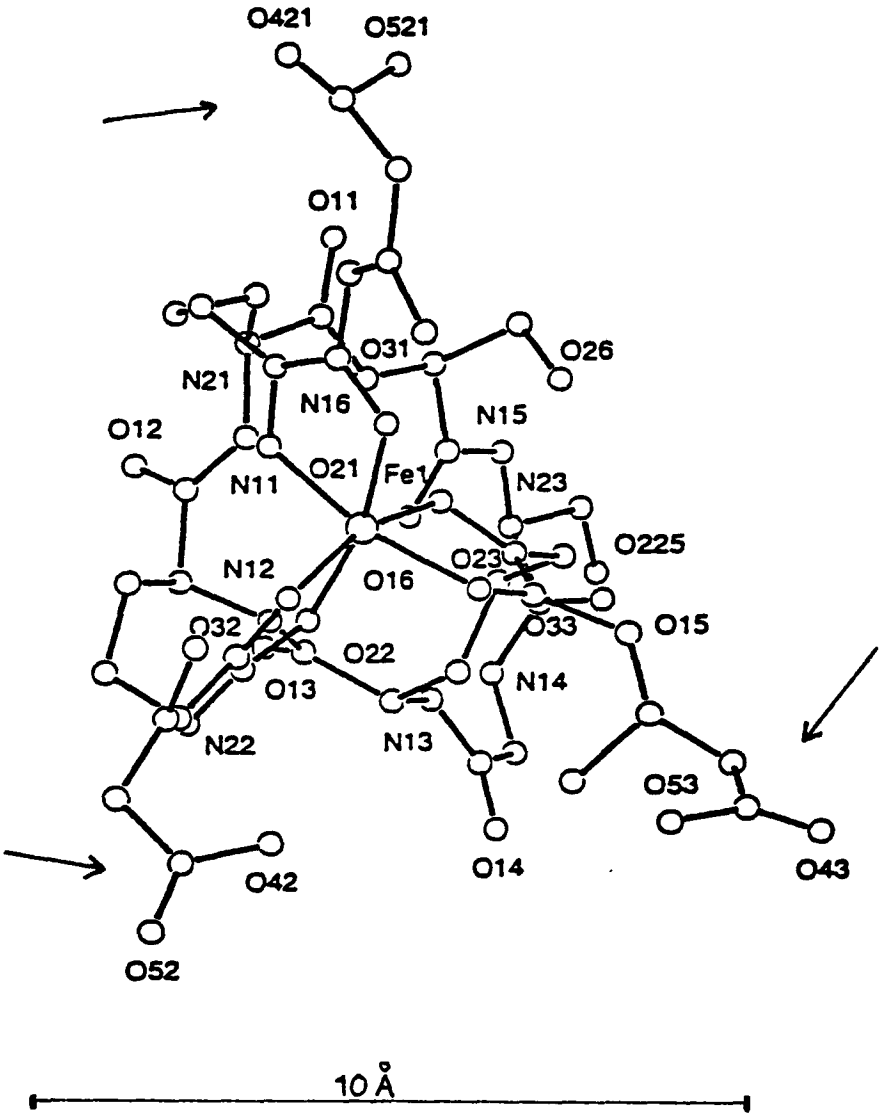

Figure 37: Crystallographic structure of ferrichrome A, showing the face with the three carboxyls (120) (the carboxyl groups are indicated by arrows).

Table XI: XPS measurements on silica slides modified with distilled or undistilled 3-aminopropyltriethoxysilane

	Atomic % of the different elements present			
	Si2p	O1s	C1s	N1s
silica modified with undistilled silane	26.41	48.86	21.23	3.75
silica modified with distilled silane	31.50	51.61	14.54	3.35

Table X: Ferrichrome A adsorption to different areas of beads. The initial ferrichrome A concentration was the same for each sample. The error listed is the standard deviation for six data points.

amount of beads used for each measurement (mg)	amount adsorbed (mg/m^2)
1	2.07±0.21
5	2.16±0.21

3.3b Effect of changing the bead area on ferrichrome A adsorption

Changing the area of the beads did not change the amount of ferrichrome A adsorbed per unit area (Table X). This implies that the ferrichrome A does not contain a significant concentration of aggregates in solution, since higher molecular weight aggregates would adsorb preferentially and would result in a higher amount adsorbed per unit area for smaller area bead samples (if the initial ferrichrome A solutions were the same volume and concentration) (79).

3.3c The adsorption isotherm: ferrichrome A adsorption as a function of solution concentration

The amount of ferrichrome A adsorbed per unit area was measured for a range of dilute concentrations of ferrichrome A (using 5 mg bead samples with six samples for each data point) and for a wider range of concentrations (using 10 mg bead samples, with two samples for each data point), see Fig. 38 and Fig. 39. Curves are fit by eye to the data points. The error bars at each point are the standard deviation of measurements of the amount adsorbed. Figure 39 also shows the amount of ferrichrome A left on the beads after washing with PBS. These experiments were done on beads modified in separate silylation procedures. Data from the two experiments agree well.

A Langmuir type adsorption isotherm was obtained, with the amount adsorbed increasing rapidly with equilibrium solution concentration before reaching a plateau. A Scatchard plot (Fig. 40) for the data obtained in dilute solutions (Fig. 38) gave a maximum amount adsorbed of 1.76 mg/m^2. This corresponds to an area per molecule of 99 $Å^2$/molecule. The same data also gave a K value of 8.26±0.99 l mol^{-1}.

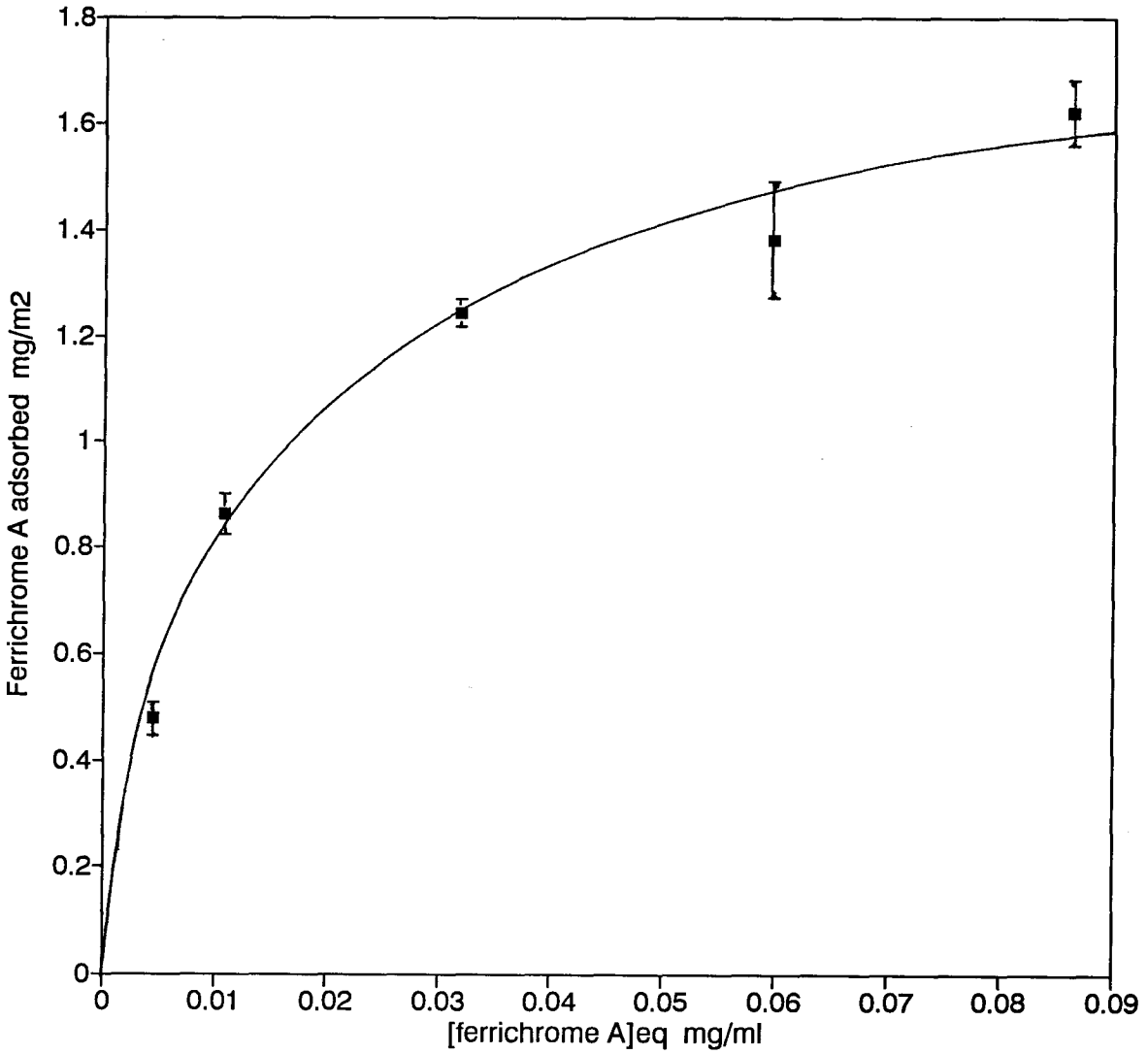

Figure 38: Adsorption isotherm for ferrichrome A in water on silylated beads at low solution concentrations (■ = amount adsorbed from solution).

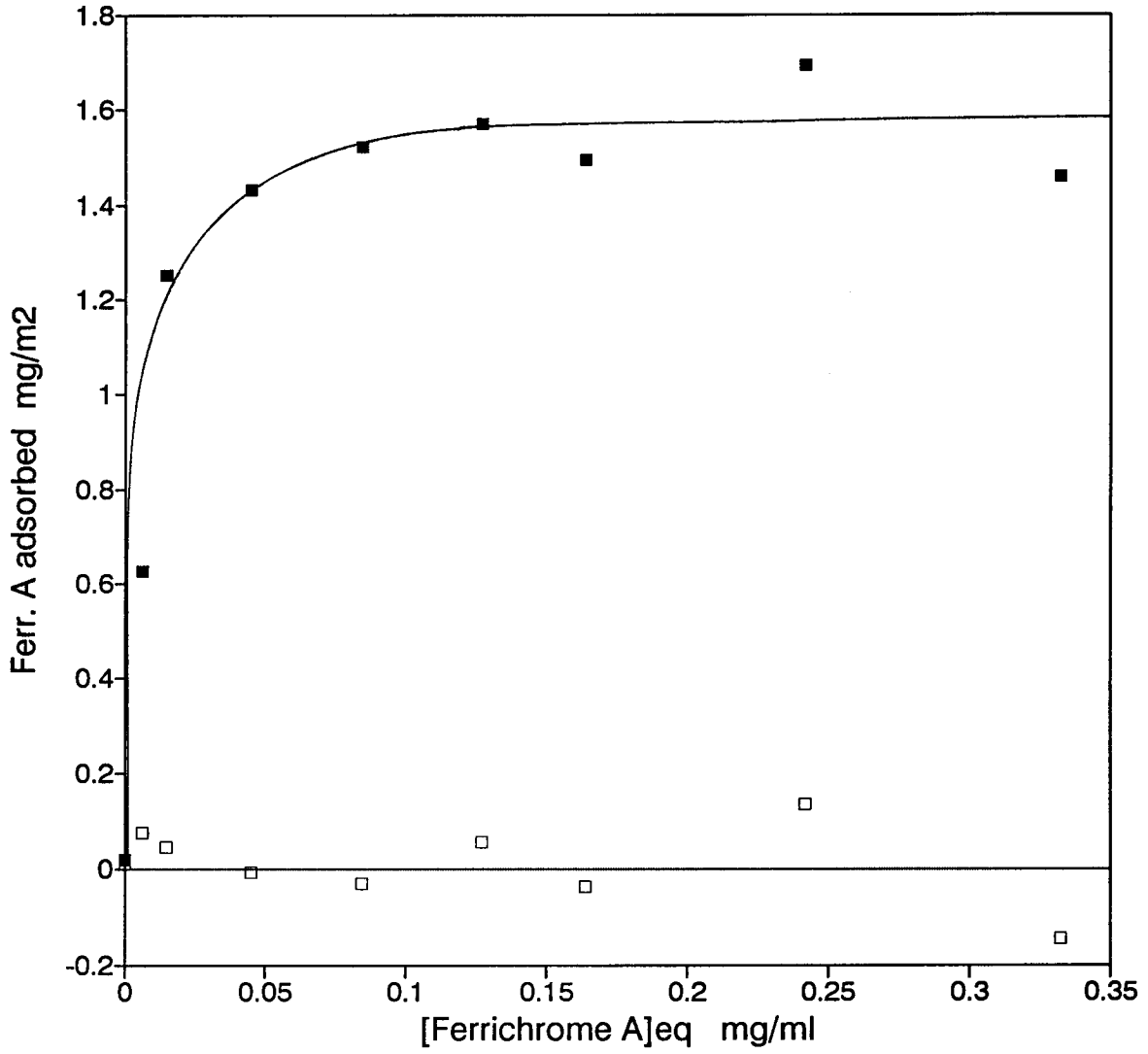

Figure 39: Adsorption isotherm for ferrichrome A in water on silylated beads (■ = amount adsorbed from solution, □ = amount left on after PBS wash).

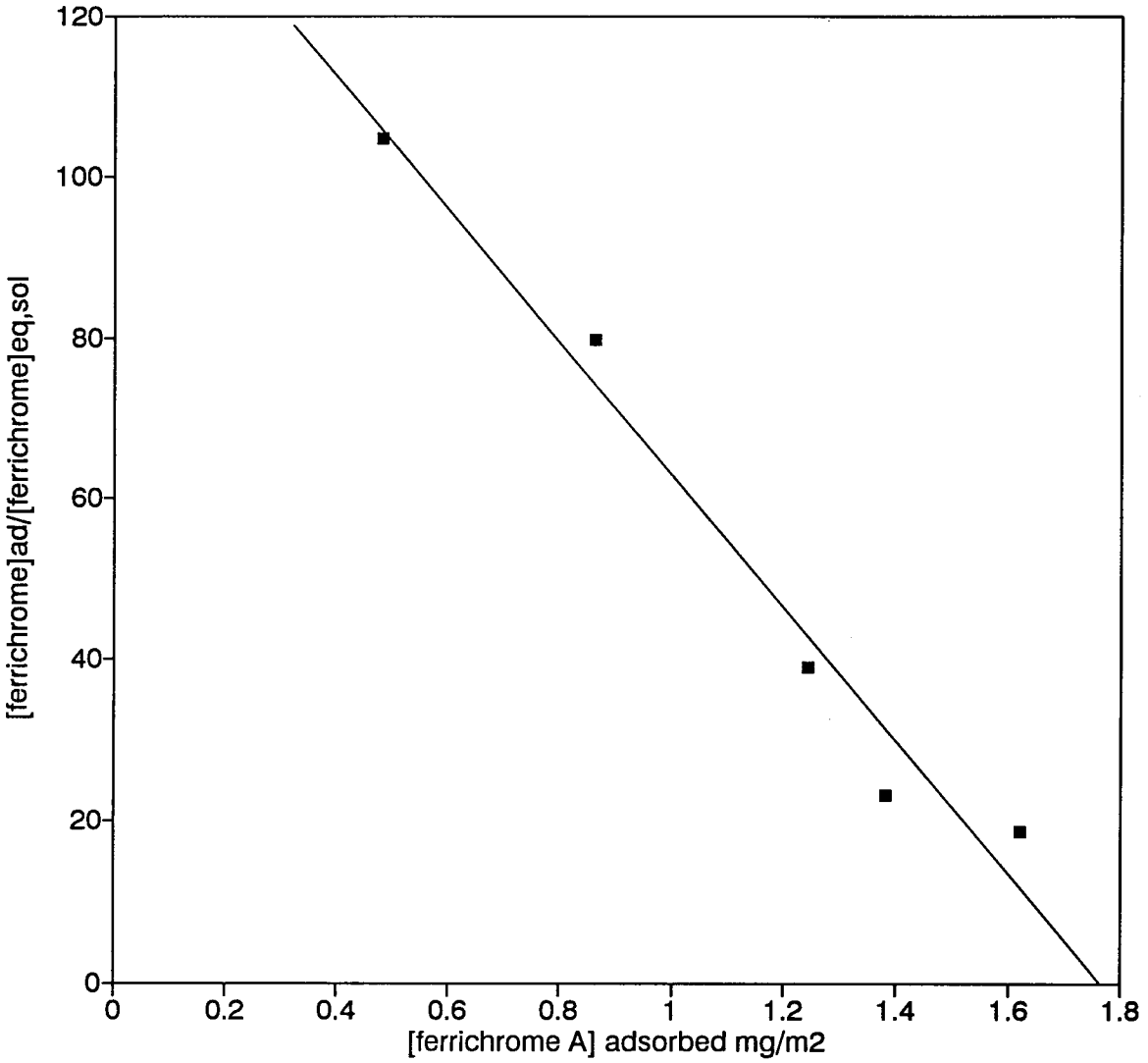

Figure 40: Scatchard plot for ferrichrome A binding to silylated beads (from the data shown in Fig. 38)

3.3d Effect of salt concentration on ferrichrome A adsorption

The amount of ferrichrome A adsorbed in increasing concentrations of sodium chloride was measured using beads that had been stored for ten days after the silylation. A series of ferrichrome A solutions was made up in distilled water and 5, 10, 20, 50 and 100 mM NaCl. Although the initial concentration of ferrichrome A was the same in all solutions, the equilibrium concentrations differed because different amounts of ferrichrome A adsorbed to the beads. The amount bound was lower than for freshly prepared beads (see Table VI). Data is presented in Fig. 41 as amount bound as a fraction of the amount bound in water.

Increasing salt concentrations rapidly decreased the amount bound; 10 mM NaCl would cause a 50% decrease in the amount bound. No detectable ferrichrome A was bound at 100 mM NaCl. The chloride ions and ferrichrome A would both act as counter ions to the positively charged amines on the silylated silica, and increasing concentrations of sodium chloride would compete with the ferrichrome A to cause a decrease in the amount of ferrichrome A bound.

The decrease in amount of ferrichrome A bound may also be partly due to the beads aggregating and decreasing the area of silica available for binding. Aggregates could be seen under the the microscope for beads in higher salt concentrations. The aggregates could also be detected in suspension because the beads settled out more rapidly in salt solutions.

3.3e Reaction of ferrichrome A with EDC

When ferrichrome A is reacted with EDC by adding a solution of EDC in water to dry ferrichrome A, an additional peak appears in the

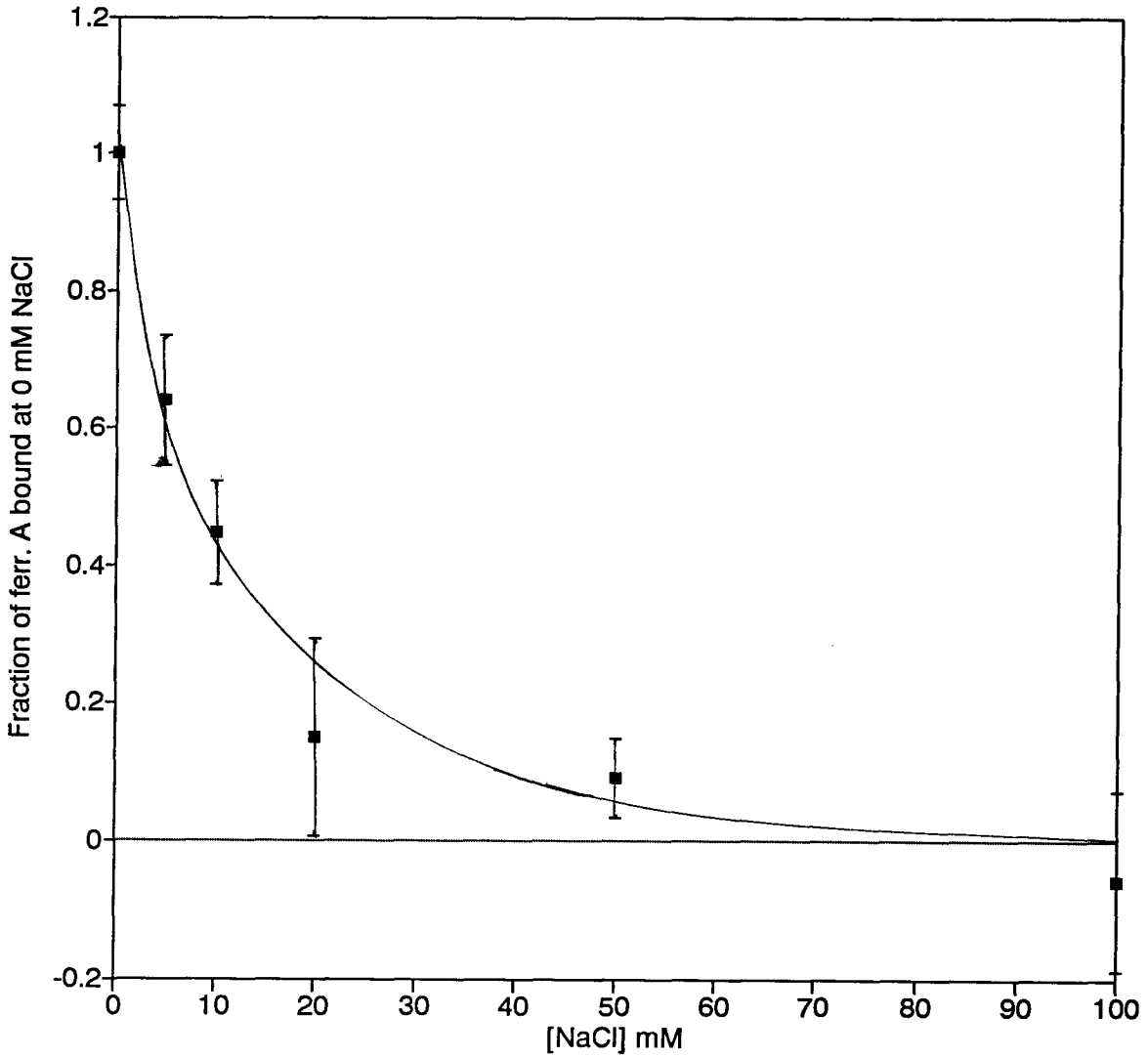

Figure 41: The effect of increasing concentrations of NaCl on adsorption to the silylated beads. Results are shown as a fraction of the amount bound at 0 mM NaCl.

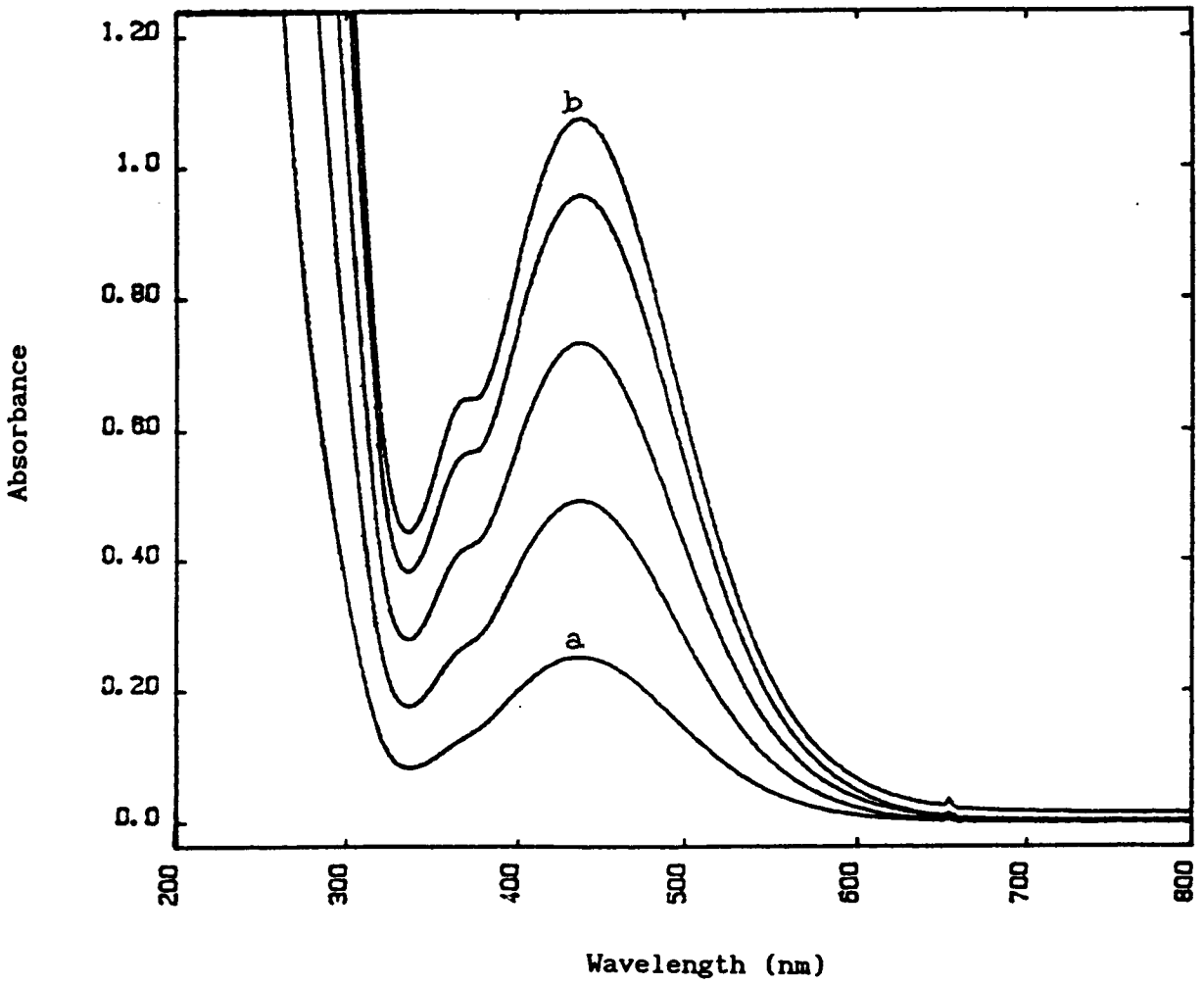

Figure 42: The absorbance of ferrichrome A mixed at different ratios with EDC, where a= the lowest EDC: ferrichrome A ratio and b= the highest ratio. Results are shown for solutions with increasing concentrations of ferrichrome A so that they may all be shown on one figure.

absorbance spectrum at 367 nm (Fig. 42). The peak at 367 nm increases with respect to the peak at 436 nm as the concentration of EDC in solution is increased (Fig. 42). This absorbance is not due to EDC. The peak at 367 nm is outside the range reported for typical 3:1 ferric trihydroxamates (420 to 450 nm, 146) and seems quite narrow, where most ferric hydroxamates have a broad absorbance peak (147). The peak is also shifted to longer wavelengths than the maximum for ferrichrome A, unlike the shift that occurs for ferric trihydroxamate as the hydroxamate groups dissociate. As the solution pH is lowered, ferric trihydroxamate will dissociate and form the 1:1 ferric hydroxamate. As this occurs, the absorbance maximum shifts from a range of 425 nm to 440 nm for the ferric trihydroxamate to 520 nm for the 1:1 complex, with a decrease in the extinction coefficient (147).

If the peak at 367 nm represents a different species, then at an EDC:ferrichrome A mole ratio of 50:1, it seems to account for only a small fraction of the total ferrichrome A.

Ferrichrome is another metabolite of *Ustilago sphaerogena* without a serine residue or any carboxyl groups. Ferrichrome does not react with EDC to produce a peak at 367 nm, implying that the hydroxamate groups are not involved in the reaction (Figure 73, Appendix 4).

3.3f The amount of ferrichrome A on the beads at a constant EDC:ferrichrome A ratio

The EDC was mixed with ferrichrome A at a mole ratio of 50:1 in water and then mixed with the silylated beads as described in section **2.11**. Figure 42 shows the amount of ferrichrome A associated with the beads at different concentrations of ferrichrome A and the amount left on the beads after rinsing with PBS, with all data points for the

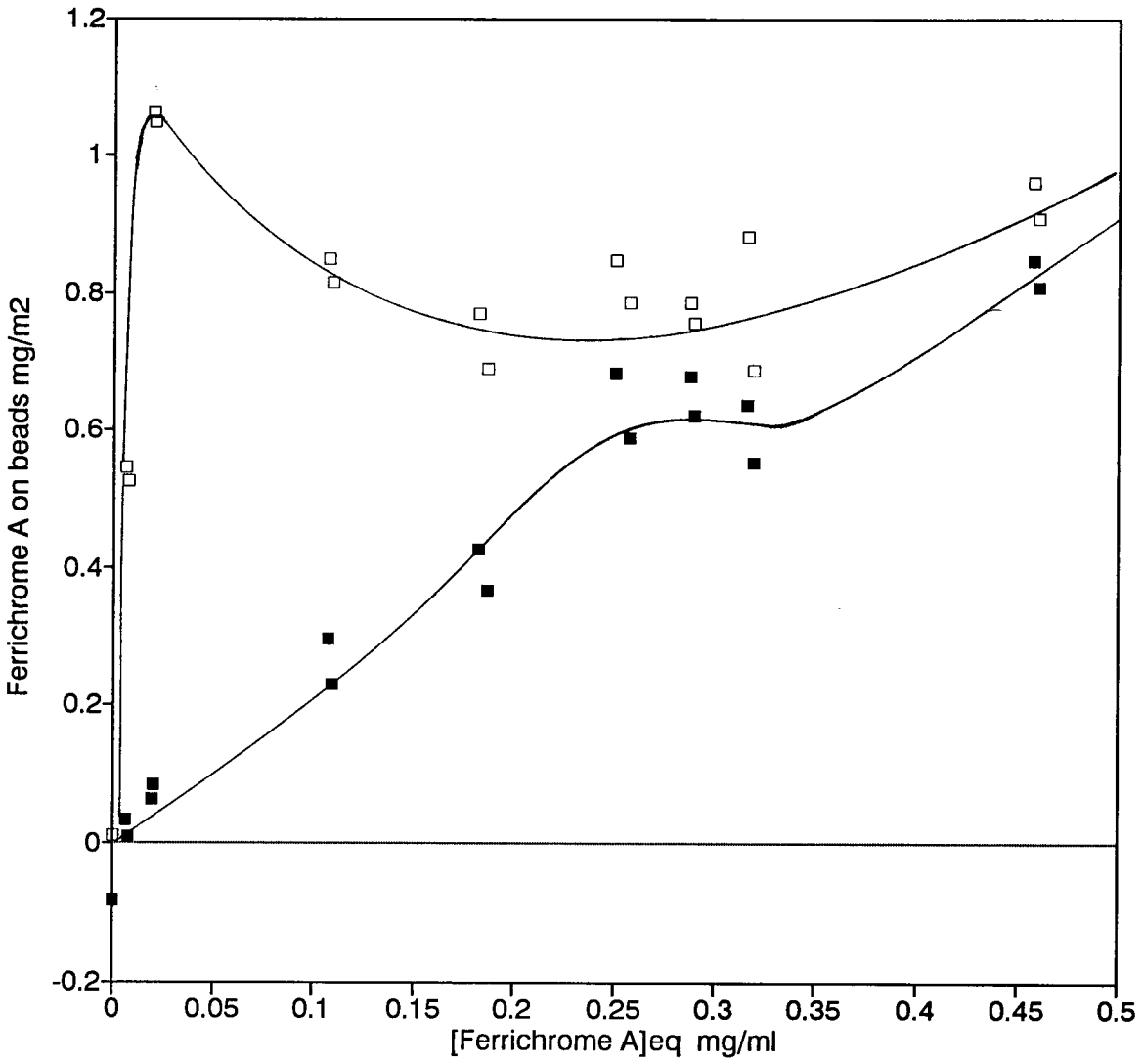

Figure 43: Coupling ferrichrome A to silylated beads at a constant EDC: ferrichrome A mole ratio of 50:1 (□ = amount of ferrichrome A associated with the beads, calculated from initial solution depletion measurements, ■ = ferrichrome A left on the beads after a PBS wash).

experiment shown. The amount adsorbed on the silica shows the initial sharp increase with equilibrium solution concentration that was seen for ferrichrome A adsorbed in water, but then decreases as the ferrichrome A solution concentration continues to increase. This is probably due to the increasing concentration of EDC, which could have the same effect as sodium chloride in disrupting the ionic interaction between the ferrichrome A and the positively charged silica.

At an equilibrium solution concentration of 0.459 mg/ml of ferrichrome A, 89% of the ferrichrome A stayed on the beads after rinsing with PBS. This is distinctly different from the negligible amount of ferrichrome A left on the beads after the PBS rinse of the ferrichrome A adsorbed in water. At higher surface concentrations of ferrichrome A on the beads, the beads remained orange after the PBS wash.

The absorbance spectrum of the ferrichrome A that washed off the beads did not show any shoulder at 367 nm.

At an equilibrium solution concentration of 0.18 mg/ml ferrichrome A, the initial ferrichrome A concentration was 0.226 mg/ml, and the EDC concentration was 11 mM. From Figure 39, a 0.226 mg/ml solution of ferrichrome A in water would give a ferrichrome A surface concentration of 1.6 mg/m^2. If EDC is a 1:1 electrolyte at pH 5.3, it would have an ionic strength equivalent to that of a sodium chloride solution of the same concentration, which caused a 50% decrease in the amount of ferrichrome A bound (Fig. 41). This is similar to the decrease observed for ferrichrome A bound to the beads in an EDC solution relative to the amount in water.

The amount left on the beads after the PBS wash increases less rapidly with solution concentration of ferrichrome A than the total

amount associated with the surface (Fig. 43). There is a kink in the binding curve corresponding to a surface concentration of 0.62 mg/m^2 or an area per molecule of 270 $Å^2$. Adsorption isotherms of proteins can show kinks where reorientations of the the protein occurs to give a more compact arrangement (87). The protein saturates the surface at one orientation, but can then reorient to allow more protein to bind.

If the ferrichrome A is attached covalently, then at least one of the carboxyl groups must be towards the surface. The other two carboxyl groups on each molecule may be originally in contact with the surface so that the triangular face shown in Fig. 37 is towards the silica surface. At higher concentrations, the molecules could reorient so that carboxyl groups not covalently bound to the silane were exposed to the solution.

Electrophoretic measurements on the same bead samples prepared for Fig. 43 showed that the beads at concentrations above the kink in the ferrichrome A binding curve had a large negative surface charge. Figure 44 shows the electrophoretic mobility of the beads as a function of solution concentration of ferrichrome A. The graph has a similar shape to the graph of the amount left on the silica after the PBS rinse as a function of solution concentration of ferrichrome A, but with a sharper increase after the apparent saturation point. The high electrophoretic mobility supports the idea that the carboxyl groups are oriented towards the solution.

The specific amount of ferrichrome A bound would be expected to reach a saturation point at the concentration observed for adsorption of ferrichrome A with no EDC, but the limited solubility of ferrichrome A in water prevented measurements at higher concentrations.

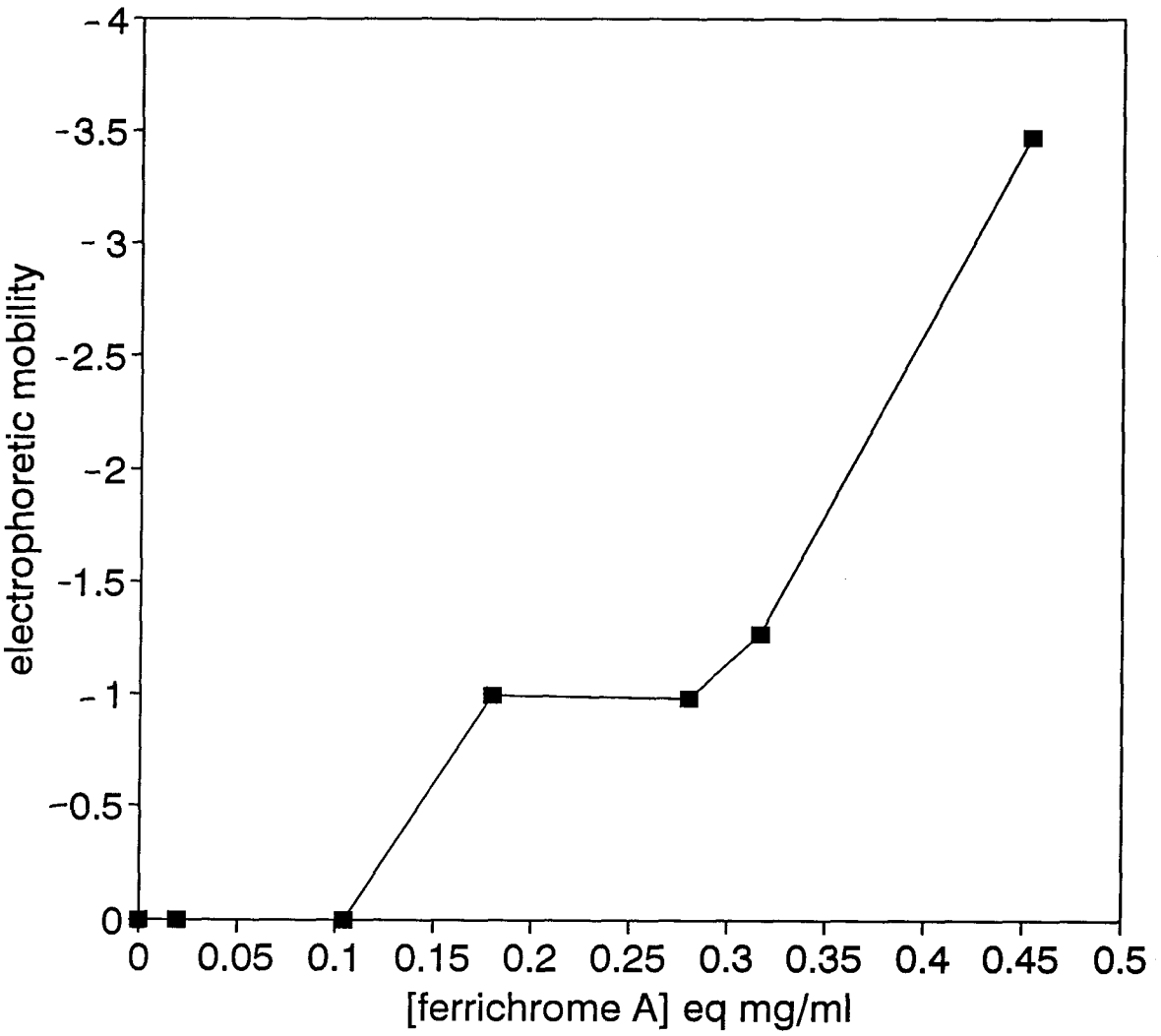

Figure 44: Electrophoretic mobility of silylated beads with ferrichrome A attached covalently at a constant EDC:ferrichrome A mole ratio. Units of electrophoretic mobility plotted are (10^{-4} cm^2 V^{-1} s^{-1}); uncertainties in data points are approximately the same magnitude as the size of the symbol).

3.3g Amount of ferrichrome A on the beads at constant EDC concentration

Another experiment was carried out varying the concentration of ferrichrome A but maintaining a constant concentration of EDC. The EDC concentration of 20 mM was chosen to give a 50:1 mole ratio for the highest concentration of ferrichrome A; the mole ratio of EDC to ferrichrome A increased for lower concentrations of ferrichrome A. The initial increase in adsorbed ferrichrome A, followed by a decrease at higher equilibrium solution concentrations that was observed in Fig. 43 was not seen, indicating that the increase was due to the low concentration of EDC in solution (Fig. 45).

Since the amount of ferrichrome A left in solution was calculated from the derivative of the absorbance using the same number that was determined for a 50:1 ratio of EDC:ferrichrome A, the results obtained will be less accurate for the lower concentrations of ferrichrome A with higher EDC:ferrichrome A ratios, but should still serve to indicate the shape of the binding curve.

The binding curves showing the amount of ferrichrome A on the beads for a constant EDC:ferrichrome A mole ratio and a constant EDC concentration were similar at higher ferrichrome A concentrations where the mole ratio of EDC:ferrichrome A was similar. At lower concentrations of ferrichrome A, increased EDC decreased the amount initially associated with the beads and the amount remaining after the PBS wash.

3.3h BCA assays of the amount of ferrichrome A on the beads

The amount of ferrichrome A left on the beads after a PBS rinse was also estimated directly with a BCA assay (section **2.14b**). This gave values similar to those obtained from solution depletion (Fig. 46).

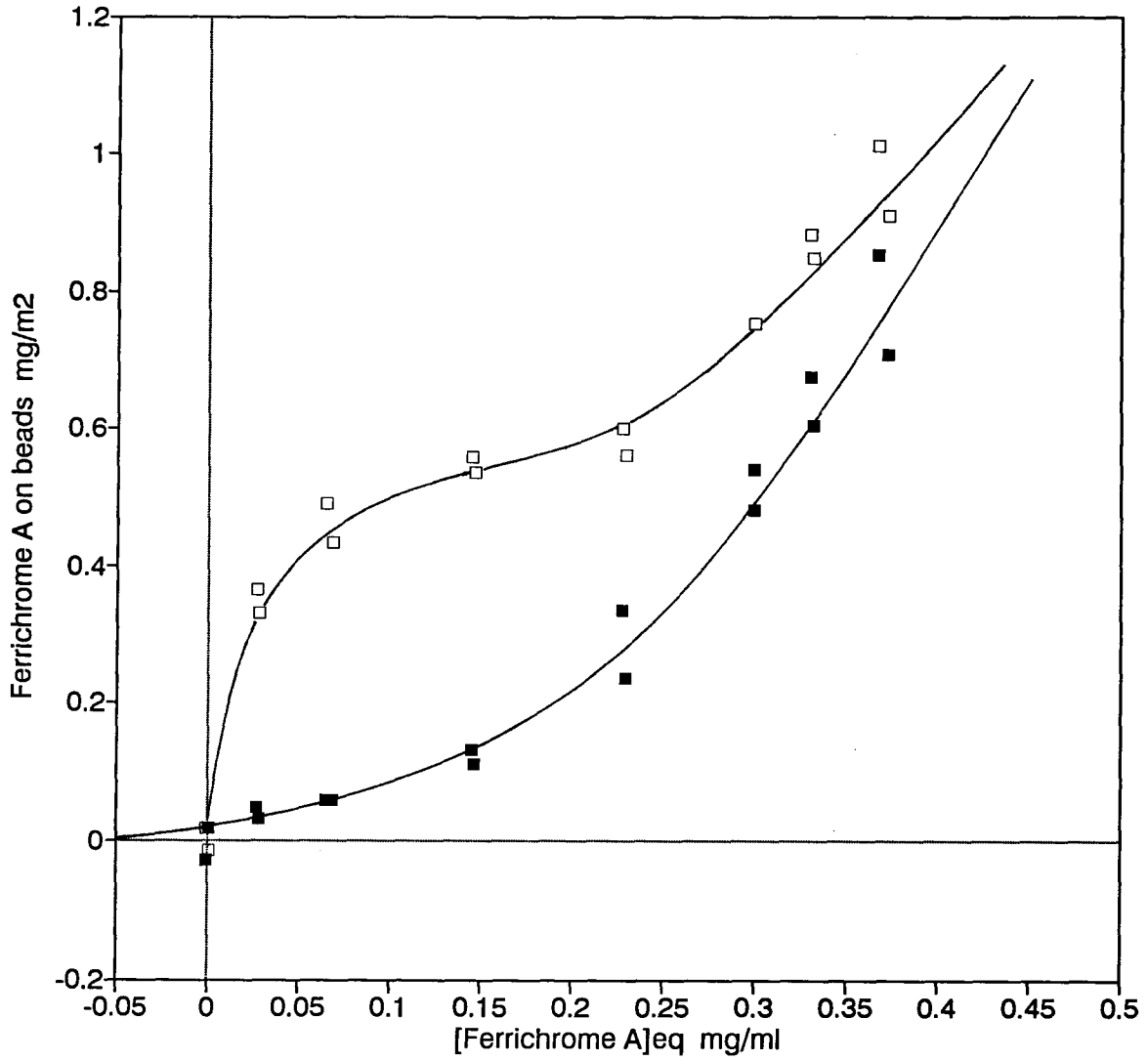

Figure 45: Coupling ferrichrome A to silylated beads at a constant EDC concentration of 20 mM, giving an EDC:ferrichrome A mole ratio of 50:1 for the highest ferrichrome A concentration used (□ = ferrichrome A initially associated with the beads, ■ = ferrichrome A left on the beads after a PBS wash).

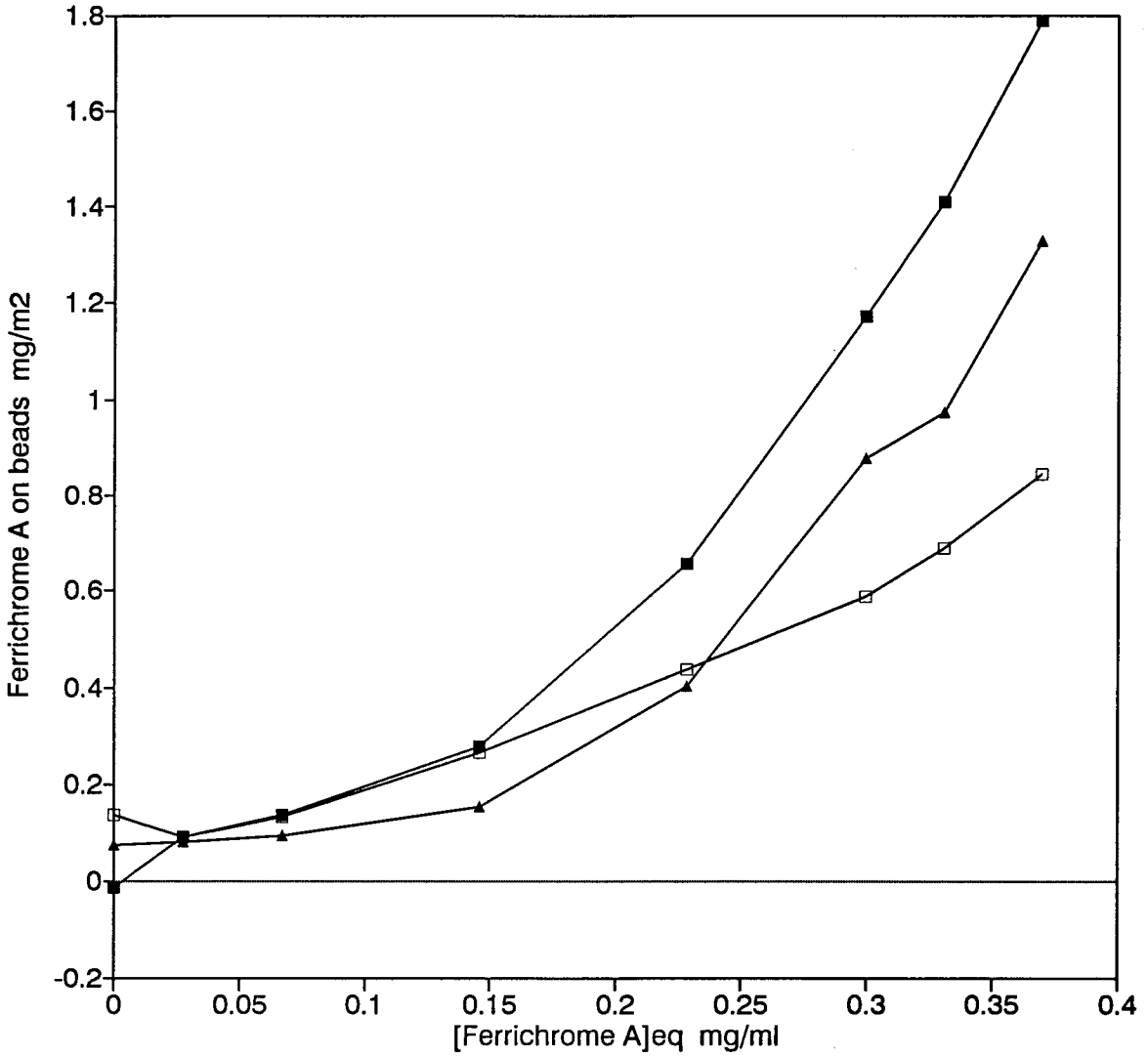

Figure 46: BCA determination of the amount of ferrichrome A on the beads after coupling ferrichrome A to the beads with a constant EDC concentration of 20 mM and washing the beads with PBS (■ = amount of ferrichrome A calculated from solution measurements, □ = BCA assay with 30 min incubation time, Δ = BCA assay with 120 min incubation).

3.2i Ninhydrin assays of silica modified with acetic acid and EDC

Ninhydrin assays of the acetylated beads were done in search of evidence for formation of a covalent bond on the surface. The beads were modified with acetic acid following the same procedure used for coupling ferrichrome A, with a 20:1 mole ratio of EDC:ferrichrome A. The acetylated beads had a surface amine concentration of 2.1×10^{-7} mol m^{-2}, as compared to the silylated beads with a surface amine concentration of 1.9×10^{-5} mol/m^2. The decrease in the measured amount of amines on the surface was not due only to ionic interactions of the acetic acid and the amines on the silica, since the assay was carried out in 100 mM acetic acid. The ninhydrin assay implies that nearly all the available amine groups on the bead surface reacted with acetic acid plus EDC.

3.2j XPS measurements of ferrichrome A on the silica

Angularly resolved XPS measurements of ferrichrome A coupled to flat silylated silica with EDC showed that the ferrichrome A covered some but not all of the surface. The Si2p signal from the underlying substrate decreased for measurements made at angles higher away from the normal, but appeared to approach a constant value at high angles (Fig. 39). This implies that some of the silica is covered with a thin layer of ferrichrome A, and that some of the silica remains uncovered.

The ferrichrome A on the surface was identified by the iron 2p peak at 711 eV (Fig. 47).

Ferrichrome A dried onto the silica from an aqueous solution with no EDC desorbed in the vacuum of the XPS machine, although the initial amount of ferrichrome A on the slide was sufficient to cause a dark red mark. This is further evidence that EDC results in formation of a stable bond between ferrichrome A and the silylated silica.

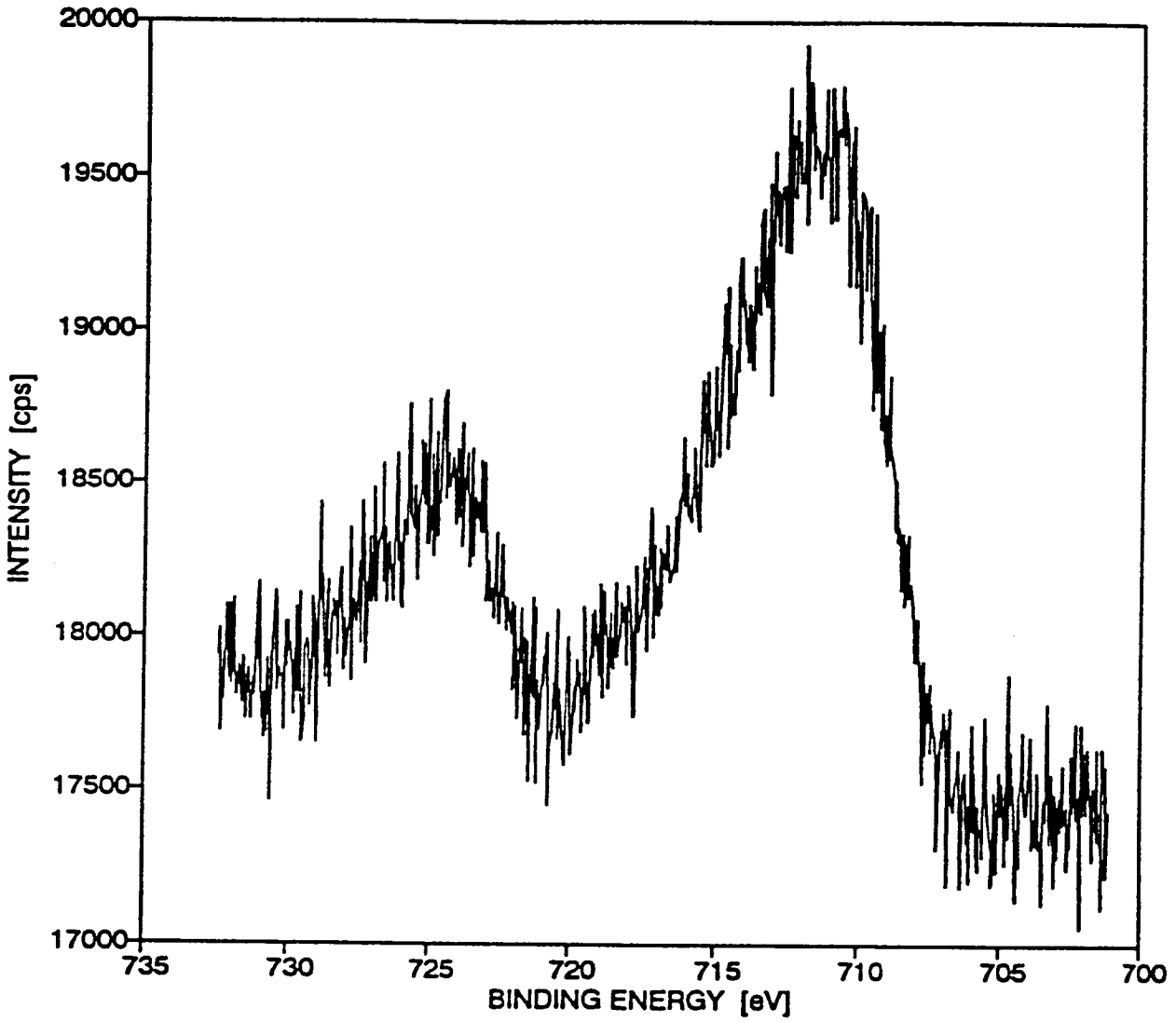

Figure 47: An XPS spectrum showing the Fe2p peak from ferrichrome A on silica (Mgkα source)

3.4 Antibody binding to the ferrichrome A-modified silica

3.4a The radiolabelled antibody

The purified IgG (section 2) was labelled with I^{125} (2.15a). The effects of the labelling were determined with SDS-PAGE of the labelled antibody and an ELISA to compare the activity of the labelled and unlabelled antibody preparations (Figs. 48a and 48b).

The SDS-PAGE indicated that the sample was pure and the ELISA showed that the labelling did not affect the antibody activity.

3.4b. Non-specific adsorption

The adsorption of the antibody to unmodified and silylated silica was measured and the effect of Tween 80 and 0.2% BSA in minimizing the non-specific binding was measured. The BSA was used instead of skim milk as a blocking agent for the adsorption measurements with radiolabelled antibody to avoid any problems that might result from components of the skim milk being centrifuged out of suspension during the assay.

Antibody adsorbed more strongly to the silylated silica than to the unmodified silica (Fig. 50). This is probably due to the positively charged surface, which is known to increase binding (148). Addition of Tween 80 decreased the binding to the silylated silica (Fig. 51) and addition of 0.2 % BSA by itself as a blocking agent caused a greater decrease (Fig. 52). The Tween 80 and 0.2 % BSA were used together for maximum effect.

A greater non-specific adsorption was seen for antibody on the beads with no antigen than for the flat silica (Figs. 52 and 53) with no antigen. This could indicate that the beads were more difficult to wash or that the beads were modified with a higher surface concentration of amines to give a more positively charged and higher binding surface.

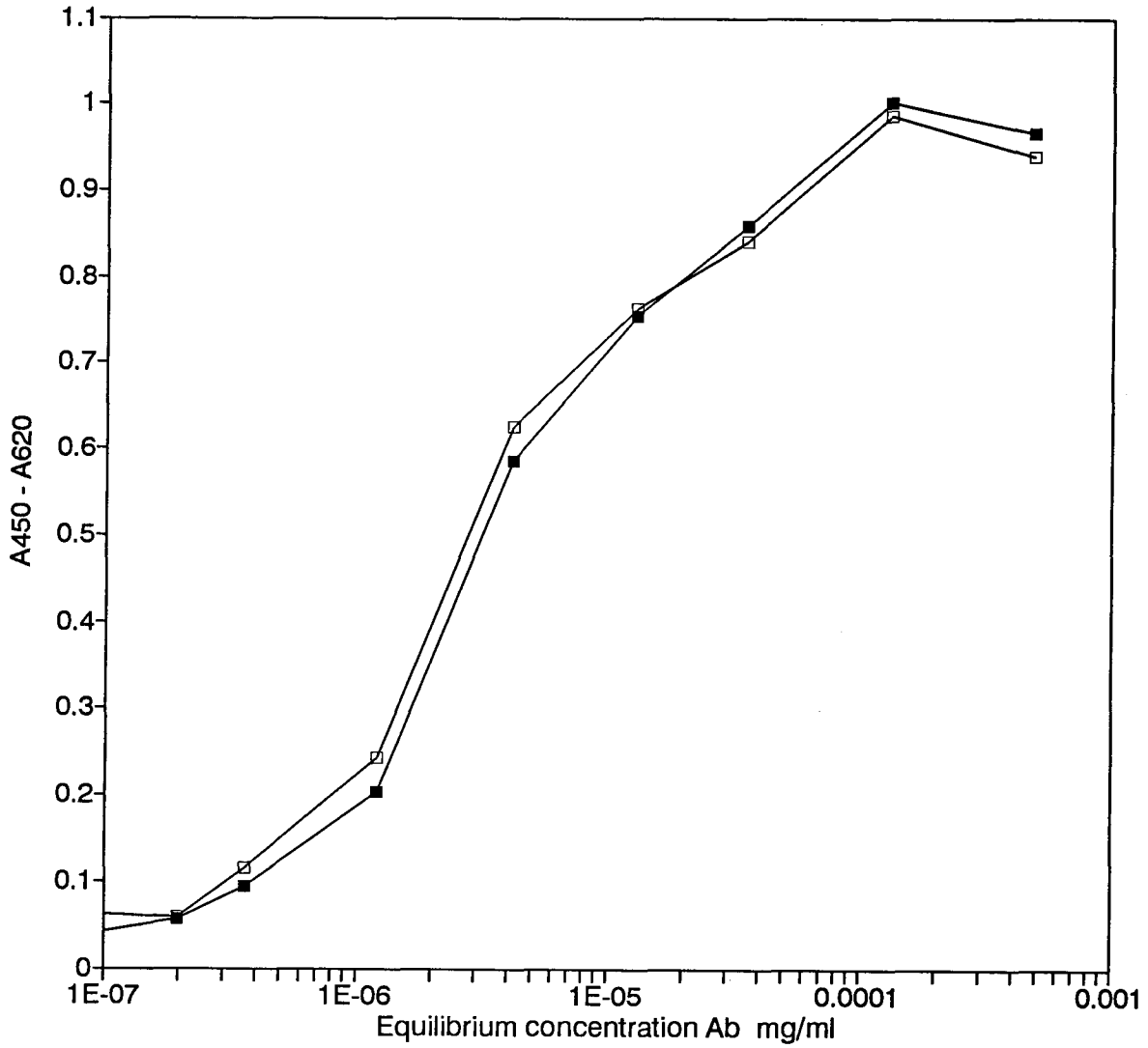

Figure 48a: An ELISA comparing the activity of labelled and unlabelled antibody, using commercial polymer microwells as the substrate (■= the labelled antibody, □= the unlabelled antibody).

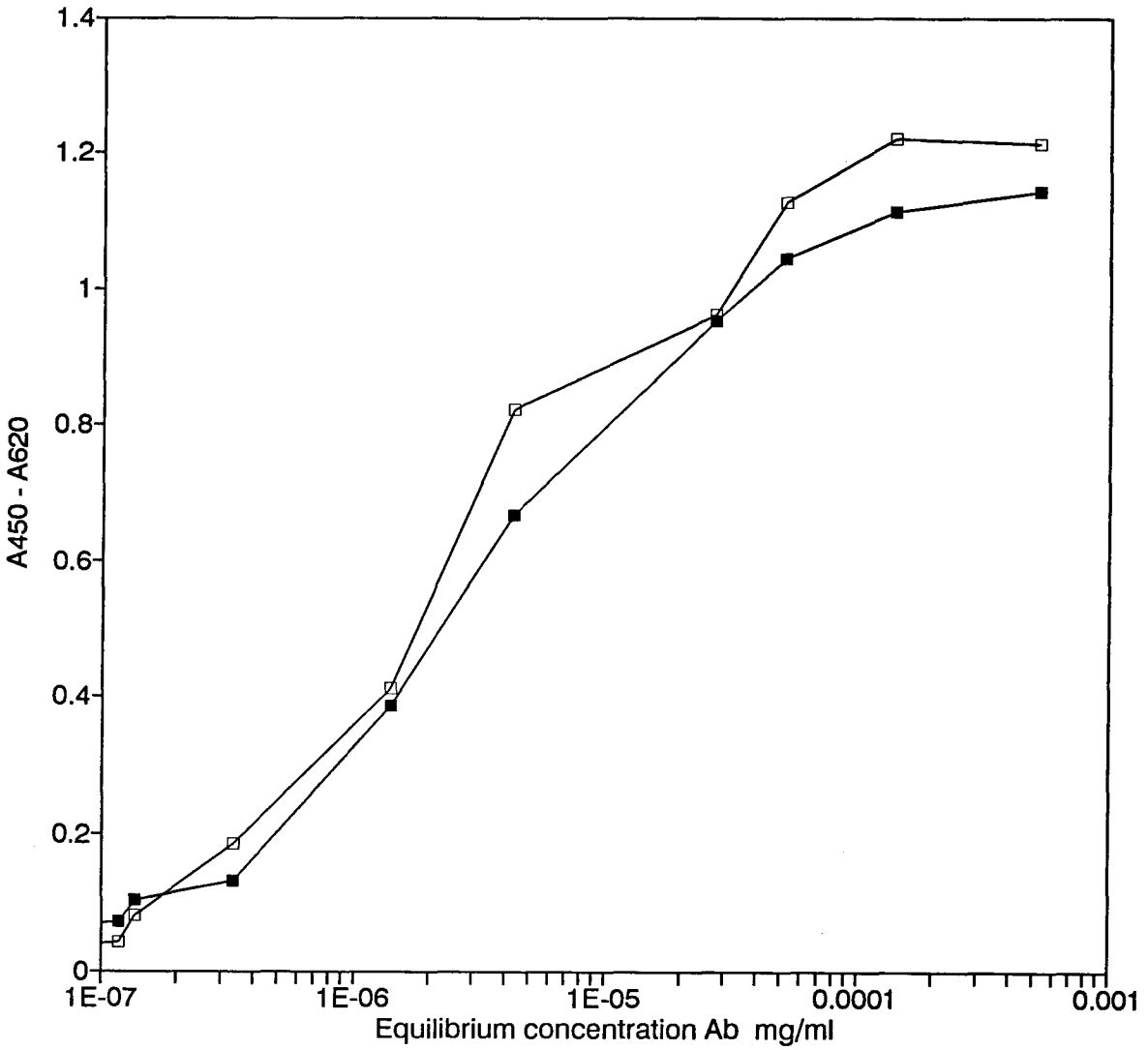

Figure 48b: A second ELISA comparing the activity of labelled and unlabelled antibody, using a different commercial assay plate. The labelled and unlabelled antibody were consistently shown to have similar activity (Fig. 48a).

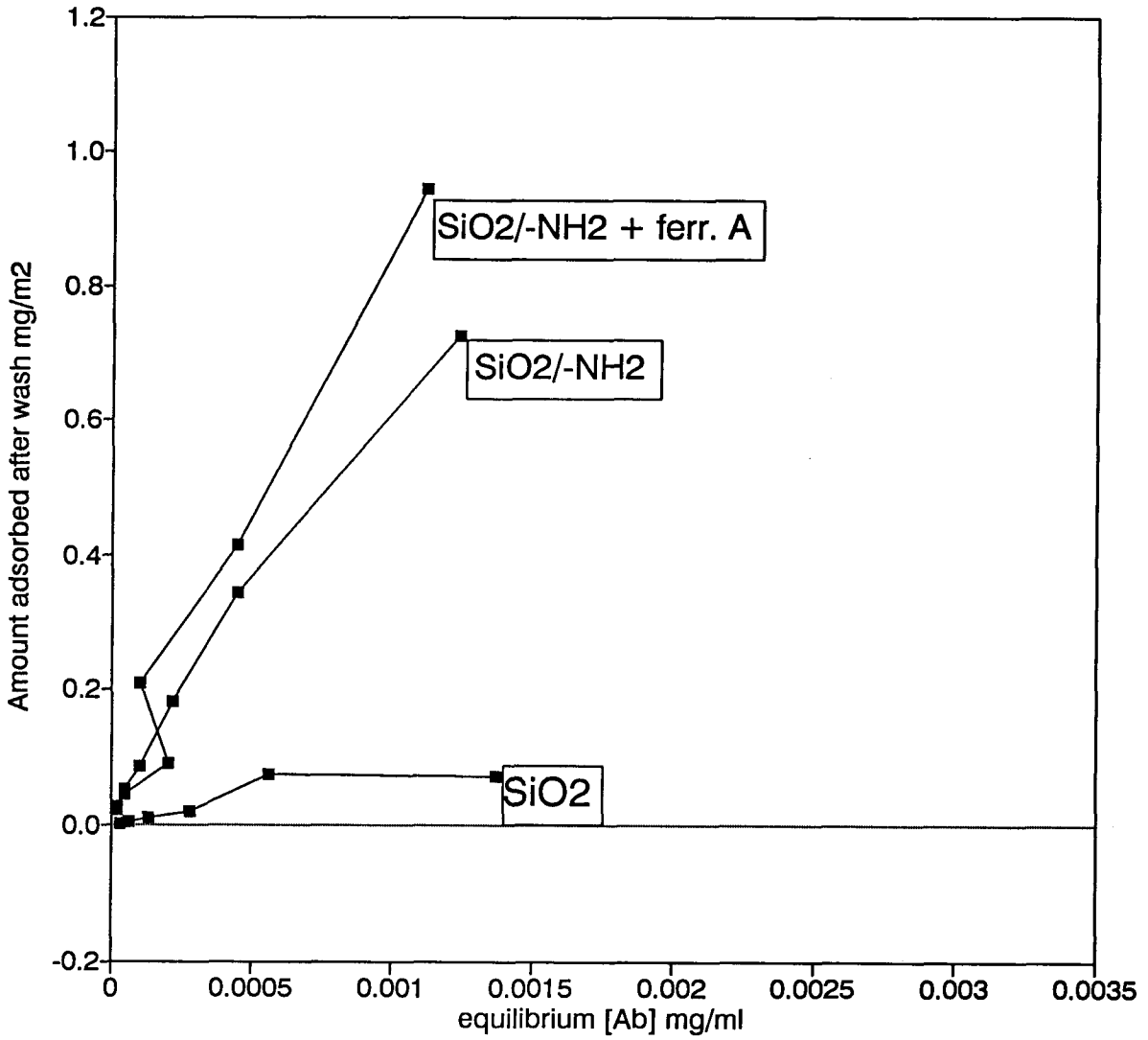

Figure 49: Antibody adsorption in PBS onto clean flat silica, silylated silica, and silylated silica with ferrichrome A.

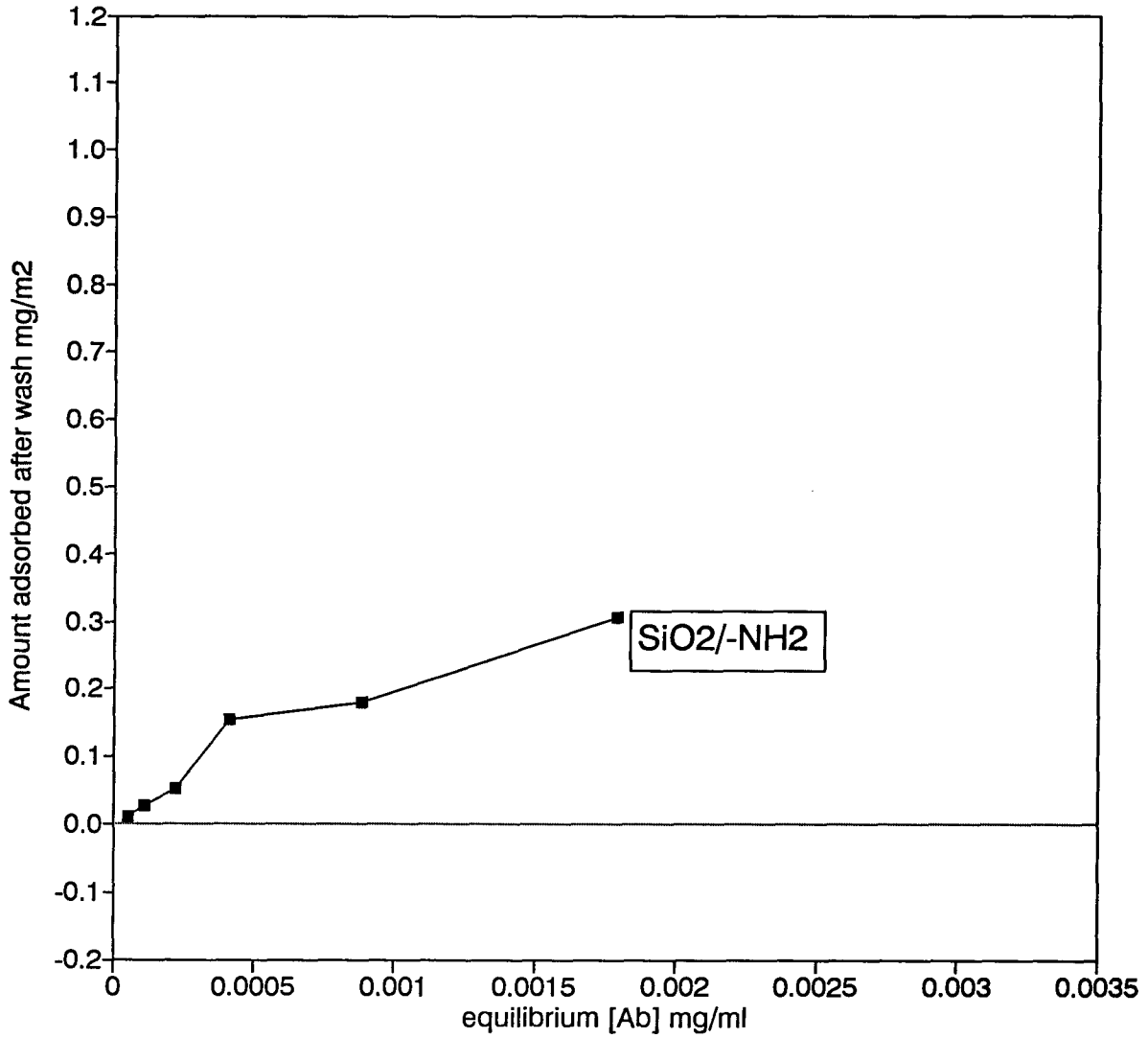

Figure 50: Antibody adsorption in PBS-Tween onto flat silica with no ferrichrome A

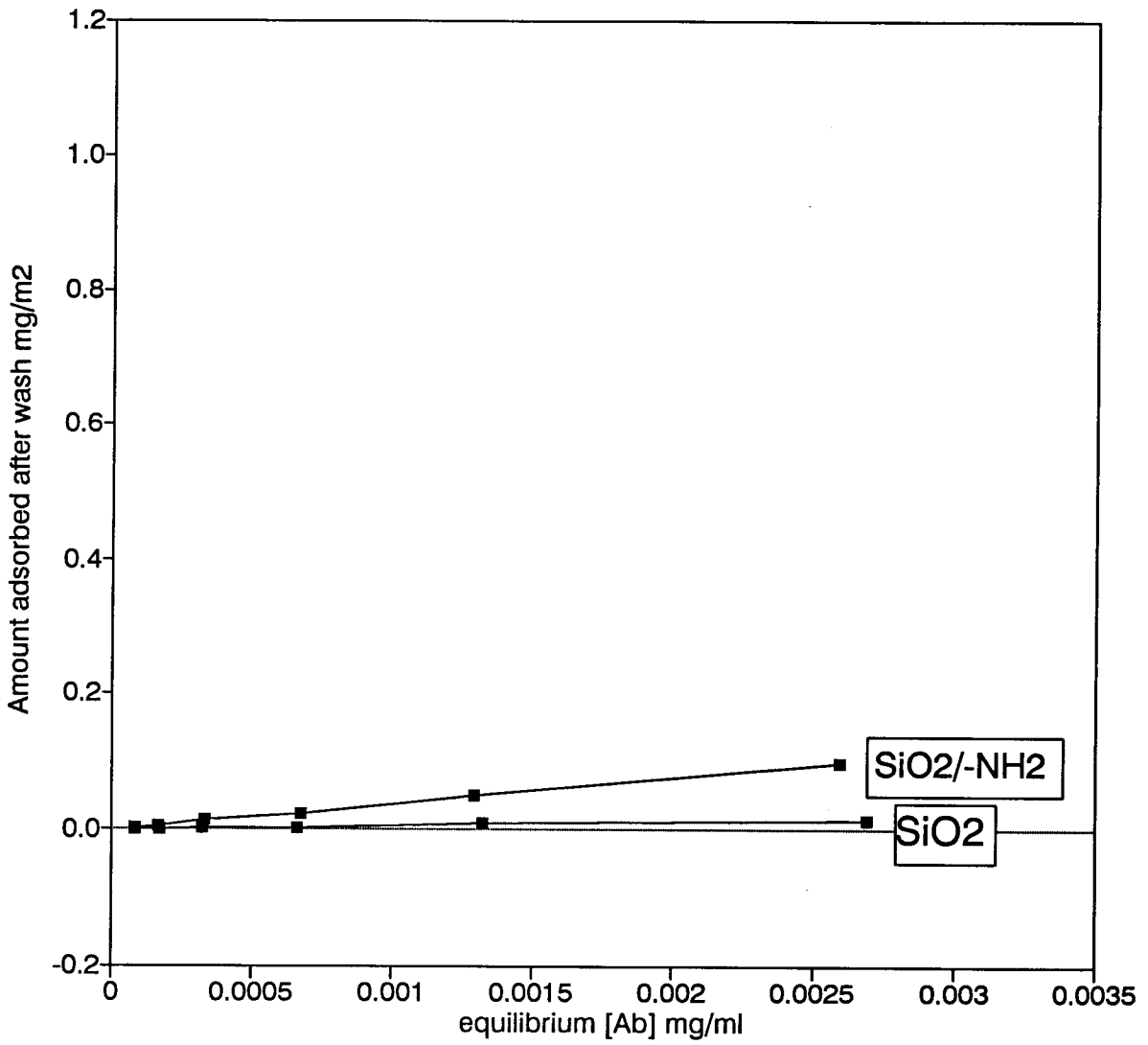

Figure 51: Antibody adsorption in PBS with 2% BSA onto flat silica with no ferrichrome A

Some increased adsorption was seen for the silylated silica modified with ferrichrome A, but it was not greatly different from the non-specific adsorption to silica without ferrichrome A.

The non-specific adsorption could be determined by labelling an unrelated IgG and using it in the assays. This would permit the determination of the amount of antibody bound non-specifically to the ferrichrome A modified surface. Although this was done as a control for some ELISAs, it was not done for the protein adsorption isotherms.

3.4c Antibody binding to ferrichrome A on flat silica and beads

Silica beads were prepared with a range of surface concentrations of ferrichrome A. Silica slides were modified with the same range of solution concentrations used to modify the beads. Both the slides and beads were used for adsorption isotherm measurements.

The amount of antibody bound to the antigen coated surfaces was calculated by solution depletion measurements and by direct counts of the amount of antibody left on the beads after washing. The antibody binding was seen to be irreversible over the washing time period used, with the amount bound from solution depletion measurements being the same or slightly greater than the amount determined from a direct count.

The surface concentrations of protein appeared to be more accurate from the direct measurements, giving less scatter and no negative values for the surface concentration of antibody and were therefore used to calculate the binding constants. The data points measured for the protein adsorption isotherm were used directly in the Scatchard plots, although this may not be the best approach, given the scatter in the data. Another way would have been to plot the data of the amount bound against solution equilibrium concentration, fit curves by eye and

then take data points off the graph.

Results for the beads and the slides are shown in Figs. 53 and 54. The beads with no ferrichrome A on the surface showed some non-specific adsorption of antibody, which may be due to the strongly positive surface. As the surface concentration of ferrichrome A increased, the amount of exposed silylated silica decreased; this would affect the non-specific binding and might result in lower non-specific binding at higher ferrichrome A concentrations. The shapes of the isotherms for beads with successively higher surface concentrations of ferrichrome A are consistent with this idea; at high solution concentrations of antibody, the isotherms for beads with high surface concentrations showed saturation, whereas the isotherms for beads with lower concentrations of ferrichrome A did not.

Additional plots included in Appendix 4 show the amount of antibody bound to the beads and flat silica as calculated from solution depletion measurements. Appendix 4 also shows the binding of antibody to beads at low antibody concentrations.

Information about systems having binding sites with two different affinities can be obtained from Scatchard plots where the data is not too scattered. The Scatchard plots can be used to estimate the two different binding constants as shown in Fig. 55. Data for the Scatchard plot of the beads with 0.086 mg/m^2 could be used to draw two lines with different slopes.

If there is a reorientation of ferrichrome A at higher surface concentrations, as postulated in sections **3.2e** and **3.2f**, the antibody might bind differently to the beads at high surface concentrations. This could possibly explain the binding isotherm for antibody on the beads at a ferrichrome A surface concentration of 0.83 mg m^{-2};if the ferrichrome A

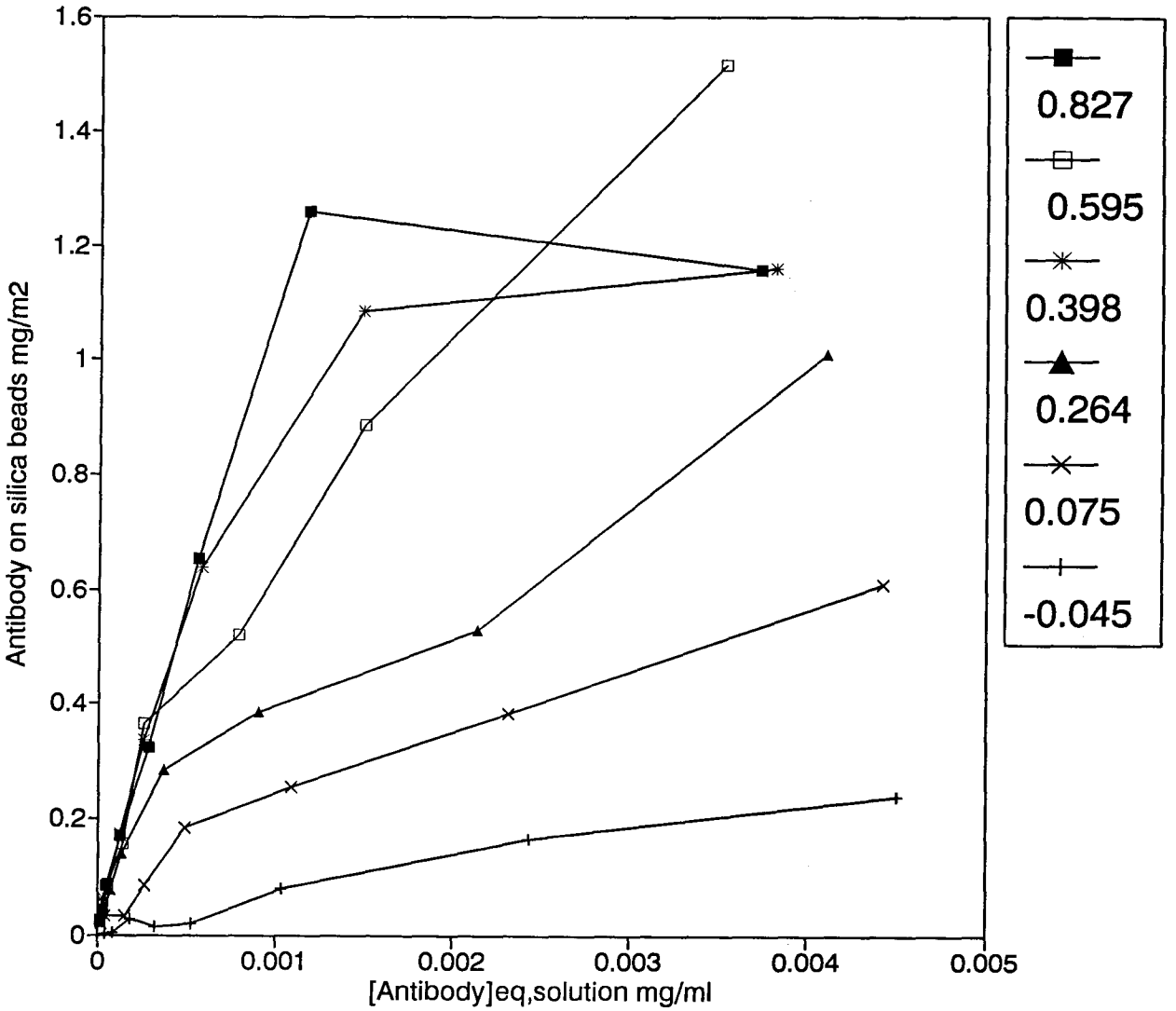

Figure 52a: Antibody bound to silica beads with a range of different surface concentrations of ferrichrome A: bound antibody determined from the amount remaining after washing. The legend shows the measured surface concentration of antigen on the surface in mg/m^2

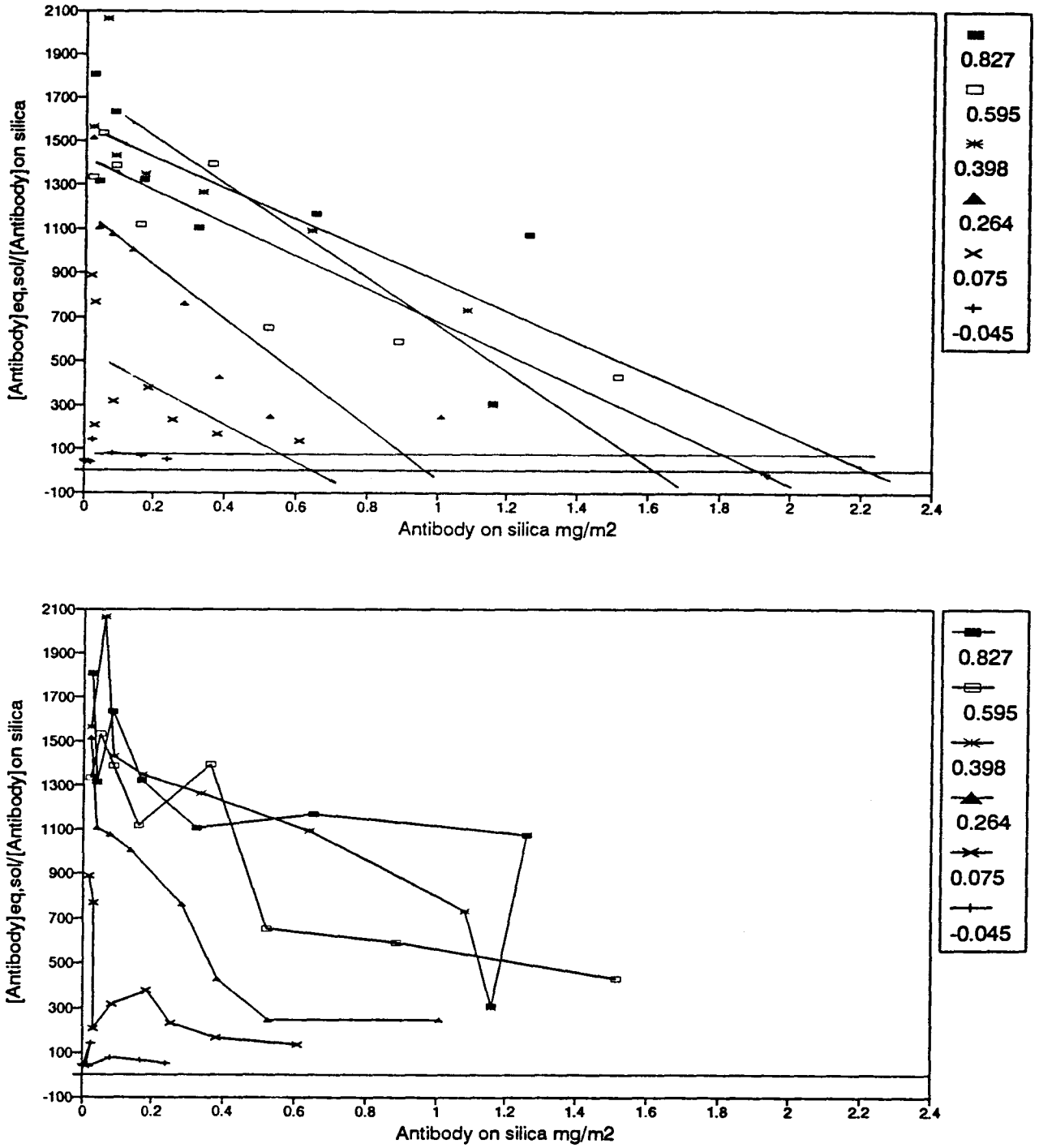

Figure 52b: The Scatchard plot for the data shown in Fig. 52, shown with and without a linear regression.

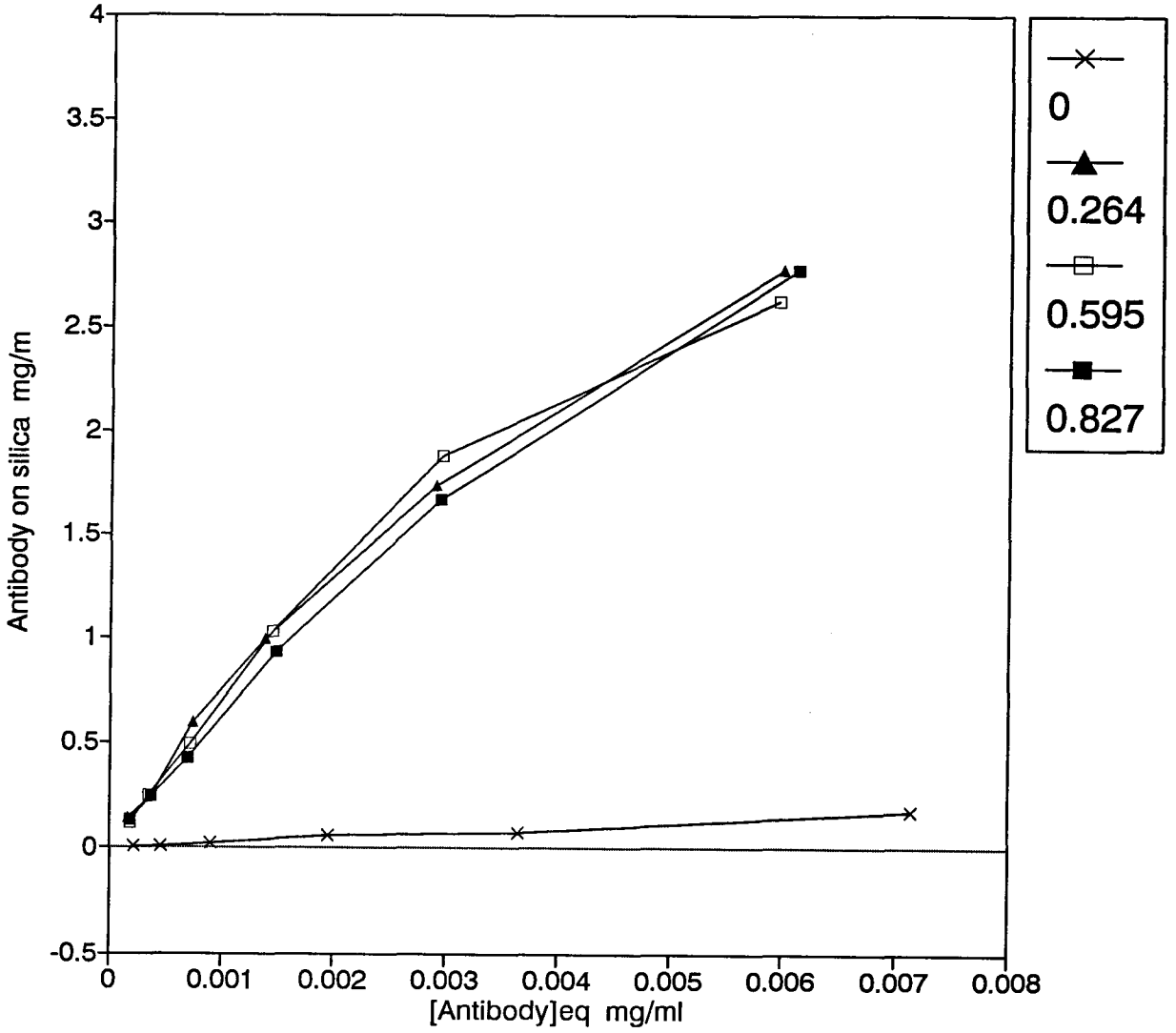

Figure 53a: Antibody adsorption to flat silica modified with a range of different solution concentrations of ferrichrome A: bound antibody determined from the amount remaining after washing. The legend shows the surface concentration of ferrichrome A (mg/m^2) obtained on beads modified with the same solution concentration of ferrichrome A.

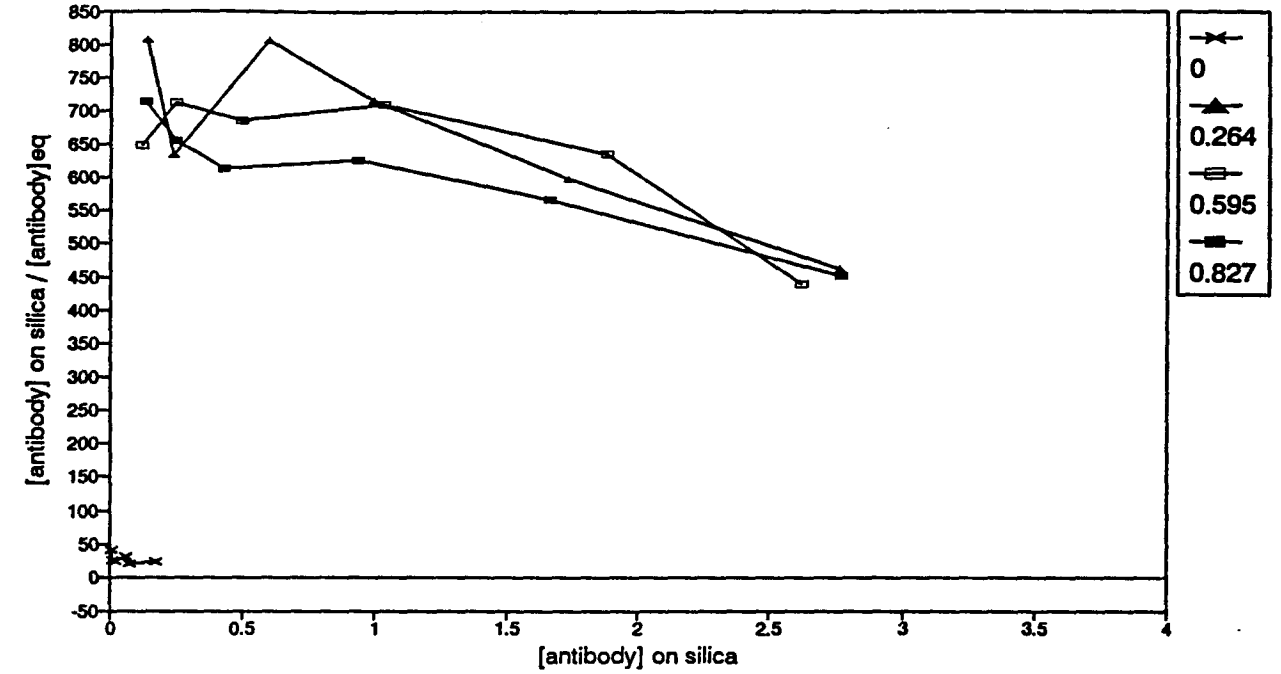

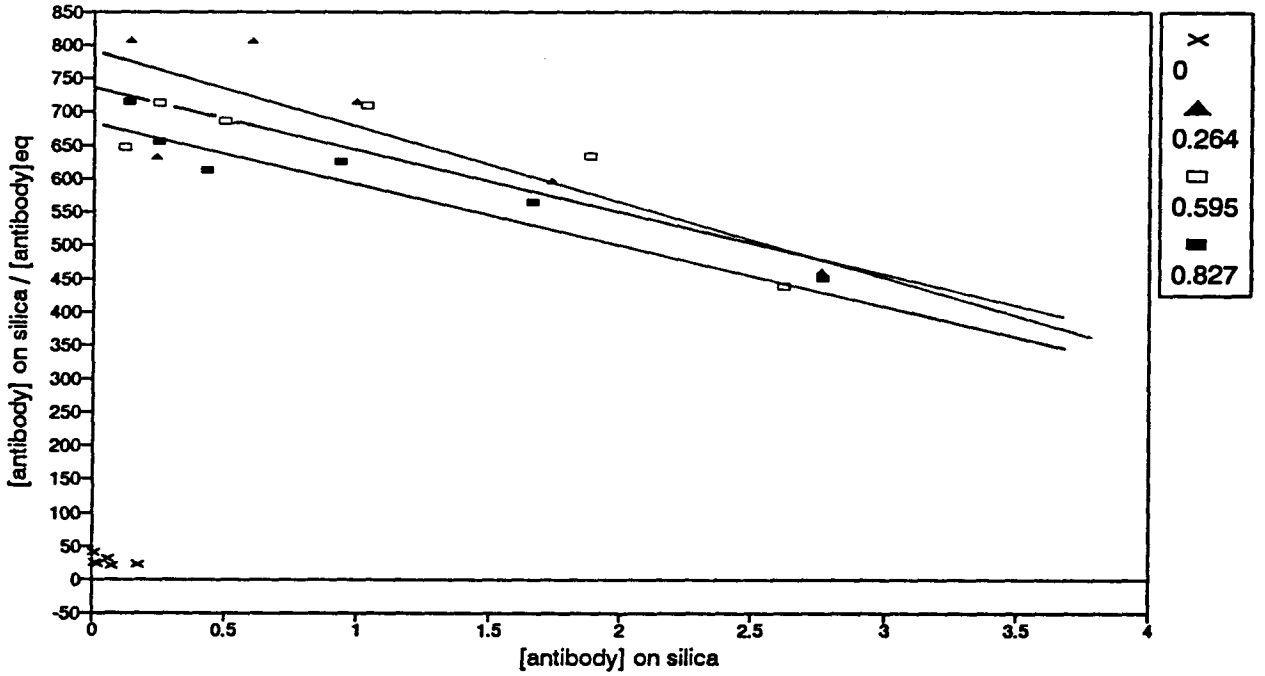

Figure 53b: The Scatchard plot for the data shown in Fig. 53, shown with and without a linear regression.

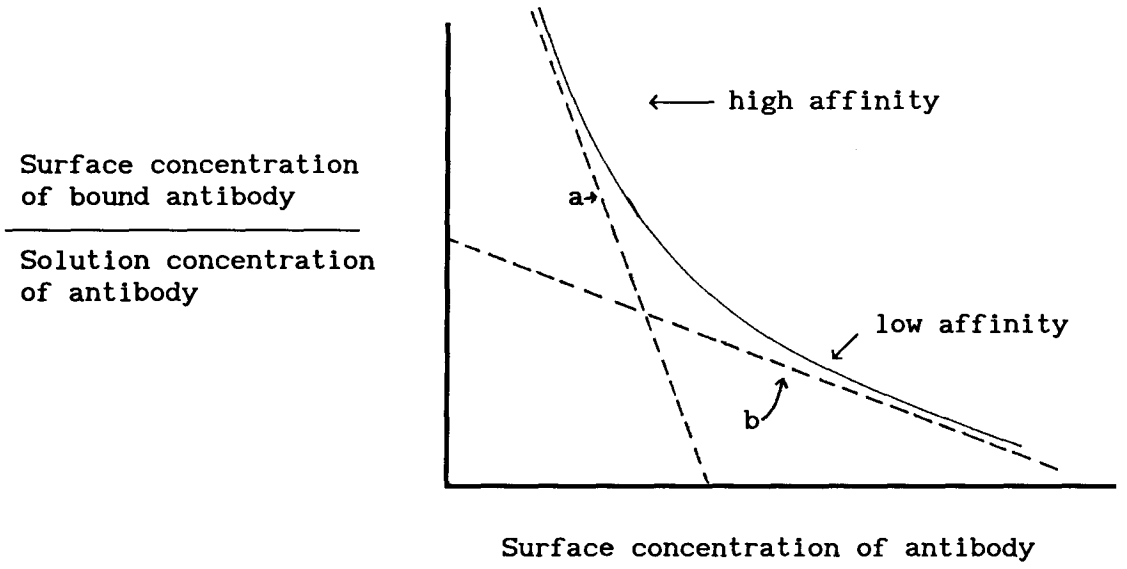

Figure 54: Scatchard plot for a system with two different binding affinities. The equilibrium constant for high affinity binding can be determined from the slope of line a, and equilibrium constant for low affinity binding can be determined from the slope of line b.

were in the more densely packed mode postulated for surface concentrations below the apparent saturation point at 1.1 mg m^{-2}, the antibody might bind less strongly, resulting in lower surface concentrations of antibody than were seen for the beads with lower surface concentrations of ferrichrome A.

The antibody did not show as much non-specific binding on the silylated flat silica (Fig. 54) as on the beads. If the non-specific binding is due to the amine groups on the surface, as is implied by the comparisons of binding on unmodified silica and on silylated silica (Figs. 50 and 52), the flat silica would seem to have fewer amine groups than the beads.

No difference was seen for the adsorption isotherms onto silica modified with the different solution concentrations of ferrichrome A that caused variations on the binding isotherms on the beads. This may be because the different solution concentrations of ferrichrome A did not in fact result in different surface concentrations. If the flat silica has fewer amine groups than the beads, the ferrichrome A modification would not be expected to give the same results. The surface concentration of ferrichrome A on the flat silica could be limited by the amine group density.

Equilibrium binding constants for the antibody binding to ferrichrome A on the beads and flat silica are summarized in Table XII. The equilibrium constants for the binding to the beads are larger than for the binding to the flat silica (approximately 1.1×10^{8} litre mol^{-1} for the beads as opposed to 1.5×10^{7} litre mol^{-1} for the binding to the flat silica modified with higher concentrations of ferrichrome A). If the ferrichrome A is at low surface concentrations on the slides and is distributed evenly on the surface, then the

Table XII: Apparent equilibrium constants for antibody binding to ferrichrome A- modified beads and slides. These constants are calculated from the Scatchard plots and do not take into account the distribution of light chains that would render one quarter of the antibodies inactive.

Equilibrium constants K for binding to slides modified with three different solution concentrations of ferrichrome A (1, 2, 3) and with no ferrichrome A (4)

	maximum amount of Ab bound mg/m^2	K in litre mol^{-1}	area per Ab molecule $Å^2$
1	7.12	1.8×10^7	3 700
2	8.77	1.3×10^7	3 030
3	8.24	1.3×10^7	3 224
4	0.68	7.2×10^6	39 000

Equilibrium constants for antibody binding to beads modified with a range of ferrichrome A surface concentrations

concentration ferrichrome A on the surface $mg\ m^{-2}$	area per Ag molecule $Å^2$	K in litre mol^{-1}	max. amount Ab bound $mg\ m^{-2}$	area per molec. $Å^2$
0.827	211	1.1×10^8	2.22	11 970
0.595	293	1.2×10^8	1.90	13 960
0.398	438	1.7×10^8	1.61	16 503
0.264	661	1.9×10^8	0.99	26 594
0.075	2 327	1.4×10^8	0.64	41 345

antibody would not be able to bridge between two surface bound antigen molecules when it bound to the surface. Bridging increases the equilibrium constant as described in section 1.5e and has been reported to increase the measured equilibrium constants by several orders of magnitude (83).

Only binding of multivalent antibodies could be enhanced by bridging between antigens. Since the antibody preparation used probably contains both divalent and monovalent antibodies, a portion of the antibodies would bind with enhanced affinity at higher surface concentrations of antigen, and a portion would bind with lower affinity. The antibody also binds non-specifically to the silylated silica, so the observed binding isotherm would be a function of antibody binding to the antigen-modified surface in three different ways and with three different affinities.

The SEM photograph in Fig. 55 shows the distribution of binding sites for a gold-labelled secondary antibody on flat silica modified with ferrichrome A and with the antibody AC3. The gold particles do not show any large clumps, implying that the antibody binding sites are evenly distributed on the surface.

Comparison of the amount of Ab predicted to be bound at saturation to beads with the measured Ag density demonstrates that the Ag density is considerably more than twice the saturation amount of the Ab. Hence, bound Abs are presumably covering antigen molecules without specifically binding to them. The ferrichrome A-modified slides have a higher maximum number of antibody binding sites as determined by the Scatchard plot than do the beads. The lower affinity constant suggests that little bridging of surface Ag by Ab is taking place and therefore the surface Ag density is lower than on the bead surface. The Scatchard intercepts for Ab binding to the slides are higher than on the beads,

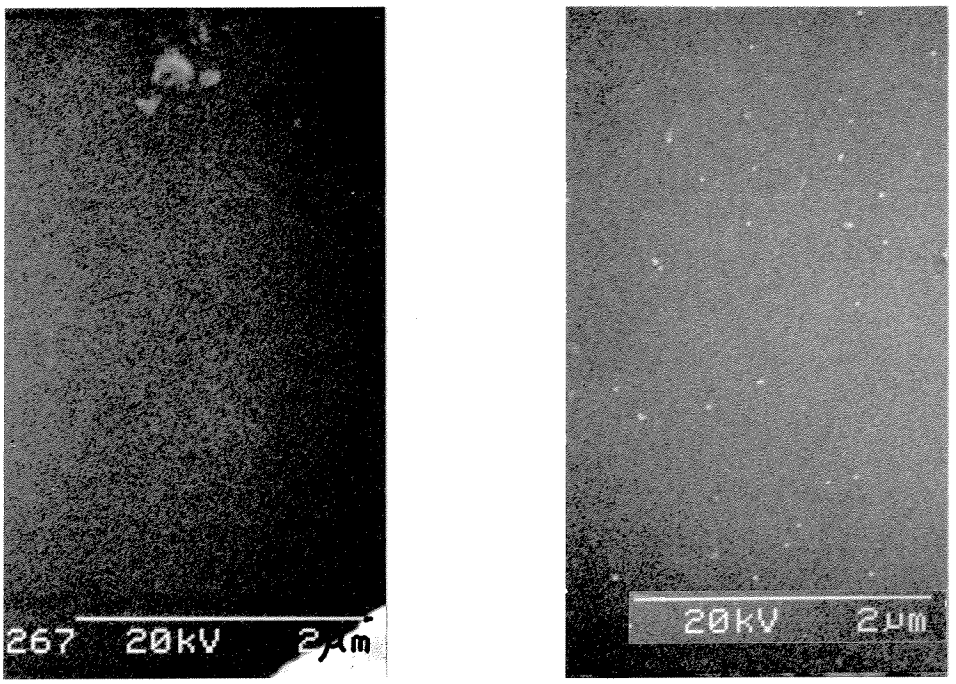

(a) (b)

Figure 55: SEM photograph showing the distribution of gold labelled secondary antibody on silica slides with immobilized ferrichrome A and adsorbed antibody. The small white dots represent gold particles (a= results obtained for no antigen on the surface and b= results obtained for antigen present)

however. This may indicate that singly bound Abs can pack more efficiently near saturation, perhaps showing more potential for rotation if the ferrichrome A is attached by only a single covalent bond, than do Abs that are more rigidly associated with the surface by binding two Ags per molecule.

There are also geometric considerations to be taken into account when comparing the beads and the slides. Antibody binding to diffusing and sedimenting particles in suspension is less likely to be limited by kinetics than is binding to a flat surface in an unstirred solution (75). If the binding of the antibody were limited by diffusion, then the equilibrium constant might be underestimated. The antibody was incubated with the silica for more than two hours at 37 ^{o}C with some stirring early in the incubation. Two hours was chosen as an incubation time as an optimum between the time required for antibody adsorption and the time during which the beads would settle out of solution.

Antibody on beads can form bridges in an additional way: the divalent antibody can bridge between two beads, to form an aggregate. Small clumps of two or three beads were seen for samples mixed with antibodies at an initial antibody concentration of about 10^{-5} to 10^{-7} mg/ml and a low measured surface concentration of ferrichrome A. Large clumps would affect the binding of the antibody due to bridges between the adjacent beads.

3.4d Inhibition of antibody binding with free ferrichrome A: a measurement of the solution equilibrium constant

Ferrichrome A in solution was used as a competitive inhibitor of the antibody binding to slides with immobilized ferrichrome A and the measurements of the amount of antibody bound as a function of solution

concentration of antigen were used to calculate the solution equilibrium binding constant as described in Appendix 1 (Fig. 56). Silica slides were chosen as a substrate rather than the beads to minimize problems with non-specific binding. The slides were modified with a low concentration of ferrichrome A in order to minimize possible bridging of the divalent antibody between adjacent antibody binding sites on the substrate.

An equilibrium constant of $2.5 \pm 0.8 \times 10^7$ litre mol^{-1} was calculated for the antigen binding to antibody in solution. This value is about half that calculated for specific binding to flat silica modified with the same solution concentration of ferrichrome A, taking the effect of light chain distribution into account: 7.1×10^7 litre mol^{-1}. This is the smallest estimate of the constant obtained in any of the systems examined, and is consistent with earlier discussion since none of the complications associated with interpretation of binding to surface-associated Ag, most of which tend to increase the apparent association constant, are relevant.

3.5 ELISAs using the beads and flat silica

3.5a Reproducibility of ELISAs on the beads

The ELISAs performed using the same batch of ferrichrome A-modified beads gave very consistent results (Fig. 57). Assays performed with a second batch of beads gave results that were similar, with the greatest change in absorbance occurring over the same concentration range of antibody in solution.

If reproducible ELISAs are desired, a large batch of beads can be modified and used for all experiments. The 10 mg bead sample sizes used were sufficient for about 300 data points at the sample area used,

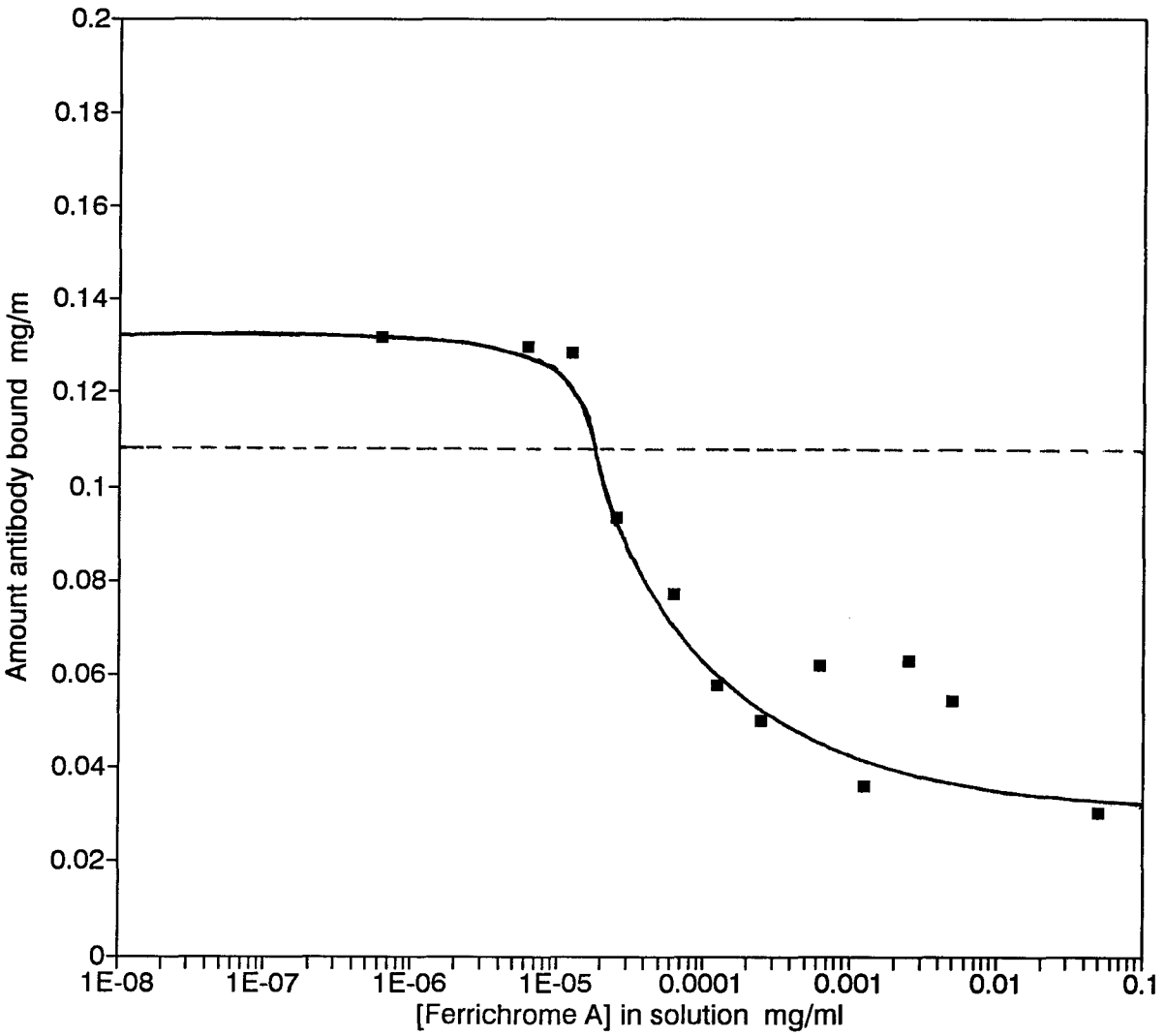

Figure 56: Antibody binding on flat silica: inhibition by free ferrichrome A. (- - -) = amount antibody bound with no inhibiting ferrichrome A.

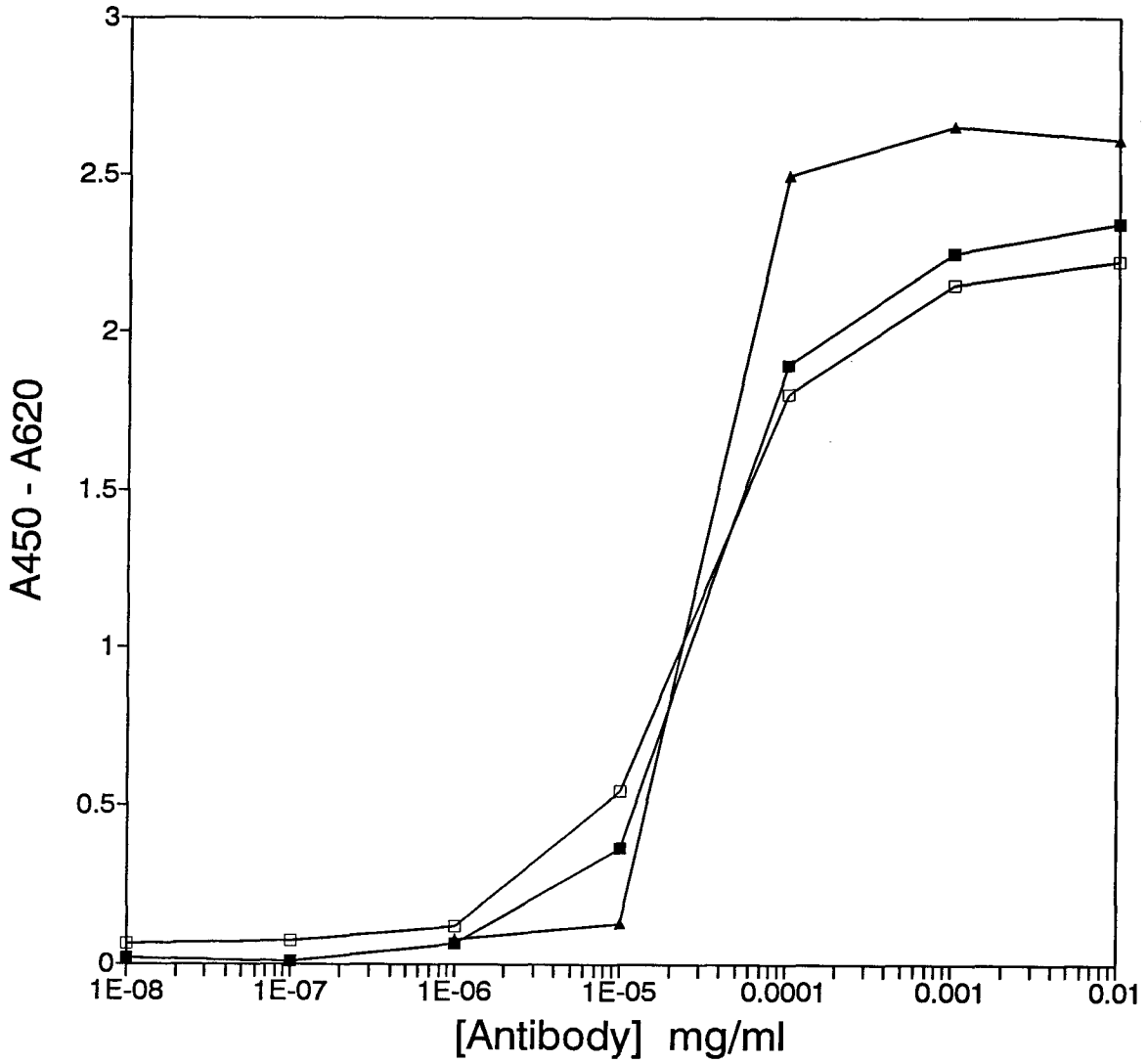

Figure 57: Reproducibility of ELISAs on ferrichrome A-modified beads (■, □ = beads modified with ferrichrome A at one time; ▲ = beads silylated and then modified with ferrichrome A in a separate experiment).

and larger bead samples could easily be modified with ferrichrome A.

In order to ensure reproducibility, the beads must be well suspended in the final assay step before addition of the substrate. Since the reaction of the substrate occurs quickly there is not sufficient time to mix and suspend the beads after addition of the substrate and incompletely resuspended beads will result in lower absorbances.

3.5b ELISAs on the beads: varying the surface concentration of antigen

Assays were performed on beads with a range of different surface concentrations of antigen (Fig. 58). There was very little difference between the two highest surface concentrations of antigen used. One of the two highest concentrations used was in the region where the kink occurs in the plot of the amount of ferrichrome A bound as a function of solution concentration and one was above it. If the ferrichrome A has in fact formed a close packed layer, it is not surprising that the amount of antibody bound does not increase. The amount of antibody bound as measured using radiolabelled antibody showed a similar pattern, with the two highest surface concentrations of antigen giving similar binding isotherms.

At lower surface concentrations of antigen, the maximum absorbance obtained decreased, and the minimum solution concentration of antibody required to give a detectable signal increased.

The shape of the ELISA plots changed as the surface concentration of antigen decreased, but this is probably only due to the fact that at the high surface concentrations of antigen and high solution concentrations of antibody, there is too much HRP in the samples to give a linear response (Fig. 23). The binding isotherms of antibody on the beads also showed a saturation, but this was at higher concentrations of antibody.

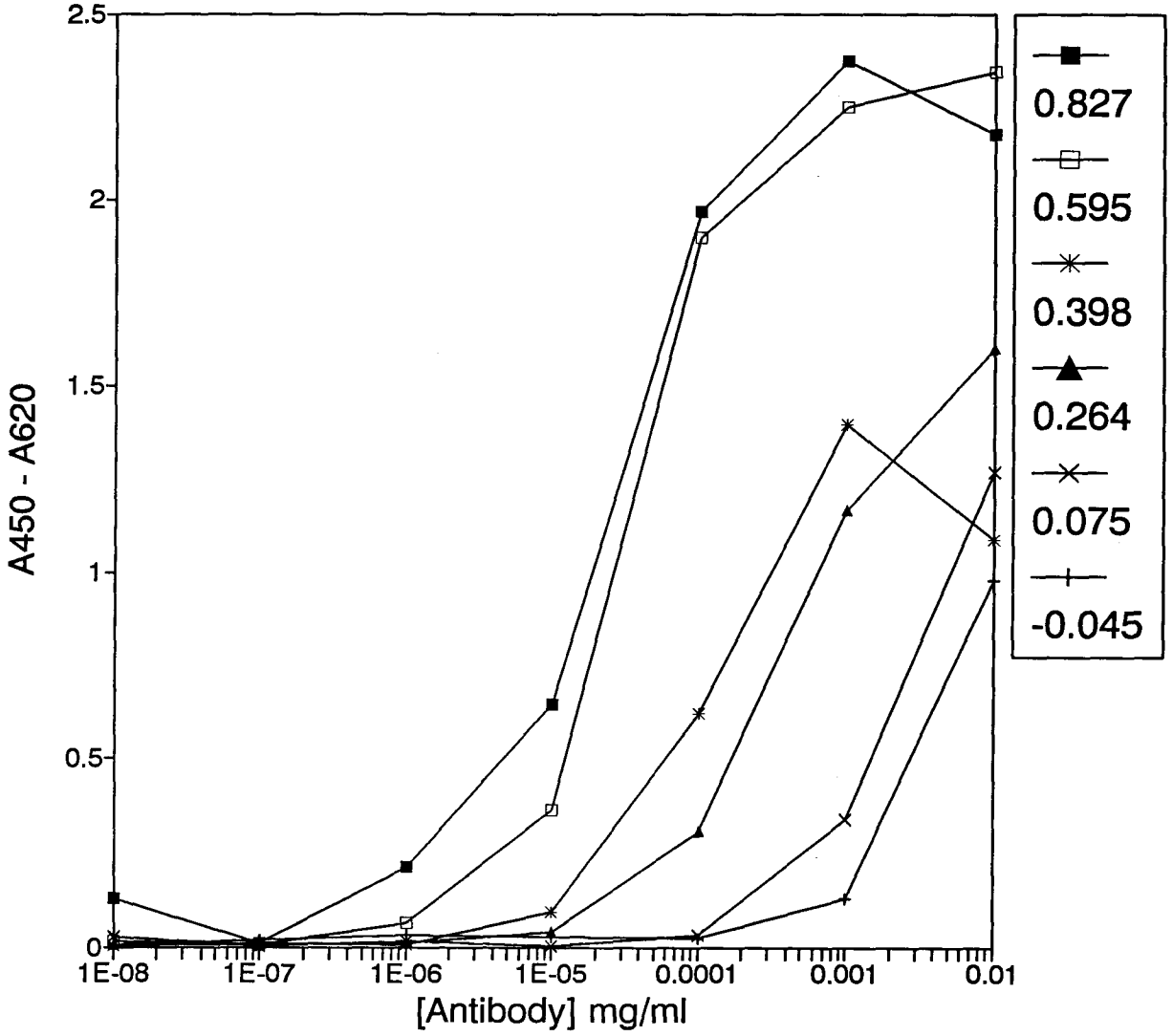

Figure 58: ELISAs on silica beads modified with a range of surface concentration of ferrichrome A. The legend shows the surface concentration of ferrichrome A in mg/ m^2.

Smaller surface areas of beads might have given a linear response due to the smaller amount of HRP that would have been present when the substrate was added, but the bead surface area used was chosen and kept at a constant value for purposes of comparison with the assays on the flat silica.

The ELISA results obtained are also plotted as a function of surface concentration of antigen for the different initial concentrations of antibody (Fig. 59). For a given solution concentration of antibody, the ELISA signal increased linearly with the surface concentration of antigen.

3.5c ELISAs on the beads: inhibition of the antibody binding with free antigen

The ELISA signal could be inhibited by free antigen, indicating that the antibody was binding specifically to the ferrichrome A.

An initial antibody concentration of 10^{-4} mg/ml was used for the inhibition assay (Fig 60), which was performed at the same time as the ELISA measuring response as a function of solution concentration of antibody (Fig. 61). The ferrichrome A inhibited the response at solution concentrations down to 10^{-5} mg/ml, or $1x10^{-8}$ M. The sensitivity of the inhibition assay may be limited since there would be very little change in absorbance with decreasing HRP concentration at the initial absorbance seen with no inhibiting antibody (Fig. 23). The assay conditions were chosen to be comparable to the beads rather than to maximize sensitivity.

3.5d Some comments on ELISAs on beads

The beads can be modified with a very high concentration of antigen. This has the advantage of giving a very high response at high solution

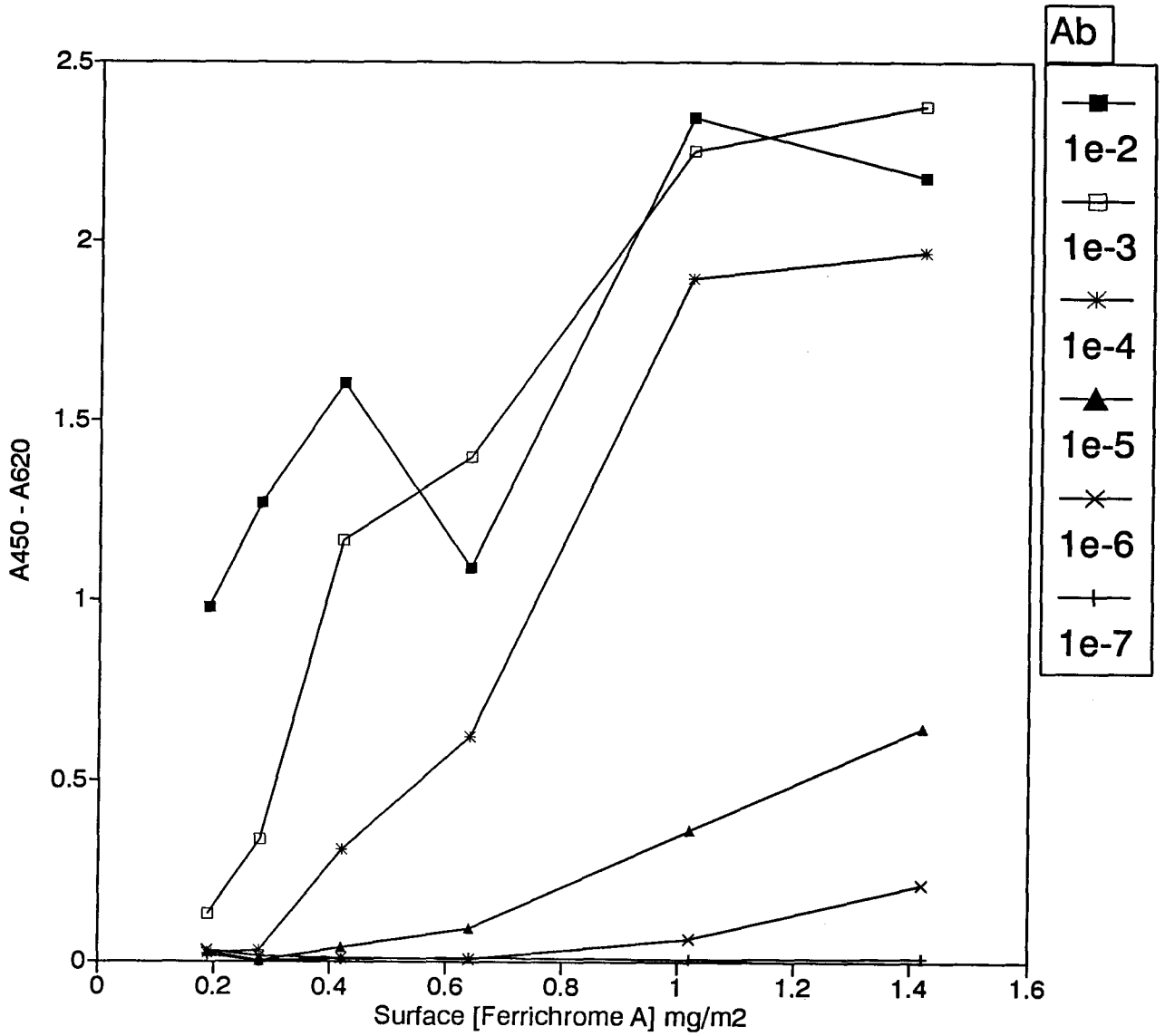

Figure 59: ELISA result for silica beads plotted as a function of surface concentration of antigen. The legend shows the initial concentration of antibody in mg/ml.

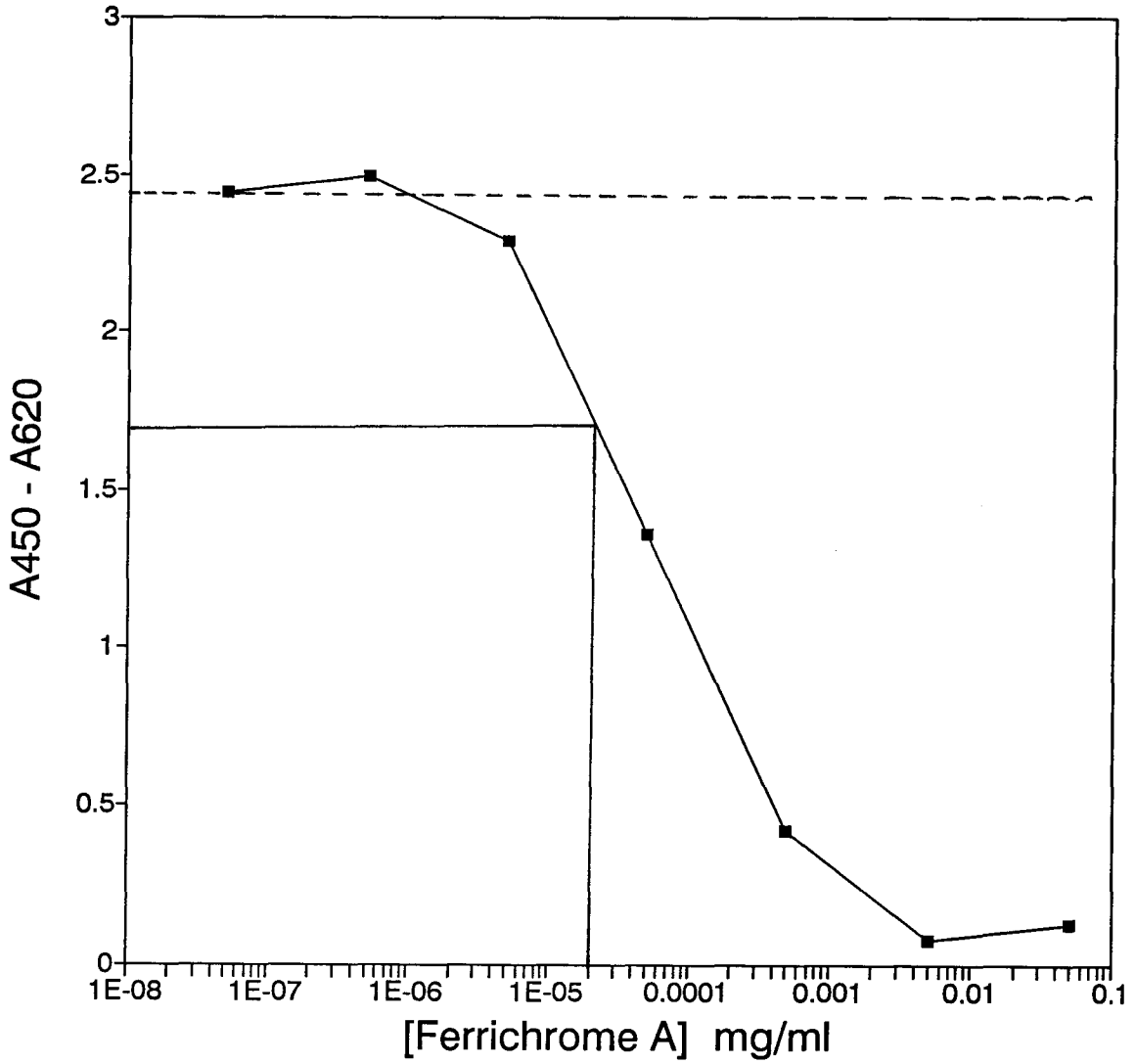

Figure 60: ELISA on beads: inhibition of antibody binding with free ferrichrome A with an initial antibody concentration of 10^{-4} mg/ml. A 30% decrease in the ELISA signal was seen at a ferrichrome A concentration of 1.1×10^{-5} mg/ml.

concentrations of antibody, with the binding of antibody likely being enhanced by the formation of bridges between adjacent antigens. There is some difficulty defining the term "sensitivity" with respect to an ELISA. The overall sensitivity is determined by the association constant of the antibody. For a given antibody, the bead assays are quite sensitive in that a very small surface area of beads gives the response that is equivalent to that obtained with ELISAs using other systems.

When the usual practice of varying antibody concentrations logarithmically (sequential halving dilutions) is used the beads are not more sensitive than flat substrates in terms of minimum concentration of antibody detected, since the response decreases to background at about the same concentration of antibody. However, by optimizing conditions it should be possible to set up an assay for soluble antigen using the beads which would be able to reliably detect lower levels of inhibiting free antigen than with the usual flat wells since a higher signal for a given concentration of Ab can be provided. This is of interest since a great many practical diagnostic assays employ inhibition of an ELISA signal for detection and quantitation of free antigen.

3.5e ELISAs on flat silica

Assays were also performed using flat silica modified with different solution concentrations of ferrichrome A (Figs. 61-63). The assays gave a much lower response than the equivalent experiments using beads with the same surface area. Larger solution volumes were used in the measurements of absorbance than for the measurements of the beads, so the results shown should be divided by two to obtain a direct comparison with the beads. This means that the beads are giving more than six times the response of the flat silica (which is comparable to the signal

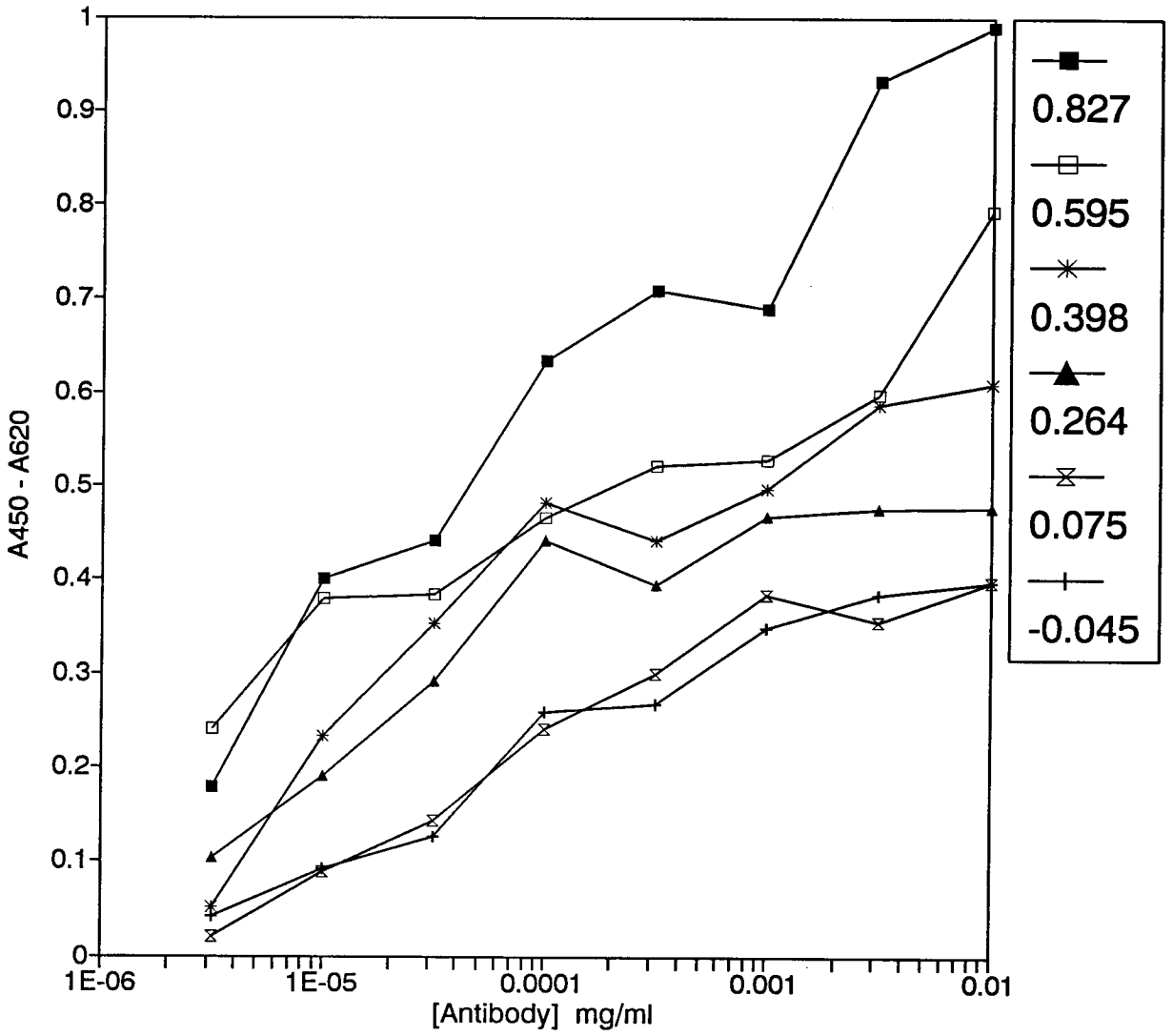

Figure 61: ELISAs on flat silica modified using a range of solution concentrations of ferrichrome A. The legend shows the surface concentration of ferrichrome A (mg/m^2) measured on beads that are modified with the same solution concentration of ferrichrome A.

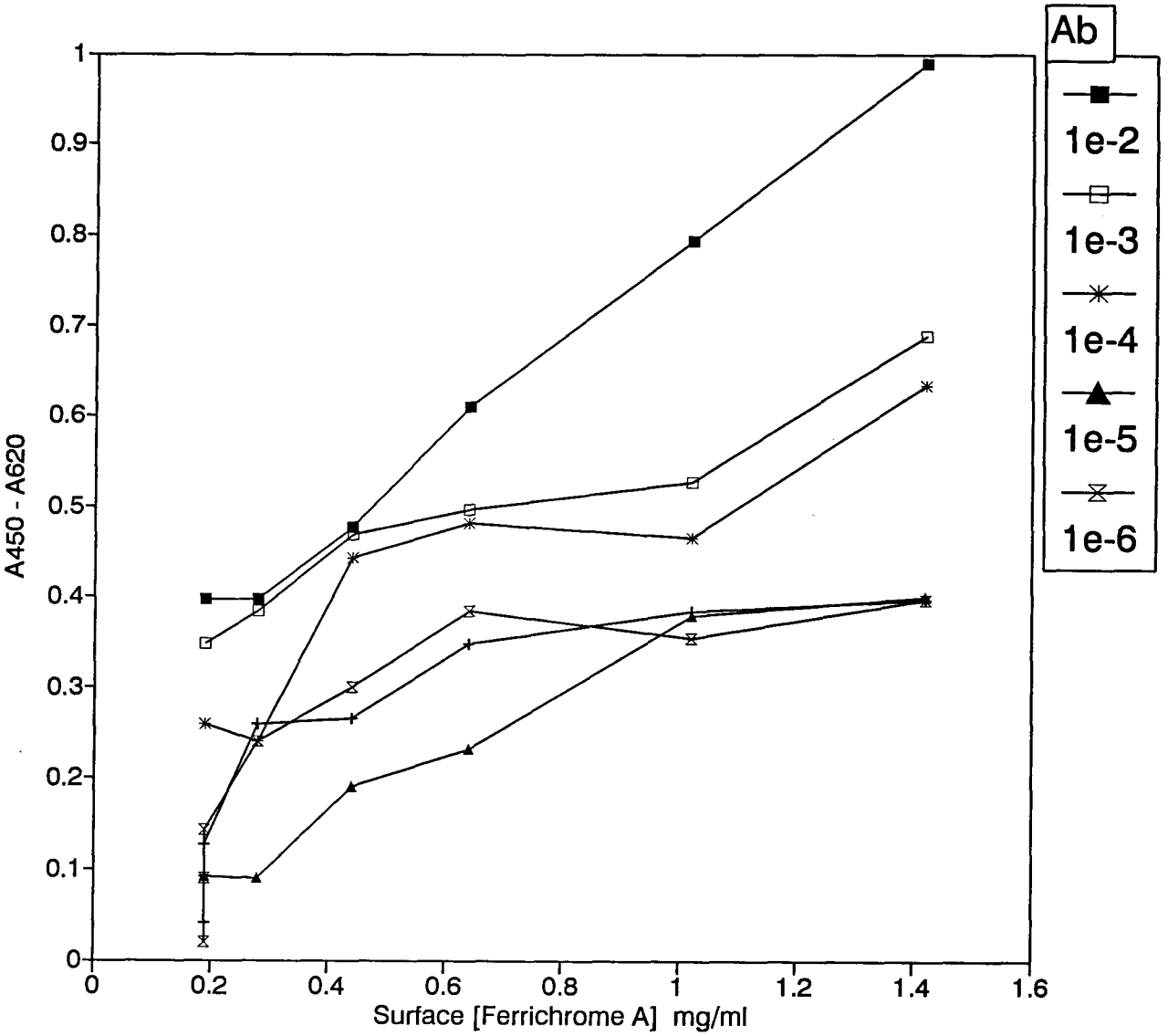

Figure 62: ELISAs on flat silica modified with a range of solution concentrations of ferrichrome A. The absorbance in the ELISA is plotted against the surface concentration of ferrichrome A determined for beads modified with an equivalent solution concentration of ferrichrome A.

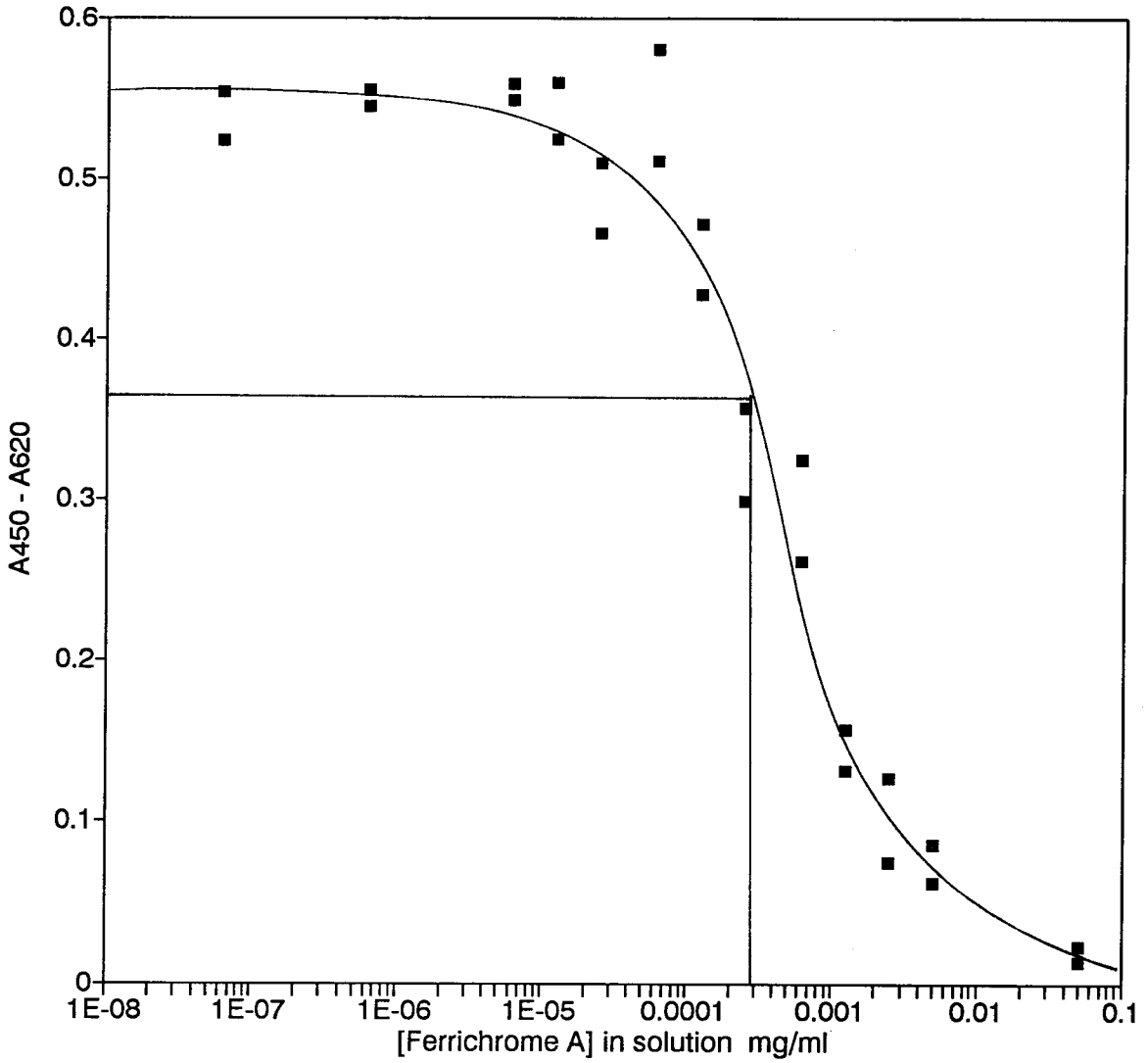

Figure 63: ELISA on flat silica showing inhibition by free ferrichrome A. A 30% decrease in the signal was seen with a ferrichrome A concentration of 1.1×10^{-4} mg/ml.

obtained with commercial plates and adsorbed, haptenated protein).

One of the problems with the low response is a simple geometric issue: the reaction occurs on a flat surface so the HRP was not distributed as evenly throughout the substrate solution as for experiments with the beads. The test tubes in which the substrate reaction was taking place were vortexed twice before that reaction was stopped, but could have been mixed more thoroughly. If the slides were allowed to sit briefly without mixing, a dark coloured layer formed adjacent to the slide.

The assays with the flat silica all give results in the range where the substrate response varies linearly with the amount of HRP present in the solution, that is, absorbances under 1.5. There was no saturation at high concentrations of antibody and high surface concentrations of antigen as was seen for the beads.

3.5d Quantitative aspects of ELISAs and comparison of ELISAs with adsorption isotherms

The surface concentration of antibody was measured directly with a radiolabelled antibody used for some ELISAs. The results showed that the response in the ELISA is not linear with the surface concentration of antibody (Figs. 64, 65), even though the absorbance readings obtained were in the range where the absorbance varies linearly with the amount of HRP present (Fig. 22). The ELISA gives a relatively higher response at lower surface concentrations of antibody, which could be due either to a relatively high amount of the the HRP-conjugated antibody being bound or to a relatively high conversion of substrate to coloured product. Binding of the HRP-labelled antibody could be enhanced at higher surface concentrations of antibody, however, where the secondary

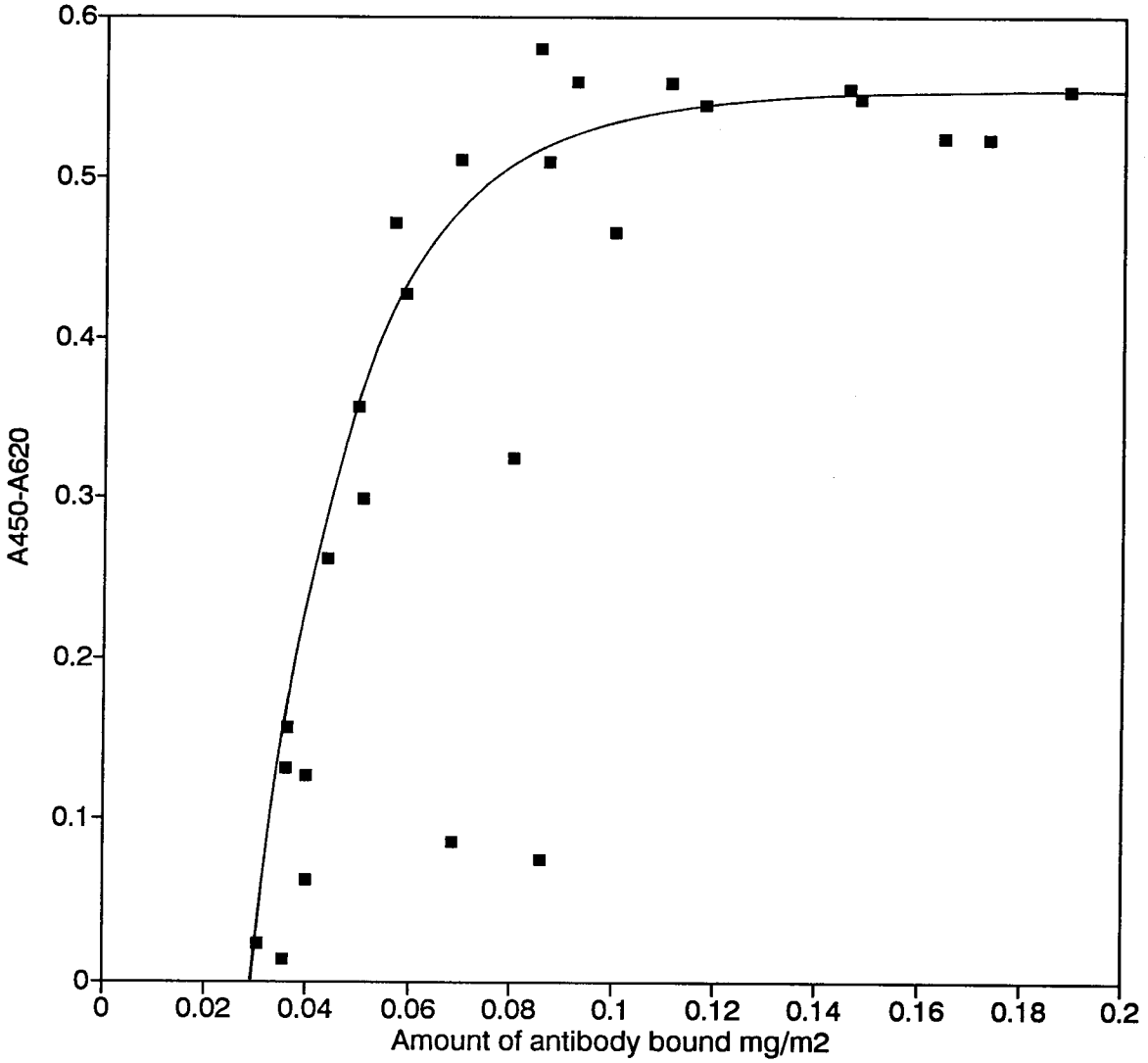

Figure 64: Absorbance in the ELISA as a function of surface concentration of antibody for an assay using flat silica. The results show that the absorbance in the ELISA is not directly proportional to the amount of antibody on the surface. The amount bound was determined from the amount remaining after washing and was therefore the amount of antibody present during the ELISA.

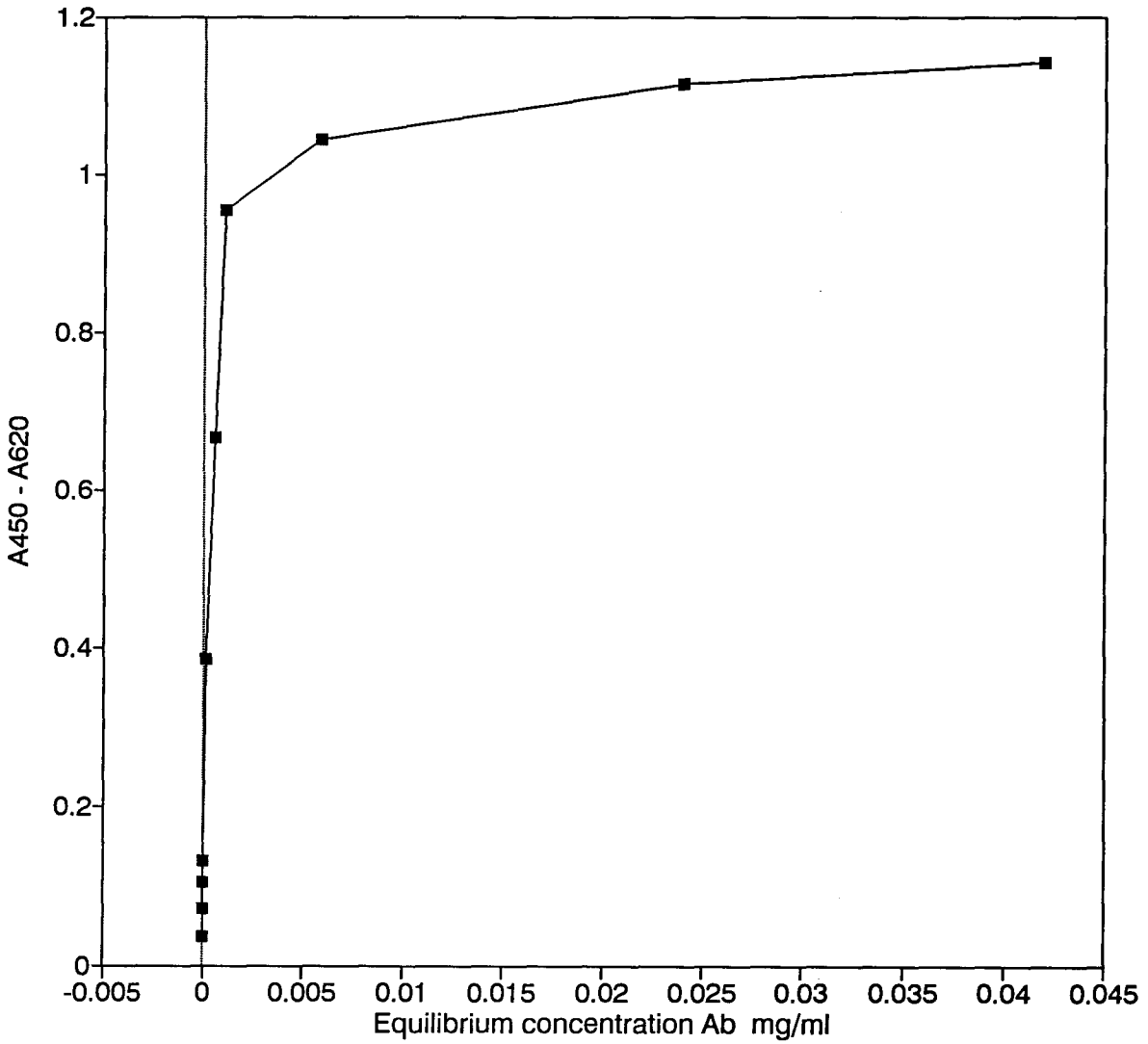

Figure 65: Absorbance in the ELISA as a function of surface concentration of antibody for an assay using a commercial ELISA plate. The amount bound was determined from the amount remaining after washing.

antibody would be able to form bridges between adjacent target antigens (the target antigens of the HRP-labelled antibody being the primary antibody).

The HRP-labelled antibody is specific towards the fc portion of the primary antibody and so binding of the HRP-labelled secondary antibody would be affected by the orientation of the primary antibody. If the primary antibody were binding in such a manner that the fc portion were less accessible, then low secondary antibody binding and a low ELISA reading would result. The binding of the primary antibody (AC3) is different on the beads and flat silica: the equilibrium binding constant and maximum amount bound both differ (Table XII). The primary antibody may bind to the silica beads in such a way that the binding of the secondary antibody is enhanced, giving a stronger ELISA response on the beads for the same amount of primary antibody bound. This could also explain the increased sensitivity of the bead assays for measuring free ferrichrome A (Figs. 60, 63): if a smaller amount of primary antibody (AC3) were bound to the beads then less free antigen would be required to inhibit the antibody binding and a lower concentration of antigen would cause a decrease in the measured ELISA signal.

Since the conversion of the substrate to the coloured product occurs at a surface over a short period of time in a poorly stirred or unstirred solution, the extent of the reaction may be limited by the diffusion of the substrate to the surface-bound enzyme. At higher surface concentrations of enzyme, this effect would become more pronounced since the substrate near the surface would be depleted more rapidly. This may be the cause of the relative loss of signal as the surface concentration of primary antibody was increased.

Thorough mixing would be expected to increase the absorbance at

higher surface concentrations of antibody. This has been demonstrated using an acoustic probe to provide mixing during all incubation steps of an ELISA. The effect was to increase the absorbance obtained in the final step of the assay, in addition to decreasing the time required for each incubation step (149).

The response of the ELISA as a function of surface concentration of antigen has been seen to vary with the affinity of the primary antibody (94); lower affinity antibodies were reported to give a relatively higher absorbance in the ELISA but no explanation for this observation was given.

Direct comparisons of the absorbance from the ELISA with the surface concentration of antigen were only made for the assays using cylindrical wells in commercial plates and for the flat silica. The surface concentration of antibody on the beads can be compared to the absorbance. The ELISA results for the beads might be more directly related to the surface concentrations of antibody, due to the distribution of the beads throughout the substrate solution. The shape of the binding isotherm on the beads seems to resemble the shape of the ELISA plot more closely than the shape of the binding isotherm on the cylindrical assay plate resembles the corresponding ELISA plot.

If the ELISAs are to be used for determination of the solution concentration of antibody, then the non-linear response of the absorbance with respect to surface concentration of antibody need not hinder the assay. The reference standards should be measured under the same conditions used for the unknown, using antibodies that have the same affinity as antibodies in the unknown sample to be measured. This can, however, prove to be quite difficult due to the large number of variables involved. Changing the assay conditions can result in

different measured antibody concentrations (88).

The antibody-antigen affinity can determine the minimum detectable concentration of antibody and can also affect the accuracy of the measurements (88) when determining concentration of an unknown antibody. Increasing the surface concentration of antigen can increase the effective affinity of the antibody for the surface due to bridging between adjacent epitopes and will minimize the dependency of the assay results on the intrinsic affinity of the antibody for the antigen (94).

Chapter 4

Concluding Discussion

Silica beads and slides can be silylated with 3-aminopropyltriethoxy silane to give a surface covered with amino groups. The silylated beads can be modified rapidly and easily with carboxyl containing antigens in a one step reaction in water. Reproducible surface concentrations of antigen which lead to reproducible assays can be obtained by using freshly silylated beads or simply by modifying at one time enough beads to use in many assays. The high specific surface area of the beads permits modification of a large area of beads using only a small reaction volume.

The EDC-mediated coupling produced a stable bond between the substrate and the small antigen used for the assays, so that the antigen could be immobilized on a surface without being coupled to a larger molecule that would adsorb non-specifically. The EDC-coupled antigen did not wash off in buffer, and antibody bound to ferrichrome A-modified silica did not desorb when washed with PBS-Tween.

The concentration of antigen coupled to silica beads by the EDC was measured as a function of solution concentration of antigen. The solution depletion measurements of the ferrichrome A on the beads and the particle electrophoresis with the modified beads gave evidence for rearrangement of the ferrichrome A at higher surface concentrations. Presence of the ferrichrome A on modified slides was confirmed by XPS measurements showing the iron peak.

Ferrichrome A was chosen as an antigen because of several features useful for analysis but it proved to be a poor immunogen in BALB/c mice,

giving a polyclonal response much weaker than in rabbits and only low affinity monoclonal antibodies. This limited the potential sensitivity of the assays, and future experiments should include the use of higher affinity antibodies.

The binding of the antibody to the antigen-modified beads and slides was different: the equilibrium constant for the antibody binding to the antigen-modified beads was higher, but the maximum amount bound on the beads was lower. The silica beads were less dense than the slides and could therefore have been porous or else could have contained organic matter from the tetraethyl orthosilicate used in the bead production. The silica beads could also have had a higher surface concentration of silanol groups, since the heating process involved in the production of the fused quartz slides decreases the surface silanol concentration. If silylation results in modification of all the silanol groups (144), then the beads could have had a greater surface concentration of amines. The antibody binding could be affected by the surface charge due to the amine groups, by the surface concentration of antigen, and by the porosity of the silica substrate, since the antigen might be more accessible if it is not fixed on a flat surface.

The ELISA response was much stronger for assays using the silica beads, which could be due to the different modes of binding of the primary antibody on the beads and on the slides affecting the binding of the secondary HRP- conjugated antibody.

The antigen-modified beads and slides were both used for ELISAs measuring the concentration of free antigen. Assays with the beads were more sensitive and could be used to detect the ferrichrome A at one tenth the concentration that could be detected with ELISAs on the slides. The sensitivity of the assays on the beads could possibly be

improved by using a lower initial concentration of antibody or a shorter development time after addition of the substrate.

Silica beads can be readily modified with amine groups for covalent attachment of high surface concentrations of small carboxyl containing antigens. The ELISAs using the beads give a strong response and provide a more sensitive system for measurement of free antigen. Since silica can be modified with many different silanes, silica beads are a useful and versatile ELISA substrate. Further experiments should include silylation of the beads with other silanes to permit covalent coupling to antigens with different functional groups, and optimization of the assay sensitivity.

References

1. Rose, N.R., Friedman, H. and Fahey, J.L. Eds., Manual of Clinical Laboratory Immunology (4th Edition), American Society for Microbiology, Washington, D.C., 1992.

2. Paraf, A. and Petre, G. Immunoassays in Food and Agriculture, Kluwer Academic, Boston, 1991.

3. Price, C.P. and Newman, D.J. Principles and Practice of Immunoassay, Stockton Press, New York, 1991.

4. Steward, M.W. and Steensgaard, J. Antibody Affinity: Thermodynamic Aspects and Biological Significance, CRC Press, Boca Raton, 1983, p.1.

5. Harlow, E. and Lane, D. Antibodies: A Laboratory Manual, Cold Spring Harbor Laboratory, New York, 1988, p.27.

6. Otterness I. and Karush F. (1982) Principles of Antibody reaction. In antibody as a tool (Edited by Marchalonis J.J. and Warr G.W.),pp. 97-137. John Wiley, New York.

7. Edwards, R. Immunoassay: An Introduction, William Heinemann Medical Books, London, 1985, p.3.

8. Ngo, T.T. and Lenhoff, H.M. Eds. Enzyme-Mediated Immunoassay, Plenum Press, New York, 1985.

9. Jaklitsch, A. Separation-free enzyme immunoassay for haptens *In* Enzyme-Mediated Immunoassay, Ngo, T.T. and Lenhoff, H.M. Eds., Plenum Press, New York, 1985, p.33-55.

10. Standefer, J.C. Separation-required (heterogenous) enzyme immunoassay for haptens and antigens *In* Enzyme-Mediated Immunoassay, Ngo, T.T. and Lenhoff, H.M. Eds., Plenum Press, New York, 1985, p.203-222.

11. Ekins, R. Towards Simpler, Faster, More Accurate Immunoassays. *In* Cost/Benefit and Production Value of Radioimmunoassay. Albertini, A. Ekins, R. and Galen R.S. Eds., Elsevier Science Publishers, 1984, 23-37.

12. Yalow, R.S. and Berson, S.A. Assay of plasma insulin in human subjects by immunological methods. Nature **184**, 1648-1649, 1959.

13. Engvall, E and Perlmann, P. ELISA. III. Quantitation of specific antibodies by enzyme linked anti-immunoglobulin in antigen coated tubes. J. Immunol. **109**, 129-135, 1972.

14. Voller, A., Bidwell, D.E., and Bartlett, A. The Enzyme linked Immunosorbent Assay (ELISA). A Guide with Abstracts of Microplate Applications, Flowline Press, Guernsey, 1979.

15. Avrameas, S., Ternynck, T. and Guesdon, J.-L. Coupling of enzymes ton antibodies and antigens. Scand. J. Immunol. **8, Suppl. 7**, 7-23, 1978.

16. Galvin, J.P. Particle enhanced immunoassay-a review *In* Diagnostic Immunology: Technology Assessment and Quality Assurance, Rippey, J.H. and Nakamura, R.M. Eds., College of American Pathologist, Skokie, 1983, p.17.

17. Maggio, E.T. Recent advances in heterogeneous fluorescence immunoassays *In* Immunoassays: Clinical Laboratory Techniques for the 1980s, Nakamure, R.M., Dito, W.R. and Tucker, E.S. Eds., Alan R. Liss, New York, 1980, p.1.

18. Heidelberger, M. and Kendall, F.E. A quantitative study and a theory of the reaction mechanism. J. Exp. Med. **61**, 563-591, 1953.

19. Maggio, E.T. Ed. Enzyme-Immunoassay, CRC Press, Boca Raton, 1980, p.9.

20. Stavitsky, A.B., Micromethods for the study of proteins and antibodies. I Procedure and general applications of hemagglutination and hemagglutination-inhibition reactions with tannic acid and protein-treated red blood cells. J. Immunol. **72**, 360-367, 1954.

21. Zrafonetis, C.J.D. and Oster, L.H. Heterophile agglutination variability of erythrocytes from different sheep. J. Lab. Clin. Med. **34**, 1216, 1946.

22. Sternberg, J.C. Rate Nephelometry *In* Manual of Clinical Laboratory Immunology (4th Edition), Rose, N.R., Friedman, H. and Fahey, J.L. Eds., American Society for Microbiology, Washington, D.C., 1992, p.33.

23. Singer, J.M. and Plotz, C.M. The latex fixation test. I. Application to the serologic diagnosis of rheumatoid arthritis. Am. J. Med. , 888-896, 1956

24. Galvin, J.P. Particle-Enhanced Immunoassays *In* Manual of Clinical Laboratory Immunology (4th Edition), Rose, N.R., Friedman, H. and Fahey, J.L. Eds., American Society for Microbiology, Washington, D.C., 1992, p.38.

25. Jaff, B.M. and Behrman, H.R. Eds. Methods of Hormone Radioimmunoassay (2nd Edition), Academic Press, New York, 1979.

26. Heyndrickx, A., Van Peteghem, C., Van den Heede, M., De Clerck, F., Majelyne, W. and Timperman, J. Insulin murders: Isolation and identification by radio-immunoassay after several months of inhumation *In* Forensic Toxicology, Oliver, J.S. Ed., University Park Press, Baltimore, 1980, p.49-57.

27. Smith, R.N. Immunoassays in forensic toxicology *In* Forensic Toxicology, Oliver, J.S. Ed., University Park Press, Baltimore, 1980, p.34-47.

28. Ratcliffe, W.A., Fletcher, S.M., Moffat, A.C., Ratcliffe, J.G., Harland, W.A. and Levitt, T.E. Radioimmunoassay of lysergic acid diethylamide (LSD) in serum and urine using antisera of different specificities. Clin. Chem. **23**, 169-174, 1977.

29. Vessella, R.L. and Lange, P.H. Monitoring of patients with testicular cancer by assays for alpha-fetoprotein and human chorionic gonadotropin. *In* Manual of Clinical Laboratory Immunology (4th Edition), Rose, N.R., Friedman, H. and Fahey, J.L. Eds., American Society for Microbiology, Washington, D.C., 1992, p.810.

30. Hollinger, F.B., Bradley, D.W., Maynard, J.E., Dreesman, G.R. and Melnick, J.L. Detection of hepatitis A viral antigen by radioimmunoassay. J. Immunol. **115**, 1464-1466, 1975.

31. Purcell, R.H., Gerin, J.L., Almeida, J.D. and Holland, P.V. Radioimmunoassay for the core of the Dane particle and antibody to it. Intervirology **2**, 231-243, 1973/74.

32. Mayberry, W.E. and O'Sullivan, M.B. The clinical utility of radioimmunoassays in the medical center and reference laboratory settings *In* Cost/Benefit and Predictive Value of Radioimmunoassay, Albertini, A., Ekins, R.P. and Galen, R.S. Eds., Elsevier Science Publishers, Amsterdam, 1984, p.65-74.

33. Mathiesen, L.R., Feinstone, S.M., Wong, D.C., Skinhoj, P. and Purcell, R.H. Enzyme-linked immunosorbent assay for detection of hepatitis A antigen in stool and antibody to hepatitis A antigen in sera: comparison with solid-phase radioimmunoassay, immune electron microscopy, and immune adherence hemagglutination assay. J. Clin. Microbiol. **7**, 184-193, 1978.

34. Chantler, S.M. and Clayton, A.-L. The use of ELISA for rapid viral diagnosis: viral antigen detection in clinical specimens *In* ELISA and Other Solid Phase Immunoassays, Kemeny, D.M. and Challacombe, S.J. Eds., John Wiley & Sons, Chichester, 1988, p.279.

35. Virtanen, M., Syvanen, C.A., Oram, J., Soderlund, H. and Ranki, M. Cytomegalovirus in urine: detection of viral DNA by sandwich hybridisation. J. Clin. Microbiol. **20**, 1083, 1984.

36. Barka, N., Tomasi, J.P. and Stadtsbaeder, S. ELISA using whole *Legionella pnewmonphilia* cells or antigen. J. Immunol. Methods **93**, 77-81, 1986.

37. Goodman, Y.E., Wort, A.J. and Jackson, F.L. Enzyme-linked immunosorbent assay for detection of pertussis immunoglobulin A in nasopharyngeal secretions as an indicator of recent infection. J. Clin. Microbiol. **13**, 286-292, 1981.

38. Rubin, R.L., Joslin, F.G. and Tan, E.M. An improved ELISA for anti-native DNA by elimination of interference by anti-histone antibodies. J. Immunol. Methods **63**, 359-366, 1983.

39. Benjamini, E. and Lesdowitz, S. Immunology: A Short Course (2nd Edition), Wiley-Liss, New York, 1991, p.40-42.

40. Deleide, V., Dona, V. and Malvano, R. Homogeneous enzyme-immunoassay for anticonvulsant drugs: Effects of hapten-enzyme bridge length. Clin. Chem. Acta **99**, 195-201, 1979.

41. Ratcliff, R.M., Mirelli, C., Moran, E., O'Leary, D. and White, R. Comparison of five methods for the assay of serum gentamicin. Antimicrob. Agents Chemother. **19**, 508-512, 1981.

42. Morris, B. and Clifford, M.N. Eds. Immunoassays in Food Analysis, Elsevier Applied Sciences, London, 1985.

43. Weisburger, E.K., Russfield, A.B., Homburger, F., Wiesburger, J.H., Boger, E.,van Dongen, C.G. and Chu, K.C. Testing of twenty-one environmental aromatic amines of derivatives for long-term toxicity or carcinogenicity. J. Environmental Path. Toxicol. **2**, 325-356, 1978.

44. Benjamini, E. and Lesdowitz, S. Immunology: A Short Course (2nd Edition), Wiley-Liss, New York, 1991, p.38-39.

45. Benjamini, E., and Leskowitz, S. Immunology: A Short Course Second Edition. 1991. Wiley-Liss, Inc. New York. p 38-40.

46. Harlow, E. and Lane, D. Antibodies: A Laboratory Manual, Cold Spring Harbor Laboratory, New York, 1988, p.5.

47. Harlow, E. and Lane, D. Antibodies: A Laboratory Manual, Cold Spring Harbor Laboratory, New York, 1988, p.128.

48. Harlow, E. and Lane, D. Antibodies: A Laboratory Manual, Cold Spring Harbor Laboratory, New York, 1988, p.56.

49. Benjamini, E. and Lesdowitz, S. Immunology: A Short Course (2nd Edition), Wiley-Liss, New York, 1991, p.40.

50. Spouge, J.L., Guy H.R., Cornette, J.L., Margalit, H., Cease, K., Berzovsky, J.A., and D. DeLisi. Strong Conformational Propensities Enhance T Cell Antigenicity. J. Immunol. **138**: 204-212. 1987.

51. Harlow, E. and Lane, D. Antibodies: A Laboratory Manual, Cold Spring Harbor Laboratory, New York, 1988, p.131.

52. Harlow, E. and Lane, D. Antibodies: A Laboratory Manual, Cold Spring Harbor Laboratory, New York, 1988, p.77.

53. Means, G.E. and Feeney, R.E. Chemical Modification of Proteins, Holden-Day Inc., San Francisco, 1971, p.147.

54. Pierce Immunotechnology Catalog and Handbook Pierce Chemical Co., Rockford, 1991, p.E8-E39. A16-A18.

55. Benjamini, E. and Lesdowitz, S. Immunology: A Short Course (2nd Edition), Wiley-Liss, New York, 1991, p.70.

56. Challacombe, S.J., Biggerstaff, M., Gennall, C. and Kemeny, D.M. ELISA detection of human IgG subclass antibodies to *Streptococcus mutans*. J. Immunol. Methods **87**, 95, 1986.

57. Balestrino, E.A., Daniel, T.M., de Latini, M.D.S., Ma,Y. and Scocozza, J.B. Serodiagnosis of pulmonary tuberculosis in Argentina by enzyme-linked immunosorbent assay (ELISA) of IgG antibody to *Mycobacterium tuberculosis* antigen 5 and tuberculin purified protein derivative.Bull. W.H.O. **62**, 755-761, 1984.

58. Goding, J.W. Monoclonal Antibodies: Principle and Practice, Academic Press, London, 1983, p.14-17.

59. Fischbach, F.T. A Manual of Laboratory Diagnostic Tests (2nd Edition), J.B. Lippincott Co., Philadelphia, 1984, p.444-446.

60. Halliwell, T.E., Jones, M.W., Diment, J. and Salam, N. Enhanced luminescence immunoassay for anti-HIV IgM. Clin. Chem. **36** (Abstract), 1090, 1990.

61. Benjamini, E. and Leskowitz, S. Immunology: A Short Course 2nd. Edition), Wiley-Liss, New York, 1991, p.75-76.

62. Benjamini, E. and Lesdowitz, S. Immunology: A Short Course (2nd Edition), Wiley-Liss, New York, 1991, p.78.

63. Silverton, E.W., Navia, M.A. and Davies, D.R. Three-dimensional structure of an intact human immunoglobulin. Proc. Natl Acad. Sci. **74**, 5140-5144, 1977.

64. Litman, G.W. and Good, R.A. Immunoglobulins, Plenum Medical Co., New York, 1978.

65. Harlow, E. and Lane, D. Antibodies: A Laboratory Manual, Cold Spring Harbor Laboratory, New York, 1988, p.16-18.

66. Köhler, G. and Milstein, C. Continuous culture of fused cells secreting antibody of predefined specificity. Nature **256**, 496-497, 1975.

67. Galfre, G. and Milstein, C. Preparation of monoclonal antibodies; Strategies and procedures. Methods Enzymol. **73**, 3-46, 1981.

68. American Type Tissue Collection. Catalogue of Cell Lines and Hybridomas. Seventh Edition, 1990. Ed. R. Hay, J. Caputo, T.R. Chen, M. Macy, P. McClintock, and Y. Reid. American Type Tissue Collection.

69. Harlow, E., and Lane, D. Antibodies: A Laboratory Manual. 1988. Cold Spring Harbour Laboratory. p 211-213.

70. Amit, A.G., Mariuzza, R.A., Phillips, S.E.V., Poljak, R.J. Three Dimensional Structure of an Antigen-Antibody Complex at 2.8 Å Resolution. J. Biol. Chem. **233**: p 747-753. 1986.

71. Harlow, E., and Lane, D. Antibodies: A Laboratory Manual. 1988. Cold Spring Harbour Laboratory. p 24-27.

72. Steward, M.W., and Steensgaard, J. Antibody Affinity: Thermodynamic Aspects and Biological Significance. 1983. CRC Press, Boca Raton, Florida. p 1-2.

73. Steward, M.W., and Steensgaard, J. Antibody Affinity: Thermodynamic Aspects and Biological Significance. 1983. CRC Press, Boca Raton, Florida. p 10.

74. Cantor, C.R. and Schimmel, P.R. Biophysical Chemistry Part III: The Behavior of Biological Macromolecules. W.H. Freeman and Co., San Francisco, 1980, 852-856.

75. Nygren, H. and Stenberg, M. Immunochemistry and Interfaces. Immunology, **66**, 321-327, 1989.

76. Mason, D.W. and Williams, A.F. The Kinetics of Antibody Binding to Membrane Antigens in Solution and at the Cell Surface. Biochem. **187**, 1-3, 1980.

77. Uzgiris, E.E. and Kornberg, R.D. Two-dimensional Crystallisation Technique for Imaging Macromolecules with Application to Antigen-antibody-complement Complexes. Nature. **301**, 125-126, 1983.

78. Ehrlich, P., Moyle, W.R., Moustafa, Z.A. and Canfield, R.E. Mixing Two Monoclonal Antibodies Yields Enhanced Affinity for Antigen. J. Immunol. **128**, 2709-2710, 1982.

79. Olal, A.D. A Surface and Colloid Chemical Study of the Interaction of Proteins with Polystyrene Latex (PSL). PhD Thesis. University of British Columbia, 1990.

80. Tamm, L.K. and Bartoldus, I. Antibody binding to lipid model membranes. The large-ligand effect. Biochemistry **27**, 7453-7458, 1988.

81. Harlow, E., and Lane, D. Antibodies: A Laboratory Manual. 1988. Cold Spring Harbour Laboratory. p 30-33.

82. Ansari. A.A., Hattikurdur, N.S., Joshi, S.R. and Medeira, M.A. ELISA Solid Phase: Stability and Binding Characteristics. J. Immunol. Meth. **84**, 117-124.

83. Kaufman, E.N. and Rakesh, K.J. Effect of Bivalent Interaction upon Apparent Antibody Affinity: Experimental Confirmation of Theory Using Fluorescence Photobleaching and Implications for Antibody Binding Assays. Cancer Res. **52**, 4157-4167, 1992.

84. Raman, C.S., Jemmerson, R.,Nall, B.T. and Allen, M. Diffusion-limited rates for Monoclonal antibody binding to cytochrome *c*. Biochemistry, **31**, 10370-10379, 1992.

85. Nygren, H., Stenberg, M. and Karlsson, C. Kinetics Supramolecular Structure and Equilibrium Properties of Fibrinogen Adsorption at Liquid-solid Interfaces. J. Biomed. Mater. Res. **26**, 77-91, 1992.

86. Steward, M.W., and Steensgaard, J. Antibody Affinity: Thermodynamic Aspects and Biological Significance. 1983. CRC Press, Boca Raton, Florida. p 5-8.

87. Andrade, J.D. Principles of Protein Adsorption. In Surface and Interfacial Aspects of Biomedical Polymers, Volume 6: Protein Adsorption. Ed. J.D. Andrade. 1985. Plenum Press, New York. p 46-52.

88. Griswold, W.R. and Chalquest, R.R. Theoretical Analysis of the Accuracy of Calibrated Immunoassays for Measuring Antibody Concentration. Molec. Immun. **28**, 727-732, 1991.

89. Fisher Scientific. Catalogue. Fisher Scientific Company, Ottawa, Ontario. 1991. p 93.

90. Fisher Scientific. Catalogue. Fisher Scientific Company, Ottawa, Ontario. 1991. p 95.

91. Wojciechowski, P., Ten Hove, P., and Brash, J.L. Pheonomenology and mechanism of the transient adsorption of fibrinogen from plasma (Vroman effect). J. Coll. Interface Sci., **111**, p. 455-465, 1986.

92. Oliver, D.G., Thermal gradients in microtitre plates.Effects on enzyme-linked immunoassay. J. Immun. Methods, **42**, 195.

93. Sorenson, K. and Brodbek, U. Assesment of coating-efficiency in ELISA plates by direct protein determination. J. Immun. Methods, **95**, 291-293, 1986.

94. Werthen, M. and Nygren, H. Effect of antibody affinity on the isotherm of antibody binding to surface-immobilized antigen. J. Immun. Methods **115**, 71-78, 1988.

95. Challand, G.S., Spencer, C.A. and Ratcliffe, J.G. Observations on the Automated Calculation of Radioimmunoassay Results. Ann. Clin. Biochem. **13**, 354-360, 1976.

96. Marschner, I., Erhardt, F. and Scriba, P.C. Calculation of the Radioimmunoassay Standard Curve by Spline Function. *In* Radioimmunoassay and Related Procedures in Medicine. International Atomic Energy Agency, Vienna, 1974, 11.

97. Kemeny, D.M., and Challacombe, S.J. Microtitre Plates and Solid Phase Supports. In ELISA and Other Solid Phase Immunoassays: Theoretical and Practical Aspects. Ed. Kemeny, D.M., and Challacombe, S.J. Wiley, Toronto. 1988. p 39-40.

98. Rasmussen, S.E. Solid Phases and Chemistries. *In* Complementary Immunoassays. Collins, W.P. Ed. John Wiley and Sons, Chichester, 1988, 53.

99. Roch, A.M., Delcross, J.G., Thomas, V., Richard, J. and Quash, G. A novel covalent enzyme-linked immunoassay (CELIA) for simultaneously measuring free and immune complex bound antibodies of defined specificity: I. Application to naturally occurring antipolyamine antibodies in human sera. J. Immun. Methods, **133**(1), 1-12, 1990.

100. Lutz, H.U., Stammler, P. and Fischer, E.A. Covalent binding of detergent-solubilized membrane glycoproteins to "Chemobond" plates for ELISA. J. Immun. Methods, **129**(2), 211-220, 1990.

101. Varga, J.M., Klein, G.F. and Fritsch, P. Binding of a mouse monoclonal IgE (anti-DNP)antibody to radio-derivatized polystyrene-DNP complexes. FASEB J. **4**(9), 2678-2683, 1990.

102. Petrarch Systems, Inc. Silicon Compounds: Register and Review, Bristol, PA, 1984.

103. Plueddermann, E.P. Silane Coupling Agents. Plenum Press, New York and London, 1982.

104. Tan, C.G., Bowen, B.D. and Epstein, N. Production of Monodisperse Colloidal Silica Spheres: Effect of Temperature. J. Colloid Interface Sci. **118**, 290-293, 1987.

105. Stöber, W. and Fink, A. and Bohn, Ernst. Controlled Growth of Monodisperse Silica Spheres in the Micron Size Range. J. Colloid and Interface Sci. **26**, 62-69, 1968.

106. Hermanson, G.T., Mallia, A.K. and Smith, P.K. Immobilized Affinity Ligand Techniques. Academic Press, Inc. Harcourt Brace Jovanovich, Publishers, San Diego, 1992, 282-284.

107. Siegbahn, K. et al. ESCA: Atomic, Molecular and Solid State Structure Studied by Means of Electron Spectroscopy. Nova Acta Regiae Societatis Scientiarum Upsaliensis. Fourth Series. **20**. Upsala, Almquist & Wirksells Boktryckeri Ab.

108. B.D. Ratner and B.J McElroy. "Electron spectroscopy for chemical analylsis: applications in the Biomedical Sciences" in R.M. Gendreau. Ed., Spectroscopy in the Biomedical Sciences , CRC press, Boca Raton, 1986.

109. Fulghum, J.E. and Linton, R.W. Quantitation of coverages on rough surfaces by XPS: an overview. Surf. Interfac. Anal., vol 13, 186-192 (1988).

110. C.S. Fadley. Instrumentation for surface studies: XPS angular distributions. J. Elect. Spect. Relat.Phen, 5 (1974) 725-754.

111. R.W. Paynter, B.D. Ratner, T. A. Horbett, and H. R. Thomas. XPS studies on the organization of adsorbed protein films on fluoropolymers. J. Colloid Interface Sci., 101, 233-245, (1984).

112. Bull, H.B. An Introduction to Physical Biochemistry. F.A. Davis, Philadelphia, 294-329, 1964.

113. Menewat, A. Henry, J. and Siriwardan, R. Control of surface energy of glass by surface reaction: conctact angle and stability. J. Coll. Interface Sci.

114. Blake, P. and Ralston, J. Controlled methylation of quartz particles, Colloids and Surfaces, **101**, 110-110 (1984).

115. Massia, S.P. and Hubbell, J.A. Covalent Surface Immobilization of ARG-GLY-ASP and TYR-ILE-SER-ARG containing peptides to obtain well-defined cell adhesive substrates. Anal.Biochem., **187**, 292-301, 1990.

116. Pashley R.M. and Kitchener J. A. Surface forees in adsorbed multilayers of water on quartz., Interface Science, **713**, 491 - 590 1979.

117. Ratner, B.D., J.J.Rose, A.S.Hoffman and L.H.Scharpen. An ESCA study of surface contaminants on glass substrates for cell adhesion. *In* Surface Contamination (Genesis Detection and Control, vol. 2. K.L. Mittal, Ed. Plenum Press, New York and London, 1979.

118. Kaplan, L.A. and Pesce, A.J. Clinical Chemistry: Theory, analysis and correlation The C.V. Mosby Company, St. Louis, 1989, 2nd edition, p. 548.

119. Garibaldi, J.A. and Neilands, J.B. Isolation and Properties of Ferrichrome A. J. Am. Chem. Soc. **77**, 2429-2430, 1955.

120. van der Helm, D., Baker, J.R., Loghry, R.A. and Ekstrand, J.D. Acta. Cryst. **B37**, 323-330, 1981.

121. O'Haver, T.C. Derivative Spectroscopy: Theoretical Aspects. Plenary Lecture. Anal. Proc. **19**, 21-33, 1982.

122. Towbin, H., Staehelin, T. and Gordon, J. Electrophoretic Transfer of Proteins from Polyacylamide Gels to Nitrocellulose Sheets: Procedure and some Applications. Proc. Natl. Acad. Sci. USA, **76**, 4350-4354, 1979.

123. Dresser, D.W. Specific Inhibition of antibody production. II. Paralysis induced in adult mice by small quantities of antigen. Immunology, **5**, 378-388, 1962.

124. Harlow, E., and Lane, D. Antibodies: A Laboratory Manual. 1988. Cold Spring Harbour Laboratory. p 96-137.

125. Wieczorek, A. Vancouver Research station of Agriculture Canada, Personal communication, 1988.

126. Goka, A.K.J. and Farthing, M.J.G. The use of 3,3',5,5'-tetramethylbenzidine as a peroxidase substrate in microplate enzyme-linked immunosorbent assay. J. of Immunoassay, **8**, 29-41, 1987.

127. Harlow, E., and Lane, D. Antibodies: A Laboratory Manual. 1988. Cold Spring Harbour Laboratory. p 94.

128. Gibco BRL Life Technologies Catalogue and Reference Guide Gibco, Grand Island, 1993, p. 94-97.

129. Taggart, R.T. and Samloff, I.M. Stable Antibody-Producing Murine Myelomas. Science, **219**, 1228-1230, 1982.

130. Harlow, E. and Lane, D. Antibodies: A Laboratory Manual, Cold Spring Harbor Laboratory, New York, 1988, p.311.

131. Stocks, S.J. and Brooks, D.E. Production and Isolation of Large Quantities of Monoclonal Antibody using Serum-Free Medium and Fast Protein Liquid chromatography. Hydridoma, **8**, 241-247, 1989.

132. Harlow, E. and Lane, D. Antibodies: A Laboratory Manual, Cold Spring Harbor Laboratory, New York, 1988, p.310.

133. Goding, J.W. Monoclonal Antibodies: Principle and Practice, Academic Press, London, 1983, p.16.

134. Fairbanks, G., Steck, T.L. and Wallach, D.F.H. Electrophoretic analysis of the major polypeptides of the human erythrocyte membrane, Biochem., **10**, 2606-2617, 1971.

135. Reisner, A.H., Nemes, P. and Bucholtz, C. The use of Coomassie Brilliant blue G250 perchloric acid solutio for staining in electrophoresis and isolelectric focussing on polyacrylamide gels. Anal. Chem., **64**, 509-516, 1975.

136. Janzen, J. Fibrinogen Adsorption to Red Blood Cells. PhD thesis, University of British Columbia. 1985. p.42-44.

137. Arkles, B. Silane Coupling Agent Chemistry *In* Petrarch Systems, Inc. Silicon Compounds: Register and Review, Bristol, PA, 1984.

138. Hermanson, G.T., Mallai, A.K. and Smith, P.K. Immobilized Affinity Ligand Techniques, Academic Press, San Diego, 1992. p. 81.

139. Hermanson, G.T., Mallai, A.K. and Smith, P.K. Immobilized Affinity Ligand Techniques, Academic Press, San Diego, 1992. p. 282-284.

140. Means, G.E. and Feeney, R.F. Chemical Modification of Proteins, Holden-Day, Inc. San Francisco, 1971, p 175-178.

141. Seaman, G.V.F. Electrokinetic Behaviour of Red Blood Cells *In* The Red Blood Cell, Sturgenor D.M., Ed. Academic Press, New York, 1135-1229, 1975.

142. Cotton, F.A. and Wilkinson, G. Advanced Inorganic Chemistry, third edition, John Wiley and Sons., New York, 1972, p. 320-321.

143. Quartz Scientific International Product Information, Quartz Scientific International, Washington D.C.

144. Chaimberg, M. and Cohen, Y. Notes on the Silylation of Inorganic Supports. J. Colloid Interface Sci., **134**, 576- 579, 1990.

145. Means, G.E. and Feeney, R.F. Chemical Modification of Proteins, Holden-Day, Inc. San Francisco, 1971, p 144-145.

146. Neilands, J.B. Hydroxamic Acids in Nature: Sophisticated Ligands Play a Role in Iron Metabolism and possibly in Other Processes in Microorganisms. Science. **156**, 1443-1447, 1967.

147. Emery, T. and Neilands, J.B. Structure of the ferrichrome compounds. J. Am. Chem. Soc. **83**, 1626-1628, 1961.

148. Gray, B.M. Methodology for polysaccharide antigens: protein coupling of polysaccharides for adsorption to plastic tubes. J. Immun. Methods, **28**, 187-191.

149. Boraker, D.K., Bugbee, S.J. and Reed, B. A. Acoustic probe-based ELISA. J. Immun. Methods, **155**, p. 91-94, 1992.

Appendix 1

Analysis of Competitive Inhibition of Monoclonal Antibody Binding to Surface-attached Antigen

D. E. Brooks

The analysis of inhibition by free Ag of monoclonal IgG Ab binding to surface-attached Ag is complicated by:

1. the presence of mixed light chains in the monoclonal Ab such that 1/4 of the IgG molecules present are expected to carry two specific Ag binding sites, 1/2 of the molecules one site and 1/4 of the molecules no specific binding sites;
2. the statistical nature of Ag binding to divalent Ab in solution. Since the Ag in question is small, it can be assumed that occupation of one of the two sites by Ab in solution will not inhibit binding of the Ab molecule to surface-bound Ag. Hence, for any of the Ab species present in solution, only those with all binding sites filled will be inhibited from binding specifically to the surface.

Both effects are taken into account in the following analysis.

Assumptions:

1. The binding isotherm for Ab to surface-bound Ag exhibits no non-specific binding due the effectiveness of blocking protein.
2. The Ab is pre-equilibrated with free Ag at various concentrations. Since the actual amount of each Ab species bound to the surface is very small compared to the solution

concentration (which is readily verifiable in the present case) it is assumed that the concentrations of Ab species that equilibrate with the surface are those which result from the initial equilibration with free Ag.

3. The antibody is radiolabelled so the total amount of IgG and the total surface concentration of IgG are known but not the concentrations of the individual species.
4. The total concentration of soluble inhibiting Ag added is known but its distribution among the various species is not measured.

Analysis:

The binding equilibrium for Ab binding specifically to surface-attached in the absence of free Ag is given by:

$$\Gamma = \Gamma_s K_g C_g/(1 + K_g C_g) \qquad [A1]$$

where Γ, Γ_s are the surface concentrations of Ab at equilibrium with Ab concentration C_g and at saturation, respectively and Kg is the apparent association constant for Ab binding to surface-attached Ag.

From measurements of Γ as a function of C_g values for K_g and Γ_s are obtained. In the presence of soluble inhibiting Ab, and taking into account the distribution of binding sites due to light chain variation, the total amount of Ab able to bind to surface sites, C_{gin}, is:

$$C_{gin} = C_{10} + C_{20} + C_{21} \qquad [A2]$$

where C_{ni} = concentration of Ab species with i of its n specific sites occupied by soluble Ag, n = 0, 1 or 2. The individual species C_{nj} can be expressed in terms of the association constant for Ag binding to Ab in solution, K_{ag}, and the equilibrium concentration of free Ag, C_{ag}, by:

$$C_{ni} = C_{no} \frac{n!}{(n-i)!\ i!} (C_{ag} K_{ag})^i \qquad [A3]$$

$$C_{no} = \frac{C_{nT}}{(1 + C_{ag} K_{ag})} \qquad [A4]$$

where C_{nT} is the total concentration of Ab bearing n specific sites in the system. Note that according to complication 1:

$$C_{1T} = 2\ C_{2T} = 2\ C_{oT} \qquad [A5]$$

so the total concentration of labelled Ab in the system, C_T, is:

$$C_T = \Sigma C_{iT} = 4\ C_{2T} \qquad [A6]$$

Once the free Ag has equilibrated with the Ab the total concentration of soluble Ag, C_{agin}, can be expressed in terms of the various Ab species C_{ni} as was the concentration of Ab available to react with the surface Ag in [A2]:

$$C_{agin} = C_{11} + C_{21} + 2C_{22} + C_{ag} \qquad [A7]$$

since there are two Ag molecules bound per molecule of C_{22}. Utilizing [A3], [A4] and [A6] and simplifying gives for C_{gin}:

$$\frac{C_{gin}}{C_{2T}} = \frac{(4 + 3z)}{(1 + z)^2} \qquad [A8]$$

and for C_{agin}, using [A7]:

$$\frac{C_{agin}}{C_{2T}} = \frac{z(4 + 3z)}{(1 + z)^2} + \frac{C_{ag}}{C_{2T}} \qquad [A9]$$

where $z = C_{ag} K_{ag}$. In the presence of soluble inhibiting Ag the binding isotherm [A1] can be written, in terms of the fractional saturation $\theta = \Gamma/\Gamma_s$:

$$\theta = \frac{K_g(C_{gin} - \Gamma A)}{1 + (C_{gin} - \Gamma A)} \qquad [A10]$$

where $C_g = C_{gin} - \Gamma A$ and A = area per ml of surface in experiment.

The object of the present effort is to estimate a value for the binding constant of Ag for Ab in solution, K_{ag}, from the inhibition of surface binding. The known or measured parameters are K_g, C_T, θ, A and C_{agin}; for a fixed choice of A and C_T, θ is measured as a function of C_{agin}. Equations [A6] and [A8] - [A10] uniquely determine K_{ag}. Their simultaneous solution gives:

$$K_{ag} = \frac{z}{C_{agin} - z\ L\ C_{2T}} \qquad [A11]$$

where:

$$L = \frac{1}{K_g\ C_{2T}(\theta^{-1} - 1)} + \frac{\Gamma A}{C_{2T}} \qquad [A12]$$

$$z = C_{ag}\ K_{ag} = (3/2L - 1) \pm (4L + 9)^{1/2}/2L \qquad [A13]$$

in which the positive root is taken and:

$$C_{2T} = C_T/4 \qquad [A6]$$

Applying this solution to the inhibition data shown in Figure 56 gives the estimates for K_{ag} in the table below. The following values for the constants were used, derived from experiment:

$K_g = 7.1 \times 10^7$ litre/mole (this value takes into account the light chain distribution)

$\Gamma_s = 0.565$ mg $m^{-2} = 3.5 \times 10^{-13}$ moles/cm^2

$C_T = 9.25 \times 10^{-9}$ moles/litre

A = 3.2 cm^2/ml

$C_{ag in}$ (M)	θ	L	z	K_{ag} (M^{-1})
9.5×10^{-9}	0.327	3.07	0.240	3.08×10^{7}
1.9×10^{-8}	0.275	2.41	0.519	3.22×10^{7}
4.75×10^{-8}	0.192	1.52	1.27	2.94×10^{7}
9.5×10^{-8}	0.157	1.19	1.82	2.02×10^{7}
1.9×10^{-7}	0.129	0.948	2.47	1.34×10^{7}

The five values for K_{ag} give an average value of:

$$K_{ag} = (2.5 \pm 0.8) \times 10^{7}\ M^{-1}$$

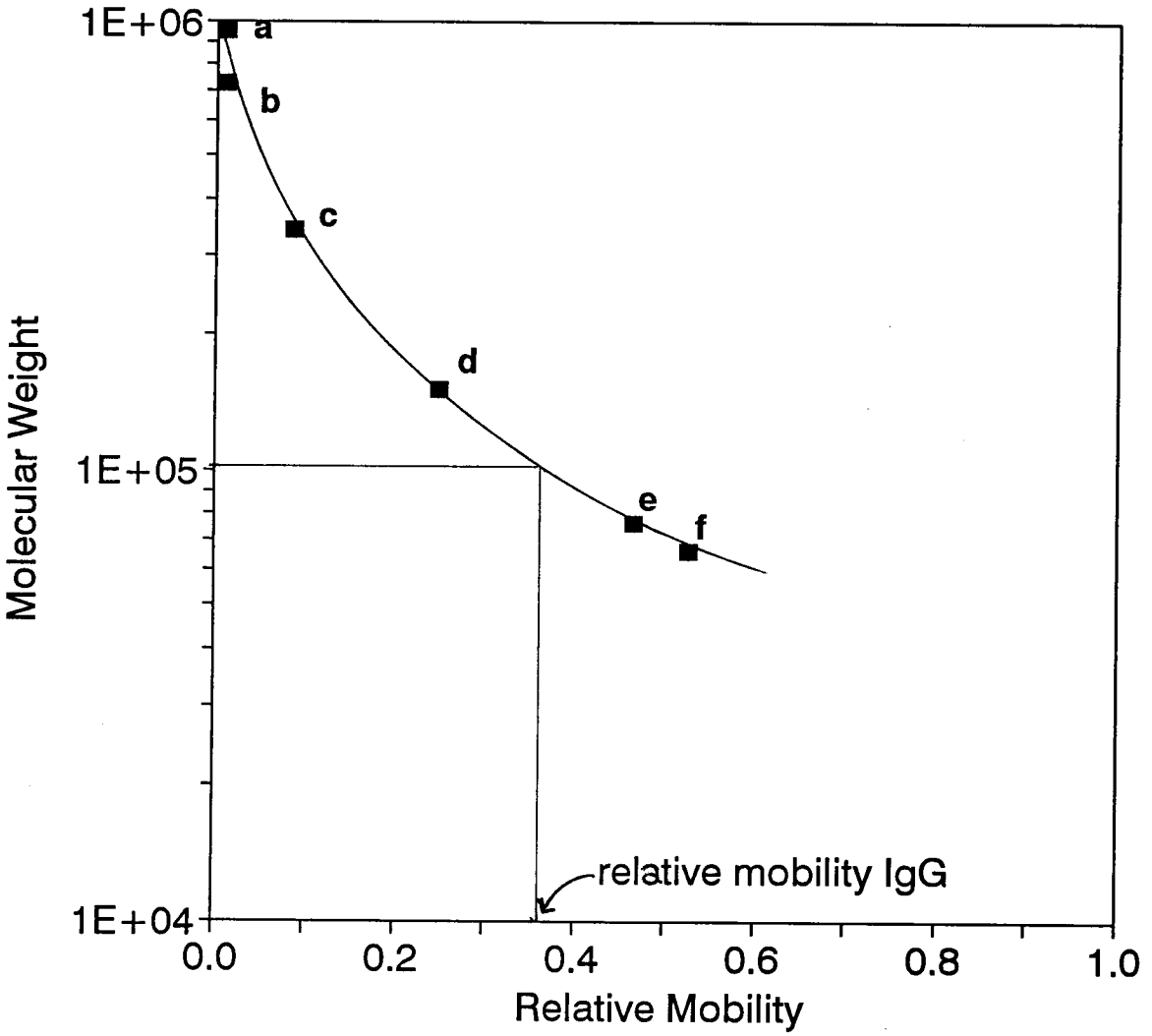

Figure 66: Determining molecular weights from SDS-page of proteins in human serum. The proteins were identified by comparison to gels run by Dr. Johan Janzen, and the peaks correspond to a= IgM (950 kD), b= α_2M, (750 kD), c= fibrinogen (340 kD), d= IgG (160 kD), e= transferrin (76 kD) and f= albumin (66 kD).

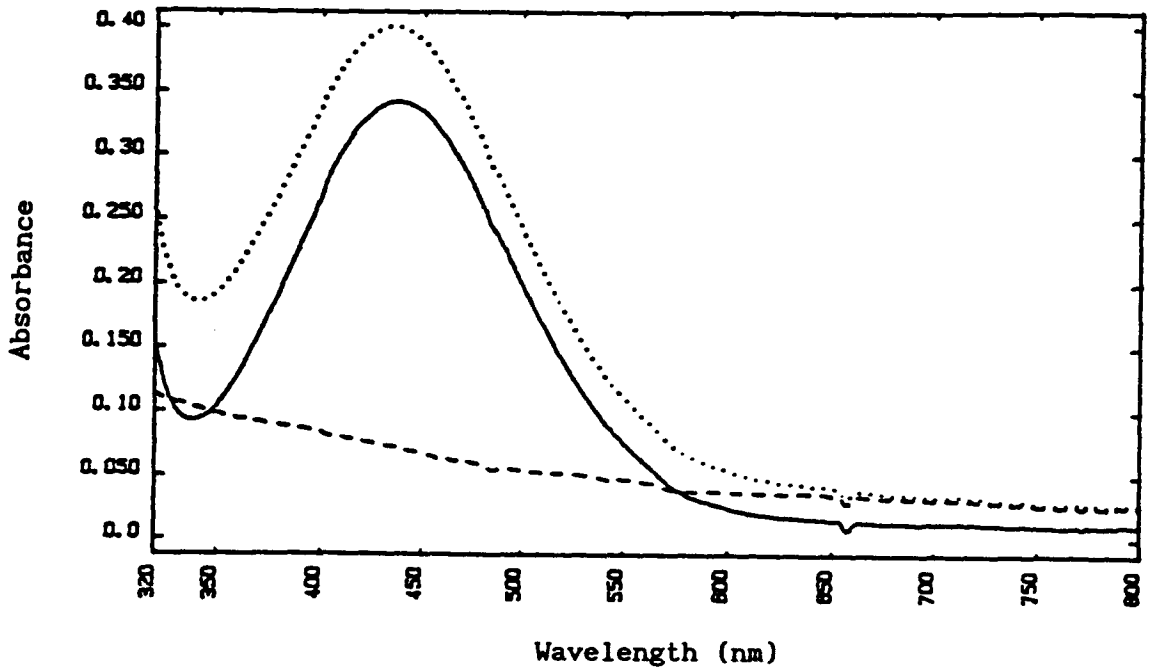

Figure 67: Sample spectra showing optical density of a ferrichrome A solution (——), a suspension of beads in water (- -) and a suspension of beads in a ferrichrome A solution (...). The two ferrichrome A solutions are at the same concentration.

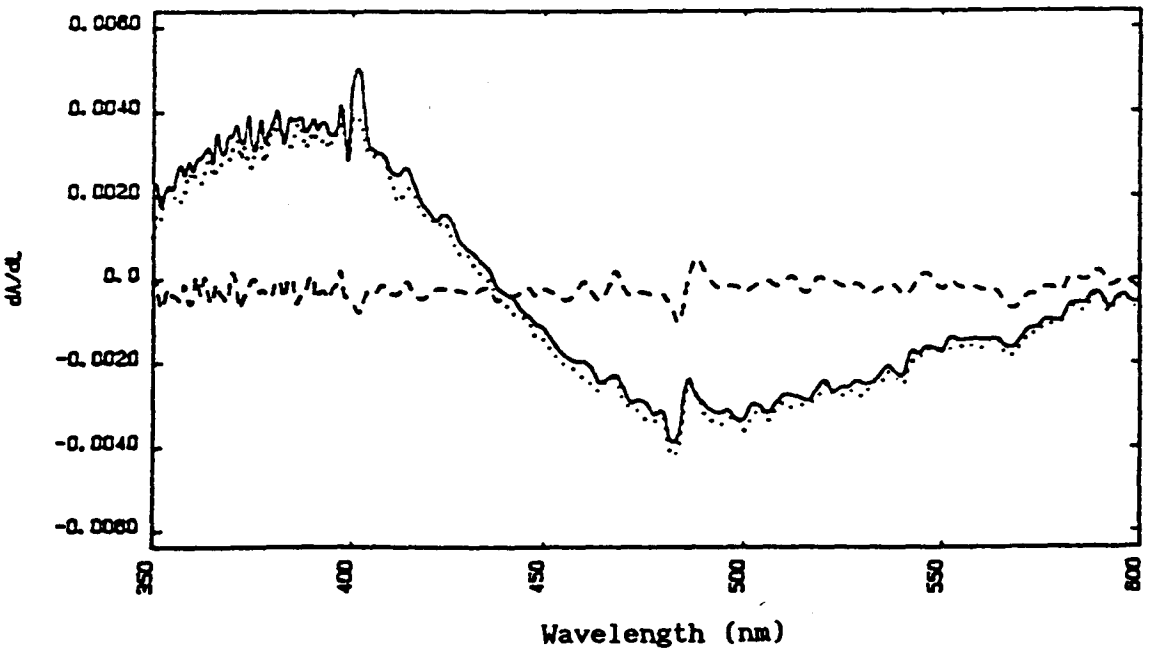

Figure 68: The derivatives dA/dλ for the sample spectra shown in Fig. 67 ((——) ferrichrome A, (- -) beads in water and (...) beads in a ferrichrome A solution).

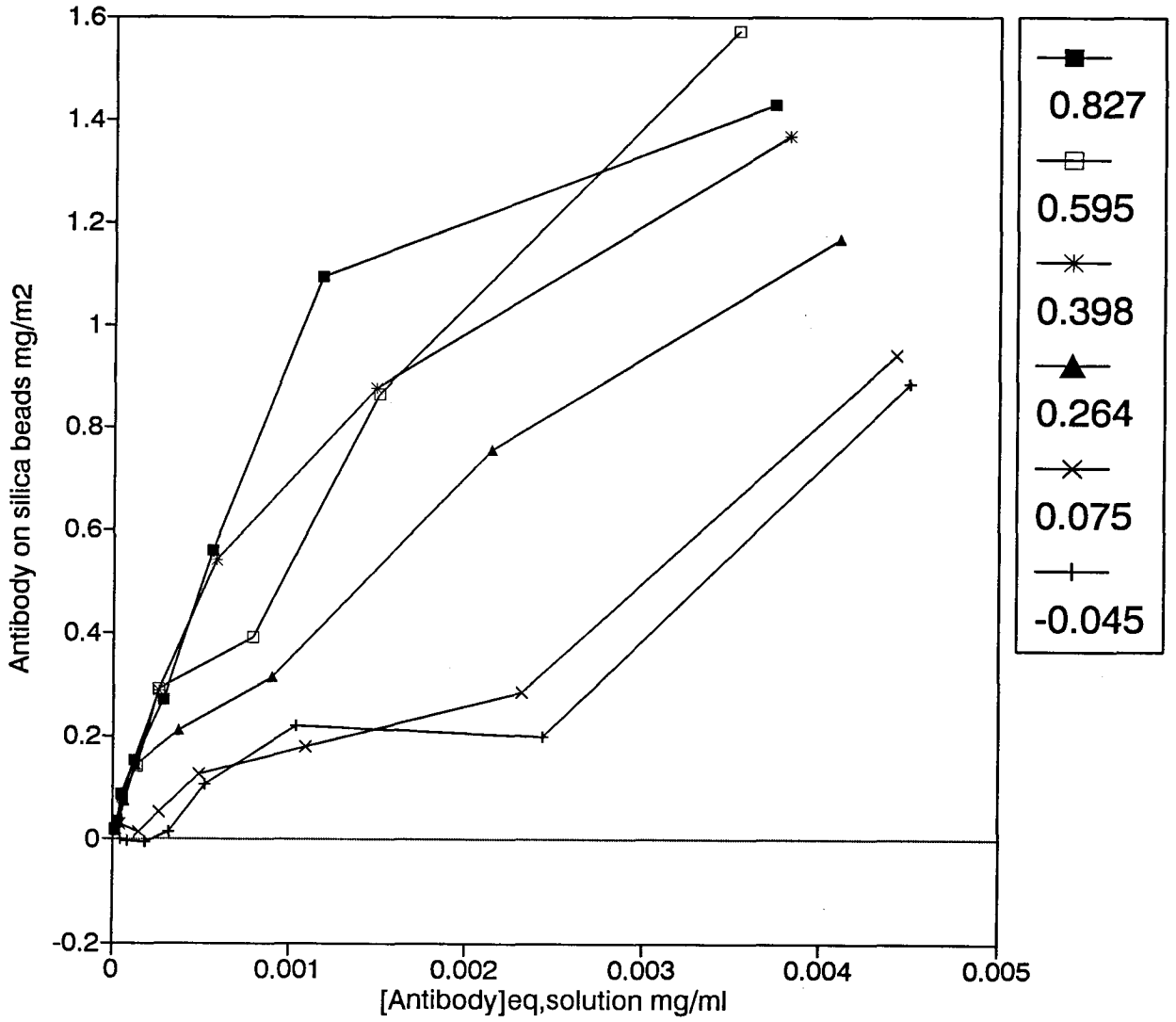

Figure 69: Antibody bound to silica beads with a range of different surface concentrations of ferrichrome A: bound antibody determined from solution depletion measurements (from the same experiment as Fig. 52). The legend shows the measured surface concentration of antigen on the silica in mg/m^2.

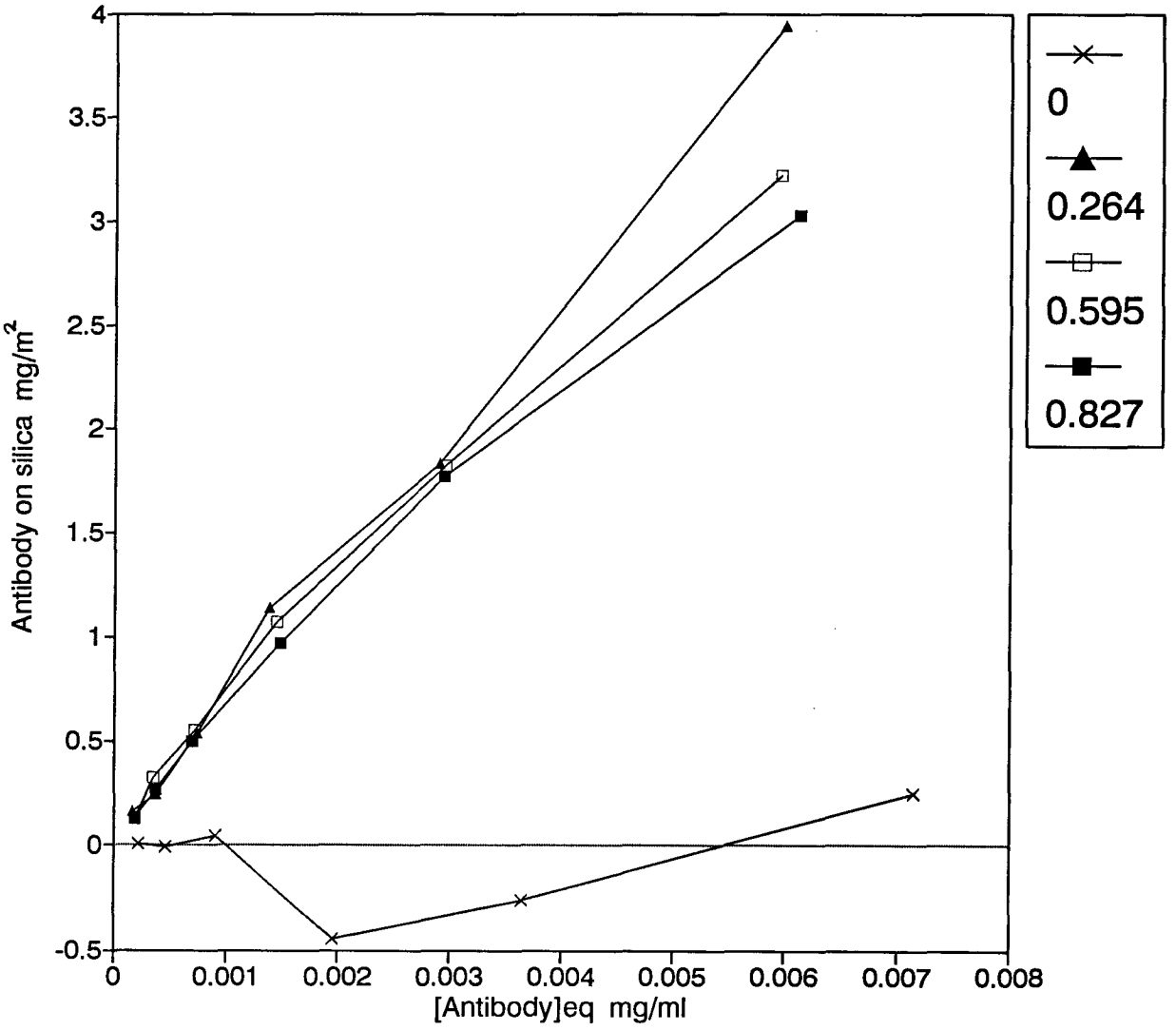

Figure 70: Antibody binding to flat silica modified with different solution concentrations of ferrichrome A: bound antibody determined from solution depletion measurements. The legend shows the measured surface concentration of antigen on silica beads (mg/m^2) modified with the same solution concentration of ferrichrome A.

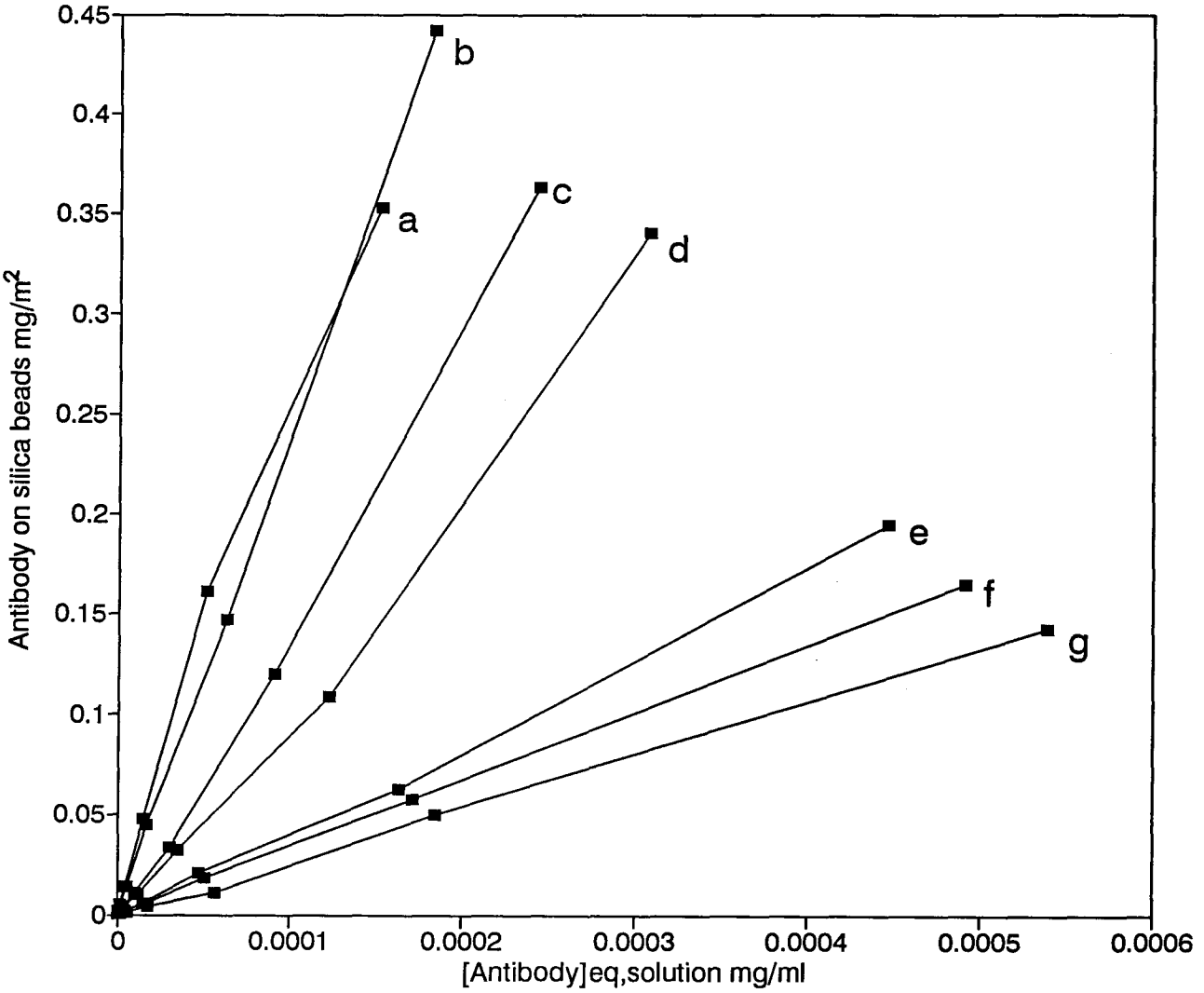

Figure 71: Antibody bound to silica beads with a range of different surface concentrations of ferrichrome A: bound antibody determined from amount remaining after wash (a=0.827 mg/m^2 ferrichrome A, b=0.595 mg/m^2, c= 0.636 mg/m^2, d= 0.398 mg/m^2, e= 0.264 mg/m^2, f= 0.075 mg/m^2, g= 0.022 mg/m^2).

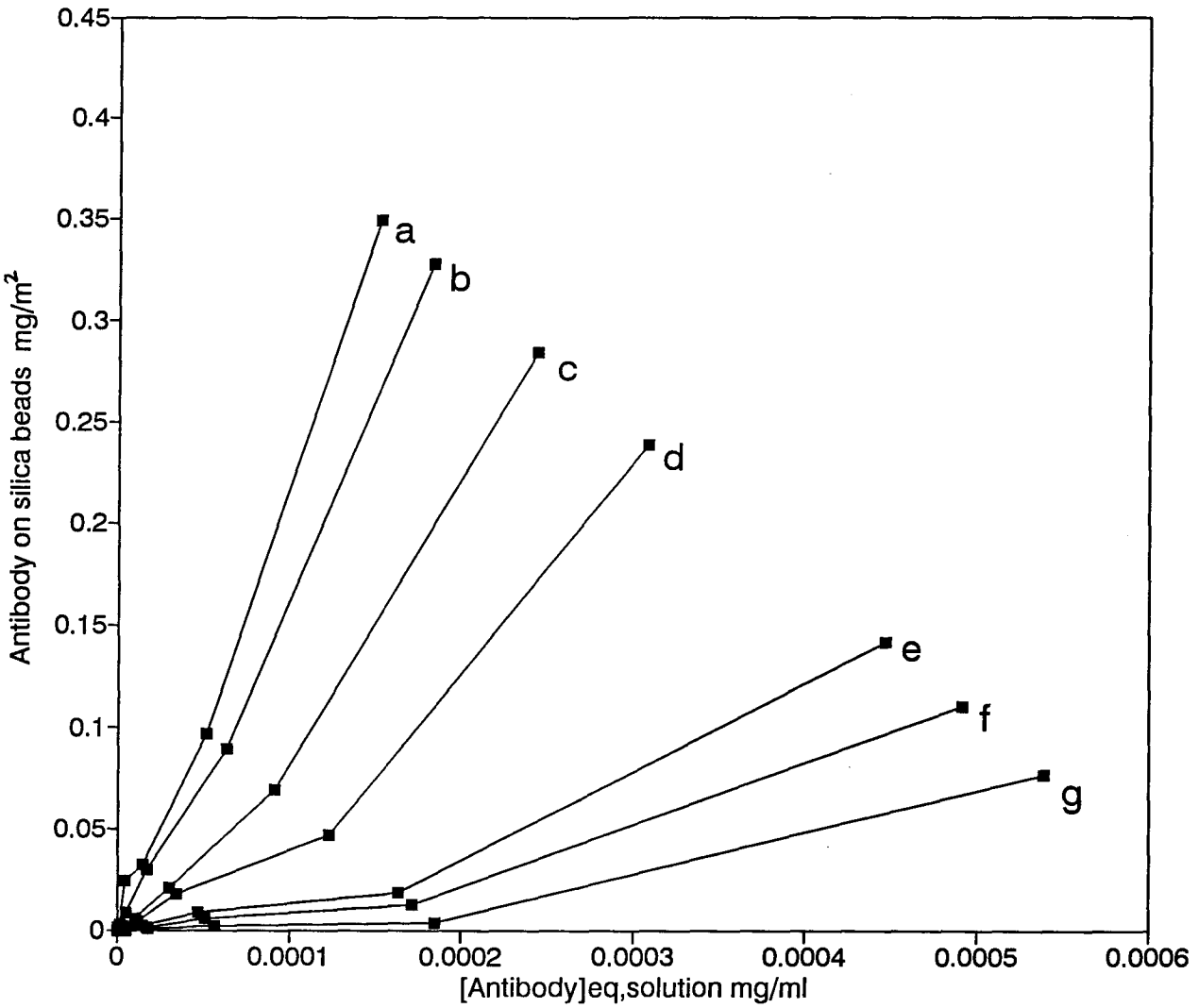

Figure 72: Antibody bound to silica beads with a range of different surface concentrations of ferrichrome A: concentration of antibody determined from solution depletion for the experiment shown in Figure 71.

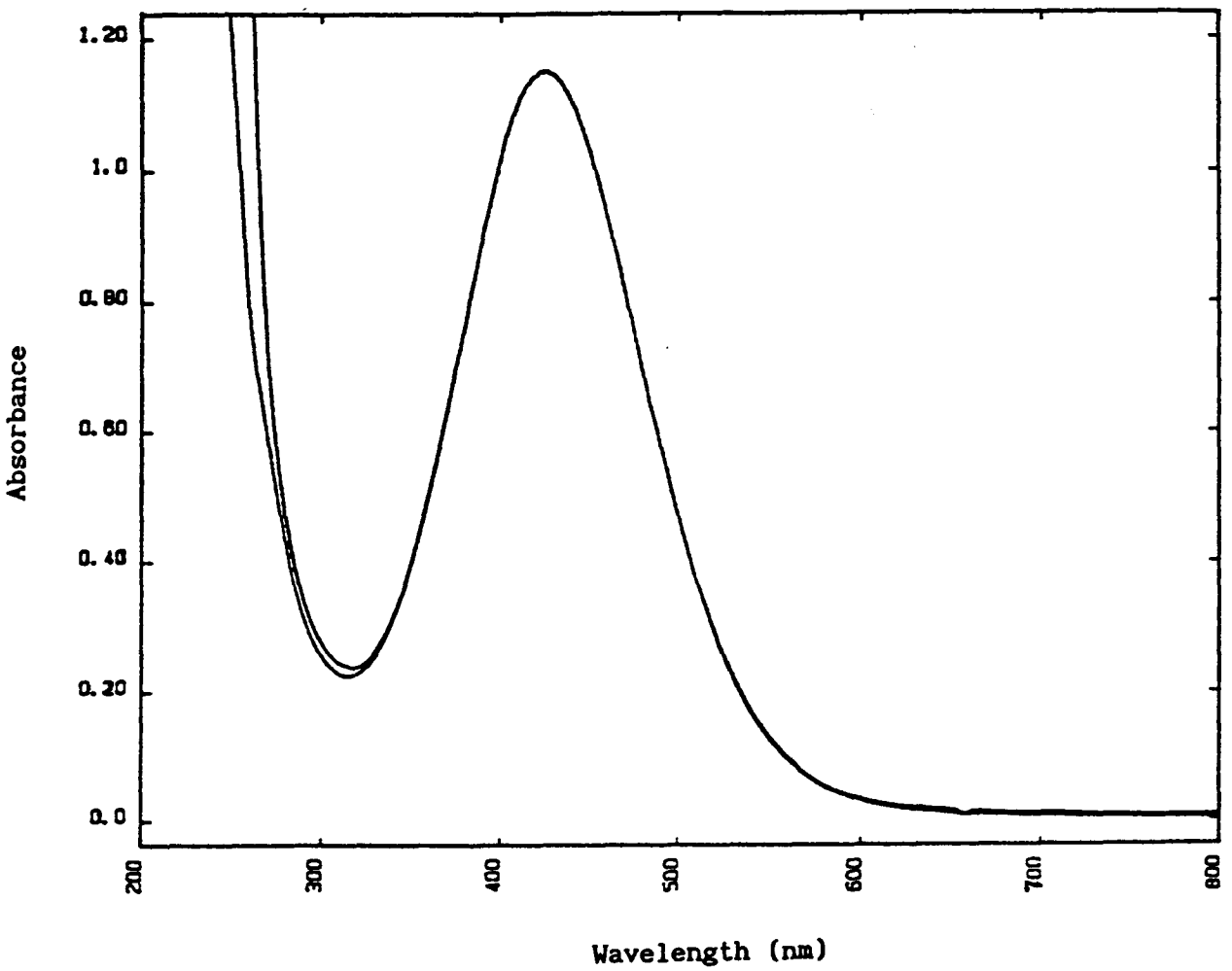

Figure 73: Absorbance of ferrichrome in water and ferrichrome with a large excess (>100:1 ratio) of EDC. There is no peak at 367 nm after addition of the EDC.